HYDRODYNAMIC BEHAVIOURS OF FINE SEDIMENT IN RETENTION STRUCTURE USING PARTICLE IMAGE VELOCIMETRY

MASOUMEH MOAYERI KASHANI

THESIS SUBMITTED IN FULFILMENT OF THE REQUIREMENTS FOR THE DOCTORAL DEGREE OF PHILOSOPHY

FACULTY OF ENGINEERING
UNIVERSITY OF MALAYA
KUALA LUMPUR

2016

University of Malaya

UNIVERSITY OF MALAYA

ORIGINAL LITERARY WORK DECLARATION

Name of Candidate: (I.C/Passport No:)

Matric No:

Name of Degree:

Title of Project Paper/Research Report/Dissertation/Thesis ("this Work"):

Field of Study:

I do solemnly and sincerely declare that:

(1) I am the sole author/writer of this Work;
(2) This Work is original;
(3) Any use of any work in which copyright exists was done by way of fair dealing and for permitted purposes and any excerpt or extract from, or reference to or reproduction of any copyright work has been disclosed expressly and sufficiently and the title of the Work and its authorship have been acknowledged in this Work;
(4) I do not have any actual knowledge nor do I ought reasonably to know that the making of this work constitutes an infringement of any copyright work;
(5) I hereby assign all and every rights in the copyright to this Work to the University of Malaya ("UM"), who henceforth shall be owner of the copyright in this Work and that any reproduction or use in any form or by any means whatsoever is prohibited without the written consent of UM having been first had and obtained;
(6) I am fully aware that if in the course of making this Work I have infringed any copyright whether intentionally or otherwise, I may be subject to legal action or any other action as may be determined by UM.

Candidate's Signature Date:

Subscribed and solemnly declared before,

Witness's Signature Date:

Name:

Designation:

University of Malaya

ABSTRACT

Siltation, or sediment pollution, is a cause for water pollution by fine particles of clay or silt. Accumulated fine sediments create murky water with low oxygen levels, potentially leading to aquatic life death. Thus, studying the hydrodynamic behavior of fine sediments is essential. However, the direct evaluation of fine particle suspension and deposition is costly and limiting. The intent of this research is to display a novel, direct outlook of the hydrodynamic behavior of fine sediments in the two-dimensional study of retention structures with different hydraulic features using particle image velocimetry (PIV). To attain this goal, the physical and mechanical properties of fine sediment are investigated extensively by applying rheological methods, laser diffraction particle size analysis (LDPSA) and scanning electron microscopy (SEM). The rheological behavior of six soil samples (fine particles with D < 63 μm) from different regions of Malaysia is explored. A rotational rheometer with a parallel-plate measuring device (two sizes: 25 mm and 50 mm) is used to observe the flow and viscoelastic properties of fine particles. The samples undergo the rheological curve and amplitude sweep test methods to investigate the effect of water content ratio, and texture and structure of particles on the rheological properties. Therefore, the hydrodynamic behavior of a mix of water and fine particles is studied in a specifically designed sediment basin. The fluid is seeded with fluorescent polymer particles of two sizes (20-50 and 1-20 μm). Then the impact of different hydraulic parameters, such as water depth, flow rate, particle diameter, varying inlet distances from the water surface, and outlet placement, on fine particle movement in the middle of the designed basin is observed. Fine particle displacement is identified by recording images with a CCD (charge coupled device) camera and using Nd-YAG laser lighting. The fine sand, clay and silt content affect the stiffness, structural stability and shear behavior of soil. Moreover, the concentration of fine sediment particles in water directly influences the rheological curve. Reduced viscosity of samples with higher water concentrations is

University of Malaya

detected. Consequently, a substantial quantity of fine sediments are distributed within the water body and remain suspended over time. As a result, the sedimentation rate slows down. Apparently, the flow rate modifies the velocity and direction of fine particles, while at the bottom of the basin, approaching the outlet, the re-suspension rate increases at higher flow rates. The same inlet and outlet level reduces fine particle dispersion, while a lower flow rate assists with controlling high siltation. The gravitational force affects the fine particles more at greater depth, thus boosting the settling level more than 50%. Thus, the supreme collecting efficiency is investigated at water surface near 80%. Furthermore, there is a direct correlation between flow rate and particle size, while a higher inlet and outlet hinder the dispersion of fine particles in the water column. Smaller spherical particles have greater influence on fine particle suspension. Therefore, controlling the hydraulic parameters can ultimately reduce the siltation problem.

University of Malaya

ABSTRAK

Pengelodakan, atau pencemaran sedimen, adalah punca pencemaran air dengan partikel halus tanah liat atau kelodak. Sedimen halus yang terkumpul menghasilkan air keruh dengan tahap oksigen yang rendah yang boleh membawa kepada kematian hidupan akuatik. Oleh itu, pemahaman tingkah laku hidrodinamik sedimen halus adalah penting. Walau bagaimanapun, kos bagi penilaian penggantungan zarah halus dan pemendapan adalah sangat tinggi dan terhad. Tujuan kajian ini adalah untuk menghasilkan novel, keterangan tingkah laku hidrodinamik sedimen halus dalam kajian dua dimensi pengekalan struktur dengan ciri-ciri hidraulik yang berbeza dengan menggunakan imej zarah velocimetry (PIV). Bagi mencapai matlamat ini, sifat-sifat fizikal dan mekanikal sedimen halus disiasat secara meluas dengan menggunakan kaedah reologi, LDPSA dan SEM. Reologi adalah keterangan sains bagi pengubahan bentuk dan aliran di bawah tekanan. Sifat-sifat reologi enam sampel tanah (zarah halus dengan D <63 mikron) dari kawasan-kawasan yang berlainan di Malaysia mula dikaji. Putaran reometer dengan alat pengukur plat-selari (dua saiz: 25 mm dan 50 mm) digunakan untuk melihat aliran dan kandungan viskoelastik zarah halus. Kaedah ujian reologi dan amplitud dijalankan ke atas sampel sampel untuk mengkaji kesan nisbah kandungan air, tekstur dan struktur zarah kepada sifat-sifat reologi. Oleh itu, sifat-sifat hidrodinamik dari campuran zarah air dan zarah halus dikaji dalam lembangan sedimen yang direka khusus. Cecair ini disemai dengan zarah polimer pendarfluor dalam dua saiz (20-50 dan 1-20 mikron). Kesan parameter hidraulik yang berbeza seperti kedalaman air, kadar aliran, diameter zarah dalam pelbagai jarak masuk dari permukaan air, perletakan alur keluar dan pergerakan zarah halus di tengah lembangan kemudiannya diperhatikan. Sesaran zarah halus dikenal pasti dengan rakaman imej menggunakan kamera CCD dan lampu laser Nd-YAG. Pasir halus, tanah liat dan kandungan kelodak memberi kesan pada kekukuhan, kestabilan struktur dan tingkah laku ricih tanah. Selain itu, kepekatan zarah sedimen halus dalam air

University of Malaya

terus mempengaruhi sifat reologi-nya. Sampel dikesan mempunyai kekurangan likatan dan kenaikan dalam kepekatan air. Oleh itu, kuantiti besar sedimen halus diedarkan dalam badan air dan tergantung dari masa ke masa. Hasilnya, kadar pemendapan semakin perlahan. Kadar aliran mengubah halaju dan arah zarah halus, manakala di bahagian bawah lembangan, dekat pada saluran keluar, kadar penggantungan semula semula semakin tinggi. Kadar masuk dan keluar yang sama mengurangkan penyebaran zarah halus, manakala kadar aliran yang lebih rendah mengawal pengelodakan yang tinggi. Daya graviti memberi kesan kepada partikel halus pada kedalaman yang lebih tinggi, dengan itu meningkatkan tahap pengenapan lebih daripada 50%. Oleh itu, kumpulan tertinggi disiasat pada 80% permukaan air. Tambahan pula, terdapat hubungan langsung antara kadar aliran dan saiz zarah, manakala salur masuk dan keluar yang lebih tinggi menghalang penyebaran partikel halus di dalam air. Zarah sfera yang lebih kecil mempunyai pengaruh yang lebih besar pada penggantungan zarah halus. Oleh itu, dengan mengawal parameter hidraulik , masalah pengelodakan boleh dikurangkan.

University of Malaya

ACKNOWLEDGEMENTS

I would like to express my sincere gratitude to my advisor Associate Prof. Dr. Lai Sai Hin for the continuous support of my Ph.D study and research, for his patience, motivation, enthusiasm, and immense knowledge. His patience and support helped me overcome many crisis situations and finish this thesis.

I would like to thank my co-advisor Prof. Dr. Shaliza Binti Ibrahim for her encouragement, insightful comments, and support.

I am also grateful to the following former or current staff at University of Malaysia, for their various forms of support during my graduate study.

Many friends have helped me stay sane through these years. Their support and care helped me overcome setbacks and stay focused on my graduate study. I greatly value their friendship and I deeply appreciate their belief in me.

Most importantly, none of this would have been possible without the love and patience of my family. I would like to express my heart-felt gratitude to my parents and my beautiful sister for supporting me spiritually throughout my life and study.

Finally, I appreciate the financial support from University of Malaya that funded this research.

University of Malaya

TABLE OF CONTENTS

University of Malaya

University of Malaya

University of Malaya

University of Malaya

University of Malaya

University of Malaya

LIST OF FIGURES

University of Malaya

University of Malaya

University of Malaya

University of Malaya

University of Malaya

University of Malaya

University of Malaya

University of Malaya

LIST OF TABLES

University of Malaya

LIST OF SYMBOLS AND ABBREVIATIONS

f	:	Focal Length
F	:	Force
G	:	Shear Modulus
G'	:	Storage Modulus
G"	:	Loss Modulus
μ	:	Kinetic Viscosity
η	:	Dynamic Viscosity
τ	:	Shear Stress
λ	:	Wavelength
ɣ•	:	Shear Rate
ρ	:	Density
AST	:	Amplitude Sweep Test
BOD	:	Biochemical Oxygen Demand
CCD	:	Charge Coupled Device
CMOS	:	Complementary Metal–Oxide–Semiconductor
COD	:	Chemical Oxygen Demand
CSD	:	Constant Shear Deformation
CSR	:	Constant Shear Rate
DID	:	Drainage and Irrigation Department
DO	:	Dissolved Oxygen
DOE	:	Department of Environment
FS	:	Fine Sediment
g	:	Gravitational acceleration
HRT	:	Hydraulic Retention Time

University of Malaya

LDPA	:	Laser Diffraction Particle Size Analysis
LVE	:	Linear Visco Elastic
MWD	:	Molecular weight distribution
NAHRIM	:	National Hydraulic Research Institute of Malaysia
pH	:	Hydrogen Ion Level
PIV	:	Particle Image Velocimetry
PP	:	Parallel Plate
Q	:	Flow rate
SEM	:	Scanning Electron Microscopy
SPSS	:	Statistical Packages for Social Sciences
SS	:	Suspended Solids
T	:	Turbidity
TS	:	Total Sediment
TSS	:	Total Suspended Solid
Vc	:	Critical Speed
Vs	:	Settling Velocity
V_*	:	Shear Velocity
WQI	:	Water Quality Index

University of Malaya

LIST OF APPENDICES

University of Malaya

CHAPTER 1: INTRODUCTION

1.1 Background

The construction of retention structures to collect rainwater, such as dam, lakes and ponds to prohibit runoff, for flood control in urban drainage systems as well as for municipal and industrial utilization have been implemented into several government program agendas. If the management and maintenance of pond systems are neglected, pond habitats deteriorate over time. Ponds have specific habitats including fish, plants and other organic and inorganic matter, which are affected by urbanization and human activity; some habitats are even dying nowadays.

Since the 1970s, the Malaysian Department of Drainage and Irrigation requires all project developments to have a retention pond for flood mitigation, the size of which is proportional to the development area and land use. As development regions are inhabited, commercial activities have attracted an abundance of facilities and markets with poor construction practices; consequently, much sediment and organic waste accumulates at the bottom of ponds, creating thick layers of anaerobic micro-activity. Humans significantly influence the amount of algae in pond water by over-fertilizing land that drains in ponds and by inadequately maintaining septic sewer systems on land close to ponds. Fish life and aquatic activity ceases and ponds evolve to “dead pond” status. The problem is further exacerbated by frequent storm events, whereby excess flow contaminates downstream waterways and estuaries.

In order to mitigate these problems, several studies have been carried out in relation to retention structures, such as water quality (Bhat et al., 2009), sedimentation (Ismail T. et al., 2010; Shamsudin et al., 2012), eutrophication (Kumar et al., 2011; Kumar. P & Wanganeo., 2012; Sarnelle et al., 2010; Sipaúba-Tavares et al., 2011), chemicals and

University of Malaya

heavy metals (Karlsson et al., 2010; Stephansen et al., 2012) and so on. However, studies related to a direct view of the hydrodynamic behavior of fine sediments in retention structures are scarce. Therefore, the focus of this study is on fine sediment, to bring new knowledge to light and assist with solving the high turbidity problem in the majority of retention structures.

1.2 Problem Statement

The problem of siltation is well-known as a major factor contributing to pollution/muddy water in most countries worldwide. However, research and knowledge of the fine sediment transport mechanisms, dispersion, interaction, relationships, etc., in retention structures for dealing with a number of problems related to siltation are limited.

Urbanization, forestry and agriculture have the potential to influence the quality and quantity of soils, sediments and pollutants in ponds. Sediment transport causes muddy water. The movement of soils and sediments during runoff creates turbid water, and the role of fine sediments is greater in this case since fine sediments float or become suspended in water. Thus, sediment re-suspension should also be considered. Sediments moving in water and accumulated sediments at the bottom scatter or absorb sunlight in water and disrupt benthic macro-invertebrates. Small particles as fine sediments of two types (cohesive and non-cohesive) affect water quality as well as engineering structures such as channels and ponds. Turbidity is a principal physical characteristic of water and the optical property expression that enhances light scatter and absorption by particles and molecules rather than transmission in straight lines through a water sample (USEPA., 1999).

A few studies have addressed the prediction of fine sediment transport (Mitchell et al., 2003), stratification and fine sediment transport mechanisms (Mitchell et al., 2006),

University of Malaya

velocity, salinity and suspended solid concentration in a turbidity maximum shallow tidal channel (Mitchell et al., 2008) and the impact of fine sediment accumulation on benthic macro invertebrates (Harrison et al., 2007). All studies have attempted to demonstrate the impact of fine sediments on water life.

Among the major problems with retention structures is siltation. The conversion of catchment areas to agriculture regions besides urbanization under rapid development negatively affects water quality and quantity. The health of aquatic ecosystems is dependent upon the physical habitats and can only be maintained if the ecosystems are protected from degradation (Harrison et al., 2007). To find a solution to this problem, surveying the foundations of programs is essential. Therefore, investigating fine sediment movement and hydrodynamic behavior in retention reservoirs may facilitate better management and maintenance quality to avoid polluted or dead ponds.

1.3 Study Objectives

In this study, emphasis is on fine sediment movement in retention structures to explore fine sediment transport in water using Particle Image Velocimetry (PIV). Primary tests on particle size distribution using laser diffraction (LDPS) and scanning electron microscopy (SEM) to categorize fine sediment size and shape along with rheometry are required to achieve superior visualization of fine sediment characteristics, which have a key role in siltation and sedimentation. The Particle Image Velocimetry (PIV) method assists researchers to capture better and closer images of fluid movement. A camera is used in PIV to record images of the studied areas and reproduce bright images of the fluid mechanism. The main study objectives are as follows:

- To investigate the physical properties of fine sediment using SEM and LDPA
- To explore the rheological and hydrodynamic behavior of fine sediment

University of Malaya

- To evaluate the effect of hydraulic parameters on collecting efficiency and settling velocity

The goal of this study is to understand the physics and basic dynamics that govern fine sediment dispersion and accumulation by utilizing PIV in a settling tank. Moreover, the mechanism of fine sediment transport in retention structures is described through a laboratory technique, and fine sediment particle size and texture are studied. The study indicates there is a significant correlation between flow rate and fine particle settling, as well as fine sediment characteristics and water depth for fine particle settling. The hydrodynamic behavior and characteristics of fine sediment are investigated using Particle Image Velocimetry.

1.4 Scope of the Study

The literature review is divided into two parts. The first section describes fine sediment characteristics, fine sediment influence on water habitats and related research on fine sediment in terms of fine sediment, and sediment transport and mechanisms. The second section expands on the methods employed in this study to explore fine sediment properties; the methods are Particle Size Distribution, Rheology and Particle Image Velocimetry. As the main goal of the study is to demonstrate fine sediment settling and movement in water, this section represents an evaluation of the relations between the selected methods and the main subject.

A literature of existing research proves that particle image velocimetry is a suitable assay for obtaining a schematic of water flow velocity (Adrian, 1991; Kuok & Chiu, 2013; Lindken & Merzkirch, 2002; Prasad & Jensen, 1995; Weitbrecht et al., 2004). However, fine sediment transport in retention structures has not yet been evaluated using particle image velocimetry. In the current study, the intent is to investigate the nature of the

University of Malaya

impact of water flow rate on fine sediment settling at various depths. To generate this relation, some primary objects, i.e. seeding particles are utilized. Because testing the hydrodynamics of fine sediment in muddy water using PIV is impossible (. Raffel et al., 2007), tracer particle samples with the same characteristics as fine sediments are required. Hence, the sediment basin is fed with seeding particles to observe the displacement of fine sediments in flow. In order to avoid excessive background noise and larger or smaller particles that would decrease the accuracy, using identical particle seed sizes is desired. Selecting an optimal seeding particle diameter is also essential to prohibit further errors and noise (high signal-to-noise ratio) during testing (Hadad, 2013). Therefore, the particle size distribution and the particles' rheological properties enable obtaining new knowledge and relations of the selected fine sediment series with siltation and sedimentation so as to design appropriate seed particles with specifications similar to those in nature. Specific particle geometric features such as size and shape influence the forces between particles and fluid (Adrian & Westerweel, 2011). Therefore, choosing suitable seeding requires several conditions to be fulfilled, as the particles' density should be similar to the fluid density to ensure buoyancy also affects the particles' ability to pursue the flow (Hadad, 2013). In liquid flow, the particle tracers are added to the liquid to obtain a homogenized fluid, after which the information is collected (Adrian & Westerweel, 2011). As observed when using a digital PIV system in liquid flow condition, the fluorescent particles scatter the laser light clearly, yielding higher image resolution (Raffel et al., 2007). Flow visualization with PIV involves seeding the fluid with particles and then measuring their movement over a particular period of time. Subsequent to data acquisition, tracer seed identification and tracking are performed (Hassan et al., 1992). This study is carried out under laminar flow, thus facilitating easier tracking of tracer particles. The seed displacement during flowing conditions is examined and the result analysis is processed in Dantec PIV software. To evaluate the PIV results, different cross correlation and auto

University of Malaya

correlation methods are applied, then based on the study objective, other methods are expanded (Yang et al., 2011).

Overall, this study presents fine sediment settling in a pond along with a comparison of the results from this research. Graph outcomes corroborate the foundation of this study.

1.5 Significance of the Study

With the ever-increasing demand for high water quality throughout the world, direct outlooks on problems such as siltation and proposing further solutions are of interest. PIV is a measurement tool used to describe the fluid mechanism in flows with visualization difficulties. Therefore, it is a novel technique for studying the hydrodynamic behavior of fine sediment with direct access. Hence, the findings of study clarify the various aspects of fine sediment mechanism behavior, which could provide significant insight with regard to producing clear water with fewer suspended particles. The study derives a new correlation between the flow rate and fine particle transport in retention structures under different hydraulic conditions. The present study may be useful by introducing interesting new insight for understanding hydrological processes and utilizing retentions to boost storm water management levels in future.

University of Malaya

CHAPTER 2: LITERATURE REVIEW

Suspended solids are known as a water pollutant factor and role as a major cause of water pollution in many countries. By decreasing the size of solid particles and depth of water more murky water was detected. In this chapter the study will discuss about the water pollution and water quality in the environment. Furthermore, the retention structure under sedimentation is been discussed. Therefore, pursuing the different aspect of fine particles could assist in solving the issue. Thus, the study is focused on the different aspect of fine particles movement and transport in flow. The sedimentation process of fine particles in tank and reduction of turbidity are debated under effective condition. By arguing about the different aspect of fine sediments, the background and principal basics of selected methods to achieve the objective of the study is discussed which are particle size distribution, rheology, and particle image velocimetry.

2.1 Water Pollution

Water pollution is commonly defined as any chemical, physical or biological change in the quality of water that causes a harmful effect on species which inhabit or consume it. When humans drink polluted water it often has serious affects on their health consequences. Water pollution can also make water incompatible for the required use (Lenntech, 2011).

In Yemen, which is ranked as one of the top five countries with water scarcity issues, the Minister of Water noted the main source of water contamination is due to two common factors - direct and indirect.

Direct sources is interred in urban water supplies that is contained sewage outfalls from refineries, factories and waste treatment plants etc. that release toxic solutions directly into our water supplies. Indirect sources include pollutants that go through the water

University of Malaya

recourses through soil/groundwater systems and the atmosphere via rain water (YemenWater, 2013). The pollutants that are produced by soil and ground water are born from human agricultural practices which use fertilizers, pesticides etc. and improper disposal of industrial waste. Humans have also changed the quality of water by introducing atmospheric pollutants to the air such as gaseous emissions from automobiles, factories and even bakeries. Such contamination can be generally classified into organic, inorganic, radioactive and acid/base (Hawai'I, 2012).

In a natural habitat, rainfall is absorbed by meadows and forests with little to no runoff. Therefore nutrients are absorbed directly by plants, and water catchments such as streams and ponds provide clean, fresh water to wildlife. Meanwhile, in an urban setting, fields of grass and groves of trees are replaced by flat pavements, poorly managed watersheds, and obstructed dams. Buildings and roads are built up, and natural habitats are destroyed or significantly reduced. Storm water drains are constructed and can easily become blocked with litter and debris causing more unnecessary water pollution (Nielsen, 2012a).

There are many factors that cause sediment pollution such as rainfall, erosion (30% is natural, 70% is created by humans), soil content, melting snow, slope of land and farmland (Nielsen, 2012b). For example, after a large rain storm, particles from soil and rock erode into land surfaces and waterways which is then carried by wind and precipitation. These particles can carry anything from excess nutrients like phosphorus to endocrine disrupters. This causes many serious problems such as endangering fresh water supplies and endangering large fish communities. The sediment in the water can limit the amount of sunlight into streams and rivers which is essential to fish and plant life. This results in changes in feeding habits and decreases the overall effectiveness of water sources (Basualto et al., 2006).

The most common and serious form of effluence is sediment runoff which causes suspended materials to cloud the clarity of water. High turbidity can have detrimental

University of Malaya

effects on phytoplankton productivity because of the reduced passage of sunlight through the water. If the suspended load has high organic carbon content, the biochemical oxygen demand will be raised, and conversely the dissolved oxygen levels will decrease. Another concern is the impact of human intervention such as farming and agricultural practices that result in harmful fertilisers and pesticides entering into our waterways.

Water pollution is a major concern that is high on the agenda for global communities to prevent and solve. As a result, there are several active projects and environmental bodies across the world that are analysing the impact of water pollution on our ecosystem (Danielle, 2010).

Research shows Malaysia has serious water pollution problems which negatively impact on the sustainability of water resources. The cost of treatment is high and some water contamination issues cannot be treated, thereby significantly reducing the availability of clean water supplies to the community (shaFAO, 2012).

2.2 Water Quality

Water quality is comprised of chemical, physical, and biological components that are affected in many ways, often caused by nature's own patterns. The seasons and physical geographical changes to our planet can impact the water quality of rivers and lakes, even where there is no pollution present.

A water quality index is a standard measure used to determine water quality levels. The overall water quality at a certain location and time based on several parameters is express by a grade by water quality measurement. The obtained results from water quality index (WQI) tests is shown by Q-value. The purpose of this index is to transpose and accurately compare different sources of water data into information that is consistent and useable(R. M. Brown et al., 1970).

University of Malaya

Table 2.1 : Interim National Water Quality Standards for Malaysia(National Hydraulic Research Institute of Malaysia (NAHRIM), 2012).

Classes							
Parameters	Unit	I	IIA	IIB	III	IV	V
Ammoniacal Nitrogen	mg/l	0.1	0.3	0.3	0.9	2.7	>2.7
BOD	mg/l	1	3	3	6	12	>12
COD	mg/l	10	25	25	50	100	>100
DO	mg/l	7	5-7	5-7	3-5	< 3	< 1
Elec* Conductivity	Umhos.cm	1000	1000	-	-	6000	-
PH	mg/l	6.5-8.5	6-9	6-9	5-9	5-9	-
Color	TCU	15	50	50	-	-	-
Odor		N	N	N	-	-	-
Floatables		N	N	N	-	-	-
Turbidity	NTU	5	50	50	-	-	-
Total Suspended Solid	mg/l	25	50	50	150	300	300
Total Dissolved Solid	mg/l	500	1000	-	-	4000	-
Temperature	^{0}C	-	normal	normal	normal	-	-
Taste		N	N	N	-	-	-
Salinity	%	0.5	1	-	-	2	-
Faecal Coliform**	counts/100 ml	10	100	400	5000(20000A)	5000(20000A)	-
Total Coliform	counts/100 ml	100	5000	5000	50000	50000	>50000

Notes:

N: No visible floatable materials or debris or No objectionable odour, or No objectionable taste

*: Related parameters, only one recommended for use

**: Geometric mean

A: maximum not to be exceeded

The other form of division, divided water to different classes that uses in different uses which are explained in Table 2.2.

University of Malaya

Table 2.2 : Classification of water (National Hydraulic Research Institute of Malaysia (NAHRIM), 2012)

Class	Water Supply	Aquatic Species
I	conservation of natural environment(practically no treatment necessary)	very sensitive aquatic species
IIA	standard treatment requires	sensitive aquatic species
IIB	recreational use with body contact	
III	extensive treatment required	common, of economic value, and tolerant species livestock drinking
IV	Irrigation	

Today global efforts have been made to maintain and protect clean water supplies by creating a standard safety level for water. The international community has focused on water quality as a first and major concern for living in a sustainable and healthy environment. These programs try to protect and improve water quality. Protecting rivers, lakes, streams and groundwater quality keeps these waters safe for a number of important needs such as consumption, marine habitant, recreation and irrigation. This is accomplished by developing and implementing water quality standards and clean water plans, regulating sewage treatment systems and industrial waste, collecting and evaluating water quality data, providing grants and technical assistance to reduce non-point pollution sources and providing loans to communities to build treatment facilities (New Mexico Environment Department, 2014).

Urbanization is one main factor that has affected water quality through the development of cities that removed the natural ecosystem and introduced pollutants into streams, lakes and rivers (Novotny, 2003). These pollutants can harm water life and drinking water supplies and include sediment, chemicals, heavy metals and oil from motor vehicles as

University of Malaya

well as pesticides used for gardens. The other fact in rise of temperature as a water pollution is the provided by runoff from parking lots and rooftops. Since the current research aimed to demonstrate the movement of fine particles thus the two factors that have higher influence on this phenomenon regarding the water quality such as the turbidity and suspended solids are selected to explain.

2.2.1 Turbidity

The measurement of turbidity indicates the waters clarity and quality. Excessive turbidity in drinking water is caused by water discharge, runoff from watersheds, algae or aquatic weeds, humic acids, high iron concentrations and air bubbles from treatment processes.

Murky water increases the water temperature where suspended particles have efficient role in enhancement of sunlight absorption. There the water gets warm and that the reason to associate with increased water temperature. With increased turbidity, water clarity is reduced resulting in a decrease in photosynthesis as less sunlight is able to penetrate the water. By decrease of water clarity more displeases of the water aesthetically, therefore it reduces the quality of water for different water uses.

Turbidity of water can be caused by silt and clay deposits as a result of soil erosion, urban runoff, bottom dwelling organisms (e.g catfish) up the sediment on the bottom of the lakes, organic matter, treatment effluent of sewage, and particulates (Terrell & Perfetti, 1996).

Nephelometric Turbidity Units (NTU) defines the turbidity measurement by an instrument called a turbidimeter. Turbidimeters with scattered-light detectors located at 90 degrees to the incident light beam are called nephelometers. This instrument measures the amount of light scattering that occurs within a given water sample by shining a bright light on one side of the sample and measuring the amount that is redirected to the detector located 90 degrees to the incident light (direction of the incoming light). Scattering from

University of Malaya

the water sample is measured relative to the amount of light scattered by a reference solution (a solution that will cause a known amount of light scattering). The scattering of light increases as the amount of suspended materials in the water increases (Wilson, 2010).

The surface water turbidity is generally determined between 1 NTU and 50 NTU. Turbidity is higher than above average after heavy rain by increase of the water levels. Although, where suspended particles have settled in still water we note turbidity can be lower than expected. The standard scale of turbidity for drinking water is measured from 0.5 NTU to 1.0 NTU, thus turbidity higher than 5 NTU demonstrates the visibly turbid water (Wilson, 2010).

Significant research has been done to examine the relationship between temperatures, turbidity and suspended solid. The University of Wisconsin 2004 studied the relationship between changing land use and water quality in Baird Creek. Results show sharp increases in turbidity were closely associated with runoff events and changes in stream discharge. In addition, linear analysis indicated a strong relationship between sediment concentrations and turbidity readings in Baird Creek. The relationship between sediment concentrations and turbidity significantly differed between the upstream and downstream sampling sites (Fink, 2005). Prestlglacomo (Prestlglacomo et al., 2007) worked on the implementation of an automated stream monitoring unit that features four probe-based turbidity (T) measurements per hour and the capability to collect frequent (e.g. hourly) samples for Total Suspended Solids (TSS) analysis during runoff events(Figure 2.1). This unit aimed to assess the dynamics of T, TSS and corresponding loads in sediment-rich Onondaga Creek. Turbidity was demonstrated to be a better predictor of TSS than Q (discharge), supporting the use of the frequent field Tn measurements to estimate TSSL (Turbidity Suspended Solid Level). During the year of intensive monitoring, 65% of the TSSL was delivered during the six largest runoff events that represented 18% of the

University of Malaya

annual flow. The high T levels and extensive in-stream deposits have negatively impacted the stream's biota and the aesthetics of a downstream harbor.

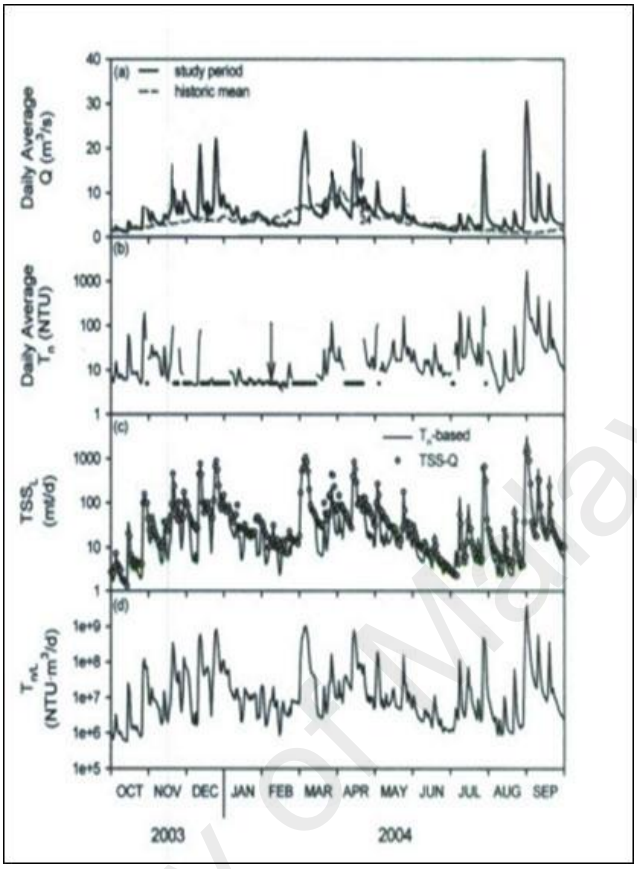

Figure 2.1 : Time series of primary study site on Onondaga Creek for water year 2004: (a) flow (Q), with runoff events labeled and long term average for comparison, (b) daily average turbidity (Tn) data intervals identified, (c) comparison of daily total suspended sediment loading (TSSL) based on Tn monitoring versus TSS-Q relationship, and (d) daily turbidity load (TA)(Adopted-Prestlglacomo et al., 2007)

Studies of fine sediment show swelled fine sediment in water can have an effect on turbidity. As turbidity reduces light penetration into the euphotic zone, it causes a reduced rate of photosynthetic production of oxygen (Mitchell et al., 2003; Rex & Petticrew, 2011; Tu et al., 2001; Woo et al., 1986). Oxygen production by rooted aquatic plants may be impacted by loss of habitat within the euphotic zone. Therefore, the subsequent disappearance of submerged aquatic vegetation can radically lower oxygen levels (Schubel, 1977).

University of Malaya

2.2.2 Total Suspended Solid

Total suspended solid (TSS) determines the solid materials dissolved in water. The dissolved materials could include silt, some organic materials and a wide range of other things from nutrients to toxic materials. Aquatic habitats need to have a constant level of minerals in the water. Any changes in this level could limit growth and lead to the death of many aquatic life forms.

Solids in water act in two forms- suspended and dissolved. Suspended solids include stirred up bottom sediment that could include of silt, sewage treatment effluent or decaying plant matter, whereas soluble salts that yield ions are involved in dissolved solids in freshwater.

Many forms of aquatic life are affected by high levels of Total Dissolved Solids (TDS), especially due to dissolved salts. High concentrations of dissolved solids such as water salinity which can dehydrate the skin of animals can add a laxative effect to water then it causes to decrease the taste and quality of water with unpleasant mineral (Dowd, 2010). The concentration of suspended solids is calculated as follows:

Suspended Solid residue (mg/L) = [(Weight (mg) of filter + residue) – (Weight (mg) of filter alone (mg)] / Volume of sample filtered (L) (2.1)

TDS levels have different levels in various water sources where the TDS range reaches to 50 to 250 mg/L. TDS may be as high as 500 mg/L in areas of especially hard water or high salinity. This level tends to be 25 to 500 mg/L in drinking water. Normally, it has conductivity of 0.5 to 1.5 mg/L in the fresh distilled water (Al-Mutairi et al., 2004; Longe & Balogun, 2010; Sargaonkar & Deshpande, 2003).

Countries with year round rain such as Malaysia need to consider this natural factor. Management programs are being introduced to keep pollutants away from water

University of Malaya

resources, chiefly suspended solids. They aim to identify and measure the rainfall and resultant pollutant in rivers to improve water quality. Malaysia in particular is impacted by ponds and lakes which collect water and create suspended solids that need to be directed to a safe place. The Department of Irrigation and Drainage (Shamsad et al., 2010) in Malaysia is charged with defining the best management plan for the development of resources, flood control and storm water management. Therefore ponds and lakes play a critical role in creating a natural and healthy ecosystem in the water supply.

2.3 Retention Structure

There are many important water resources in Malaysia such as reservoirs and lakes. The quality of water resources body have been significantly under effect of the rapid pace of development in the lake catchment areas (Sharip & Zakaria, 2007). Ponds are one of the most effective tools at providing channel protection and pollutant removal in urban streams (Swann, 2001). Essentially, retention ponds provide water quality and quantity control (EPA, 2001). Two common classifications of retaining ponds are either "wet" or "dry." Wet ponds, known as retention ponds, continually have a pool of water in them called dead storage. Dry ponds, or detention ponds, do not have dead storage and dry out between storms (EPA, 2001).

Information available on the retention structures in Malaysia is very confined. No retention structure has been investigated broadly on an integrated approach to enable the development of a proper database on the lakes and reservoirs of Malaysia (National Hydraulic Research Institute of Malaysia NAHRIM, 2012).

Lakes and reservoirs are storage basins for municipal and industrial water supply, agriculture and hydropower. The construction of reservoirs in some cases is for balance the different flow of water during wet and dry seasons and act as flood control detention

University of Malaya

storage units. Common problems in lakes and reservoirs include weed infestation, sedimentation and eutrophication.

A major problem is eutrophication for ponds in Malaysia. Rapid construction of cities through conversion of catchment areas to agriculture and increased urbanization has had a negative impact on the quantity and quality of water (Sharip & Zakaria, 2007).The health of the aquatic ecosystems is dependent upon its physical habitat and can only be maintained if the ecosystem is protected from degradation (Harrison et al., 2007).

Although man-made, the pond has two principal problems. Ponds continuously accumulate pollution as there is no mechanism to remove the pollution permanently. Only biomass or removal of sediment could help to keep the retention structure alive. Where there is a high accumulation of biomass and sediment in water, oxygen and nutrients are consumed at a higher rate, therefore there is insufficient surface for other life forms to develop and the pond will die. The other problem is weed control in the pond as they are typically shallow around the perimeter. Therefore the weeds spread. The control equipment or solution should be placed close to where the rainwater falls so as to collect the runoff. There are also other management methods that treat the surface water in different level of treatment such as using filtration, biological degradation, adsorption and natural processes of sedimentation. The surface water management drain addresses the runoff quantity and quality at all stages of the drainage system (CIRIA., 2000). Bio-Ecological Drainage System (BIOECODS) is a pilot project in Malaysia (Prestlglacomo et al., 2007) that applies the concept of the surface management train (Ab. Ghani et al., 2004). The components of BIOECODS include ecological swales (source control), dry ponds and wet ponds (site control) and detention ponds (regional control). Nowadays the management of drainage systems is carried out through data collection and the comparison of different areas and the conditions for discovering the source of the pollution and the methods for reducing it.

University of Malaya

2.4 Sediment and Sedimentation

Sedimentation is the process where a state of suspension or solution in a fluid deposit solid material, usually air or water (Mackay, 2001). Materials from glacial ice and those materials collected under the gravity force, as in talus deposits, or accumulations of rock debris at the base of cliffs can be denominated as deposits (Britannica, 1964). The sedimentation process is achieved when the particles will no longer remain in suspension by decreasing the velocity of water in relation to bottom. Gravity removes the particles from the flow since velocity does not carry the particles (World Bank, 2012).

In geology, sedimentation means the effect from the formation of sedimentary rock which results in deposits of sediment forming. Many studies have noted that sedimentation depends on the field and the transport of fluid particles by means of true bed load transport or by saltation which follows after sedimentation. Moreover, it could refer to end of settling, when the suspended solids settle down in the liquid particles. Even more, the separation of particles ranging in various sizes from dust pollen, single molecules such as proteins and peptides to large rocks which are suspended in water is referred to as sedimentation. In biology, sedimentation helps in separation of cells from cultured medium.

The size, charge and type of particles to be removed have a significant effect on the sedimentation. Depending on the density of particles, some can be eliminated (e.g. silt and clay are removed easily). The particle shape also influences in its settling behaviors. For example, a particle that has ragged or irregular edges will sink slower than a spherical particle (Cammem, 1982).

The temperature of water is a significant parameter in the sedimentation basin- when it decreases; the rate of settling becomes slower. Moreover, the density of the solids varies in the concentration of solids and temperature of the water. Major reasons for the rapid

University of Malaya

rate of sedimentation is the increase in land development activities upstream of waters sources which contributes substantially to filling the bottom lakes with sediment within a 60 year period (Ayub et al., 2005).

Sediment is defined as the organic and inorganic flow of materials or solid fragments derived from the weathering processes of sand, pebbles, silt, mud and loess (fine-grained soil) (Kamarudin et al., 2009). These fragments can be carried by wind, ice or other naturally occurring agents. Sediments can also be defined as the materials which settle at the bottom of rivers such as silt (Ekhwan et al., 2009).

The size of sediments is different. The concentration of silt or clay in sediment determines the size. Nutrients are carried in water by sediment, therefore has an important impact on water, plants and fish. It is important that the sediment is moved through the water flow therefore the flow rate speed influences its transportation and breadth of reach. An increase in fine sediment can change the suitability of the substrate for some taxa, increase macro-invertebrate drift and affect respiration and feeding activities (Harrison, 2007).

Sediment is categorized based on the size and shape (Table 2.3), which include (in order of decreasing size)- boulders (> 256 mm), cobble (256-64 mm), pebble (64-2 mm), sand (2-1/16 mm), silt (1/16-1/256 mm) and clay (< 1/256 mm). The modifiers in decreasing size order are- very coarse, coarse, medium, fine and very fine. For example, sand is sediment that ranges in size from 2 millimeters to 1/16 mm. Very coarse sand ranges from 2 mm to 1 mm; coarse from 1 mm to 1/2 mm; medium from 1/2 mm to 1/4 mm; fine from 1/4 mm to 1/8 mm; and very fine from 1/8 mm to 1/16 mm (Wikipedia, 2012).

The load of silt and clay, which have a diameter smaller than 0.0625 mm is called sediment load (siltation). The fine sediment load includes the electro-chemically interacting clay particles which affect the fluid properties and settling velocity of larger particles (Woo et al., 1986). "Wash-load" and "Fine Sediment Load" are not synonymous.

University of Malaya

Loading of silt and clay is fine sediment load and wash-load refers to the part of the total load that is washed through the channel and not found in significant quantities in the bed. The transportation of material is explained by the sediment load, and the term sediment discharge assigns the rate of transport of the sediment load (Woo et al., 1986).

The sediment loads can have an effect on the shawling of estuaries, by enhancement of turbidity level makes the limitation in light penetration and photosynthesis, change in habitants, for example the increasing in mangroves distributed. Meanwhile the strong chemical bonds in the soil create strong vegetation growth which prevents erosion as they reduce run-offs and provide a dampening effect to the kinetic energy of rainfall on soil surfaces (Ekhwan et al., 2009), increased organic matter degradation (Cooke et al., 2012).

Table 2.3 : Graph of particle size (grain size)(Wikipedia, 2012)

φ scale	Size range (Lucas et al., 2010)	Size range (inches)	Aggregate class (Wentworth)	Other names
< -8	> 256 mm	> 10.1 in	Boulder	
< -8	> 256 mm	2.5–10.1 in	Cobble	Pebble
-6 to -8	64–256 mm	1.26–2.5 in	Very.coarse.gravel	Pebble
-5 to -6	32–64 mm	0.63–1.26 in	Coarse gravel	Pebble
-4 to -5	16–32 mm	0.31–0.63 in	Medium gravel	Pebble
-3 to -4	8–16 mm	0.157–0.31 in	Fine gravel	Granule
-2 to -3	4–8 mm	0.079–0.157 in	Very fine gravel	
-1 to -2	2–4 mm	0.039–0.079 in	Very coarse sand	
0 to -1	1–2 mm		Coarse sand	
1to 0	0.5–1 mm	0.020–0.039 in	Medium sand	
2 to 1	0.25–0.5 mm	0.010–0.020 in	Fine sand	
3 to 2	125–250 µm	0.0049–0.010 in	Very fine sand	
4 to 3	62.5–125 µm	0.0025–0.0049 in	Silt	Mud
8 to 4	3.9–62.5 µm	0.00015–0.0025 in		Mud
> 8	< 3.9 µm	< 0.00015 in	Clay	Mud
>10	< 1 µm <	0.000039 in	Colloid	

University of Malaya

Additionally, a series of laboratory experiments was conducted in order to examine how sediment grain size and volume affects the mobility of bed material in gravel bed channels (Venditti et al., 2010). Scientist noted the amount of sediment a river can transport changes over time. Hydrologists take measurements and samples as the stream flow goes up and down during a storm (Kinnaman et al., 2012).

A part of suspended sediment is fine sediment that has two types- cohesive and non-cohesive. These kinds of sediment create problems in two ways, siltation of engineering constructions such as harbors and channels, and environmental mixing and dispersion of contaminants that often contain heavy metals and pesticides as a result of their cohesive nature. Both require an understanding of physical processes relating to their transport, deposition, and resuspension (erosion), followed by parameterization of those processes in predictive models that can be used for practical engineering and environmental applications (Tu J. et al., 2001).

The impact of fine sediment in nature is studied in the prediction of fine sediment transport in the turbidity maximum (Mitchell et al., 2003), stratification and fine sediment transport mechanisms (Mitchell et al., 2006), velocity, salinity and suspended solids concentration in a shallow tidal channel (Mitchell et al., 2008) and impact of fine sediment accumulation on benthic macro invertebrates (Harrison et al., 2008).

The heavy metals included in sediments as a contaminant an interesting area of study in relation to sedimentation. Sediment carries heavy metals in estuarine areas, where freshwater encounters seawater which are characterized by a lateral variation in salinity and can be represented as a transfer box for the sediment between land and the open ocean (Meade, 1972). Contamination caused by heavy metals affects both ocean waters- those of the continental shelf and the coastal zone where, besides having a longer residence time, metal concentrations are higher due to input and transport by river runoff and the

University of Malaya

proximity to industrial and urban zones (Alagarsamy, 2006; Karageorgis et al., 1998). Other studies show estuaries were moderately enriched by Pb, while the Cu occurs naturally and not greatly caused by anthropogenic and human activities. Therefore, human activity polluted waters (Yunus et al., 2010).

2.4.1 Sediment as Physical Pollutant

Since researchers have estimated different values in terms of sediment transport, it has shown the difficulty in finding a reliable value that explain for discharge and sediment concentration and in different countries. Therefore some hypotheses are created, and the accelerated erosion opposing effects due to human activities such as road construction, deforestation, poor agricultural practices is related the construction of dams which results in sediment storage relative (Milliman & Syvitski, 1992). Further, Milliman and Syvitski (1992) in the mid-20th century noted that human activity caused an increase of sediment transfer from rivers to the ocean by 30% southern Asia. The high relief on islands of Oceania are associated with almost 50% erosion of the global total comes. As a physical pollutant, sediment affects on income water in the following principal ways.

The physical disruption of the hydraulic characteristics of the channel is created by high levels of sedimentation in rivers. It can decrease the depth of the channel and rivers and directly increase flooding because of the reduced capacity of the river channel to efficiently route water through the drainage basin.

2.4.2 Sediment as Chemical Pollutant

The amount of particulate organic carbon associated with the sediment, and the particle size of sediment attribute the role of sediment in chemical pollution. The sediment chemically active fraction is commonly cited as the particle which is finer than 63 μm (silt + clay) fraction. Particle size is of primary importance due to the wide surface area of very fine particles for phosphorus and metals. Ionic exchange sites of clay particles

University of Malaya

with the iron and manganese coatings highly attract phosphorus and metals that commonly occur on these fine particles. The several constants, toxic organic contaminants and bio-accumulating, especially chlorinated compounds including many pesticides are strongly associated with transportation of organic carbon sediment as part of the sediment load in rivers.

An organic chemical is described by its octanol-water partitioning coefficient form the affinity for particulate matter (Krzaklewski et al., 2004). This partitioning coefficient is well known as the basis for predicting the organic chemicals environmental fate and for most organic chemicals. Chemicals can have two KOW (The octanol/water partition coefficient) values which with high values are described as "hydrophobic" and tend to be associated with particulates, whereas those with low values are readily soluble. Due to the very low solubility of the chlorinated compounds such as DDT (Chlorophenothan) and other chlorinated pesticides which are known as very hydrophobic thus, analyze of them in water samples are not easy. Organic chemicals transport as part of the sediment, and the most important component of the sediment load appears to be the particulate organic carbon fraction. The association of partitioning coefficient with the organic carbon fraction (KOC) is further refined by scientists.

The concentration of sediment specially <63 mm fraction is another important variable in the water column. Even highly hydrophobic chemicals will be found in trace levels in soluble form. Where the suspended load is very small, the amount of water is so large relative to the amount of sediment, thus the bulk of chemical load may be in the soluble fraction.

By microbial degradation that occurs during sediment transport in rivers and in deposited sediment complicate the transport and destiny of sediment-associated organic chemicals dissimilar to phosphorus and metals (Ongley, 1996). However, the role of sediment in the

University of Malaya

transportation and agricultural chemicals fate, both for pesticides, metals, and nutrients is not deniable and must be taken into account when monitoring these chemicals, and should be used during watershed level and applying models. Therefore, it have proven the efficiency of models using the fugacity in predicting the fate of contaminants and environmental pathways (Mackay & Paterson, 1991).

Sediment with organic chemical contents enters into the food chain in a variety of ways. Fine sediment (especially the carbon fraction) is the food provided for benthic organisms which, in turn, are the food source for high organisms eventually, toxic compounds bio-accumulate in fish and other top predators. Hence, the runoff and erosion process that transport off the land are include pesticides which accumulate in top predators including man (FAO, 2012).

2.5 Decay of Sediment

The study of the behavior of sediments after sinking in water is essential. The way in which each particle settles to the water bed depends on its weight, shape and size. The process of sedimentation in water and the dynamic activity which happens after is significant. An analysis in the changes of sediment properties in representative cores must be preceded by an identification of sedimentation conditions as this considerably influences the spatial diversity of sediment successions.

The process of sedimentation (Figure 2.2) in water begins with the source then the deposits from air, after that re-suspension from sediment which leads to first decay at the end outflow from the lake. In the beginning, the particles deposit in the water, then diffuse which creates decay(Kilic et al., 2005).

A variety of factors of natural and anthropogenic origin are influenced the rate and character of accumulated sediments. The rate or type of sediment is measured depended

University of Malaya

on sediment erosion, transportation and accumulation zones. By using radio isotopic methods and radio metric dating of the youngest sediments (Murray & Olley, 2002), it can estimate the value of these differences and compute the age of parameters based on metals in sediment.

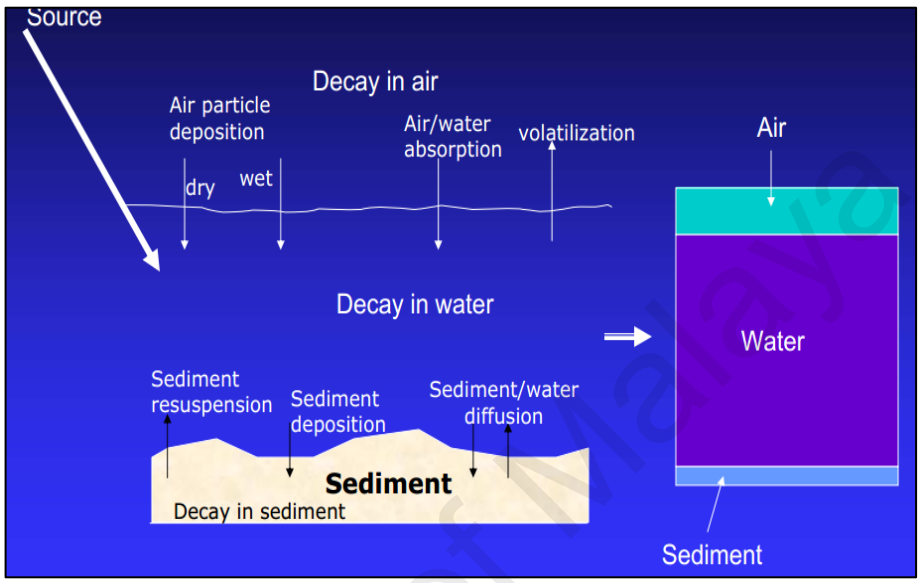

Figure 2.2 : Natural process in the lake(Kilic et al., 2005)

Organic matters like microorganisms play a key role in the decay of sediment. Alison R. et al 2012 assessed varying bacteria and water quality standards in surface water through investigation of decaying E.coli rates and its influence on sediments and associated organic matter.

Research in sediment deposits has proven that when in contact with the water column, it decreases the bacteria decay rate, and therefore should be utilized when designing storm water treatment measures. In addition, it has been found that high levels of organic carbon in sediments temporarily amplify bacteria concentrations in the water column. This can solve the issue of high effluent of bacterial concentrates in the detention basins and constructed wetlands, therefore additional analysis of sediment, organic carbon and water column depth should be conducted (Alison et al., 2012).

University of Malaya

Furthermore, other studies have proven the increase in temperature resulted in an increase in decay rate for all organisms in overlying water, and to a lesser extent in the surface sediment layer. Thus the concentration of faecal coliforms in sediments is higher than the water layer.

Therefore in the event of re-suspension of sediment in the water column, the sediment acts as a reservoir hence this phenomenon can increase exposure risk.

$$k = \alpha e^{\beta T} \qquad (2.2)$$

Where, k = decay rate and T = temperature (^{0}C)

Values for α and β for sediment is -0.05 and 0.11 respectively (Craig et al., 2002).

To determine the rate of decay, the amount of area, deposition and re-suspension of sediment and wet or dry deposition rate is required.

$$V_s Z_{bs} \frac{d_{Fs}}{d_t} = (Q_{dep}\, Z_p + K_{sw}\, A_s\, Z_w)\, F_w - (\, k_s V_s Z_s + Q_{res}\, Z_s + K_{sw}\, A_s\, Z_w\,) F_s \qquad (2.3)$$

(Kilic et al., 2005) Where V_s = volume of sediment, Z_{bs} = bulk sediment fugacity capacity, Z_p = particle fugacity, Z_s = sediment fugacity, F_w = water fugacity, F_S = sediment fugacity, Q_{dep} = Particle deposition rate, Q_{res} = Particle resuspension rate, K_{sw} = sediment equilibrium constant, and W_{ate} = Particle fugacity capacity.

2.6 Sediment Transport and Mechanisms

Sediment transport is defined as the displacement of solid particles under gravities force or the fluid movement which contains sediment. Sediment transportation is considered in the fields of geomorphology, environmental engineering, sedimentary geology and civil engineering.

University of Malaya

The sediment transportation is determined by the flow strength that carries sediment in specific parameters such as density, size, shape and volume. Powerful flow of water will raise the lift and drag of the particle causing it to rise, whilst larger or more dense particles will be more likely to fall through the flow (wikipedia).

Gravel, rock and boulders downstream are moved by rolling or sliding along the bottom of the waterbed through the high level of water movement. A series of jumps lead small grains of sand and gravel at the bottom and suspension transports smaller particles of sand, silt and clay which mix in the turbulent water and gives the appearance of muddy water.

To measure the bed load transport, two measuring methods are available- simple mechanical trap-type samplers (collecting the sediment particles transported close to the bed) and the recording of the bed profile as a function of time (bed form tracking)(Van Rijn, 2007).

2.6.1 Types of Sediment Transport

Sediment transport is normally classified into three categories- suspended, bed and wash load. When waves break, sediment particles are mixed with the water due to the turbulence of water flow, therefore, the model is called suspended sediments. The sediments which are transported as suspended sediments are small, with stronger waves it forces bigger particles to be transported, and there will be more concentration in the water. Bed load is a form of sediment transport when particles are dragged by the seabed or in other definitions where pebble and sand move along the stream bed without being permanently suspended in the flowing water. Particles in the bed load are too big to be moved with the flow of water, and too small to be transported by drag force. Sheet flow happens under strong waves or strong current forces which cause sediments on the seabed to move in a thin layer. The difference between sheet flow and bed load is that in bed load

University of Malaya

only bigger particles are transported, whilst in sheet flow a thin layer with both suspended sediment and bed load are driven by a strong current (Myrhaug & Holmedal, 2007).

2.6.2 Fluvial Process

Fluvial process is the physical interaction of flowing water and the natural channels of rivers and streams. Such processes play an essential and noticeable role in the denudation of land surfaces and the transport of rock debris from higher to lower levels. This movement is dependent on the velocity of water, viscosity, density and decay rate of particles (Britannica, 1964). Based on the fluvial process, when the discharge and velocity increase, the amount of sediment being carried by the stream generally rises correspondingly (Pidwirny, 2006).

2.6.2.1 Drainage basin

The basic fluvial system is a drainage basin, the spatial geomorphic area occupied by a river system. The drainage basin is an open system that water initially moves down slope in a thin film named sheet flow, or overland flow. Rills or small-scale downhill grooves are included in the surface runoff which may expand into a stream course in a valley and deeper gullies (Vincent, 2001). The watershed catchment area is a division of a drainage basin at a high ground separating one valley from another and directing sheet-flow. This is termed an inter flume. Patterns of drainage refer to the channels arrangement in an area as measured by the variable rock resistance, hydrology, steepness, variable climate, relief of the land and structural controls imposed by the landscape. There are seven basic drainage patterns generally found in nature- dendritic, trellis, radial, parallel, rectangular, annular, and deranged. Stream channels vary in width and depth. The streams that flow in them vary in velocity and in the sediment load they carry. When all of these factors are increased, it may also increase the discharge (Horton & DeCelles, 2001).

University of Malaya

2.6.3 Coastal Process

The forces that erode, transport and deposit sediment along shorelines is explained as coastal process. The conditions of the coastal environment are determined by the forces of wind, waves, currents and tides. Beaches are composed of sediment in various sizes, from large boulders to fine sand or mud (Davies et al., 2004).

The coastal process is important because of the type of dredge and transportation of contaminated materials which impact the environment. It is scour protection in resist movement, dissipate energy, and relieve pressure (Davies et al., 2004; Komar, 1998; Reading, 2009).

2.7 Fine Sediment

Woo, (2003) defined the load of silts and clays, which have diameters smaller than 0.0625 mm as fine sediment load. In this phenomenon the electro-chemical interation is happened between clay particles which affect the fluid properties and settling velocity of larger particles. Fine sediment could prevent sunlight reaching phytoplankton and plants in the water and therefore destroy life. Therefore investigation of fine sediment transportation is important. There are studies that investigated the parameters affecting transport and rate of fine sediment accumulation (Van Kessel & Blom, 1998; Vermeulen, 2004; Woo et al., 1986; Yu et al., 2013).

There are many sediment transport equation which determine the total load and the most well-known equations are Zeller-Fullerton, Yang, Engelund & Hansen, Ackers & White, Laursen, Tofaletti, Woo-MPM, MPM-Smart and Karim-Kennedy. Each formula was based on unique river conditions.

University of Malaya

2.7.1 Ackers-White Method

In the Ackers-White method, sediment transport is determined based on Bagnold's stream power concept using dimensionless parameters including a mobility number, representative sediment number and sediment transport function. Only a portion of the bed shear stress is effective in moving coarse sediment. The total bed shear stress contributes to the suspended fine sediment transport (Huang, 2007; Valentine et al., 2001). The Ackers-White approach tends to overestimate the fine sand transport.

2.7.2 Karim-Kennedy

The Karim-Kennedy equation (Karageorgis et al., 1998) is defined as a nonlinear multiple regression relationship based on velocity, bed form, sediment size and friction factors for a large data set. They used for large rivers with non-uniform sand/gravel conditions.

The sediment entering the control segment can be (Ismail et al., 2010) from the upstream segment and from tributary inflows. The amount of sediment (q_{su}) entering the control segment during a time interval of Δt can be expressed as follows (Krishnappan, 2000):

$$q_{su} = QC_{i-1}\Delta t + Q_i C_i \Delta t \tag{2.4}$$

Where C_{i-1} is the sediment concentration in the upstream segment, C_t is the concentration of sediment in the tributary inflow to the control segment, and Q_i is the tributary inflow rate (Krishnappan, 2000).

The direction of sediment movement can be varied based on the current flow conditions. When, closer to the inflow, the shear stress of the sediment quantity is lower than upstream. If the shear stress in the control segment is equal to or greater than the upstream segment, then the sediment arriving from the upstream segment would have gone through the deposition process already and would have reached the steady-state concentration. Therefore, this sediment has to be routed straight through the control segment. The

University of Malaya

amount that would deposit in the control segment, can therefore be calculated as (Krishnappan, 2000):

$$q_{su} = (QC_{i-1}\Delta t)f_d + (Q_iC_i\,\Delta t)f_d \qquad if\ \tau_i < \tau_{i-1}$$

$$q_{su} = (Q_iC_i\,\Delta t)f_d \qquad if\ \tau_i > \tau_{i-1} \tag{2.5}$$

Where q_{su} is the amount deposited during the current time step. And the amount remaining in suspension is q_{ss}. f_d shows the fraction of sediment deposited; τ_i is shear stress.

The suspended sediment concentration in the control segment at the end of the current time step is (Krishnappan, 1997):

$$C(i) = {}^{q_{ss} + q_{st}}/_{(Q\Delta t)} \tag{2.6}$$

In the transport of fine sediment, a variety of factors are affected on sedimentation such as water level, wave, and gravitation circulation. Depending on the area that is studied, other parameters like tidal asymmetry, seasonal effect (impact of wind and wave on fine sediment transport) or biological impacts could be important (Estproc, 2003).

There are two different types of sediment- cohesive sediment which is an accumulation of mud with silt, and non- cohesive sediment that is submereged in water until it transports sediment and then settles on the bottom.

University of Malaya

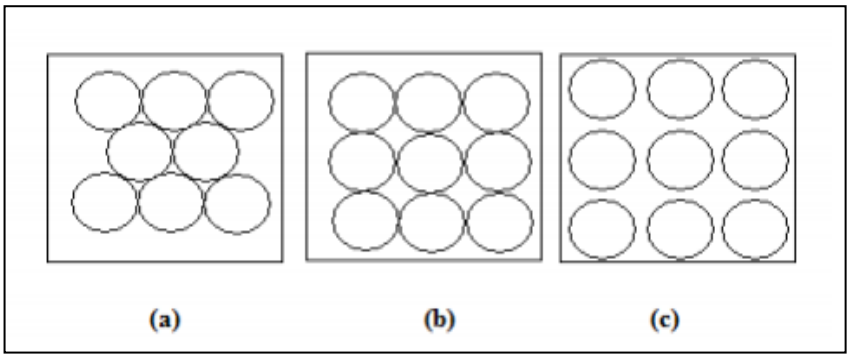

Figure 2.3 : Network structure in a sand bed for different volume fractions of sand.(a) volume fraction less than critical volume content for sand; (b) volume fraction same as critical volume content for sand and (c) volume fraction more than critical volume content for sand (Ahmad et al., 2011)

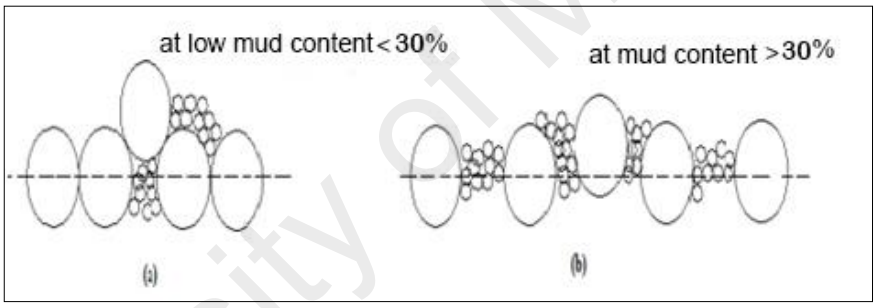

Figure 2.4 : Ideal models for (a) mixture of mud and sand with mud by weight or volume less than 30%; (b) mixtures of mud and sand and with mud content more than 30% (Ahmad et al., 2011)

This model of transport behavior has been reported by researchers such as Mitchener and Torfs 1996 where they suggest the transition is in a range of 3-15% mud content. Houwing, 2000 reported the critical shear stress for erosion is a significant parameter in forecasting the morphological behavior.

The range of size in fine sediment is different in rivers or ponds because of the flow and kinds of solids that carries sediment is different. According to the British Standard test

University of Malaya

sieves, the grain size of fine sand is between the ranges of 0.06 to 2 mm, silt between the ranges of 0.002 to 0.06 mm and finally for clay is less than 0.002 mm.

With large concentrations of fine sediments in suspension, the range of particle sizes in the bed broadens to the extent that the sediment size corresponding to D10 is arbitrarily defined. The shear stress for erosion of natural bed shows the different threshold depending on the composition of the sand, slit, clay and water (Markgraf et al., 2012).

The exchange of sediment particles between the bed and the suspended level creates a lower settling velocity which causes a viscose fluid and the concentration of clay decreases. The sediment transport capacity under those conditions remains very poorly defined (Woo et al., 1986).

For particulate elements, flocculation processes are roughly accounted for by relating the settling velocity Ws to the total suspended sediment concentration in the following manner:

$$Ws = min[W_{max}, max\ (W_{min}, W_1 \times SPM^{W2}\ )] \quad (2.7)$$

W_{max}, W_{min}, and $W_{1,2}$ depend on the type of particles, with the model allowing the simulation of several classes (Le Hir et al., 2001).

The deposition rate is computed from the Krone formulation (Le Hir et al., 2001) but with a very large critical bottom stress for deposition (equal to 10 N m22), which means that deposition is always possible. This is reasonable as erosion of fluffy deposits can occur instantaneously, when turbulence is high enough (Le Hir et al., 2001).

2.8 Turbid Water and Settlement Basin

In wastewater treatment there are some basic definitions which need to be described**.** The first concept is sedimentation which causes the settling of solid particles from suspension

University of Malaya

due to gravity. Clarification refers to a similar action such as flotation and filtration which is the sedimentation tank function in suspended matter removal from the water to provide a clarified runoff. Whereby the settled impurities are concentrated and compacted on the bottom of the tank and in the sludge-collecting hoppers the process of thickening in settlement basins is occurred.

2.8.1 Sedimentation Processes application

The sedimentation process is generally applied in resulted impurities removal from coagulation and flocculation during turbidity and color removal. Processes such as using chemical precipitation to softening of water are also used to remove impurities. In general, solid separation or sedimentation is the first stage in wastewater treatment where 50 to 70 % of the suspended solids are removed from the wastewater thus the BOD is decreased 20 to 45 % in sedimentation together with biological treatment. It should be noted that the lighter particles or organic matters remain in suspension. Absolute knowledge of the principals governing the various forms of sedimentation behavior is important for an efficient operation and design of sedimentation tanks.

2.8.2 Arrangement of Settling Behavior

The diameter and size of a particle may cause different behavior, where this settling velocity can be distinguished based on the concentration of particles in the water column. Therefore, single particles can be separate (sand grains) or flocculent (most biological and organic materials). The classification of settling behavior through the concentration of particles in water (Figure 2.5) is categorized based on the following four classes:

Class I- Infinite settling of distinct particles

Class II- Dilute suspensions of flocculent particles settling

Class III- Zone settling and hindered settling

University of Malaya

Class IV- Compression settling (compaction).

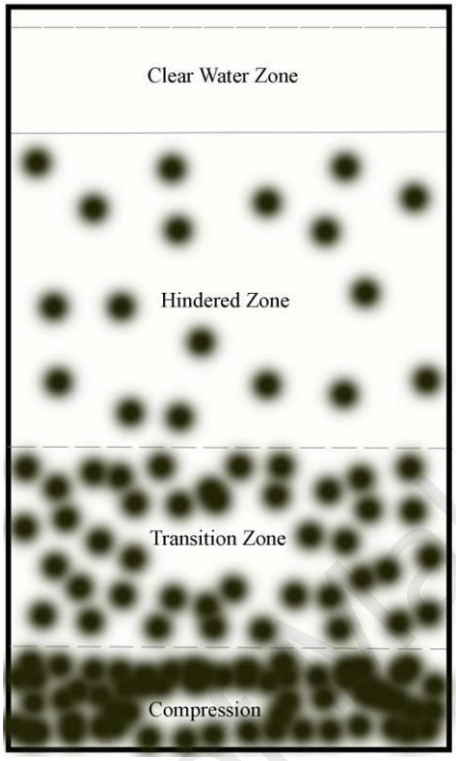

Figure 2.5 : Sketch of sedimentation levels in a settlement tank

2.8.2.1 Sedimentation class I - infinite settling of distinct particles

In clear water zones the settling level of discrete particles is low, in this zone particles settle freely without interaction force between them. During sedimentation, particles move down in a fluid, and it accelerates until the particle's submerged weight is equal to the fluid resistance due to its motion.

Therefore the particle will reach terminal velocity and this particle velocity V_s is achieved based on the weight of particles. Another type of velocity is settling velocity that is evident in sedimentation tanks where the rate of settling velocity for uniform fluid flow and non-flocculent particles is constant throughout the settling time. This is used for studies and designs in settlement basins.

University of Malaya

$$V_s = {(\rho - \rho_l) g d^2}/{18\mu} \tag{2.8}$$

There are three common types of tanks that are effective in sedimentation- circular radial flow, rectangular horizontal flow, and up-flow reservoirs. In this study the designed basin is rectangular; therefore more specifications of this tank are described. The ideal rectangular horizontal flow settlement basin is deemed to be categorized into four zones -inlet zone, settling zone, outlet zone, and sludge zone (Figure 2.8). The flow is generated at the inlet zone and carries the particles to a uniform forward direction. The particles subsequently begin to settle while the water flows towards the outlet, the flow then congregates upwards to the pour column which is more clear and forwarding to outlet. In this area between the sludge zones is where the particles settle and collect, and are therefore removed from the flow.

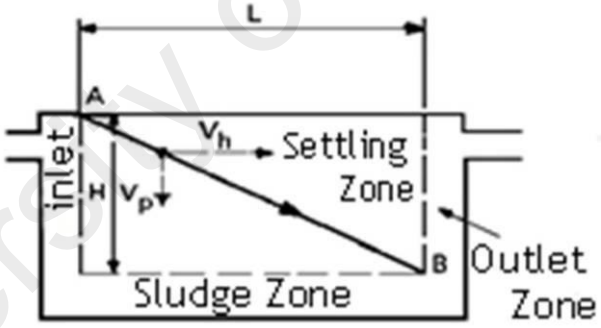

Figure 2.6 : Settling zone in tank

The inlet and outlet design is critical for improving the effectiveness of the sediment basin. The velocity components of such a particle are shown by V_h (represents as U in PIV result) in the horizontal direction and V_s (represents as V in PIV result) the terminal settling velocity, in the vertical direction. The retention time or required time to settle the particles in a tank is calculated by

$$t_0 = {Length}/{V_s} \tag{2.9}$$

University of Malaya

Where according to the relationship, the settling velocity of Q/A in an ideal sedimentation tank could be expected where the slowest settling particles are completely removed. With the exception of up-flow tanks, when the settling velocities is higher than the Vs the particles can be removed partially in an ideal settlement basin with a horizontal or radial flow pattern.

2.8.2.2 Sedimentation class II - flocculent particles settling in dilute suspension

Flocculation of particles make them heavier and increases the particle size, therefore the settling of sediments is better**.** In a rectangular tank, it may be possible that some particles move in a circle or curved path and move quicker rather than transferring to a straight line when settling. Therefore, a larger height makes the longer detention time for growth of particle and reaches to the settling velocity and settled down. Thus, in a tank with less depth implanting baffles or tubes assists the process of sedimentation. They are regularly installed at an angle where efficiently enhances the vertical displacement between two plates.

2.8.2.3 Sedimentation class III - zone settling and hindered settling and sludge blanket clarifiers

The condensation of particles increases in hindered zone, where the particles get closer to each other and there is more interaction between them. Therefore no more individual movement will be seen at this level and more floc settling is observed in this zone. Although some upward flow can be seen from particles in this zone. This is known as hindered settling where higher concentration of particles cause higher settling velocity, and composing of particle is found in this zone. The high concentration leads to a higher chance that particles collide and accumulate which removes many of the very fine particles.

University of Malaya

2.8.2.4 Sedimentation class IV - compression settling (compaction)

A high concentration of particles directs the settling particles to reach the floor of the sedimentation tanks. Compression zones show the settled particles in gravity thickening process. The importance of this zone is more related to active sludge fraction.

2.8.3 Sedimentation Tank

The surface loading rate Q/A is considered as the primary factor influencing the settling function as it illustrates the critical particles settling velocity for complete removal. It notes the sedimentation in settlement of flocculent particles in dilute suspension requires the adequate depth (H) and detention time (HRT to t_0) to prepare the particles for flocculation. The density and the viscosity that is related to temperature of fluid is always noticeable. The H and HRT factors always exert to all tanks (three types) normally applied for class II and III sedimentation, namely square up flow tanks, circular radial flow tanks, and rectangular horizontal flow tanks. The forward velocity has a decisive role in rectangular tanks, as the scouring and re-suspension of settled sludge could happen by excessive velocity. This requirement impacts the length-to-width ratio selected for such tanks. The inlet must be appropriate, in the right place and allows the spread of water flow in all direction.

2.9 Particle Size Distribution

Measuring the particle size diameter or distribution is a method which investigates the shape, size and volume of particles with different techniques and instruments. Many studies have been done regarding the effect of particle size distribution on the different properties and materials such as in reactive as catalysts (Victoria, 2000), tablet in pharmacology, stability in suspension as sediment (Cammem, 1982), efficiency of delivery in medicine and drug, texture and feel in food industry, viscosity and flow ability

University of Malaya

(Heath et al., 1997), and packing density and prosperity. Many industries aiming to improve the quality and efficiency of materials invest in research on particle size distribution of materials. In sedimentation studies the movement and transport of particles is a significant matter, therefore measuring the particle size and especially the variables regarding this method is essential. There are many techniques to determine the particle size of material which depends on the method and objective of study such as to seek knowledge in the stability, performance, appearance of materials or formulation. Although some types of materials are the reason for low performance of some methods. The conclusive results of these different methods will vary because during the scanning mobility of the particle spectrometer, there is an assumed equilibrium particle charge distribution and it is correctly measured, The charge fraction, optical and mobility sizing differ, therefore differences persist with the calibration factors. For solution of this matter, treating these various methods independently is essential, and merging them into a single distribution will produce inherent "bumps" during the transition of the solution.

There are different methods to measure the particle size such as microscopy, sieving, sedimentation techniques, optical and electrical sensing zone method (Nègre et al., 2004; Whalley & Krinsley, 1974), laser light scattering techniques (Segal et al., 2009; Stanković et al., 2012) and surface area measurement techniques (Markgraf et al., 2012). It is necessary to select an appropriate method that suits time constrains and specification requirements of the experiment in order to accurately estimate particle size range, solubility, toxicity, flow ability and financial factors such as capital and ongoing operational costs.

For particle size distribution the D values is the most evaluated technique. The D10, D50 and D90 are commonly used to represent the midpoint and range of the particle size of a given sample. The sieved sample are mostly investigated by creating an S-curve of cumulative mass retained against sieve mesh size, and calculating the intercepts for 10%,

University of Malaya

50% and 90% mass. Although the new methods just measure the numerical range and not the mass of particles.

A D value can be assumed as a mass division diameter. The diameter of all particles in a sample are arranged in ascending order of mass, and divided by the total samples mass to give an individual percentage value for each particle. The percentage mass of a particle below the diameter of interest is the number expressed after the D value. The D50 is also known as mass median diameter as it divides the total sample equally by mass. The particle volume distribution and cumulative volume graphs of the sample demonstrate that the particles in a given size, range by percentage of the total sample volume, whilst the cumulative volume curve tracks the total volume of all size ranges as they approach 100%.

2.9.1 Rayleigh Theory

Rayleigh theory is described as the scattering of light from a small particle size to the wavelength of incident light. In that moment the whole surface of the particle makes a homogenous surface act as an electric field. The light penetration time is short compared to the polarization of the particle and incident of light. The intensity of scattering is in different directions.

The polarizability α is a tensor, but all three perpendicular components are the same in case of optically isotropic materials. Although α is a function of particle volume and particle shape and effects the intensity of scattering light, all particles scatter light without defined structure. Rayleigh theory in regards to natural light can be defined in equation 2-8 (Xu R., 2000).

$$I = (1 + \cos 2\theta) k_0^4 |\alpha|^2 I_0 / 2r^2 \quad (2.10)$$

University of Malaya

Where *I* is intensity of scattered light, θ is scattering angle, k_0 wave vector of incident light, α polarizability of the particle, I_0 intensity of incident light, and r is distance from scattering center.

For small particles the formula of Rayleigh theory can be represented also as in equation 2-10 (Xu R., 2000).

$$I = \frac{16\pi^4 a^6}{r^2\lambda^4}\left[\frac{m^2-1}{m^2+1}\right]^2 sin^2\psi \qquad (2.11)$$

Where *I* is intensity of scattered light, a is radius of the particle, r is distance from scattering center, λ wavelength of incident light, m is relative refractive index, ψ is angle between incident and scattered light (Xu R., 2000).

2.9.2 Mie Theory

Mie theory relates to the scattering of light in conjunction with particles that can be small, large, transparent or opaque (Figure 2.7). This theory covers a wide range of details regarding scattered light (Eshel et al., 2004). The intensity of scattering from the surface of the particle (primary scattering) can be predicted with the refractive indexes of the particle and the medium, also the light refraction with the particle (secondary scattering) which is very important when particle diameter is below 50 μm.

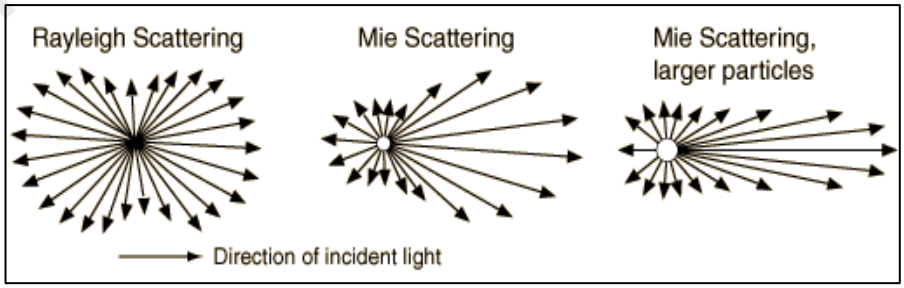

Figure 2.7 : Mie Scattering produces the white glare around the sun during the high concentrate of particulate material in the air and is weakly wavelength dependent (Williamson & Cummins, 1983)

University of Malaya

It is important that with large particles (solid line) the peak of intensity is stronger than with small particles (dashed line), and the minimum intensity is much closer to the axis of the incident light (Kippax, 2005). The intensity of peaks are in the same location in the both positive and negative angles because of the symmetrical nature of scattering (Segal et al., 2009).

2.9.3 Sieving

Sieving is a traditional and old method using the simple premise of weight distribution. The material is passed through the different pore sizes of complex nets. The top sieve has larger hole which is placed over those with a smaller aperture size below. The different sieves can be distinguished by the mesh size or sieve number (Figure 2.8). The mesh size is the number of wires per linear inch in US unit. The mesh size is based on the number of wires, for example 250 µm equals to No. 60 to 125 µm which is equal to No. 120. Approximated size range could be defined by standard woven wire sieves from 5µm - ~3mm, though in the sieves of electroformed micromesh at the lower range is (< 20µm) and the punch plate sieves at the larger range of 20µm.

Figure 2.8 : A images of Sieve Series (Federal Highway Administration, 2006)

There is a different classification of particle size based on each countries standard. Based on US classification, where not more than 40 % passes through a number 355 sieve and

University of Malaya

not less than 95% crosses through a number 1400 sieve, the particles are coarse. For moderately fine powder, the rate of passes through a number 355 sieve is not less than 95%passes, and not more than 40% passes through a number 180 sieve. Fine powders are those particles where not more than 40% crosses through a number 125 sieve and not less than 95% goes through a number 180 sieve. According to the British Soil Classification System for engineering purposes BS 5930:1981, the soil fine particles are categorized as fine sand 0.06-0.2 mm, silt 0.06-0.002 mm and clay <0.002mm.

Sieving can be executed in wet or dry estate, by machine or manually. In this method the time of experiment can be fixed or completed when all particles have passed at a constant low rate through the sieve. There are various instruments used to clear the sieves such as wet sieving ultrasonic (Eshel et al., 2004), air jet sieving, shaking or vibration machines.

This method is cheap and easy to perform in a wide range of sizes, but the particles can be incorrectly classified or size estimation can be in incorrect because the pore size of the sieve was not exact, it was hard to clean and nowadays the accuracy of this method is considered low.

2.9.4 Measurement Techniques

Sedimentation techniques are used to measure the particles coarser than one micrometer (>1μm), the principal of sedimentation is depended on the fact that increase of particle size resulted increase of the terminal velocity of a particle in a fluid. This technique is applied based on the weight distribution. The particle size distribution is defined with Stokes's law, therefore the settling velocity and the particle size relation will be determined through the below equations:

$$V = {(\rho_f - \rho_s) g d_{sph}^2}\Big/{18\eta} \tag{2.12}$$

University of Malaya

Where the V is defined as terminal velocity of sphere, ρ_s is particle density and ρ_f is fluid density.

$$d_{sph} = {}^{18\eta}\Big/_{(\rho_f - \rho_s)d}\ {}^{x}\Big/_{t} \tag{2.13}$$

Where the g is acceleration due to gravity, the η is viscosity and the d_{sph} is diameter of sphere.

Generally the Stokes's diameter (d_{st}) is denominated as the sphere diameter that would sink down at the same rate as the particle. The distribution of fine particle sizes can be measured by testing the sedimentation of the fine particles suspension as hydrometer (wet sieve). There are two categories used in determining the particle size, first is incremental, which is applied when there are changes in the concentration over time, or density of the suspension at known depths are known. Secondly is cumulative which describes the rate at which the powder is settling out of suspension. As an example the accumulated particles are measured at a fixed level after all particles between it and the fluid's surface have settled. In sedimentation of suspension two methods of the pipette and the photo-sedimentation technique are used. The pipette method is processed by allowing a homogenous suspension settle in a station cylinder in time and the different displacements in time give the concentration of coarse and fine particles. This method is cheap and simple equipment is required, it has high accuracy and reproducibility in measurement a wide range of sizes. However the sedimentation analysis should be conducted at sufficiently low concentrations to diminish interactive effects between particles, thus the collected data from their terminal falling velocities to be equal to the isolated particles. The next issue is temperature dependence which is suppressing convection currents. Moreover, Brownian motion for progressively smaller particles is more important at the lower limit of particle size. The particle of sand (re-aggregation) should be completely insoluble in the suspending liquid during extended measurements.

University of Malaya

2.9.5 Particle Size Distribution Determination by using Electrical Sensing Zone Method (Coulter Counter)

This method is based on volume distribution. In this method an instrument is used with two electrodes, therefore the size and number of suspended particles in an electrolyte is assessed by causing them to pass through an orifice as both sides are immersed in an electrode. The measured particle volume by this instrument can be expressed as the sphere diameter which shows the same volume as the particle. So the variation in resistance or electric impedance occurs as particles transport per the orifice and produce voltage pulses whose amplitude is proportional to the volumes of the particles. This method gives results with high resolution in a extensive confine of particle diameter measurements (approximately 0.5- 400µm) and true volume distribution. However the calibration for each set up is required and with porous particles errors can be observed. Moreover there is difficulty with high density materials and low concentration of particles.

2.9.6 Laser Light Scattering Techniques

This method involves two techniques, one is Laser Diffraction Particle Size Analysis that can measure the particle size between range of 0.02-2000µm to 0.01-3500 µm and the second is Photon Correlation Spectroscopy which can determine particle size in the range 1nm to 5µm.

2.9.6.1 Laser diffraction particle size analysis (LDPSA)

In general the laser diffraction methods determines distributions of particle size by examining the angular variation in intensity of light scattered as a laser beam passes through a dispersed particulate sample (Segal et al., 2009). In this method an instrument is manufactured with laser light and the main application of it is created with light scattering. The combination of distilled water and material is passed through the light

University of Malaya

beam and the angle of scattered light is collected and analyzed as particle diameter. The particles pass through an expanded and collimated laser beam in front of a lens whose focal plane is positioned in a photosensitive detector consisting of a series of concentric rings. In this technique the shape of particles cannot be identified (Andrews et al., 2010).

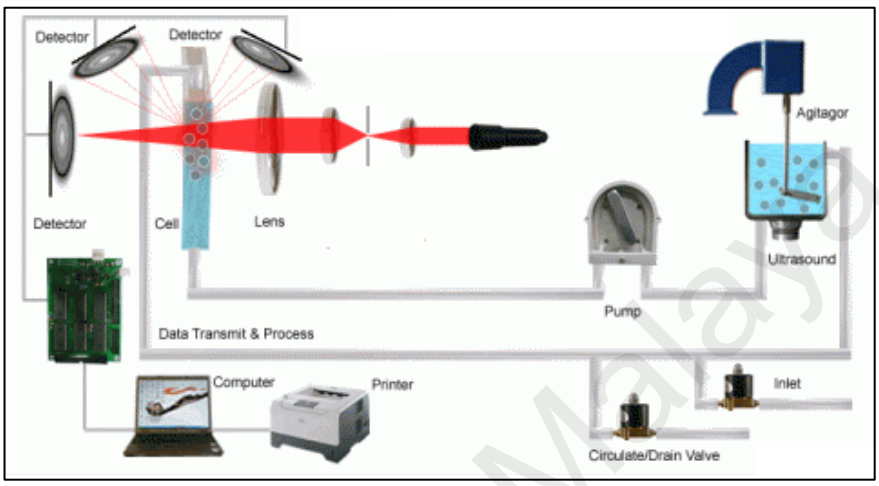

Figure 2.9 : Laser Diffraction Particle Size Analysis (HMK, 2014)

The research proved small angles relative to laser beams provided through the large particles scatter light and small particles scatter light at large angles. In addition**,** the angular scattering data was examined to determine the particles size that produced this pattern using the Rayleigh/Mie theory (Adrian, 1984). Based on the Mie theory of light scattering and the volume of the equivalent sphere model, the optical properties of the dispersant and sample being measured is understood. it is a volume equivalent sphere model, then with knowledge of the optical properties (refractive index (Eshel et al., 2004) and imaginary component) of both the dispersant and the sample being measured. The distribution of scattered intensity is analyzed by a computer to yield the particle size distribution (Di Stefano et al., 2010; Dudderar et al., 1988).

In some cases, errors can arise in the results of LDPSA; therefore it is necessary to try avoid this. Sample dispersion, air bubbles, misalignment in the presence of external vibration, **i**ncorrect obscuration, electrical interference, sudden changes in temperature can cause misalignment as well as changes to the measured electrical offsets.

University of Malaya

This method can measure the wide dynamic range of particle size from submicron to the millimeter size range, and the results generated in less than a minute with a large number of particles able to be measured in each sample. The researcher has the ability to monitor and control the particle dispersion process and performed hundreds of measurements per day without calibration. Even though there must be a difference between particles and suspending medium's refractive index, during the test the study proved the best refractive index for soil particle size distribution is 1.4 (Stojanović et al., 2012).

As it discussed in particle size distribution part of the result is evaluated by the D value system. Therefore based on a division of the mass of a sample by diameter, from the diameter values obtained for each particle a relative mass can be assigned.

$$\text{Mass of a sphere} = {}^{\pi}/_{6}d^{3}\rho \tag{2.14}$$

Where ρ is constant for all particles and cancelling all constants from the equation:

$$\text{Relative mass} = d^{3} \tag{2.15}$$

So each particles diameter could give its relative mass. These values can be determined from the total relative mass of the sample measured. The values may then be arranged in ascending order and added iteratively until the total reaches 10%, 50% or 90% of the total relative mass of the sample. The corresponding D value for each of these is the diameter of the last particle added to reach the required mass percentage.

2.9.6.2 Photon correlation spectroscopy (PSC)

In the photon correlation spectroscopy method, the principals of the technique are similar to LDPSA as the signal of light is collected as sample and matched with itself at several time periods using digital correlated and exerted computer software. The coarse particles travel at low speed than fine particles, thus the light scattered sway rate from them is also

University of Malaya

lower. Subsequently the light fluctuations rate and variations are determined by measuring the size distribution of the particles scattering light. Therefore to analyze the particle size distribution, a comparison is taken of each speckle pattern with another taken a microsecond after. As time is the variable factor and directly affects the position of the speckles, this also impacts size. At the final stages of analysis, the particle size distribution is estimated using the relationship of the auto-correlation function obtained to time intervals. The PSC method is quick, non-intrusive when determining the wide size range. Viscosity and refractive index (R.I) values are dependent on solids in liquid or liquid in liquid samples, which can be described as disadvantages.

2.9.7 Microscopy

The numerical distribution of particle size is determined using microscopy. In this method two techniques are used- Electron microscopy (0.001µ) and Optical microscopy (1µm) by this method each particle is investigated individually therefore the microscopy is considered as an absolute particle size measurement. This method can distinguish individual particles within an aggregation, and when analyzed using computers, each area can be investigated and bring out a distribution. The depth of focus with this technique is about only 0.5µm at x1000 and 10µm at x100. As discussed before, with fine particles, the enhance of diffraction effects could cause blurring at the edges. Hence the two methods of Scanning Electron Microscopy (SEM) and Transmission Electron Microscopy (TEM) are used to investigating the submicron elements. The analysis of data from microscopy can be performing using different criteria such as**,** Martin's diameter (M), Feret's diameter (F), Projected area diameter (d_a or d_p), Longest dimension, Perimeter diameter, and Maximum chord.

In Martin’s diameter method, a line in drawn by ruler in any direction but must be constant for all image measurements with the length of the line which bisects the particle image.

University of Malaya

Moreover, the distance between two tangents on opposite sides of the particle, parallel to some fixed direction is defined as Feret's diameter. This is also the longest dimension described in this value when a measured diameter is equal to the maximum value of Feret's diameter. Maximum chord is determined by a diameter equal to the maximum length of a line parallel to some fixed direction and limited by the contour of the particle.

The Projected area diameter and Perimeter diameter are defined as the diameter of a circle having the same area as the particle viewed normally to the plane surface on which the particle is at rest in a stable position. Furthermore the pointed area also has the same circumference as the perimeter of the particle.

Overall, the microscopy method is relatively inexpensive and records the images of small sample sizes. Nonetheless it is time consuming without information on three dimensional shapes. Thus the Scanning Electron Microscopy has been suggested.

2.9.7.1 Scanning electron microscopy

The Scanning Electron Microscopy was developed in the 1950's with wide possibilities and interest in investigating its use. This instrument processes with electrons instead of light. The SEM is a big microscope that generates a variety of signals at the surface of solid specimens by operation of a focused beam of high-energy electrons. The SEM covers the wide aspects of science by studying both morphology and composition of biological and physical materials (Figure 2.10).

University of Malaya

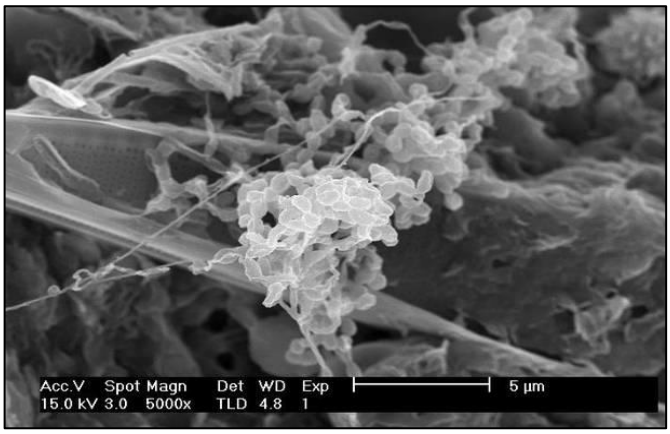

Figure 2.10 : A sample of scanning electron microscopy with 15.0 kV and 5 µm zoom (Cranfield, 2014)

In addition, it should be considered that the SEM has processed electrons which are backing scattered electrons or BSEs, secondary electrons and characteristic x-rays (Figure 2.11). There are several other kinds of signals generated during the specimen electron beam interaction, which could be used for micro structure analysis. They are Auger electrons, cathode luminescence electrons, transmitted electrons and specimen (or absorbed) current.

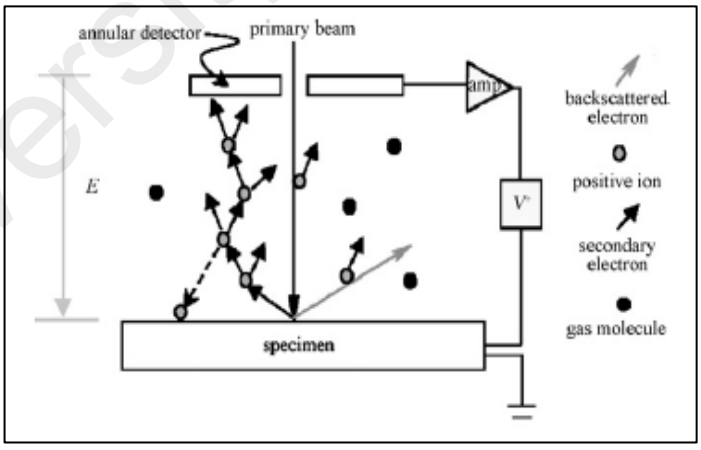

Figure 2.11 : A schematic of the amplification process due to collisions between the secondary electrons and gaseous molecules. Image courtesy of Stokes (2003) and the Royal Society of U.K (Bogner et al., 2007).

This microscope could produce electrons and accelerates them to an energy level of 0.1–30 keV. Electromagnetic lenses and apertures are used to focus and define the electron

University of Malaya

beam and to form a small focused electron spot on the specimen. The air is evacuated in SEM to produce a high-vacuum environment, this allows electron travel without scattering in the air. When the signal detection occurs, the surface is observed and processed with an image recorded of the specimen surface.

For better vision of nanoparticle, nanostructure, nanocarbons, nanotube materials (Bonard et al., 2002), cells (Clarke, 1974) the preparation of a sample is required since errors can result from the reflection of electrons (Figure 2.12). Two main approaches exist to improve the SEM resolution: decrease the lens aberrations, or increase the source brightness (Bogner et al., 2007). Therefore, a way to eliminate or decrease the source of brightness is through the preparation of samples before the SEM test. Freeze drying, air drying and dehydration can be applied for sample preparation to remove the water or moisture from the sample. The other method of sample preparation for samples of biological specimen is Critical Point Drying (CPD) which allows chemical fixation and exchange with an intermediate fluid (ethanol or acetone) and then a a transitional fluid such as liquid carbon dioxide (CO2) which subsequently undergoes a phase transition to gas in a pressurized chamber. Moreover, the bioorganic specimens naturally include low atomic number elements that emit the secondary and BSE yields during the test, therefore it is coated with metals such as gold, silver, gold/palladium, and platinum (Nègre et al., 2004; Whalley & Krinsley, 1974). In an argon atmosphere the damage of bioorganic specimen surface is reduced but can still lead to structural decoration with large grain uneven film thicknesses as the metals provide conductivity.

University of Malaya

Figure 2.12 : Different models of specimen with metals coated (Ted Pella, 2014)

Particle shape can be measured using SEM but this method is expensive and time consuming in sample preparation, has low throughout, is not suitable as a routine technique and some materials are impossible to investigate using this method.

All the particle size distribution instruments and methods are developed to measure the particle size distribution of a sample. There are a few instruments that operate to give a single type of information regarding the sample otherwise all the rest give variations of information regarding the particle size and shape which leads to better knowledge in science and industry.

2.10 Rheology

Rheology is the study of the materials flow in stress conditions. This science is focused on the deformation of material under applied forces. Primarily this method is used in a liquid phase, but it is distributed in solid phase as well to investigate the plastic and elastic behavior of material. This method is applicable to all materials such as dilute solutions of polymer to semi solids such as pastes and creams to solid material. Rheological properties could be measured with different instruments such as a mechanical rheometer, and in a micro scale using a micro-capillary viscometer or micro-rheology. Many factors influence the rheological behavior of dispersions including volume concentration of the

University of Malaya

dispersed phase, viscosity of suspending medium, size of the dispersed phase, size distribution of the dispersed phase, surface chemistry of the dispersed phase and shape of the dispersed phase (Mazzeo, 2008). Since this study is focused on sedimentation, some aspects of rheological properties relation and sedimentation will be studied. The particle shape has effect on its settling characteristics. For example a circular particle, will settle faster and easier than a particle that has ragged or a typical edges (Cammem, 1982). Major reasons for sedimentation is fast urban development activities upstream of waters that supply extensive sediment to the lake and fill the deck within 60 years (Ayub et al., 2005). Thus, studying different effects of sediments is necessary as fine sediment plays a substantial role in sedimentation which has been investigated in a variety of behaviors recently. The modeling of fine sediment transport in rivers (Yu et al., 2013; Hsu et al., 2012), influence climate change on fine sediments (Goswami & Mishra, 2013), and the management of coastal fine sediment systems (Kirby, 2013) proves the importance of fine sediment role. However all of these studies have tried to survey their goals whilst considering the rheology behavior.

Rheometric refers to the measurement of rheological properties and is applied when a force called shear is placed on the area. Shear is the relative movement of parallel adjacent layers. In rheology, shear rate and shear stress are the basis of rheometry. The shear stress is the component of force that leads to movement in parallel layers of materials, thus the shear rate describes the rate of change of shear strain in time. In capillary tests these two value are applied. There is another test in rheology which used oscillation force (Markgraf et al., 2012) and tests the shear modulus G that is provided from strain G’ and storage G” modulus. The ratio of shear stress to its corresponding shear strain is called the shear modulus (Biswas et al., 2002). At the end, the angel of properties deformation depends on the behavior called shear thickening (dilatant), an increase in viscosity with increasing shear rate during steady shear flow or shear thinning.

University of Malaya

The first idea or basis of the rheology is provided by the Deborah number (Denn & Porteous, 1971):

$$D = \text{time of relaxation/time of observation.} \tag{2.16}$$

Therefore, the difference between solids and fluids is defined by a magnitude of D. In case of a long observation time followed by a very small relaxed time, material flowing is fluid The Deborah number concept is of significant importance in rheology.

Isaac Newton and Robert Hooke played a big role in rheology. As with fluid mechanics, the research of the materials physic is divided in two categories- Newtonian fluids which not depart strain rates proportional to the applied shear stress and Non- Newtonian fluids (Schowalter, 1978) which go through strain rates proportional to the applied shear stress. Solid mechanics is investigated based on the elasticity and plasticity of material. Elastic material is described as material that returns to a normal shape when removing applied stress. Moreover plastic materials after a sufficient applied stress gets permanently deform.

In fluid mechanics the Reynolds number (Re) is a significant dimensionless number. The Reynolds number measures the ratio forces to viscous forces and the effect of both forces on flow condition. Under the low Reynolds number the material is viscous and the flow is laminar, while at the high Reynolds number the flow is turbulent (Rott, 1990).

$$Re = \frac{\rho V_s^2/L}{\mu V_s/L^2} = \rho V_s L/\mu = V_s L/\nu \tag{2.17}$$

Where the L is the characteristic length, [m], ρ is fluid density, [kg m^{-3}], μ is (absolute) dynamic fluid viscosity, [N s m^{-2}] or [Pa s], V_s is fluid velocity, [m s^{-1}], ν is kinematic fluid viscosity: $\nu = \mu / \rho$, [m^2 s^{-1}].

University of Malaya

Furthermore, the other scientist has tried to introduce new behavior of materials in physics. Thus the fluid is showed a different range of behavior. Maxwell (1867) as demonstrated by an equation for linear viscous fluid which is related to stress σ and strain ɣ of the form:

$$\sigma + \lambda \frac{d\sigma}{dt} = \eta \frac{d\gamma}{dt} \tag{2.18}$$

Where t is time, λ a time constant and η is the viscosity. Based on this rule when the time constant equals zero, the fluid behavior is Newtonian and when it is large number the elastic behavior or Hookean (Hooke, 1931) is observed. Therefore the fluid in this stage is elastic-viscous liquid or elastic liquid, and declared as Maxwell fluid (Maxwell, 1867). In addition another scientist Lord Kelvin established the Kelvin-Voigt model which was related to viscous solid as a comparison (Thomson, 1865).

$$\sigma = G\gamma + \eta \frac{d\gamma}{dt} \tag{2.19}$$

Where, G is a material constant. Generally, these two equations and models are known as Linear Viscoelasticity which is an important part in rheological properties.

Jeffry's model introduced a new equation regarding the simple elastic liquid. This equation was made after Maxwell's model (Jeffreys, 1929).

$$\sigma + \lambda \frac{d\sigma}{dt} = \eta[\frac{d\gamma}{dt} + \lambda \frac{d\gamma}{dt}] \tag{2.20}$$

2.10.1 Fundamental Rheological Properties

For a better understanding of rheology properties, an understanding of the behavior of materials and physic laws related to viscosity is required. Materials could behave as a plastic, elastic, viscoelastic, viscoelastic or viscous. Elastic is where the mechanical energy used to produce a deformation is stored in the material and returned through the

University of Malaya

release of stress. During a low value of deformation force, the matter is solid and in a stressed elastic state which is termed the yield stress (Iverson, 2003), and in plastic material this value is exceeded. Dissipation and stress are independent of the deformation rate when the material performs at an ideal plastic flow. Moreover a time dependent fluid or material under stress which produces a viscous and an elastic response at the same time is viscoelastic behavior. This type of material exhibits viscous flow under constant stress, but a part of mechanical energy is released after stress recovery. These type of properties are determined as a response to an instantaneously applied or removed constant stress or strain or a dynamic stress or strain, such as polymers. Viscoplastic (Kaide, 2012) is material that behaves like a solid below some critical stress value, the yield stress, although flows like a viscous when the stress is increased (Iverson, 2003). And the last behavior is viscous where there is tendency of a liquid to resist flow as a result of internal friction when mechanical energy is dissipated as heat and the stress that develops depends on the rate of deformation.

The main object of rheometry is viscosity. In the rheology science many type of viscosity have been identified. These values are evaluated using different methods of rheometry as viscosity is applied in capillary method, coefficient of fluidity, coefficient of viscosity, complex viscosity, plastic viscosity, kinematic viscosity, intrinsic viscosity, inherent viscosity, infinite shear viscosity. This study will introduce some of them. As apparent viscosity is the value of viscosity evaluated at some nominal average value of the shear rate.

Coefficient of viscosity value ($\eta=\sigma/\dot{\gamma}$) proves the behavior of material between Newtonian and Non-Newtonian behavior (Gotoh & Nawa, 2012). When the quotient is independent of shear rate (i.e. follows the Newtonian model), it is considered a material constant. When the quotient is dependent on shear rate (i.e., non-Newtonian), it should be referred to as the non-Newtonian viscosity. The fraction of shear stress to shear rate

University of Malaya

under simple steady shear is called coefficient viscosity. Moreover, during the oscillatory test the dynamic viscosity (Yu et al., 2013) ($\eta' = G^{"}/\omega$) is measured as the ratio of the loss modulus to the angular frequency, determined during forced harmonic oscillation (dynamic) measurements.

2.10.2 Basic Terms in Rheology

The experimental fluid performs in different ways with variations in physical actions. Each property is extends the rheological behavior in different stages. In terms of better understanding rheology properties, consciousness of these points is required. The study categorized them as follows:

Deformation is the displacement of particles of a material body in combination with other parts which caused the continuity of the body and is not destroyed, and resulting in a change of shape or volume or both. Dynamic Equilibrium is when the viscosity is constant at a given shear rate and during the steady shear flow the material is broken down, and subsequently rebuilt at a similar rate. Apparent Yield Stress is occurred in Bingham (plastic – visco-plastic) model as in non-ideal viscoplastic materials, where the yield stress (the point the material has started to flow) is definite, for example, by extrapolation from the linear, high shear rate portion of the flow curve to the stress axis.

Dilatant is the term of increasing resistance to shear with an increasing shear rate (shear thickening) also the increase of volume while being sheared. Shear Thickening is a behavior of material where the viscosity increases with increasing shear rate during steady shear flow (Olhero & Ferreira, 2004). Shear-Thinning (Pseudoplastic) is the viscosity decreasing with increasing shear rate during steady shear flow. Thixotropy behavior is when the shearing causes a breakdown in structure overtime. It is time dependent, decreasing in viscosity at a particular shear rate. Rheopexy describes negative thixotropy, when a

University of Malaya

material recovers some of its pre-sheared viscosity at a faster rate when it is gently sheared compared to when it is allowed to stand.

2.10.3 Classification of Flow Curve

The rheometry of materials is evaluated using a variety of tests. The flow curve test and oscillation tests are two main methods Rheological properties of material under equilibrium conditions is measured using the flow curve test (Hashimoto et al., 2005). The materials in the steady-shear flow curves may exhibit a variety of behaviors over a limited range of shear rates. Moreover, some materials may exhibit more than one distinct behavior over different shear rate regions of the same flow curve. Several types of behavior can be categorized according to their characteristic shape. Herewith the most common type of characteristics is discussed. As mentioned above, fluids are classified in Newtonian and Non-Newtonian materials.

1. Newtonian - the viscosity is constant with shear rate.

2. Shear-thickening - viscosity increases continuously with shear rate.

3.Shear-thinning [pseudoplastic] - viscosity decreases continuously with shear rate (without the yield value) (Olhero & Ferreira, 2004).

4. Shear thinning [pseudoplastic] - with yield response, viscosity decreases continuously with shear rate once the apparent yield stress has been exceeded (Lev et al., 2012).

5. Bingham plastic (ideal plastic) – follows the Bingham relation completely. The plastic viscosity or the differential viscosity is constant, while the coefficient of viscosity decreases continuously to some limiting value at infinite shear rate (Yu et al., 2013).

6. Bingham plastic (non-ideal) - while the coefficient of viscosity decreases continuously above the apparent yield stress, the differential viscosity approaches a constant value with increasing shear rate.

University of Malaya

6*. Extrapolation of the flow curve from the linear, high shear rate region (plastic region) to the stress axis gives the apparent Bingham yield stress.

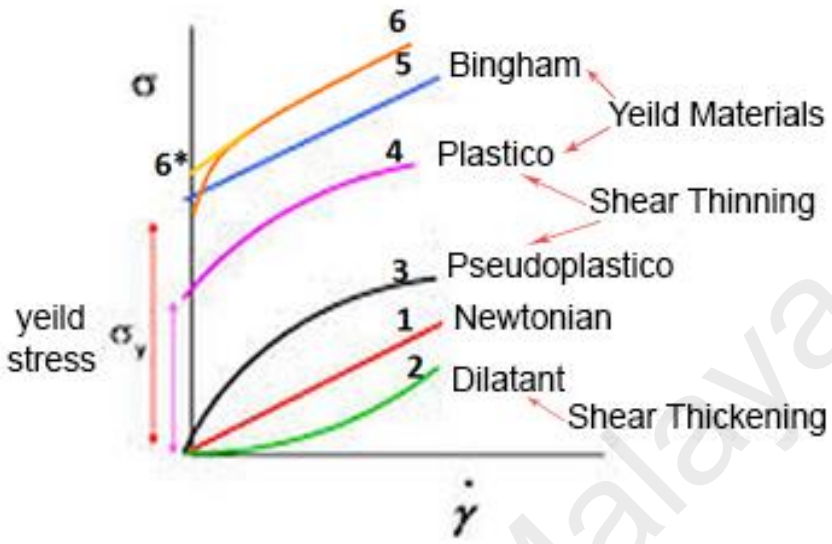

Figure 2.13 : The classification of properties in Flow Curve (http://www.iq.usp.br/mralcant/About_Rheo.html, 2013)

2.10.4 Expressions for Describing Steady Shear Non -Newtonian Flow

In this section, the relation in non-Newtonian behavior of fluids under equilibrium and steady shear flow conditions are categorised. Many different models and laws have been developed which relate to the study of rheological properties.

Carreau-Yasuda (with no yield stress**)**, Cross (with no yield stress**)**, Ellis (performing a power-law relationship between shear stress and shear rate, with a low shear rate asymptotic viscosity), Meter, power-law [Ostwald-de Waele] (shear-thickening behavior in materials that show a negligible yield response and a varying differential viscosity) are all models which describe the Pseudoplastic behavior under different conditions.

Bingham, Casson, and Herschel- Bulkley models are determined by the viscoplastic fluids. Bingham relation uses two parameters to describe the viscoplatic fluids exhibiting a yield response (Iverson, 2003).

University of Malaya

$$\sigma = \sigma_B + \eta_{P1}\dot{\gamma} \tag{2.21}$$

$$\dot{\gamma} = 0 \; for \; \sigma < \sigma_B$$

A linear relationship between shear stress and shear rate, with a constant differential viscosity equal to zero the plastic viscosity is called viscoplastic flow. $\dot{\gamma}$ is yield stress. Casson describes the flow behavior in viscoplastic fluids with yield response. This relation is same with Bingham model but the point of yield stress is zero.

$$\sigma^{\frac{1}{2}} = \sigma_y^{\frac{1}{2}} + \eta_{P1}^{\frac{1}{2}}\dot{\gamma}^{\frac{1}{2}} \tag{2.22}$$

$$\sigma < \sigma_y \quad \dot{\gamma} = 0$$

Herschel-Bulkley describes viscoplastic behavior as the yield response in power law relationships between shear stress and shear rates above the yield stress when using three parameters.

$$\sigma = \sigma_y + k\dot{\gamma}^n \tag{2.23}$$

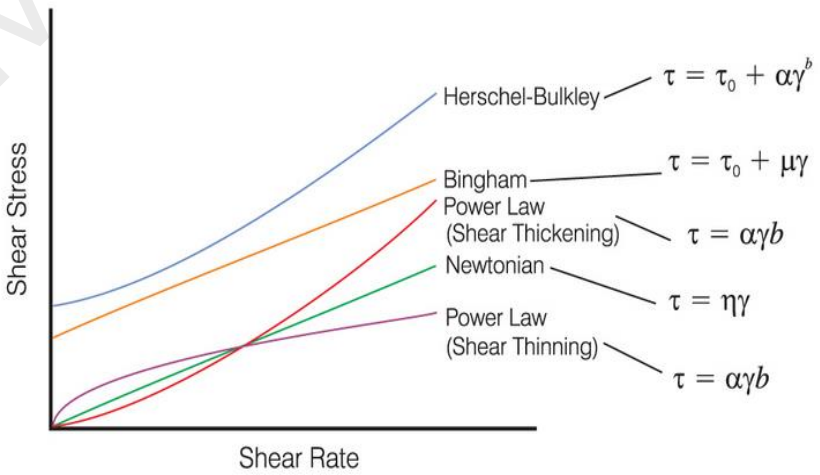

Figure 2.14 : Flow curves represent shear stress vs. shear rate (Debs, 2013)

University of Malaya

The Herschel-Bulkley relation reduces the equation for a Bingham plastic when *n*=1. Krieger-Dougherty is an ideal model to describe the effect of particle self-crowding on suspension viscosity, where M is the particle volume fraction, ϕ_m is a parameter representing the maximum packing fraction and ϕ_n is the intrinsic viscosity.

$$\eta = (1 - \frac{\phi}{\phi_n})^{(-n)\phi} \tag{2.24}$$

Powell-Eyring is related to molecular fluids, but can be used in some viscous model as well and viscoelastic polymer solutions over a wide range of shear rates.

$$\eta = \eta\infty + (\eta_0 - \eta\infty)\frac{\boldsymbol{sin\, h^{-1}\, \tau\dot{\gamma}}}{\boldsymbol{\tau\dot{\gamma}}} \tag{2.25}$$

2.10.5 Oscillatory Measurements

The other form of rheometry test is oscillation as a dynamic rheometric test in which both stress and strain vary harmonically with time, and both viscous and elastic parameters are derived from the material response. These categories of tests are applied in the linear viscoelastic regime, which is considered by a linear response of dynamic viscosity and elasticity with increasing strain amplitude.

2.10.5.1 Functions derived from oscillatory tests

In a typical sinusoidal oscillation experiment the applied stress and resulting strain wave is obtained. The basic principal of an oscillation test is to include a sinusoidal shear deformation in the sample and measure the response to stress. The time scaled probed is evaluated by the shear deformation (ω). The time dependent strain is shown by $\gamma(t) = \gamma.\sin(\omega t)$ and the stress shown as σ(t) (Markgraf et al., 2006).

University of Malaya

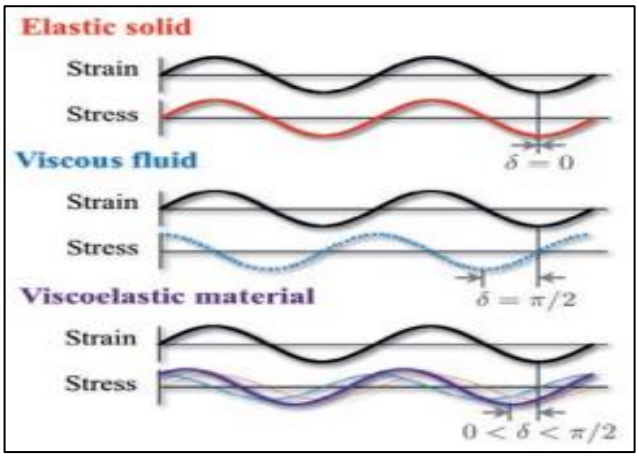

Figure 2.15 : Schematic stress response to oscillatory strain deformation for an elastic solid, a viscous fluid and a viscous material (Weitz et al., 2007).

The storage modulus (G') represents the in-phase (elastic) component of oscillatory flow, and the out-of-phase (viscous) component is termed the loss modulus ($G^{"}$) which defined as (Markgraf et al., 2006):

$$G' = \frac{\sigma_0}{\gamma_0}\cos\delta \tag{2.26}$$

$$G^{"} = \frac{\sigma_0}{\gamma_0}\sin\delta \tag{2.27}$$

Thus the complex shear modulus, G* is defined as (Markgraf et al., 2006) :

$$G^{*} = G' + jG^{"} \tag{2.28}$$

$$\tan\delta = \frac{G^{"}}{G'} \tag{2.29}$$

The function $G^{"}, G'$measures the relative importance of viscous to elastic contributions for a material at a given frequency (Yamamoto & Sawa, 2011).

$$If\ \gamma^{\cdot} = j\omega\gamma \tag{2.30}$$

$$\eta^{*} = \eta' + j\eta^{"} \tag{2.31}$$

University of Malaya

$$\eta' = \frac{G''}{\omega} \tag{2.32}$$

$$\eta'' = \frac{G'}{\omega} \tag{2.33}$$

Where the η'' termed the dynamic viscosity.

2.10.6 Measurement Device

For rheometric measurements on fluid systems, two common methods have been developed. The capillary (Hashimoto et al., 2005) and rotational methods are examined with a viscometer and rheometer. A viscometer is applied for a viscosity measurement though a rheometer which is a device used to determine the rheological properties in varied condition.

2.10.6.1 The capillary method

In this method the test fluid flows through a narrow tube to investigate the effect of applied pressure and hydrostatic. The glass capillary viscometer and extrusion capillary viscometer are devices used to measure the viscosity of material and solutions. The glass capillary viscometer is used to measure the viscosity of Newtonian fluids, including dilute solutions and suspensions. This technique is time consuming since the solution is poured in a U shaped tube which gets narrower at the bottom. The results of the device is calculated based on Poiseuille's law.

Extrusion viscometers use a cylindrical piston to force the test fluid from a reservoir through the capillary tube at a constant velocity. This device measures the pressure drop across the capillary as a function of flow rate for multiple capillaries in the same diameter to achieve the viscosity rate related to shear rate.

University of Malaya

2.10.6.2 Rotational methods

Nowadays, different companies have developed new rheometers with varied ability in the control of temperature, rheometric parameters as shear rate, variation level of stress and oscillation force. With these new devices, the viscoelastic or plastic material can be examined. In general, rotational methods are easier to test gels, paste and concentrated suspensions as compared to capillary methods (Markgraf et al., 2012). Rotational measurements have ability to control the stress and rate of force**.** In stress controlled measurements, the rotation speed is determined with a constant torque measurement tool. The rotation speed can be converted into a corresponding shear rate. In rate controlled measurement, the stress sensed as torsion spring or strain gauge, is measured with a constant rotation speed.

In the rotational rheometer, different companies such as Brookfield, Malvern (Fang et al., 2012) have the ability to change accessories and tools in making different types of force in a unit area. The tools are selected based on the phase of material. The three famous basic tool geometries for rotational rheometer are concentric cylinder, cone and plate and parallel plate. The concentric cylinder (also called Couette or Coaxial) can rotate either the inner, outer or both cylinders at the same time (Figure 2.16).

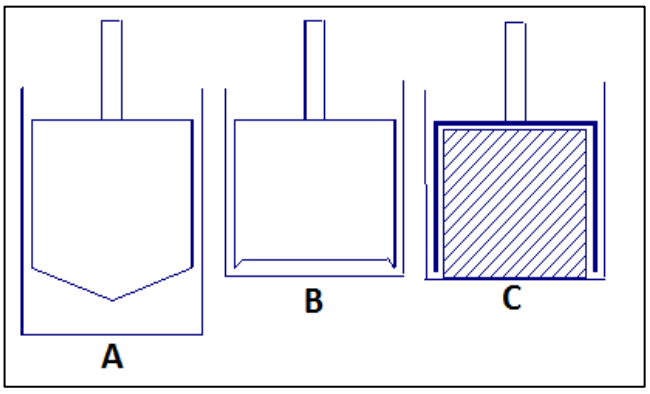

Figure 2.16 : Schematic of cone and Cylinder tools A. DN Coaxial Cylinder, B. Mooney Cell, C. Double Gap (LLC, 2014)

University of Malaya

Another tool is called the double gap configuration which has a larger contact surface and therefore more suitable for low viscous material. The last type of this model is called cone and hollow cavity configurations which are designed for less slip and a perfect tool for rheometry of fluid suspension. The cone and plate geometry (Yamamoto & Sawa, 2011) is manufactured to have close contact with a lower plate as the cone has an angle of less than 4 degrees. The parallel plate geometry (Markgraf et al., 2012) is considered a simple version of the cone and plate with zero angels. The gap is narrow between two surfaces (Figure 2.17). This geometry is mostly used for highly viscous pastes, gel (Kaide, 2012) and concentrated suspensions.

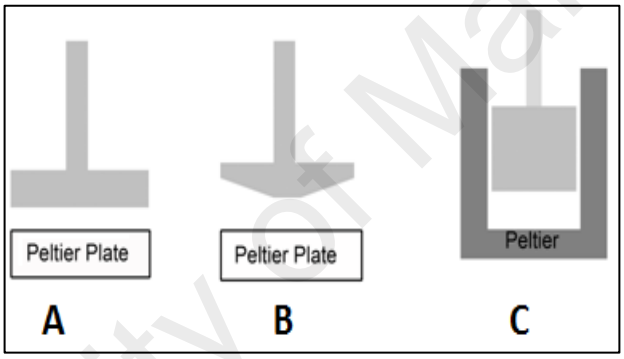

Figure 2.17 : Schematic of rotational rheometer tools, A. Parallel Plate, B. Cone and Plate, C. Cylinder (Yamamoto & Sawa, 2011)

In addition, various vane geometries (Biswas et al., 2002) when used in concrete rheometers to measure the material with coarse particles, such as two point test of Tattersall, BML and IBB (Figure 2.18).

University of Malaya

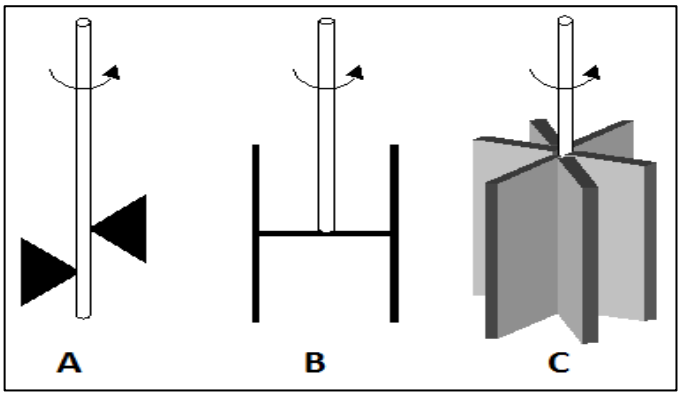

Figure 2.18 : Diverse geometry of vanes used in concrete rheometers: A. two-point test or Tattersall, B. IBB, C.BML (Hackley & Ferraris, 2001)

2.11 Particle Image Velocimetry

PIV techniques have been applied in hydraulics since the early 1980s (Adrian, 1991). Since it requires large storage and RAM memory, digital PIV techniques have benefited from the advancement in computer architecture, especially since late 1990s (Ferreira, 2011). It has been 30 years since the Particle Image Velocimetry (PIV) was developed. PIV is a technique to measure the field of fluid flow and to promote the image of velocity over time. PIV enables the recording of small tracer particles (seeds) over a period of time. When injected to the flow their motion used to estimate the kinematics of local fluid velocity and this is recorded (Prasad, 2000a). PIV can be described as a measurement tool to describe the fluid movement in the flow with the visualized problem. PIV was able to capture two and three dimensional images in a single frame and identify tracer particles from plate to plate using a recording of multi frame.

Adrian was the first person to expand the initial groundwork based on the PIV theory (R.J. Adrian, 1984). Adrian described the expectation value of the auto-correlation function as a double-exposure continuous PIV image. Thus the experiment design rules were described within this framework (Adrian, 1999). Afterwards, the theory was expanded to include multiple-exposure recordings and cross-correlation analysis.

University of Malaya

Therefore it was able to provide an adequate description for the analysis of highly resolved PIV photographs, which was the common mode of operation for a considerable time (Westerweel, 1993).

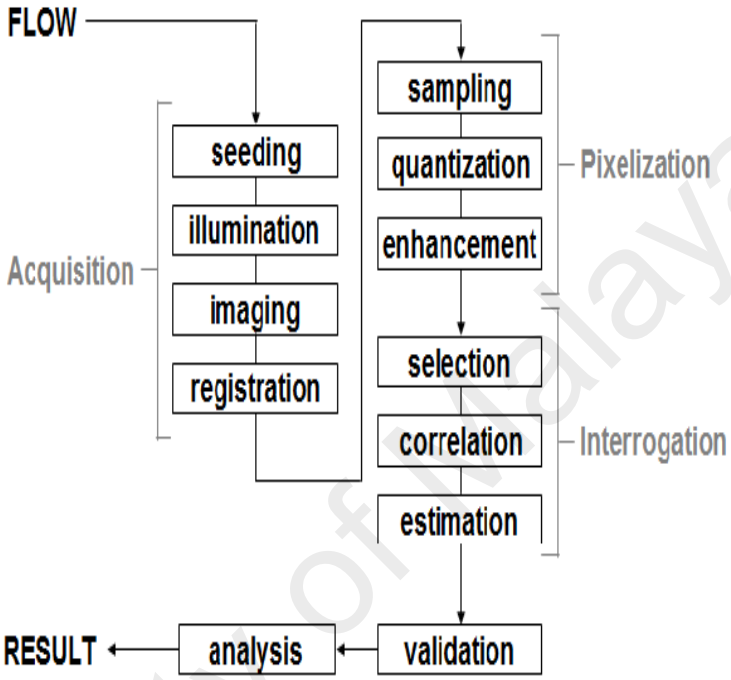

Figure 2.19 : A theoretical description of PIV involves many different disciplines, such as fluid mechanics, optics, image processing and signal analysis (Westerweel, 1993)

Following this, sediment transportation which uses PIV in different zones as measurements of inflow and around scour holes is studied (Prestlglacomo et al., 2007). In addition the velocity field of both phases in Aeolian sediment transport by using PIV with fluorescent tracer particles (Yang et al., 2011) was determined by using micron seeding in fluid and a rotor hovering above a sediment bed. This was studied using high-speed flow visualization and particle image velocimetry (Johnson et al., 2009).

In PIV the tracking of seeds is done by applying the scattering of light. As the PIV machine is included in camera CCD- or CMOS- , light source (laser) and computer

University of Malaya

software is used to collect and analyze the images. Therefore, by a light plane of which instantaneous images are recorded the tracer particles currents are brightened. The images are thereby investigated and an entire flow fields can be determined.

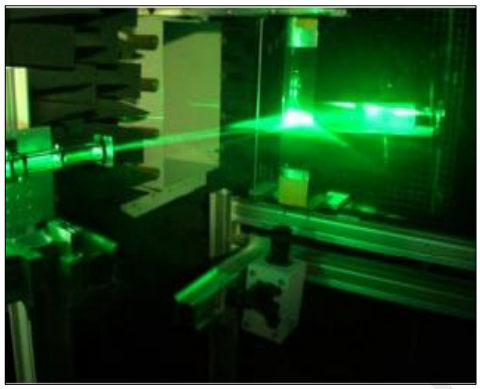

Figure 2.20 : Illumination and imaging (4D-PIV advances to visualize sound generation by air flows, Fulvio Scarano, Delft University of Technology, Aerospace Engineering Department – Aerodynamics Section) (Van Rijn, 2007)

There are other traditional methods such as Laser Doppler Velocimetry (LDA) and Hot Wire Anemometry (HWA) in two-dimensional velocity fields. The PIV technique has advantages compared to the traditional methods as mentioned above, although in high temporal resolution, the LDA and HWA are more applicable (Bastiaans, 2000). The principle of the PIV measurements technique works based on the physics definition of velocity as a differential quotient. The trajectory of many tracer particles which follow the flow faithfully can be captured with a CCD- or CMOS-camera by illuminating a plane in the flow with two very short light pulses (few nanoseconds) within a time difference of a few microseconds. The two particle images captured at time t and t' are stored on two frames of the CCD- or CMOS- sensor (Schütte & Lüdeke, 2013).

2.11.1 The Principal of Operation

In the experimental setup the process has different aspects, but the main objective of the technique is introducing the seeded in fluid and recording the track of illumination of

University of Malaya

particles with a camera. Therefore the illumination of tracer particles has to be in a path of the flow slightly twice in a period of a short time interval. The scattering light of particles is taken on a single frame or on multi frame. The movement of tracer particle images between laser light pulses is determined through assessment of the PIV recording. The investigation of fluid using PIV could be explained by the process of adding small tracer particles to the flow, then based on the particle size distribution, the thickness of light sheet is adjusted as previous studies demonstrated thinner light sheet enhances the resolution of light scattering in images (Guasto et al., 2006). The two equations below are a suitable guide to choose the correct particle size diameter based on the light scattering:

$$\text{Side intensity } (90^0) \text{ / forward intensity} = 10^3 \tag{2.34}$$

$$\text{Laser light intensity / CCD captured light intensity} = 10^5 \tag{2.35}$$

In the PIV technique, the first step in recording of images is determining the place or frame of study which is called the point. It is expected that the particles follow the fluid motion and at the identical time by the form of scattered light can play as transmitters of information, based on the Mie theory. In addition the concentration of the tracer particles in the fluid should be sufficient and be the right size. The size and concentration of particles is an important aspect of PIV because the scattering of laser light of all particles should be recorded on a memory of film (Hadad, 2013). The light scattering by tracer particles must be considered. The scattered light power is under direct effect of contrast of the PIV and in addition the particle image intensity recording, therefore, by choosing the scattering particles increasing the image intensity rather than higher power of laser is more effective with more economical benefits. Consequently, it can be said the light scattered is dependent on the particle diameter, polarization and observation angle. Mie's scattering theory can be involved for round particles with diameters, dp, larger than the wavelength of the incident light λ,. The intensity scales are plotted in logarithmic scale

University of Malaya

so that, the intensity for neighbouring round differs by a factor of 100. The normalized diameter(q) could characterized the Mie scattering, q defined by (Raffel et al., 2007):

$$q = {}^{\pi d_p}/_{\lambda} \tag{2.36}$$

If q is larger than unity, approximately q local maxima appear in the angular distribution over the range from 0° to 180° (Raffel et al., 2007) .

The time of recording is clarified by determining the time difference between laser light intervals depending on the magnification at imaging and the average flow velocity. The assumption is that the seeds are replaced between the two illuminations with local flow velocity (Önal, 2010). Then the recording is managed by a lens with high quality either on a single frame or two separate frames. The one frame lens could be a high-resolution digital or film camera and the special cross-correlation digital cameras such as (CCD or CMOS cameras) could be an example for two separate frames kind of recorder as the light is scattered by tracer particles. The modern charge coupled device (CCD) cameras captured 100 or more PIV recordings per minute. The CMOS sensors allow for acquisition in the kHz range on complementary metal-oxide semiconductor with high speed recording (Raffel et al., 2007). Consequently, the scanner develops the recorded images and the memory of a computer directly memorizes the output of the digital sensor (Jahanmiri, 2011). Since CCD cameras are limited by a finite exposure time and image pair separation time, the point of study must be chosen to cover a relatively large image area to adequately capture a significant number of tracer particles (minimum ten particles) that would otherwise drop-out within that time (Guasto et al., 2006). Interrogation areas are divided by digital image recorded to small subareas that lead to better evaluation. The positional movement trajectory for the tracer particles of the earliest images and latter illumination in each interrogation area can be determined by means of statistical methods

University of Malaya

such as -cross and auto correlation methods (Prasad, 2000a). The assumption is the all particles homogenous movement within one investigation area between the two illuminations. The calculation of the trajectory displacement is done based on the path of the vector in the local flow velocity into the light sheet area (two-component velocity vector), taking into account the time interval between the two illuminations and the magnification at imaging (Di Felice & Pereira, 2008; Johnson et al., 2009; Saleh et al., 2010).

In order to explain the main mathematically technique behind PIV, refer to the system used to determine the coordinate system x, y, z (Figure 2.21).

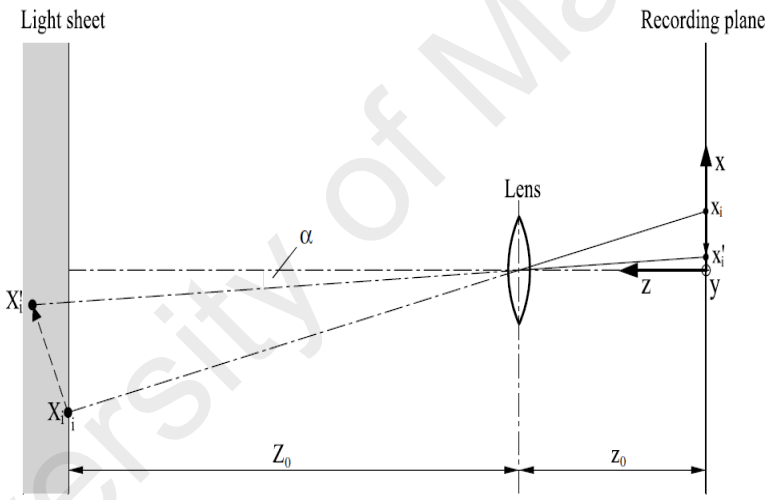

Figure 2.21 : Imaging of a particle within the light sheet on the recording plane (Raffel et al., 2007)

Therefore the taken image through the lenses is calculated to ideal imaging conditions. Additionally, the homogeneous coordinate system in a more general way is a good explanation of this calculation or it can be defined by trigonometric considerations. So the displacement of particle is defined as Dx, Dy, Dz between the light intervals. At the moment the particle displacement from x_i to position $x_{i'}$ is obtained with below relation (Prasad, 2000a).

University of Malaya

$$\tan(\alpha) = {x_i'}/{z_0} \tag{2.37}$$

Then the image displacement is obtained of $d = x_i' - x_i$, so(Grant., 1997):

$$x_i' - x_i = -M(D_x + {D_z x_i'}/{z_0}) \tag{2.38}$$

$$y_i' - y_i = -M(D_y + {D_z y_i'}/{z_0}) \tag{2.39}$$

The particle displacement is assumed to be two dimensional in X and Y direction (Dz =0). Therefore by multiplying the image displacement in (-M), the result of that with geometric parameters means the velocity measurement can be determined. However, in practical cases a flow field is never strictly two-dimensional over the whole observation field (Raffel et al., 2007).

The dedicated software algorithms are available that perform analysis of reduced precision within fractions of a second. The software could figure out the one digital PIV recording with several thousand instantaneous velocity vectors, depending on the dimension of the recording, the interrogation area and processing algorithm which is repeated for all the PIV recording interrogation areas.

Particle image velocimetry can be applied in different regions or situations as non-intrusive velocity measurements that help determine the high flow velocity even in boundary layers or near walls and indirect velocity measurement by adding the tracer particles in fluid. The other feature of PIV is it captured the image with high spatial resolution in different phase of fluid with high speed of flows, therefore is a whole new field technique (Lindken & Merzkirch, 2002). Based on the fluid phase as gaseous or liquid the velocity lag and illumination of tracer particles must be noted. When adding the seed to fluid, and following the flow and then tracking the light scatterings with a camera, the accuracy of the size and density of particles that lead to follow the flow

University of Malaya

properly is essential. The small particles faithfully follow the flow better than the large particles, and the large particles illuminate the light (Van Doorne & Westerweel, 2007). Thus the larger particles are more suitable in liquid fluid as they illuminate light better (Adrian, 1991). There are more features of PIV that Raffel et al. (2007) mentioned, therefore these subjects are important. To avoid the blurring of the image, the period of the illuminating beam of light pulse must be concise enough to ascertain the path of the seeds during the exposure of pulse. Contrariwise, it is significant to put intervals between the illumination pulses long enough to afford the better displacement measurement between the images of the seeds with sufficient resolution. In addition, it should be short enough to avoid particles with an out-of-plane velocity component leaving the light sheet between subsequent illuminations (Jahanmiri, 2011).

Furthermore, the particle tracers have to distribute in a homogeneous rate with medium density that promote higher quality of PIV recording in order to obtain optimal evaluation. Based on the paper of Adrian (Adrian, 1991) the particle image density has an effect on the PIV evaluation. The low image density is required to detect the particle individually so the image of the same particle can be tracked from its origination to different illuminations. This estate is Particle Tracking Velocimetry (PTV) technique. Density is required to apply the statistical PIV evaluation techniques in the case of medium image, although the PTV method could use as well. Nevertheless, this technique has no ability to distinguish image pairs by visual inspection of the recording. The high image congestion is estimated in terms of Laser Speckle Velocimetry (LSV). Due to overlapping of the images, individual imagary detection is not possible.

Additionally, the number of illuminations per recording is considerable. Other PIV features include the number of components of velocity vector, extension of the observation volume, temporal resolution, spatial resolution and repeatability of evaluation.

University of Malaya

2.11.2 Basic Requirement of Particle Image Velocimetry

2.11.2.1 Seed (tracer particles)

The first objective of PIV technique is seeding the flow. The material of these seeds must be able to reflect light in order to record the flow field. It is necessary to consider the size of particles as it needs to be large to reflect the laser light and small to follow the flow. So PIV is density depended. The characteristics of scattered light, the capability of aerodynamic tracking and the material of particles based on the applied PIV method is different (Adrian, 1984). The method of seeding based on the experimental phase is different, where natural seeding exists, it is not necessary to consume tracer particles in condition of clear visibility. In the liquid phase of the experiment, seeding would be easy by suspending and mixing solid particles into the fluid until ensure a homogeneous distribution (Melling, 1997). There are many methods for seeding the fluid flow appertain of the experimental phase, as liquid or gas. In addition, there are techniques for seeding the powder characteristic seeding of air flows (dried oxide metals), droplet of oil, air flows seeded (by Laskin nozzle), (Yu & Liu, 2007), and soap bubble seeding for air flows (Melling, 1997; Shields et al., 1968).

The numbers of suitable particles in liquid or gas phase are classified in Table 2.4 and Table 2.5. If the particles are homogeneously distributed, and the flow field is incompressible, then the particles always remain distributed homogeneously. Thus, the statistics of the tracer particles are independent of the flow field. This implies that the measurement is not biased with respect to the distribution of tracer particles. Then it can be defined by Liouville's theorem (Cybulski & Mucha, 1997; Westerweel, 1993) and with homogeneous seeding (Liouville's theorem (Cybulski & Mucha, 1997)).

$$\frac{\partial \rho}{\partial t} + U.\nabla\rho + \rho\nabla.U = 0 \qquad 2.40$$

University of Malaya

Where $\frac{\partial \rho}{\partial t} = 0$

And incompressible flow*:* $\nabla \rho = 0 \quad \nabla . U = 0$

A simple way to determine the particle size diameter is by evaluating the settling velocity of the particles under gravity. Assuming that the process is governed by Stokes drag law, the settling velocity U_s is given by (Prasad, 2000a).

$$V_s = U_p - U = U_g \tag{2.41}$$

Where the 'U_p' is the particle velocity.

If the particle density is much greater than the density of fluid the step response of Up typically follows an exponential law (Raffel et al., 2007):

$$U_P = U[1 - \exp(-\frac{t}{\tau_s})] \tag{2.42}$$

with τ_s (the relaxation time) apparent by (Raffel et al., 2007):

$$\tau_s = d_p^2 \rho p / 18\mu \left(\cong d^2 / v \right) \tag{2.43}$$

Studies demonstrated the fluorescent particles are the most suitable seed in liquid flow as the PIV technique successful obtained image recordings with fluorescent particles as the light emitted perfectly. Specifically they are advertised for use in aqueous suspension for micro-PIV. For several reasons, the fluorescent particles are not easily applicable to gaseous flows. First, in general the fluorescently-labeled particles are accessible as aqueous suspensions. And the size of them is not suitable for gaseous phase (Adrian & Westerweel, 2011).

University of Malaya

Table 2.4 : Seeding materials for liquid flow (Raffel et al., 2007)

Type	Material	Mean diameter in μm
Solid	Polystyrene	10-100
	Aluminum flakes	2-7
	Hollow glass spheres	10-100
	Granules-for-synthetic coatings	10-500
Liquid	Different oils	50-500
Gas	Oxygen bubbles	50-1000

Table 2.5 : Seeding materials for gas flow (Raffel et al., 2007)

Type	Material	Mean diameter in μm
Solid	Polystyrene	0.5-10
	Aluminum Al_2O_3	0.2-5
	Titania TiO_2	0.1-5
	Glass micro- spheres	0.2-3
	Glass micro- balloons	30-100
	Granules-for-synthetic coatings	10-50
	Dioctylphathalate	1-10
	Smoke	<1
Liquid	Different oils	0.5-10
	Di-ethyl-hexyl-sebacate(DEHS)	0.5-1.5
	Helium-filled soap bubbles	1000-3000

2.11.2.2 Light sources (laser)

The other basic element in PIV technique is light. The source of light used is the laser which was developed during these years. The reason for using laser in PIV is its ability for high energy density of monochromatic light emission to illuminate and record the detector particles without chromatic aberrations which can be simply clustered into thin light sheets (Jahanmiri, 2011).

University of Malaya

Laser is classified based on the wavelength and power source to gas laser (continuous wave), Helium-neon lasers (He-Ne lasers λ = 633 nm) as in the visible range it has the utmost efficient lasers, have mostly been used for the optical evaluation for photographic images in PIV.

Copper-vapor lasers (Cu lasers λ = 510 nm, 578 nm) as neutral metal vapor lasers are characterized by high average power (1-30 W), therefore the CW operation is not possible due to the long life-span of the lower laser level. The wavelengths of Cu lasers are within the yellow and green spectrum (Raffel et al., 2007).

Argon-ion lasers (Ar^{+} lasers λ = 514 nm, 488 nm) are similar to the He-Ne lasers with very high currents for ionization and excitation and are gas lasers, hence this is technologically much more complicated compared to He-Ne lasers. Semiconductor lasers are produced very compact being 1 cm tall and having in the order of 1mm diameter (Raffel et al., 2007).

Ruby lasers (Cr^{3+} lasers λ = 694 nm) are pumped optically through a flash lamp. The first model of them used as the active medium by ruby crystal rods contained $Cr3^{+}$ ions.
Neodym-YAG lasers λ = 1064 nm and λ = 532 nm are the famous type of laser nowadays. As an advantage it can be clarified that various host materials can be incorporated into the beam is generated by Nd^{3+} ions which is The most important solid-state laser for PIV.

YAG crystals (yttrium-aluminum-garnet) are usually used for laser applications. Nd:YAG lasers have a good mechanical and high reinforcement and thermal qualities (Figure 2.22). By non-radiative transitions and high reinforcement into the upper laser level the excitation is performed (Adrian & Westerweel, 2011).

University of Malaya

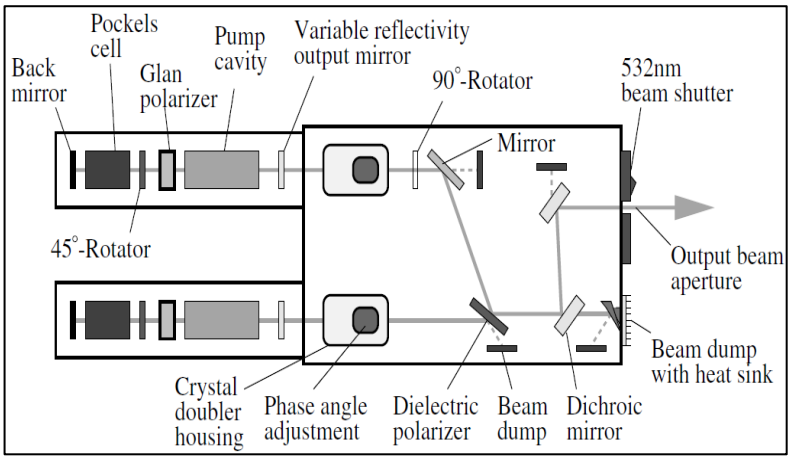

Figure 2.22 : The inside sketch of Nd:YAG lasers made laser system of double oscillator with paramount resonators (Raffel et al., 2007)

Neodym-YLF lasers (λ = 1053 nm and λ = 526 nm) are utilized in applications. It enables efficient frequency conversion through a credible high average-power laser source that produce visible wavelengths involved high-speed PIV methods. The Nd:YLF (neodymium: yttrium lithium fluoride) laser produces the highest pulse energy and average power with the ability to operate at different fundamental wave lengths. It has reiteration rates ranging from minimum of a single pulse up to around 10 kHzl (Adrian, 2005; Raffel et al., 2007).

Different types of laser or light sources could be used in PIV (Grant, 1997) such as more optimally, pulsed lasers or continuous wave (CW) laser. Grant (1997) classified different aspects and the development of laser application in PIV. Laser scanning is the first point in laser development that is considered in this review. For the creation of laser, the beam sweeps or periodically sweeps continuous wave (CW) laser beams through a plane in the flow. In this area the light is emitted directly and the effective illumination level is much higher. Therefore it is an advantage where the laser power is a limiting factor, although it is applicable in low speed flow. Thus the double-beam system is used for higher speed flows near 15 m/s. In addition mirror scanning systems sweep beams of different colour which was devised to record images with higher resolution. Therefore the emitted light

University of Malaya

from a laser is broken by mirror and recorded by camera. Subsequently, flows with higher Reynolds number and with limitation of $R_e = 1000$ is studied using an oscillating mirror as a means of scanning the sheet (Brücker, 1993; Brücker & Althaus, 1992).

Generally in PIV technique to produce argon-ion in the range of a few watts, the continuous wave lasers are used. The frequency-doubled Nd : YAG (neodymium : yttrium aluminum garnet) lasers are typical pulsed lasers that producing 0.1 to 0.3 joules/pulse (Jahanmiri, 2011), at a iteration rate of tens of Hz. The pulsed laser could brighten the particles in a short duration to receive more information regarding the flow field in a shorter time. This laser could divide the pulses interval time to nanosecond pulses. Therefore even very small particle displacement could be recorded easily. Pulsed lasers (laser 1 and laser 2) generate by following the laser pulses through release the stored energy in banks of capacitor at individual time intervals to the flash-lamp. A constant repetition rate of a few tens of Hz obtains the laser (Prasad, 2000a). The delay box produces the required trigger signals, to ensure the camera, computer, lasers and other hardware are synchronized. The cinematic PIV data with a frame-rate symmetric to the lasers repetition rate can be obtained by a suitable hardware. It is necessary ensure overlapping of each laser sheet in order to prohibit poor correlation and unsatisfactory results. Generally, by increase of flow velocity the amount of CW laser energy incident upon a particle decreases thus locates an upper bound on the flow velocity. In contrast, in regard of pulsed laser, the modality of particle images is not in relation with the flow velocity. It is notable that the power of laser and the speed of flow and type and size of particles in illumination can be significant (Raffel et al., 2007).

2.11.2.3 Digital camera (CCD-,CMOS-)

Recently, using electronic imaging through the optical and electronic characteristics of sensors has been replaced by photochemical processing. With the architecture of current

University of Malaya

electronic sensors, the principal of image capturing has been improved. Although the application of these electronic sensors as charge injection devices (CID), CMOS and CCD are modified to PIV technique but considering the errors is essential. In recent years the fast growth of technology in chip production has resulted in the manufacture of the sensor (CMOS) with high quality of resolution and an improved signal-to-noise ratio. However, these sensors cannot apply for high-speed PIV and more suitable for machine vision and digital photography.

The CCD camera converts the light (photons) into electric charge (electrons). A pixel is the individual CCD element in the sensor that is determined between 10×10 μm2, or 100 pixel/mm. A high resolution capacity of the order of 10 000 to 100 000 electrons per pixel is the description of typical CCD sensors (Raffel et al., 2007).

The CMOS sensors which are processed by each pixel electro-optical principal is photoiodiode. These sensors are highly sensitive and have a low noise level relatively. The photodiodes in CMOS sensors can be controlled separately by MOS-FET transistors in comparison to CCD pixels. The new model of CMOS sensors allowed images to be captured using very large scale integration techniques. Moreover, for higher framing rates in place of image resolution is allowed by indicating the region of interest (ROI) (Adrian & Westerweel, 2011).

2.11.2.4 Image capturing

PIV can be recorded in two categories, firstly, a single frame from the lighten flow on and secondly, for each illumination pulse, a single illuminated image (multi frame) which is called “single frame/multi-exposure PIV” and “multi-frame/single exposure PIV” respectively (Adrian, 1991).

University of Malaya

The ability to choose among a single or multi frame lead to the application of PIV in different methods as the assessment of each type is different and variable from other model. In capturing the image some parameters are important such as:

Depth of field (DOF): the optical system used to clarify thickness of the measurement frame, thus based on the focus and focal length of camera lenses the depth of particle fall is significant, or the correlation depth z_{corr}. To obtain a sharp image it is required to determine the DOF. The focal plane may be relocated from the distance point of a source of light and produce an acceptably DOF (focused image) yet, whereas the depth of correlation refers to the correlation function which is contributed with the distance of the focal plane a particle (Raffel et al., 2007). Generally the narrower the width laser sheet image to proper density of particles could lead to a better and clearer image.

The DOF (δ_Z) could calculated with (Marett, 1967) :

$$\delta_Z = 2F(1+M)^2 f\#/10^6 M \tag{2.44}$$

Or (Pan & Center, 1995),

$$\delta_Z = 4(1+1/M)^2 f\#^2 \lambda \tag{2.45}$$

Image size: Adrian (Adrian, 1984) mentioned image size is related to particle diameter d_p , the magnification of lens M, and the point response function (PRF)of the lens(Jahanmiri, 2011). In a gaseous phase the image size could be described as below. An estimate of the depth of field and diameter of particle influence can be obtained using by Gaussian functions and replacing both the Airy function and the particle image, which instruct to the approximation for the image diameter $d\tau = M^2 d_{2GI} + d_{2A}$ generally, M=1, f#=8 and λ=0.6993μm presume in a PIV experiment (Jahanmiri, 2011). When d_P is larger than 50μm then the size of image is effectively the geometrical particle image size (Jahanmiri, 2011). There are two reasons for optimizing the dτ, firstly the particle image diameter strongly affects on the error in

University of Malaya

the velocity measurements (Jahanmiri, 2011). Thus in order to diminish the error and to have a sharp image involves minimizing the diameter of image $d\tau$, and the unpredictability in locating the image centroid or correlation peak centroid respectively (Raffel et al., 2007). Secondly, the image areas decrease with quadratically increasing of the light energy per unit area in order to acquire a particle image intensity enhancement with constant light energy emitted by the seeds particle (Jahanmiri, 2011). Therefore, sharp and small particle images are important (Raffel et al., 2007).

The spatial resolution is calculated by using camera aperture f# determination of the vertex angle (α) of the cone of light and the light wavelength λ. The crossover resolution is determined by the Rayleigh criterion (Jahanmiri, 2011) based on $d1 \approx \lambda/\alpha$ and the longitudinal resolution as $d2 \approx \lambda\alpha 2$ with discounting of constant multiplicative factors (Born & Wolf, 1999). Depend on the required resolution and the recording size of flow field, the recording medium fix on. Fiber optic system for laser delivery is another distinguished subject in PIV system. Therefore in order to have a sharp image, the size of core and rate of energy is important. A combination of a series of mirrors and lenses to produce a thin sheet of light that illuminates the flow field is manufactured by a laser. Laser less PIV is another hardware that has been innovated to captured sharp images. A chip is located in the PC to avoid a high volume of laser, and this chip can control the CCD camera to be triggered automatically by external events or software control. Therefore software controlling allows multiple exposures of different duration within the same digital frame. Previous difficulties with resolution in image intensifier systems were overcome by direct lens coupling between intensifier and CCD sensor array (Grant, 1997). The CCD camera records the images in separate frames with high spatial resolution and could capture multiple frames at high speed with high sensitivity.

University of Malaya

2.11.3 Particle Image Velocimetry Techniques

2.11.3.1 DPIV

Digital particle image velocimetry (DPIV) is the expansion of digital cameras at 512×512 to 2048×2048 pixels and beyond (Jahanmiri, 2011). Pixel is an acronym referred to a single cell within a digital image or on a digital sensor that is concluded from a picture element (Jahanmiri, 2011). Each pixel in an image is associated with a numerical intensity value describing the local gray value or colour (Raffel et al., 2007). The achievement of a PIV image in digital form makes the evaluation of multi-frame and ensemble measurements easier and abolishes the photographic and opto-mechanical stage, thus this method supersedes the PIV. In order to enhance the dynamic range, the composition of multiple framing and multi pulsing can be used in DPIV (Lim et al., 1997). In video imaging, the individual frame to next frame seeds tracking cross correlation has been applied (Grant, 1997). The disadvantage of using DPIV (Jahanmiri, 2011) is the loss of spatial resolution and the low data rate at 25 Hz (Willert & Gharib, 1991). Digital PIV is evaluated in association with Young's fringes formula and expanded by numerical simulation. The tracking algorithms in engineering flows either the relevance analysis methods and even in transonic flows have been proved a profitable method to evaluate the DPIV (Bryanston-Cross et al., 1995).

The DPIV is applied when two ordinal digital images are overlapped and analyzed at one specific area through an interrogation frame. Subsequently an average spatial modification of particles is provided in the illuminated plane. This spatial shift is illustrated quite simply with a linear digital signal processing model, an area named as input with variables of m and n, and the other area in the next images as output named g(m,n) correlate with the sampled area of another image taken at a time Δt later (Jahanmiri, 2011). These two components are called spatial displacement, and an additive

University of Malaya

noise process. Where the direct displacement of tracer particles is from the edge to sampling region, the effect of three dimensional motions disappear the particles in the laser sheet, thus the reduction of the total number of particles present in the window emerged (Westerweel & Nieuwstadt, 1991).

2.11.3.2 High-Speed DPIV

This new method has been developed for quick process monitoring and improved flow measured through an ultra-high-speed video (Johnson et al., 2009; Raffel et al., 1995; Stasicki & Meier, 1995). The system delivers up to eight frames and display times are decreased to 0.06 ms and intervals of 50ns. The used camera has a beam splitter mirror and eight frame-grabber cards and the time of image capturing is controlled by the electronic shutters (Jahanmiri, 2011).

2.11.3.3 Cinematic PIV

The other method under investigation is the temporal and spatial resolution of flow fields applied in cinematic PIV. Earlier related work used shadowgraphs recorded as high-speed motion pictures which were digitally analyzed to study fluid mixing (Lindken & Merzkirch, 2002). In this method a high-speed drum camera has been used to conduct time-resolved PIV studies in low seeding density conditions. Recent studies have focused on a high seeding density regime using the cinematic PIV method to obtain high-resolution measurements in a free shear layer (Oakley et al., 1996). With the setup of a laser scanning system synchronized with the camera capture of three images for each particle per frame, there was a consequent improvement in the signal-to-noise ratio in the correlation plane.

University of Malaya

2.11.3.4 Three component methods

In spite of the advantages of PIV, this technique has a disadvantage in tracking the particles. All tracer particles could only be identified in the time that particles were in the thickness of the laser sheet light, and when out of that, this method lost the motion of particles. Therefore the other type of setup did add to the PIV. All methods used have considerable experimental and processing difficulties. Raffel et al. (1998) classified the other methods used as stereo graphic (Chang et al., 1984), holographic (Thompson, 1989), multiple-plane (light sheet) (Utami & Ueno, 1984) in methodology, with some studies combining these techniques (Grant et al., 1991).

In order to understand the out of plane velocity component, an investigation into the errors identified is required. Moreover, in three dimensional particle image velocimetry, the number of equipment required increases. The second camera is added in the basic level of PIV in 3D, and the images captured will provide further knowledge of the plane vectors which are generally referred to as stereoscopic PIV recordings (Adrian, 1999). Whilst the distance to the principal imaging optics axis expands the loss of local velocity vector error increases. Therefore managing the selection of wide viewing distances in comparison to the imaged area is the solution to reduce or diminish the projection error. By changing the focal length of lenses this goal is achieved.

In stereoscopic methods two different approaches can be used, the angular approaches of cameras must be at a specified angel with the sheet of illumination. The illuminated sheet is perpendicular to the distance between the optical axes of the cameras and strictly related to the stereoscopic effects. Nevertheless, the common field can be easily increased by changing the position of the back of the camera in relation to the lens (Prasad, 2000b). Currently the use of angular displacement arrangement of CCD cameras is more accepted between researchers (Prasad, 2000b).

University of Malaya

Figure 2.23 shows the stereogrammetry lateral observation system which utilizes two adjacent identical cameras C_L and C_R, with a parallel optical axis. The center of the two image planes are O_L and O_R. The relationships between the object point, P(*X*, *Y*, *Z*), and the corresponding images on the two film planes are where *i* is the distance of the image plane from the lens center. This is identical for the two views since the cameras are identical, and *d* is the camera separation. Three-dimensional measurements are only possible in the region where there is overlap of the two views (Grant, 1997).

$$X_R = \frac{X-d}{z} i \, , X_L = \frac{X}{z} \, i \tag{2.46}$$

$$y_R = y_L \frac{y}{z} i \, , Z = \frac{i}{x_L - x_R} \, d \tag{2.47}$$

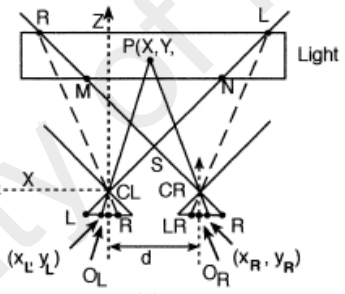

Figure 2.23 : Lateral displacement stereogrametry (Grant, 1997)

Figure 2.24 shows the other point of view in PIV stereogrametry. The camera lens centres are located at C_F and C_B on the optical axis. The real-world coordinate system is taken as cylindrical with the origin at C_F and the Z axis which coincides with the optical axis. The relationships between the real-world point P(*R*, a, *Z*) and its images (r_F, a_1) (r_B, a_2) are:

$$\frac{r_B}{i_B} = \frac{R}{Z+D} \qquad \frac{r_F}{i_F} = \frac{R}{Z} \tag{2.48}$$

$a_1 = a_2 = a$

or

University of Malaya

$$Z = \frac{r_B i_F}{r_F i_B - r_B i_F}\, d \tag{2.49}$$

$$R = \frac{r_F i_B}{r_F i_B - r_B i_F}\, d \tag{2.50}$$

Where i_F and i_B are the image distances from the respective image planes to the corresponding camera lens centres. The two cameras have different magnifications but corresponding image points are found at the same azimuthal angle in the two images (Grant, 1997).

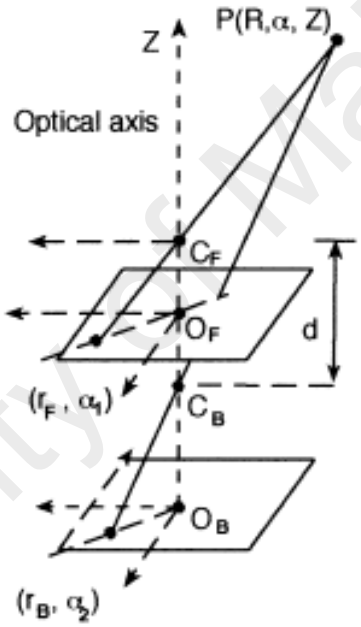

Figure 2.24 : Axial stereogrammetry (Grant, 1997)

Therefore, the temporal and spatial resolution achievable more or less is similar between stereo (3C) and 'classical' 2C PIV (Jahanmiri, 2011). The lack of access to achieve a comprehensive fluid velocity is the reason different PIV methods are used to achieve a common goal.

University of Malaya

2.11.3.5 Multi-plane stereo PIV

Multi-plane stereo PIV is a method that uses 1 to 4 cameras in combination with mirrors to catch the vectors, especially out of plane vectors (3dimensional) in order to simulate the flow velocity. Several surfaces of the flow field to be irradiated simultaneously requires in this method. A separate camera records the image of particles within each of the light sheets. The correlation of images is processed by different wavelengths polarization of laser light used for illumination. However this method does not capture a complete volume but depicts the same properties as stereo PIV (Jahanmiri, 2011).

Based on this method, displacement can be calculated based on the different velocity fields available on different planes and with space-time correlation. With this method the key equipment required is the polarization and color filters on sensors as well as cameras. The angel of the two cameras must be placed in one direction and the illumination of these two cameras will be broken using mirrors to reflect in the opposite direction of the other two stereo PIV systems.

2.11.3.6 Holographic PIV (HPIV)

In order to illustrate the flow velocity fields completely in three dimensional images the Holographic PIV methods (HPIV) are applied (Grant et al., 1991; Thompson, 1989). The particle images are introduced on high resolution photographic material (photochemical holographic PIV (P-HPIV)) and without temporal resolution a high spatial resolution in a medium sized volume achieve. This process is applied by CCD sensors (digital holographic PIV (D-HPIV)) capturing at a faster rate in small volumes.

University of Malaya

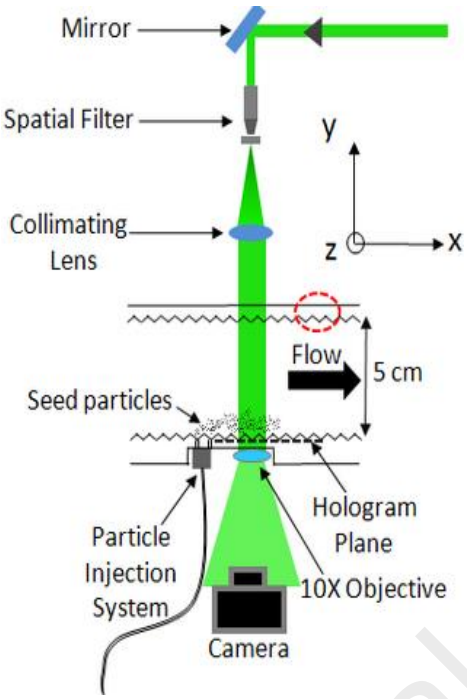

Figure 2.25 : Schematic of HPIV set up (Hopkins, 2014)

2.11.3.7 Volumetric PIV

The other new technique is volumetric PIV (volume PIV or tomographic PIV) which is carried out in a depth of content through simulation perception. This uses multiple cameras in various viewing angels to catch information.

2.11.3.8 Image properties and multiple-sheet methods

In the image properties method two parallel light sheets of different colors are used. An indication of the cross-sheet motion can be obtained from an inspection of the color of the images. Depending on the size of the particles and the brightness of them in the reflection of light, the blur particles or out of plane vectors are assumed to be depth indicators (Dinkelacker et al., 1992).

The other method for estimating the out of plane vectors is the multiple-sheet method which assumes the magnitude of the correlation peak from single-sheet measurements is a means of estimating out-of-plane motion. Despite achieving a normalization purpose,

University of Malaya

the other impacts of having a second light sheet are irrelevant It is also feasible to make out-of-plane velocity measurements by spatial cross-correlation of particle images lying within parallel light sheets (Grant., 1997).

2.11.3.9 Micro PIV

Many areas in the industry and science require the study of micron scale equipment, especially in engineering, to investigate micron scale of the flow field. The micro-fabricated fluidic devices application in industry describe in aerospace (Bayt et al., 2001; Bin Yang et al., 2012), computer (Ayon et al., 2001), automotive and biomedical industries. This method is usable in gaseous and liquid phase.

History shows Santiago et al. (1998) asserted the first Micro PIV device which recorded images in microscopic systems with a spatial resolution sufficiently small to exert reliable measurement in this level. This method was used in slow flow rates with a spatial resolution of $6.9\times6.9\times1.5\mu m^3$ and velocities in the order of hundreds of microns per second (Raffel et al., 2007) . The principal of this method is the same as the PIV method for large scales. The difference being that in a two-dimensional measurement plane, the optical velocimetry technique is operated using digital imaging methods and conventional microscopy for the quantitative determination of two-component velocity data.

Figure 2.26 : Schematic of Micro-PIV(Lavision, 2014)

University of Malaya

The area of investigation for a 5×magnification lens and a 100×magnification lens could be in a range of 1×1 mm^2 to 50×50 μm^2, respectively. Based on the interested target zone, information of velocity interval is selected at 1 μm (Lindken & Merzkirch, 2002). Currently, the maximum spatial resolution adjusts at approximately 1μm in these advance techniques. As previously discussed, the density of particle tracer and the focus of the camera must be noted as the seeds follow the flow faithfully. The highest possible sensitivity/quantum efficiency should be tuned in camera to capture a high image quality. Moreover, for reducing the interval of time between two consecutive recordings to 1μs using of double-shutter cameras is effective, thus it allows measuring the high velocities at high magnification. Researches prove the fluorescence tracer particles are more suitable in the μPIV technique (Raffel et al., 2007).

2.11.4 Error in PIV System

All of the measuring techniques have errors in wide to small ranges, as there is always noise in the recorded images called random error. By attentive selection of experimental conditions the certain errors can be reduced, although attention to noise or other errors cannot be completely achieved as some natural conditions always exist in image recording by PIV systems. The Bias error is the process of computing the signal peak location to sub-pixel accuracy. This mistake is a result of pixel-locking whereby the nearest pixel influences on the signal peak location and it is biased towards it whilst replacing a curve-fit or centroiding schemes with the discretized signal with sub-pixel accuracy (Prasad, 2000a). Moreover, deformation and rotation of the turbulent flow within an interrogation spot leading to loss of correlation causes the gradient fault. As mentioned before, the size and density of particles is significant because if particles do not follow the flow without the slip, tracking errors will result. Acceleration error is one that typically exists. It is happened from the Lagrangian motion of tracer particles that approximating creates the local Eulerian velocity (Adrian, 1991).

University of Malaya

2.11.5 Particle Image Velocimetry Analyzed

When a small quantity of seeds acting as scattering point are added to a studied area, the motion of these tracer particles is tracked by digital camera. The collection of images is then captured in a short video and saved as jpg files on a disk. At that point, these images are analyzed by software which processes this type of program. Based on the calibration images which are taken at the first of experiment, the software categorizes where the centre of the image is and determines x(up) and y (horizontal) length scales. In addition, the PIV software is able to solve and analyze the images with cross or auto correlation, and perform others analysis using adaptive correlation or mathematic etc.

To achieve a meaningful analysis it is essential to consider all the details of an experiment. The viscosity and density could influence the result, therefore the experiment phase with tracer particles is examined by the Brownian motion(R. L. Brown, 1931). The equation 2-48 establishes a relation between the colloidal diffusion coefficient Di (relation between the thermal agitation and viscous forces) and the colloidal properties (Afonso et al., 2011).

$$D_i = {}^{kT}/_{6\pi\eta r_p} \tag{2.51}$$

Where T is the temperature, η the fluid viscosity, r the particle radius and k is Boltzmann's constant. The larger the radius of the particle, the lower importance it will have on the Brownian motion. The standard deviation of a random displacement of a particle is given by the equation (Einsten, 1903).

$$\sigma_P = \Delta x_P \sqrt[n]{2D}\delta t \tag{2.52}$$

Thus it is important to focus on larger tracer particles to avoid error due to Brownian motion. As the larger particles based on the density and their weight could settle faster so, have an effect on sedimentation. Hence, the equation 2-50 (Prasad, 2000a) is used to calculate the velocity**.** It is demonstrated by images belonging to a pair. In PIV systems,

University of Malaya

the average motion of small groups of particles contained within small regions is known as interrogation spots and is used to investigate displacement. Fundamentally, the whole frame is divided into interrogation spots, and the correlation function is computed sequentially over all spots providing one displacement vector per spot. Therefore when disregarding errors in the images, the determination of the average particle displacement is accomplished by using software to determine the spatial auto-correlation, or it depends on the images of the cross correlation of particle images (Prasad, 2000a).

Within each interrogation area (8 to 64 pixels), the mean displacement (D) is calculated and divided by the inter-pulse (Δt) to reach the local mean velocity. In auto correlation analysis the displacement D must be significant enough to satellite peaks to be discernible from the central peak with directional ambiguity. It means it must be calculated at three peaks of displacement on a computer plot. On the other hand, in the cross correlation analysis the directional ambiguity is not important data even where very small displacements can be measured (~dp). In auto correlation analysis the images are performed from the same frame for both laser pulses recorded on the same sensor(single-frame/double-pulse). The equation 2-50 is used to determine the displacement. The auto-correlation function $R(S)$ of the intensity pattern $I(X)$ of the interrogation spot is (Prasad, 2000a).

$$R(s) = \int spot\ I(X) I\ (X + S) dX \tag{2.53}$$

The direct computation of auto correlation with equation 2-50 is prohibitively expensive. Therefore the auto-correlation function is computed via a two-dimensional Fast Fourier Transform (FFT) of the digitized intensity pattern. Where ♦ represents the correlation operation, and * the convolution operation (Prasad, 2000a).

$$R(S) = I\ (X) \blacklozenge I\ (X) \tag{2.54}$$

University of Malaya

$$= I(X) * I(-X), F[R(S = F[I(X)] \times F^{*}[I(X)] \quad (2.55)$$

$$= |F[I(X)]|^2, R(S) = F^{-1}[F[s|I(X)|^2] \quad (2.56)$$

Furthermore, for the determination of larger particle displacement, the simplest method is time separation. A suitable time separation (Δt) between exposures for a given experiment can be approximated by roughly knowing the expected flow velocity in the object plane (U), the recording magnification (M), and the interrogation spot size in the image plane (d_I). As a general guideline the autocorrelation technique can be used (Adrian, 2005).

$$\Delta t \leq 0.25 \frac{d_I}{MU} \quad (2.57)$$

In the case of recording images from either the first pulse or the second pulse, but not both, the process of cross correlation analysis can be done on the first frame whilst the second yields a unique signal peak without directional ambiguity. Therefore even the high speed aerodynamic flows can be analyzed with the cross correlation method. PIV used Fast Fourier Transform (FFT) cross correlation to digitally examine and track the flow from two digital images (Kuok & Chiu, 2013).

$$F(u,v)+S(u,v)+D(u,v) = G(u,v) \quad (2.58)$$

F(u,v) = [image 1]

G(u,v) = [image 2]

S (u,v) = [spatial shift

D (u,v) = [noise]

The cross-correlation function $C(S)$ of the intensity patterns $I_1(X)$ and $I_2(X)$ of interrogation spots 1 and 2 is:

University of Malaya

$$C(S) = spot \int I1\ (X) I2\ (X\ S)\ dX \tag{2.59}$$

Using the FFT, it is shown that (Prasad, 2000a):

$$C(S) = F^{-1}[F\ [I_1(X)].F * [I_2\ (X)]] \tag{2.60}$$

Overall this study was aimed at illustrating the hydrodynamic behavior of fine sediments (small particles) in retention water using the PIV and exploring the efficiency of the tank in sedimentation using Stock's law. In order to achieve this goal, some primary tests were performed to understand siltation and the relationship between particle size and rheological behavior on hydrodynamic behavior of fine sediment. By applying the particle size distribution test through laser diffraction devices and SEM instruments, in addition the rheological properties were using the rotational rheometer.

University of Malaya

CHAPTER 3: MATERIALS AND METHODS

The increasing concentration and accumulation of suspended sediments (<63 μm) causes siltation, which is most often a result of soil erosion or sediment spill. The high rate of suspended particles causes ecological degradation of a water ecosystem. Thus, studying the hydrodynamic behavior of fine sediments is essential. In this chapter the laboratory techniques are described by preparation of sediment tank which acts as a retention structure and the collection of six soil samples from different regions of Malaysia. To investigate different aspects of fine particles, three experiments were explored. The experiment was started by the investigation of physical characteristics using laser diffraction and scanning electron microscopy. Moreover, the concentration test of fine sediment was related to turbidity, total suspended solid, particle size distribution and color clarification which were studied. Then, the rheological behavior of soil series was examined through rheometry operation. The assessment of fine particle suspension and deposition is costly and restraining. This study intents to show an unprecedented direct view of fine sediment hydrodynamic behavior in retention structures with different hydraulic features using particle image velocimetry (PIV). Finally, the impact of size, depth, flow rates and outlet configuration in settling velocity was surveyed.

3.1 Preparation of Sediment Basin

Two tanks of different sizes were prepared to perform the experimental testing required for this study. The larger tank was $60 \times 45 \times 35$ cm^3 and the smaller tank was $40 \times 45 \times 35$ cm^3. To create a water circulation system, three pipes connected the two tanks and there was a valve on each pipe. The last section designed was a long pipe that bridged the small tank to the large tank and a pump was embedded on this pipe.

University of Malaya

Figure 3.1 : The studied area of experiment with flow direction from left to right side

3.2 The Experiment Preparation

Six different soil series were collected from various regions of Malaysia for the experimental study. The soil characteristics are defined in Table 3.1. The six soil samples were sieved (<63 μm) and the pH was measured using 0.01M calcium chloride solution and exchangeable cations (Stojanović & Marković, 2012).

Figure 3.2 : Images of the sieved (<63μm) soil samples: 1/Sample 1 Loamy sand, 2/sample 2 Sandy loamy clay, 3/Sample 3 Sandy clay loam, 4/Sample 4 Clay, 5/Sample 5 Clay, 6/Sample 6 Sandy Clay.

In this study, the percentage of different grain sizes within a sieved soil sample was determined by different methods including Laser Diffraction Particle Size Analysis (LDPSA) and Scanning Electron Microscopy (SEM). Hence, an S-curve could be drawn for these tests. Moreover, the texture and shape of particles were clarified with more detail

University of Malaya

using SEM. All these fine particle characterization results led to identifying the properties and behavior of the soil samples using Particle Image Velocimetry. The next test for more clearly visualizing these six soil series involved studying the rheological properties of the fine particles.

Table 3.1 : Real soil samples characteristic

Number of soil samples	Sand% Actual Soil	Silt % Actual Soil	Clay% Actual Soil	Texture	Bulk Density g/cm^3	Location in Malaysia	SOIL TAXONOMY 1992
Sample 1	80	8	12	Loamy sand	1.348	Lombong Besi	Aluvium
Sample 2	53	33	14	Sandy loamy clay	1.370	Bukit.Besi, Terengganu	Aluvium
Sample 3	63	19	18	Sandy clay loam	1.274	Kg,Gumum,Tasiki Chini,Pahanag	Siri Bungor
Sample 4	35	11	54	Clay	1.222	Kei,Milai,Tasiki Chini,Pahanag	Siri Rasau
Sample 5	25	31	44	Clay	1.214	Kei,Milai,Tasiki Chini,Pahanag	Siri Rasau
Sample 6	44	30	26	Sandy Clay	1.246	Kei,Milai,Tasiki Chini,Pahanag	Siri Melaka

All results from the above tests were compared so as to order the simulated seed particles for PIV analysis (Figure 3.3).

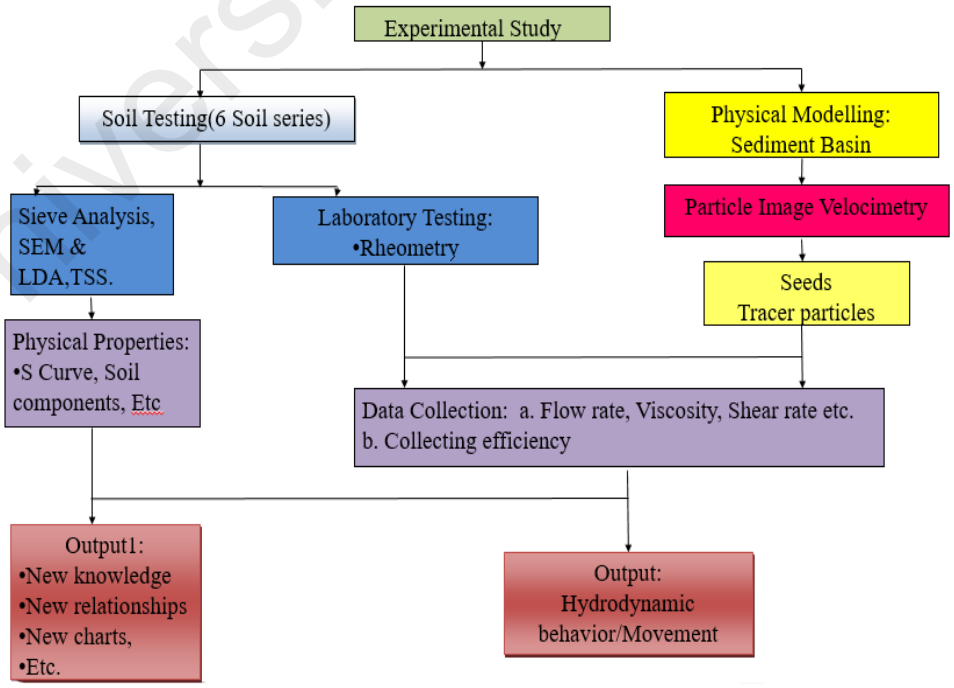

Figure 3.3 : The Procedures step of experiment

University of Malaya

3.3 Examination Method

The main focus of this study is to investigate fine sediment transport in water using particle image velocimetry. Therefore, the design of the independent and dependent variations in the simulated structure (the tank described in the first part of this chapter) was planned. Three different laboratory tests were expanded to examine the different aspects of the fine particles. The physical characteristics were explored by laser diffraction and scanning electron microscopy, then the rheological behavior was examined through rheometry testing. These two tests helped understand and describe the other hydraulic parameters affecting sediment movement. Finally, particle image velocimetry was developed. Here, the various conditions of the hydraulic parameters were expanded.

As the main question of scientists regards the different appeal of fine sediment for various retention structure levels, some natural conditions were designed in the laboratory to explore the influence of hydraulic parameters on fine particle movement. Since retention structures generally have an inlet and an outlet, depending on the water depth the upper valve was opened as an inlet, and two different outlets were explored. The next variation was water flow velocity. The maximum pump flow rate in the designed basin was used with 11 L/m flow velocity and the second velocity was studied at 5.5 L/m. Therefore, the water flow was transitional and the fine particles moved in water with similar to natural behavior. The small tank acted as a reservoir for the large tank. Thus, the impact of particle size, depth, inlet and outlet configuration, and flow rate on the larger tank was determined. The water and fine soil mixture (15% soil+ 85% water volumetric concentration) with mixed fluorescent particles at 20 - 50 µm (sample 1) and 1 - 20 µm (sample 2) was poured into the large tank (study area) up to the selected depth in each

University of Malaya

experiment to study the impact of water level on fine particle settling in the entire retention structure.

The depth of 25 cm was selected for the first experiment. The middle of the three connecting pipes was open as an inlet and it was the pipe nearest to the water surface. The lowest pipe was in front of the inlet near the bottom of the tank, and it was open as an outlet point (Figure 3.4). Based on the particle size distribution results, various fluorescent polymer particle sizes ranging from 20 to 50 µm and with different diameters (Hadad, 2013) were applied to investigate the hydrodynamic behavior of fine particles in a retention structure. The study locations are marked in Figure 3.4.

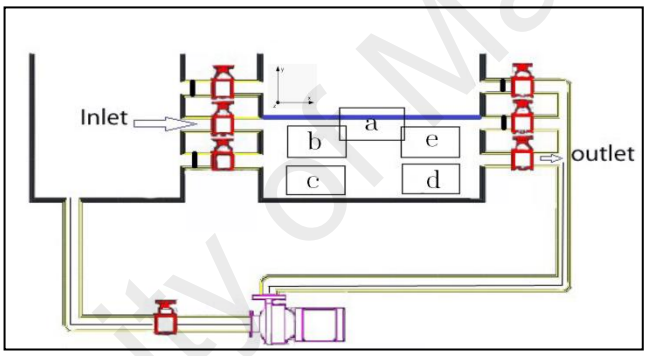

Figure 3.4 : Sketch of designed sediment basin drawn in AutoCAD. The points signify the points of examination: (a) Water Surface level, (b) Near the Inlet (Up) NIU, (c) Near the Inlet (Bed) NIB, (d) Near the Outlet (Bed) NOU, (e) Near the Outlet (Up) NOB. Depending the water level and outlet location other valves are closed.

In the next experiment, using the same fluid concentration and at two selected depths (20 cm and 44 cm), the impact of water level on fine particle settling in a retention structure pond was studied. Depending on the water level, the inlet location was adjusted nearest to the water surface. The last pipe near the bottom of the tank was open. In the second phase of the experiment, the outlet pipe was moved between the first pipes to the same height as the inlet pipe. Two different fluorescent polymer particle sizes (Hadad, 2013)

University of Malaya

were ordered to investigate the hydrodynamic behavior of fine particles in a pond retention structure. The study frame was set in the middle of the tank at a distance of 5 cm from the bottom of the tank and 15 cm from the inlet.

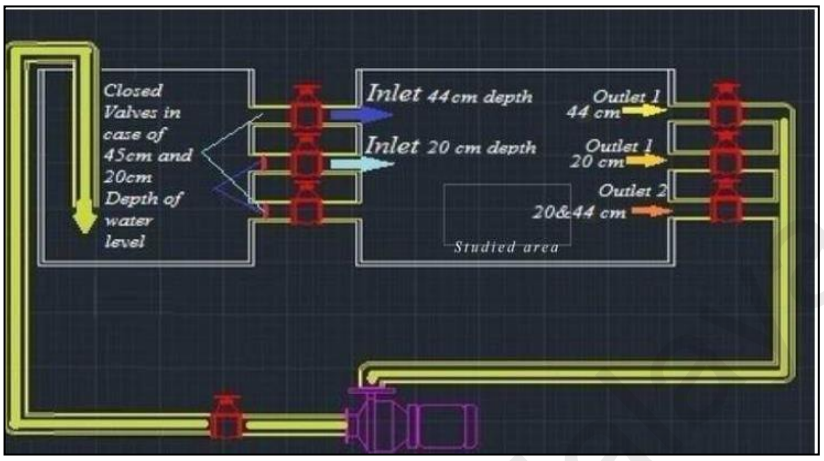

Figure 3.5 : Sketch of designed sediment basin in two water depths. Depending on the water level and outlet place, some valves are closed.

Then the sediment basin was filled up to three water levels: 16.5, 19 and 22 cm (Figure 3.6). The adjusted depths allowed for the investigation of fine particle displacement in the designed sediment basin with different incoming water conditions. According to the distance of the inlet pipe from the water surface the three water inflow stages were higher, in the middle and lower than the water level. The study frame was set in the middle of the tank close to the inlet flow and far enough from the inflow bubbles at a distance of 5 cm from the bottom of the tank and 10 cm from the inlet.

University of Ma

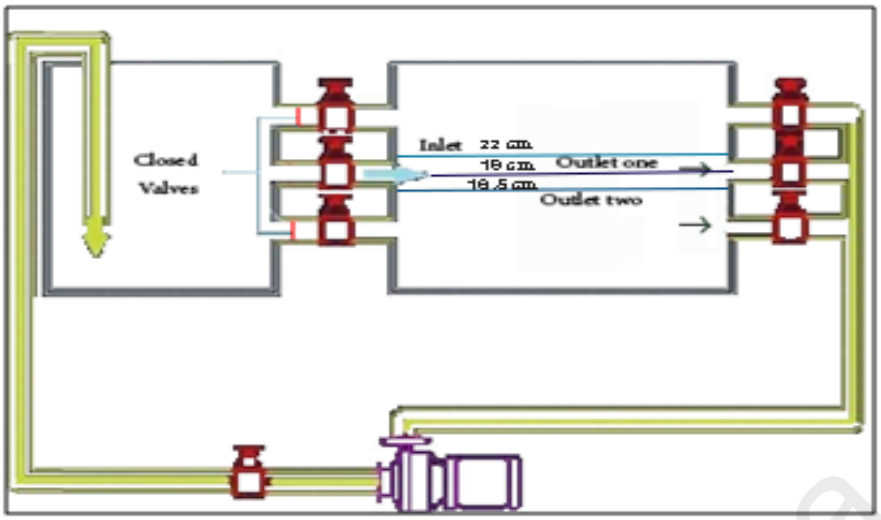

Figure 3.6 : Sketch of designed sediment basin in three water depths, water surfaces are drawn.

All these steps were quantified using the PIV machine that will be described in detail in the next paragraphs. In this study, an attempt was made to model the decay of sediment in changing circumstances. After attempting to use pumping to create water movement that caused a greater flow rate in the tanks. The last aim was to illustrate the relationship between fine particle distribution and decay rate.

3.4 Turbidity and Total Suspended Solids

To realize the effect of turbidity (T) and total suspended solids (TSS), three samples selected with the mentioned characteristics in Table 3.1 are examined. The sieved samples 1, 3 and 4 were selected because of their richness in different type of fine particles.

Suspended and colloidal matter causes water turbidity. It is an optical property expression that causes light to scatter and be absorbed rather than transmitted. Turbidity is measured with a spectrometer and no sample preparation is required except shaking the sample bottle well before analysis. The sample is simply poured into a glass tube and placed inside the instrument with the reference solution and the result is read directly from the instrument in terms of NTU measurement.

University of Malaya

TSS was measured using a water quality probe. First, the water quality probe was calibrated with distilled water, which gives a value of 0 mg/L. Then the probe was inserted into the water sample and a TSS water sample value was obtained in mg/L. The TSS also represents the turbidity of the water.

Therefore, the three sieved samples were weighed, after which the weights of fine and coarse sediments were measured. Next, a beaker was filled with 2 liters of distilled water and 0.5 g of fine sediment (250 mg/l) were added (Figure 3.7). In the next test level, this amount was increased to 1.0 (500mg/l), 2.0(1000mg/l), 3.0(1500mg/l), 4.0(2000mg/l), 5.0 (2500mg/l), 6.0(3000mg/l), 7.0(3500 mg/l), 8.0 (4000 mg/l), 10 (5000mg/l) and 12g (6000 mg/l). At those times, the TSS content and turbidity of the water samples were measured using a TSS analyzer and spectrophotometer, respectively.

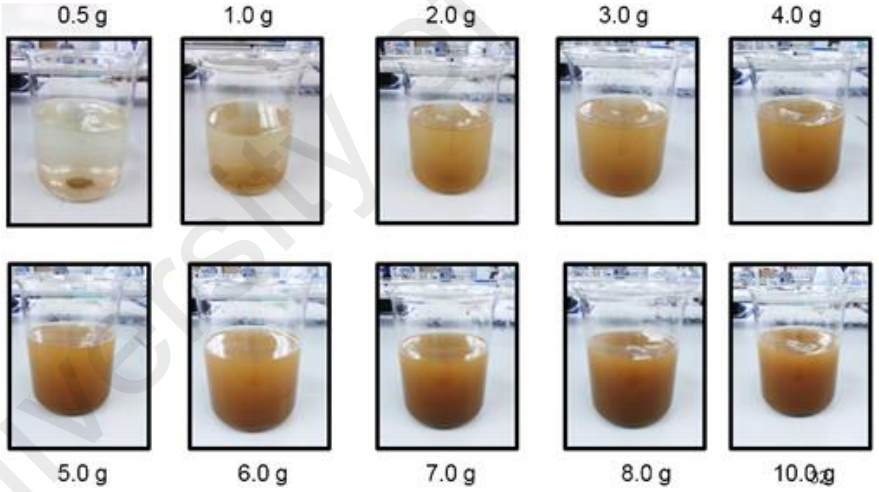

Figure 3.7 : Sieved Samples with different amount of soil

3.5 Laser Diffraction Particle Size Distribution

The fine particle size distribution was obtained after the sieved samples were measured with Laser Diffraction Particle Size technique (LDPS, Malvern Mastersizer 2000 Particle Size Analyzer). 800 mL of distilled water was poured in a specific plate of the machine. After the plot of the aligned measuring software process showed the laser diffraction

University of Malaya

instrument was ready, a very small sample amount was added by spoon to the distilled water. Then the 16-18% concentration was observed through software detection in plots after instrument measurement started. The particles were passed through a laser beam and the light they scattered was collected over a range of angles in forward direction over time. Subsequently, the diffraction angles were, in the simplest case, inversely related to particle size with a refractive index of 1.4. The selected refractive index produced the best result in particle size distribution (Eshel et al., 2004; Stojanović & Marković, 2012). The raw data were software-analyzed in the next step using laser diffraction that allows scientists to redo the analysis process by changing the optical parameters. The laser diffraction device must be calibrated each time after use, so the designed plate was filled with distilled water and the machine was run at different speeds of 3000, 2500 and 2000 rpm for 6 minutes.

The diameter result calculation in the plots was based on Rayleigh/Mie's theory, where it is assumed that a particle is a perfect sphere. To calculate the diameter of particle size the following equation was used:

$$D[m,n] = \left[\sum V_i {d_i}^{m-3} \Big/ \sum V_i {d_i}^{n-3} \right]^{1/m-n} \tag{3.1}$$

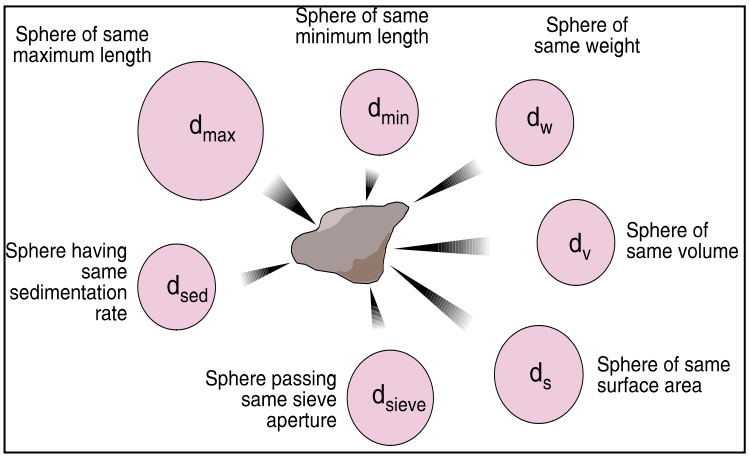

Figure 3.8 : The variation of spheres and the definition (Kippax, 2005)

University of Malaya

The soil colors were measured using the Munsell chart.

Figure 3.9 : The variation of six samples color

3.6 Scanning Electron Microscope

Scanning electron microscopy (SEM) is a technique well-suited for the characterization of the inner surface of soil samples and the texture of fine particles to determine the surface roughness as well as to monitor the formation of soil particles. Through SEM, all qualitative and quantitative information regarding the morphology of soil samples with greater details as pores are obtained by minimizing the complexity and time required for analysis. Scanning electron microscopy (SEM) was performed by SEM-FIB – Zeiss Auriga, operating at 1 KeV at a working distance of 5 mm and with no metal or carbon coating of the samples. To avoid the effect of moisture on soil particles, the soil samples were dried in an oven for one day at 100˚C. The six sieved samples were mounted onto carbon tape, and then the residuals of the sieved soils were blown away with compressed air. The attractive force between fine particles and the stub was strong enough to keep the fine particles in place and a separate fixture was not required. Moreover, the SEM stub with the soil samples was located in a chamber of the SEM system. The SEM had resolutions of 1.0 nm at 15 kV and 1.9 nm at 1 kV, and acceleration voltage between 0.1 and 30 kV.

University of Malaya

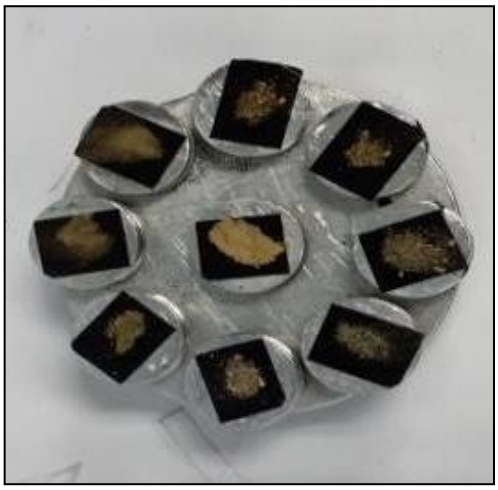

Figure 3.10 : Sieved soil samples onto carbon tape (the black background of soil is carbon tape).

Monochrome photographs were taken by integrated reflex camera. Such photographs provide semi-quantitative information of textural properties, particle shape (Whalley & Krinsley, 1974) and surface roughness (Negre et al., 2004). The soil structure can potentially affect the soil's rheological properties, as it is mentioned in this study that the composition and texture of fine sediments considerably influence the consistency and transport behavior of sediments (Greiser & Wurpts, 2008).

3.7 Rheometry

The rheological properties of fine sediments are investigated in this study to clarify the influence of fine particle texture and roughness on siltation and soil deformation. Six soil samples from different regions of Malaysia (Table 3.2) were sieved with a sieve number <63 μm and prepared to examine at 3 different volumetric concentrations: 70% (70 gr soil / 100 gr water), 45%, and 25%. The different water depth levels showed the selected fine sediment concentrations in water circulation: during runoff 25% of fine sediment can rise up to the top, 45% can be present at the middle level, and 70% can be close to bottom, a phenomenon that can occur during settling. The prepared samples were in homogenized

University of Malaya

phase since the main aim is to study the hydrodynamic mechanism between these particle fractions. The rheological approach developed by Markgraf (Markgraf et al., 2006) was used, where a rotational rheometer (MCR 302, Anton Paar, USA) with parallel plates operating in flow mode and amplitude sweep mode were used to determine the constant shear rate (CSR) and stress-strain parameters in controlled shear deformation (CSD) of the soil structure, respectively. Scanning electron microscopy and laser diffraction provided further data about particle shape and surface properties, which can be incorporated into the rheological findings.

The rheological behavior was examined using a modular compact rheometer MCR 302, Anton Paar, USA with a profiled parallel-plate measuring system with 50 mm and 25 mm diameters (Markgraf et al., 2006). The plate geometry of the rheometer MCR 302 with the parallel-plate measuring system (PP MS) was determined by the plate radius R. Because the soil particle size and the particles' muddy phase need to be stable and not break during rheometry, the parallel plate measuring system was designated. The distance between the measuring plates was 2 mm. While performing all the tests, a constant temperature of 20˚C was maintained and regulated by a Peltier unit. The generated normal force averaged between 0 and 12 N, which should not exceed during testing (Markgraf et al., 2012).

Flow curve testing was done at a constant shear rate and three different volumetric concentrations for six sieved samples to investigate their rheological behavior. Following this, a small amount of soil was taken out of each sample using a spatula, and the soil was later placed on the measuring plate of the rheometer. The results were represented in a Herschel-Bulkley model. The high sensitivity of the device was supported by an air bearing. The flow test with constant shear rate facilitated measuring the viscosity of fine sediments with various water content levels; the viscosity was then classified according

University of Malaya

to the obtained models as thixotropic, dilatant with pseudoplastic, viscoelastic, viscous, or elastic fluid (Hashimoto et al., 2005).

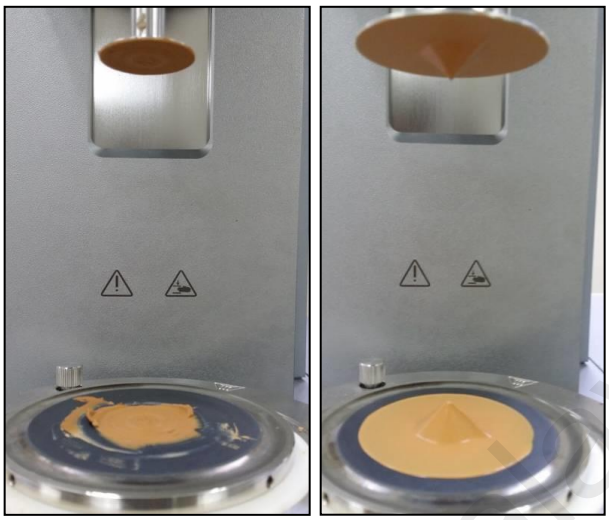

Figure 3.11 : The left image shows the Parallel Plate system 25 mm and the right image shows the parallel plate system 50 mm

Amplitude sweep tests (AST) were done under shear stress, either under steady state or oscillation. In order to quantify and investigate the structural changes of dispersions and/or soil substrates, the stress-strain parameters in controlled shear deformation (CSD) were determined to obtain information about the flow behavior of a substrate and especially its elastic part (stored elasticity), the LVE deformation range (as mentioned in the second chapter), also called the area between the points of the parallel running curves of the storage modulus and loss modulus, and their transition (Fang et al., 2012). Consequently, the information given by yield stress is similar to the deformation limit γ_L; before γ_L is reached, the elastic component prevails the plastic in the case of substrates, which act as a gel in resting state. During γ_L surpassed substance demonstrate plastic (viscous) behavior.

University of Malaya

By conducting the oscillatory test as a subset of the amplitude sweep test, the degree of elasticity-viscosity ratio could be calculated. In amplitude sweep testing, the term 'sweep' characterizes a function with a variable parameter.

A standard resting time of 60s was allowed prior to each test. Meanwhile, the brittle behavior of the clay caused a limitation during testing. Researchers agree that the test duration should be less than 15 minutes (Markgraf et al., 2012). Otherwise, the sample loses humidity and dries up; consequently, the elasticity or viscous behavior of the soil would disappear and the sample would break easily.

The curve characteristics determined by the amplitude sweep test (AST) were influenced by the water content and soil texture during testing. The data are described based on the parameters G' (storage modulus) and G" (loss modulus), where G' is 0 in purely viscous materials and G" is 0 in purely elastic materials, while between these there is viscoelastic behavior. This shows the rheological properties of the samples (fine sediment) as viscoelasticity with water content, texture and particle size. At low strain, the loss modulus and storage modulus are constant. Hence, the increasing strain breaks down the material structure so it does not behave in a linear range and so G' and G" decrease. In the amplitude sweep test, an important indication of the structural integrity range is measurement by varying the applied strain (Van Kessel & Blom, 1998). A concise description of the amplitude sweep test along with the theory of soil rheology was given by (Markgraf et al., 2006). Table 3.2 explains the functions that operate in rheometry.

Table 3.2 : General pre-settings of a flow test and an amplitude sweep test (AST)

Parameter	Amplitude sweep test	Flow test
Plate distance	2mm	2mm
Plate radius	R= 25 mm and 50 mm	R= 25 mm and 50 mm
Shear deformation	γ=0.0001…100%	-
Angular frequency	$\omega=\pi$ s−1 (f=0.5 Hz)	-
Measuring points	30 points	60 points
Duration approx.	15min	360 seconds

University of Malaya

3.8 Particle Image Velocimetry

Particle Image Velocimetry (PIV) is a technique that allows for detailed visualization of fluid flow. Measuring the velocity field of fine sediment flow is of major importance in flood control and water sanitization applications. Traditional PIV setups are limited to single plane measurements. The present study involves an extension of the PIV method to two-phase flow velocimetry. The objective of this study is to conduct velocity measurements to analyze flow consisting of fine particle seeding U_s at two flow rates and different water levels. Based on particle size distribution, two different sizes of fluorescent particles (Hadad, 2013) were ordered to investigate the hydrodynamic behavior of fine particles in water. The specifications of the fluorescent particles are provided in Table 3.3. The experimental setup implemented guarantees obtaining this information using a PIV system to calculate flow velocity fields and a high-speed camera to define the velocity of fine particles.

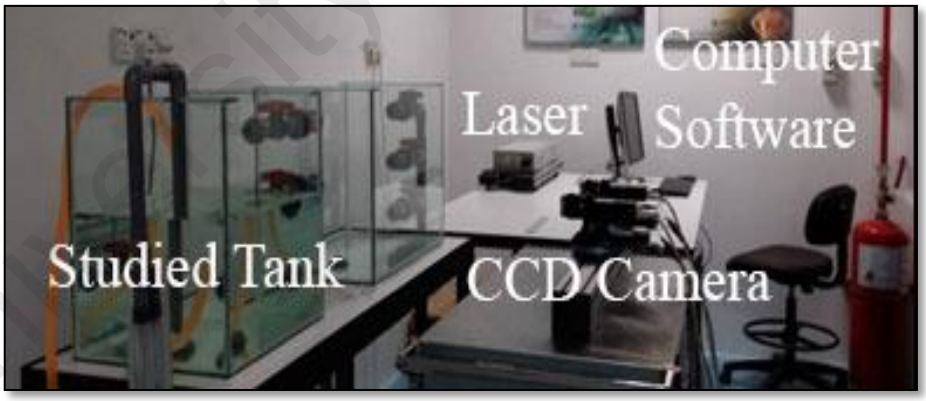

Figure 3.12 : Experimental setup

Seed fluorescent polymer particles of constant density (1.19 g/cm^3) and various sizes were added at a concentration of 10.5 ppm. Since floating or rapid seed settling yields error (Adrian, 1991; Raffel et al., 2007), the density of tracer particles had to be close to water density to avoid error. The seeding had to be constant and sensibly concentrated in

University of Malaya

order to follow the flow as well as possible. The seed particles were injected into the designed sediment basin using a pipette. The fluorescent polymer-based seed particles were homogeneously distributed through the entire particle volume. Then to attain a homogenized fluid, data collection started 15 minutes after seeding the studied tank (Raffel et al., 1998). The duration of data collection was set same in all conditions. In terms of high background level, fluorescent polymer particles can remarkably refine the quality of vector maps from PIV measurements (van Doorne et al., 2007). The experimental setup implemented guarantees obtaining information using a PIV system to determine flow velocity fields and a high-speed camera to define the fine particles' velocity. The receiving optics must be equipped with a filter centered on the emission wavelength (excitation max.: 550 nm; emission max.: 590 nm).

Table 3.3 : Description of seed particles from Dantec Dynamics company

FPP (Fluorescent polymer particles)	
Mean particle size (µm)	10, 30
Size distribution	1 - 20 µm 20 - 50 µm
Particle shape	Spherical
Density (g/cm3)	1.19
Melting point (°C)	125
Refractive index	1.479
Material	Poly(Methylmethacrylate)(Labeled with Rhodium B)

The experimental setup consisted of a transparent tank. Tracer particles were injected in the large tank using a pipette. It is recommended to add the particles in liquid phase and wait until they homogenize in the water (M. Raffel, Seelhorst, U., Willert, C. , 1998), and to use optical equipment aimed to produce laser sheets and to obtain fine particles movement images. The experimental setup depicted in Figure 3.1 shows the $60 \times 45 \times 35$ cm^3 tank with a square cross-section. Three of its sides were transparent glass and the other side was covered with black. The base of the tank was made of glass and the top was

University of Malaya

open. The setup was connected to a pump that produced the flow rate during the experiment. Therefore the maximum flow rate was about 11 L/m with 12000 Reynold number. The fluorescent tracer particles were transported to all areas of the tank with almost laminar flow (C. Van Doorne & Westerweel, 2007).

Figure 3.13 : Fluorescent Particles (Seeds) of two sizes from Dantec Dynamic

Moreover, a drain tap was fitted at the bottom of the column to evacuate the liquid easily after each series of experiments. A CCD camera captured two images within a short period of time in order for the same individual particles to appear in both images. The CCD (Charge-Coupled-Device) camera (Flowsense 8 bit, Dantec Dynamics, 1600´1186 ppi) facilitated registering 8 pairs of photos per second with 256 levels. The camera was placed at different levels for each series of experiments: first it was near the inlet, up and down, then it was set close to the water surface, and finally, near the outlet, up and down. In other experimental runs it was set in the middle of the tank near the bottom.

The experiment was done in a dark room with a laser and image acquisition system provided by Dantec Dynamics. The PIV system comprised the laser and image acquisition system provided by Dantec Dynamics. The laser beam was produced by an Nd-YAG laser (15 Hz, Quantel Big Sky – Twins λa=1064 nm - 532 nm) with maximum power of 800 mJ. The laser beam was transformed into a laser sheet through a thin spherical lens. The laser sheet crossed the column vertically, in a parallel plane. Each time the laser was used,

University of Malaya

the cooling level was checked. This level must be 80% of the volume capacity (800 ml). It had to be ensured that the laser plane was fine by adjusting the spherical lens.

The PIV images were acquired through Dantec Dynamics Version 3.31 software, which has the ability to calculate the size of the examination areas (from 16×16 to 128×128 pixels). Although the resolution is better in a smaller interrogation area, more analysis time is required. Moreover, the overlap value of the image frame can be applied by this program at 25%, 50% and 75%. It means when the value is for example 25%, the tracer particle exploration zone is expanded to 25% of the surrounding areas. This circumstance introduces interdependence and allows following the particles that initially leave the study field. The time between two laser pulses according to the experiment model's velocity and the time between two images captured by the camera can be determined with this software.

The tracer particles were Fluorescent Polymer Particles made by Dantec Dynamics. At the time of image analysis and velocity field determination, the number of tracer particles per area of integration must be noted with the objective of achieving an acceptable velocity field. This number had to be between 8 and 10 (Adrian, 2005). As long as the aim is to obtain the correct velocity field, the tracer particles must follow the flow perfectly.

The seeding had to be uniform and reasonably concentrated in order to follow the flow as well as possible. Therefore, floating or rapid settling of seeds is an error. Thus, the density of fluorescent particles had to be close to the water density to avoid errors (Adrian, 1991).

The velocity vectors were derived from subsections of the target area of particle-seeded flow by measuring the movement of particles between two light pulses.

$$\mathrm{V} = {}^{\Delta X}/_{\Delta t} \tag{3.2}$$

University of Malaya

The time between pulses was 3000μs at 4Hz since the flow was laminar and small particles moved in liquid phase slowly.

For each series of experiments, the first stage entailed focusing the CCD camera on the laser sheet in the presence of fluorescent tracer particle solution with two different particle sizes and the selected water depth. Then the images were recorded to reach calibration and finally, the best syringe advance velocity conditions were tested and determined to achieve clear images of fluorescent tracer particles in the set image frame. The images were then analyzed with Dantec Dynamic's software program version 3.31.

3.9 Collecting Efficiency

Sediment basin used for turbid water sedimentation is evaluated based on the size. This evaluation is based on several equations that are related to the size of the tank and flow rate. The shape of settlement basin can be circular or rectangular. The flow speed (v) in the basin is calculated based on the flow rate (Q) divided by height (H) on the width (W) of the tank.

$$V = {}^{Q}/_{HW} \tag{3.3}$$

HRT (hydraulic retention time), or transit time, is a calculation of the required time for a solid to remain in a storage unit. Where, $t(\theta)$ is the hydraulic retention time.

$$\mathrm{HRT}(t(\theta)) = {}^{\text{Volume of sedimentation tank}}/_{\text{Inflow rate}} \tag{3.4}$$

In this study, two flow rates and two mixture volumes were tested in a settlement basin: 11 L/m and 5.5 L/m at heights of 44 cm and 20 cm. Therefore, the retention time at a higher flow rate would be nearly 7 minutes. If *v* shows the vertical speed, then *h* shows the length that particles travel in the tank. θ is the amount of feed inside settlement basin.

University of Malaya

$$h = V.\theta \tag{3.5}$$

Therefore, if h ≥ H (height of fluid), then the particles reaching the bottom of the basin before the end of the tank are collected. If h < H, then the particles may or may not hit the bottom, depending on the level at which they start. It means particles that begin to settle at a small distance from the bottom will settle and the ones that start to settle far from the bottom will not fall downwards and they will escape with the outflow.

Finally, to understand the collecting efficiency of a tank (the removal of solid particles from a suspension by settling under gravity), the ratio of settling velocity (v) divided by the critical speed is measured. Here, the critical speed (v_c) or surface loading approach by $V_c = {}^{Q}/_{A}$.

The designed rectangular basin can be assumed to be a settlement tank, and based on the information resulting from PIV, the tank's collecting efficiency was accrued. The real flow rate of the tank was calculated by $Q = V/A$, where Q shows the flow rate, v represents velocity and A (width * height) is the tank area. The resulting value can be used to evaluate the sedimentation flow rate in a tank. Sedimentation flow rate describes the movement of sediment inside of tank under influence of hydraulic parameters.

Generally, the settlement rate is measured in a column bath that is connected to several valves at different heights. The sample is collected over time from different regions and the suspended solid is found. Then a table will be drawn with this information. The settlement velocities are calculated in this type of batch through height over difference in time. The settlement ratio is calculated by V_x/V_0, where V_x is the velocity of settlement in different zones and V_0 is the settling velocity in the whole tank.

Here, the same method of analysis was used to study the settling velocity ratio in the tank. Since particle diameter is one of the effective variables on settling rate, in this study an

University of Malaya

attempt was made to evaluate the tank's efficiency under different conditions of flow rate, location, water depth and outlet place.

Consequently, Stoke's Law defining the settling velocity (V_s) can be used to measure the relation between the gravitational acceleration (g), particle diameter (d), density of particles and fluid (ρ) and fluid viscosity (μ).

$$V_s = {d^2 g(\rho_f - \rho_s)}/{18\mu} \tag{3.6}$$

This equation shows the influence of particle diameter on settling velocity. Here, the settling velocity of fine particles from 1 to 50μm with 5 μm diameter interval was calculated. Then the efficiency obtained for this particle size range was determined using the real settling velocity obtained using the PIV method. The settling velocity result for each methodology series was divided into each size settling velocity, thus the relation between particle size and the settlement efficiency of the designed tank by relying on the PIV result was investigated. It indicated that a higher flow rate and less settling time reduced the sediment collecting efficiency.

3.10 Estimation of Settling Velocity

Many researchers have tried to predict the different aspects of sediment transfer in rivers or ponds with the aim to achieve the velocity of particles at the bed or water surface. Generally, it is attempted to solve the problem to reach better solutions with lower expense. However, the part that is neglected regards the extent to which the parameters resulting from the equations and simulations are reliable. In fact, the sensitivity of an applied method cannot cover all influencing factors in nature. With some assumptions, this study assayed to contrast the collected PIV results with the developed equation.

University of Malaya

According to the assumptions, the settling velocity of particles decreases with reduced particle diameter.

Zhiyao et al. (2008) attempted to create a settling velocity prediction formula and compare it with other prediction equations. They ultimately compared the resulting velocities. All formulas are based on the dimensionless particle size d_*, which is calculated by:

$$d_* = (\frac{\Delta g}{\nu^2})^{\frac{1}{3}} d \tag{3.7}$$

Where $\Delta = \rho_s/\rho - 1$(ρ_s and ρ represent the density of particles and the density of the fluid, respectively) , and g is the gravitational acceleration. And d is the particle diameter and ν is the fluid kinematic viscosity.

From Zhu and Cheng (1993):

$$V_s = \frac{\nu}{d}\, d_*^3 (\frac{1}{12cos^3\alpha + \sqrt{144\cos^6\alpha + (4.5\cos^3\alpha + 0.9\sin^2\alpha)d_*^3}}) \tag{3.8}$$

Where α = 0 for $d_* \leq 1$ and $\alpha = \pi[2 + 2.5(logd_*)^{-3}]^{-1}$ for $d_* > 1$.

From Cheng (1997):

$$V_s = \frac{\nu}{d}(\sqrt{25 + 1.2d_*^2} - 5)^{1.5} \tag{3.9}$$

From Ahrens (2000):

$$V_s = \frac{\nu}{d} d_*^{1.5}(C_1 d_*^{1.5} + C_2) \tag{3.10}$$

Where coefficients are calculated

$$C_1 = 0.055\, tan[12d_*^{-1.77} \exp(-0.0004d_*^3)]$$

University of Malaya

$$C_2 = 1.06\, tan[0.016 d_*^{1.5} \exp(-120/d_*^3)]$$

From Guo (2002):

$$V_s = \frac{v}{d} d_*^3 [24 + \frac{\sqrt{3}}{2 d_*^{3/2}}]^{-1} \quad (3.11)$$

From She et al. (2005):

$$V_s = 1.05 \frac{v}{d} d_*^{1.5} [1 - \exp(-0.315 d_*^{0.765}]^{2.2} \quad (3.12)$$

Thus, in this study, the equations were compared with the results for 1, 20 and 50 µm particle sizes according to particle image velocimetry (PIV). The PIV experiment was run using two types of fluorescent particles with various diameter sizes: one type had particles ranging from 1-20 µm and the other from 20-50 µm. Hence, the lowest measured velocity assumed was at 1 µm and the highest velocity was for the 20 µm size for type one; the maximum velocity value resulting from the second type of fine particles was placed for 50 µm. This assessment was applied to the results of different fluid heights and flow rates and the same inlet and outlet height to prevent any error with regard to outlet location.

University of Malaya

CHAPTER 4: RESULTS AND DISCUSSIONS

In this chapter the study demonstrates the results and discuss about it. The aim of this study was to investigate the hydrodynamic behavior of fine sediment. To achieve this goal, some primary experiments were required. Therefore, the particle size distribution was examined using laser diffraction particle size analysis and scanning electron microscopy methods, and the rheological properties of six soil series (< 63µm) were examined to order the tracer particle for Particle Image Velocimetry (PIV). In this chapter, for result clarification, the outcomes of the mentioned experiments are connected to define the relations between particle diameter and shape and the rheological properties in the beginning section. The results of the rheological properties are discussed by considering the LDPSA and SEM results. Further, the relation between rheological behavior and physical characteristics of fine particles and hydrodynamic behavior of fine sediment has been analyzed and particularity discussed.

4.1 Concentration Test

There are three different types of soil being tested in this study. The soil samples of 1, 3 and 4 used. From Table 4.1, it shows the value of Total Suspended Solid and Turbidity with different amount of weight.

University of Malaya

Table 4.1 : Value of Total Suspended Solid and Turbidity in 3 types of soil (Hern et al., 2014)

Weight(mg/l)	Type 1(sample1)		Type 2(sample3)		Type 3(sample4)	
	TSS(mg/l)	Turbidity(NTU)	TSS(mg/l)	Turbidity(NTU)	TSS(mg/l)	Turbidity(NTU)
250	25	2	81	5	109	5
500	58	5	152	10	249	15
1000	121	10	283	16	505	30
1500	207	11	443	26	827	45
2000	234	12	680	37	1150	62
2500	338	24	788	45	1480	78
3000	383	28	954	52	1730	90
4000	593	36	1450	79	2550	117
5000	606	60	2010	88	3120	142
6000	721	75	2500	104	3950	170

4.1.1 Total Suspended Solid (TSS)

For three different types of soil the quality factors of Total suspended solid (TSS) and turbidity were examined. Depend on the proportion of clay content the impact of fine sediment on TSS and turbidity are varied (Hern et al., 2014). Graph in Figure 4.1 proved there is correlation between the fine sediment and TSS, as the the weight of fine sediments increased TSS also increased in all types of soil sample. It is realized the higher content of clay, lead to the higher value of TSS and turbidity where sample 1 with 54% of clay has the highest TSS, then the samples with name of Siri Bungor and Aluvium with clay content of 18% and 12% placed at the next stages (Hern et al., 2014). TSS values has a constant growth from 250mg/l until 3000mg/l and showed rapid expand from 3000mg/l till 6000 mg/l(Hern et al., 2014). The TSS at 8g of fine sediment weight enhanced rapidly to 593mg/L, 1450mg/L and 2550mg/L for soil sample type 1, 2 and 3 respectively (Hern et al., 2014). The TSS had the highest values at 721mg/L, 2500mg/L and 3950mg/L in Sample 1, 2 and 3 respectively (Hern et al., 2014).

University of Malaya

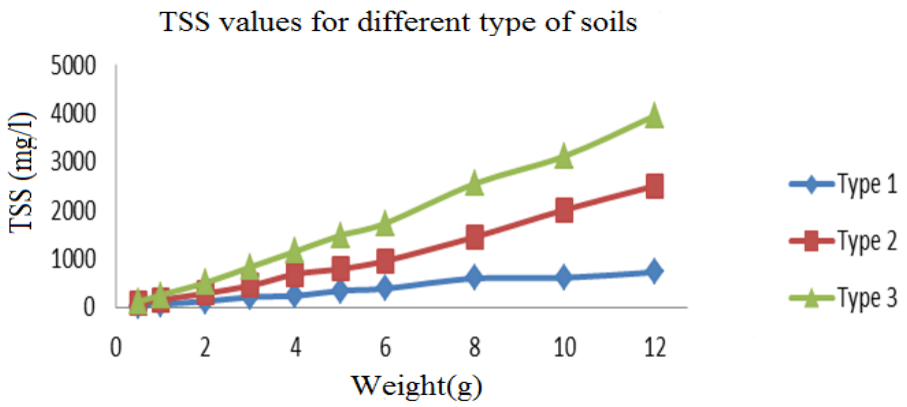

Figure 4.1 : Comparison of Total Suspended Solid (TSS) for different type of soil sample with different amount of weight

4.1.2 Turbidity

The study shows by increases the weight of fine sediments the turbidity increases as well. Other study has investigated there is a linear relationship (Figure 4.2) between suspended silt concentration gravimetrically with turbidity (Divakaran & Sivasankara, 2002).

Therefore, it could be concluded the influence of fine sediment weight on both TSS and turbidity is similar. In here, the experiment results demonstrated sample 3 has the highest turbidity at varying weight of fine sediment followed by sample 2 and sample 1 (Hern et al., 2014). The highest turbidity value was detected at 75NTU, 104NTU and 170NTU for soil Sample 1, 2 and 3 respectively, in weight of 12g fine sediment in all tested soil samples (Hern et al., 2014).

University of Malaya

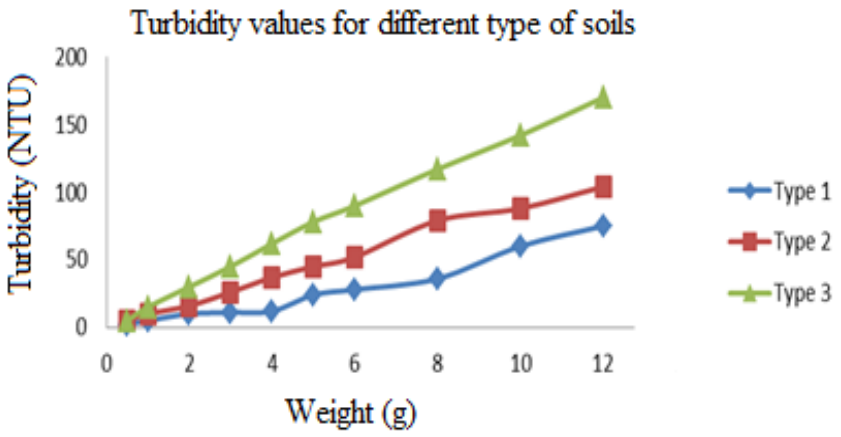

Figure 4.2 : Comparison of Turbidity for different type of soil sample with different amount of weight

Relationship between Total Suspended Solid (TSS) and turbidity had been analyzed for sample 1, 3, and 4. From Figure 4.3, the graph shows that the value of turbidity increased when the amount of TSS increased. Clay soil has the highest R-square value, which is 0.99061 followed by sandy clay loam with 0.972 and loamy sand with 0.8895. The R-square for all type of soil is approach to 1 which means TSS corresponds to turbidity in the high accuracy.

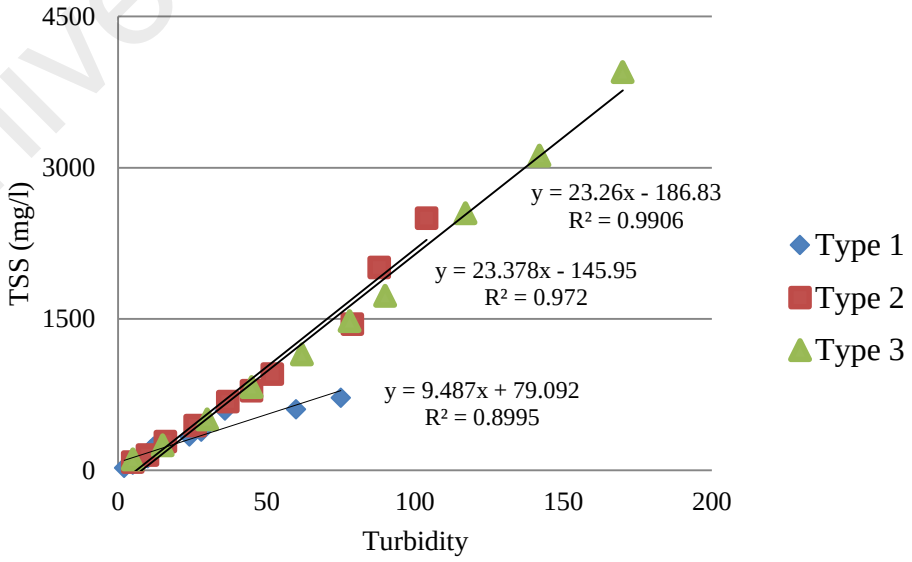

Figure 4.3 : Correlation between TSS and Turbidity in 3 examined soil samples

University of Malaya

4.2 Analysis of Turbidity and TSS

The correlation between TSS and turbidity (Figure 4.3) was established to offer more efficiency in predicting total suspended solids concentration in a retention structure. A positive relationship between total suspended solids concentration and turbidity level suggested that the measurement of turbidity is possibly the most economic option for estimating total suspended solids concentration in a retention structure. The relationship between Total Suspended Solid (TSS) and turbidity significantly differed between the different types of soil sample. TSS can be predicted in real time using turbidity as an indicator parameter. There is a high correlation between TSS and turbidity with a correlation value of 0.9906. Generally it is observed (Figure 4.3) there is a correlation between TSS and turbidity (Bukhari, 2008; Tu et al., 2001) . All graphs demonstrated a positive correlation relationship between TSS and turbidity with a coefficient of determination, R^2=0.9629 (Hern et al., 2014).

4.3 Particle Size Distribution and Color Clarification

4.3.1 Laser Diffraction Particle Size Analysis

The color of samples was recorded based on the Munsell system, Figure 3.2 illustrates the colors of fine sediments and they were classified as sample1 = 10YR4/6 (Dark Yellow Brown), sample2 = 10YR5/6(Yellow Brown), sample3 = 2.5Y5/6(Light Olive Brown), sample4 = 5YR7/6(Reddish Yellow), sample5 = 5YR6/8 (Reddish Yellow), and sample6 = 7.5YR5/8(Strong Brown) which means the influence of organic matter and minerals as iron or manganese are source of the color range (Shields et al., 1968).

According to the British Soil Classification System for engineering purposes BS 5930:1981, the soil fine particles are categorized as fine sand 0.06-0.2 mm, silt 0.06-0.002 mm, and clay <0.002mm. The graph of the particle size distribution is illustrated in Figure

University of Malaya

4.4. The highest volume in the soils was silt. Based on the graph (Figure 4.4), samples 1, 2, 3, and 6 had high-volume particle sizes around 0.05 mm whereas samples 4 and 5 contain high-volume particle size around 0.04 mm. Thus, the results prove that samples 4 and 5 include finer particles in comparison with the other samples. Since the silt and clay encompass more cohesive particles than the sand, this fact might cause different behaviours during the rheological test (Fang et al., 2012).

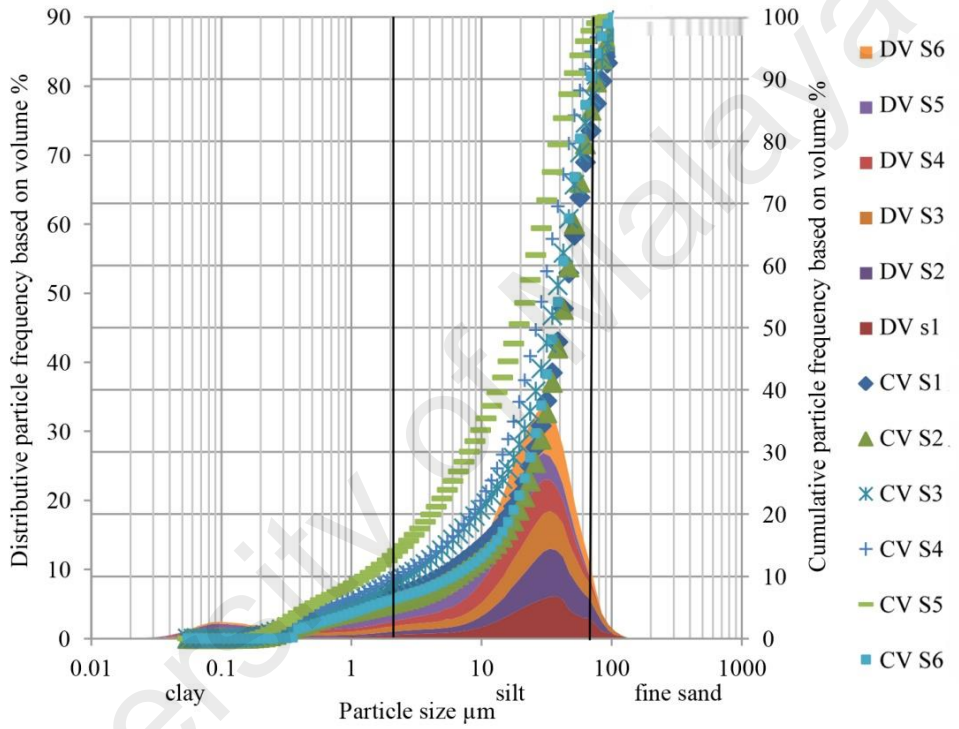

Figure 4.4 : Graph of particle size distribution (Laser diffraction method) of 6 sieved (<63µm) soil samples, Distributive volume (DV), and Cumulative Volume (CV)

4.3.2 Scanning Electron Microscopy (SEM)

The best preparation of soil sample for SEM investigation was drying. Observations of the scanning electron micrographs for soil samples 1 to 6 are depicted in Figures 4.5 to 4.10 which provide semi-quantitative information on the textural properties, the particle shape, and the surface roughness. Since the exchange capacity, the type of cautions, the size of clay particles (Neaman & Singer, 2004), the stress history, the hydraulic state, the

University of Malaya

soil chemistry, and the mineral history influence both the macro and micro fabric of a clayey soil (Al-Mukhtar et al., 1996).

It could be observed the sieved sample 1 particles with 1.00 Kx magnified had more angular shapes with more stability Figure 4.5, also this feature can be observed in the sample 2 (Figure 4.6) which it means the fine sand amount is significant.

Sample 3 (Figure 4.7) showed a feature between sample 1, 2 and sample 4, as it was illustrated the outlook of particles with angular shapes in addition of smooth wall in some particles, however the images with higher resolution showed the stepping plates. The other image (Figure 4.8 and 4.9) showed the particles with roughness as sample 4 and 5 with plates in close resolution.

University of Malaya

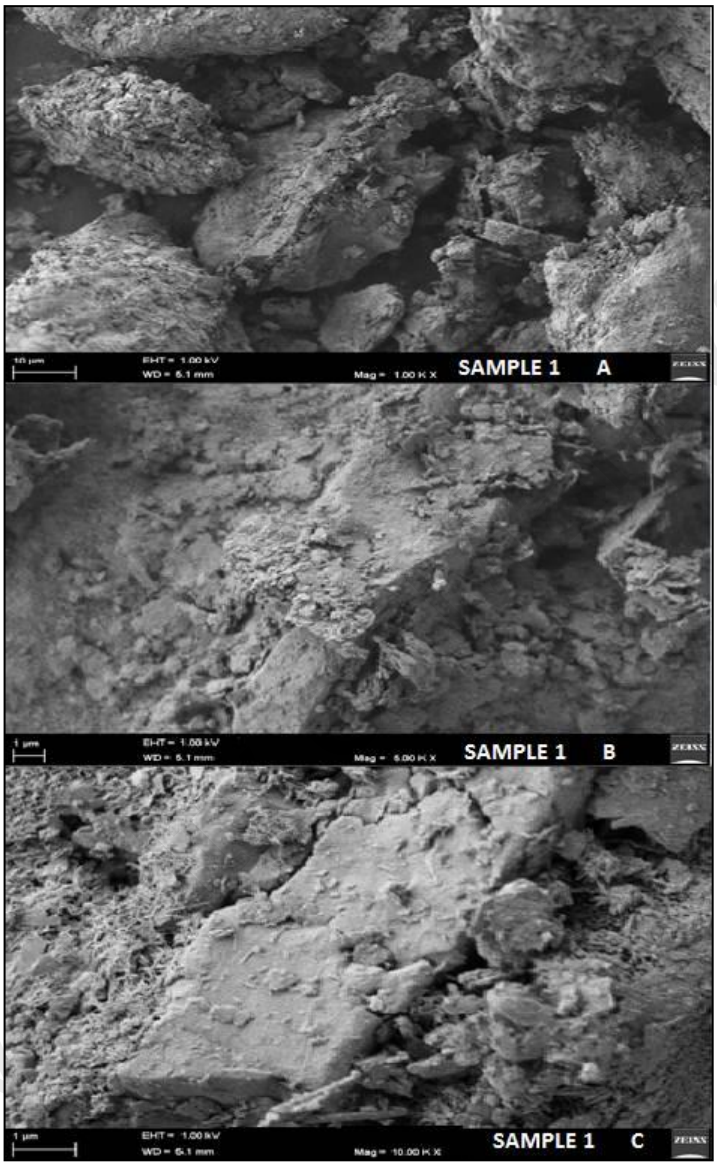

Figure 4.5 : Sample 1 A. 1.00x, B. 6.00Kx, C. 10.00 Kx magnified SEM image of the clay dry-pressed at room temperature

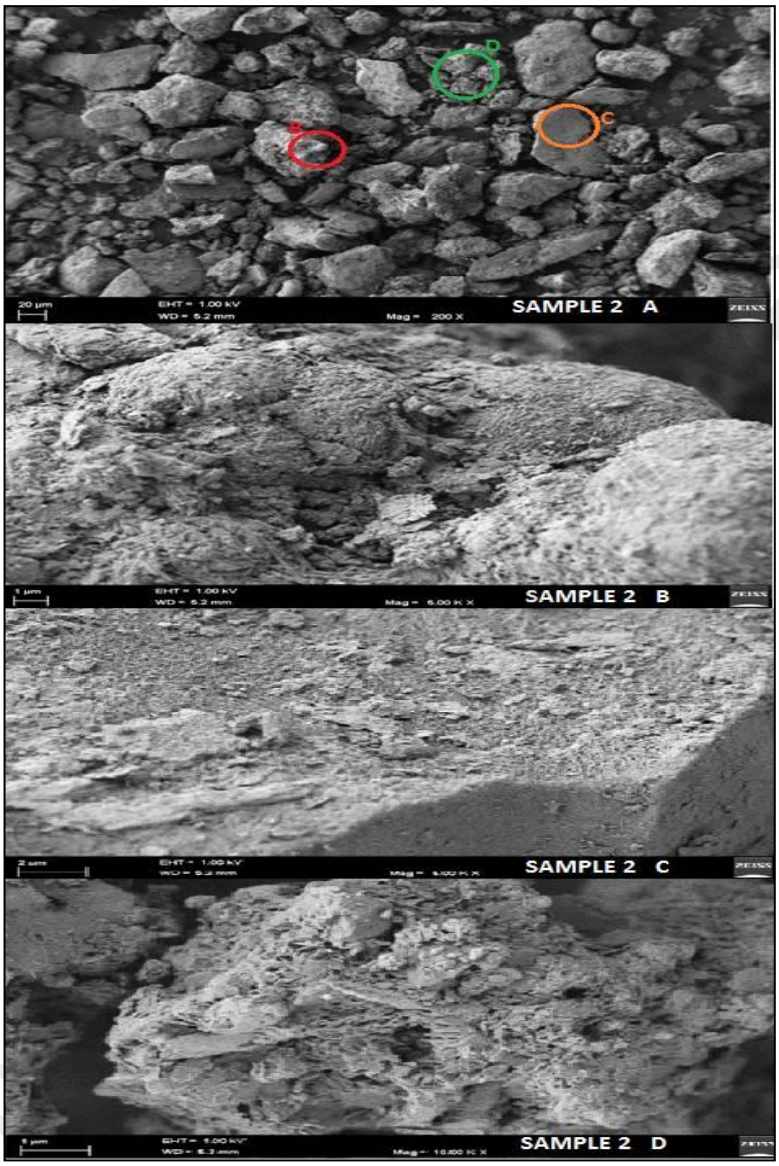

Figure 4.6 : Sample 1 A. 2.00x, B. 6.00Kx, C. 6.00 Kx, D. 10.00 Kx magnified SEM image of the clay dry-pressed at room temperature, more different texture as C. fine sand, B and D. two different type of clay are seen in sample 2.

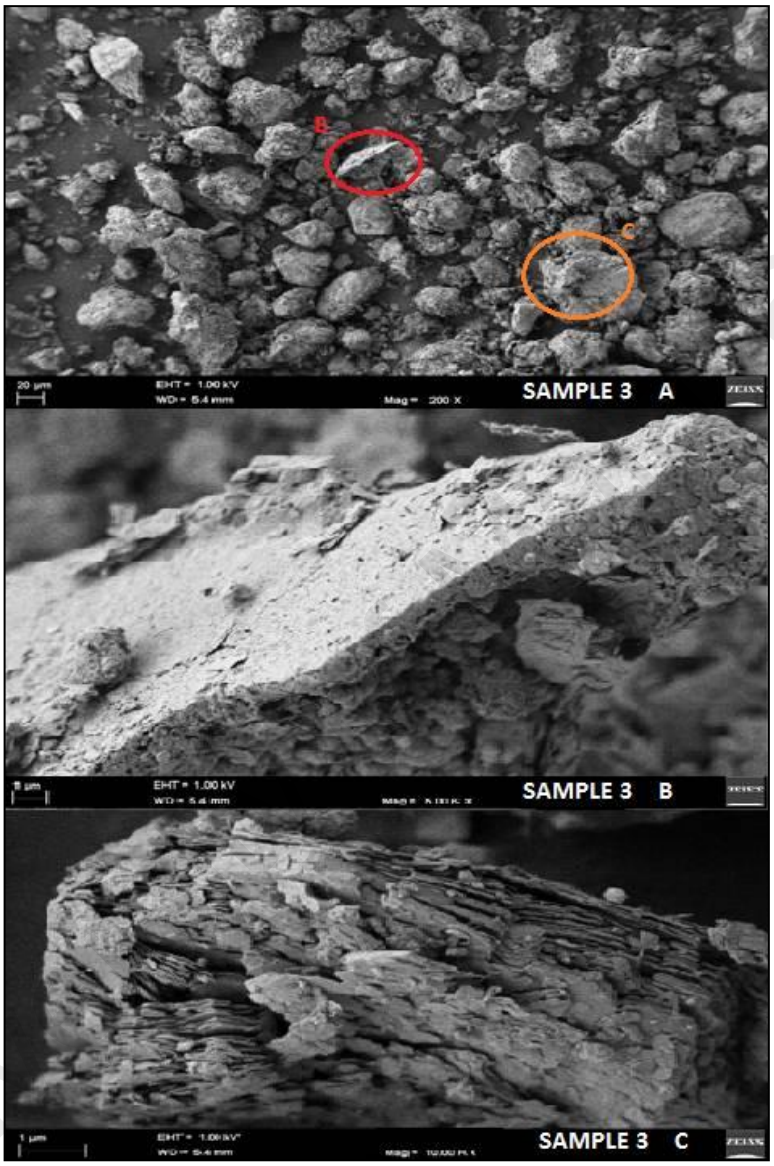

Figure 4.7 : Sample 3 A. 1.00x, B. 6.00Kx, C. 10.00 Kx magnified SEM image of the clay dry-pressed at room temperature, Sample 3 shows both textures of sample 1, 2, 4, and 5.

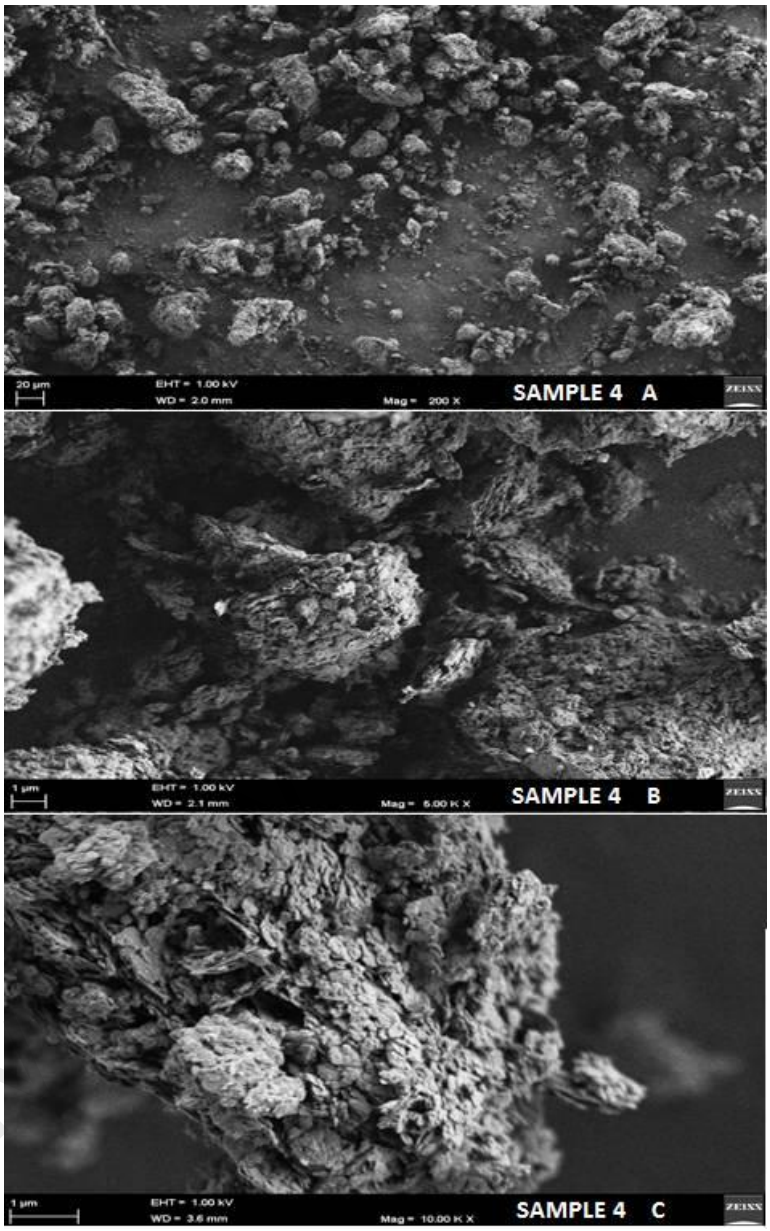

Figure 4.8 : Sample 4 A.2.00 x, B. 5.00Kx, C. 10.00 Kx magnified SEM image of the clay dry-pressed at room temperature

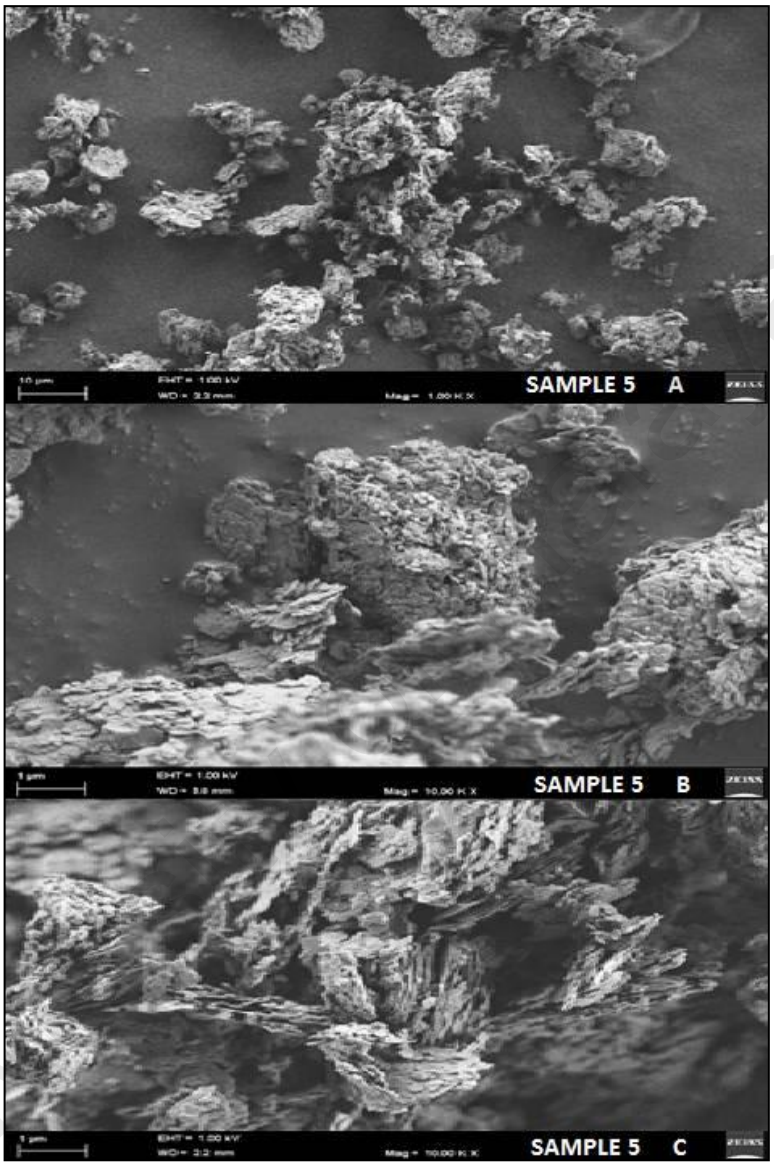

Figure 4.9 : Sample 5 A. 1.00 x, B. 10.00Kx, C. 10.00 Kx magnified SEM image of the clay dry-pressed at room temperature

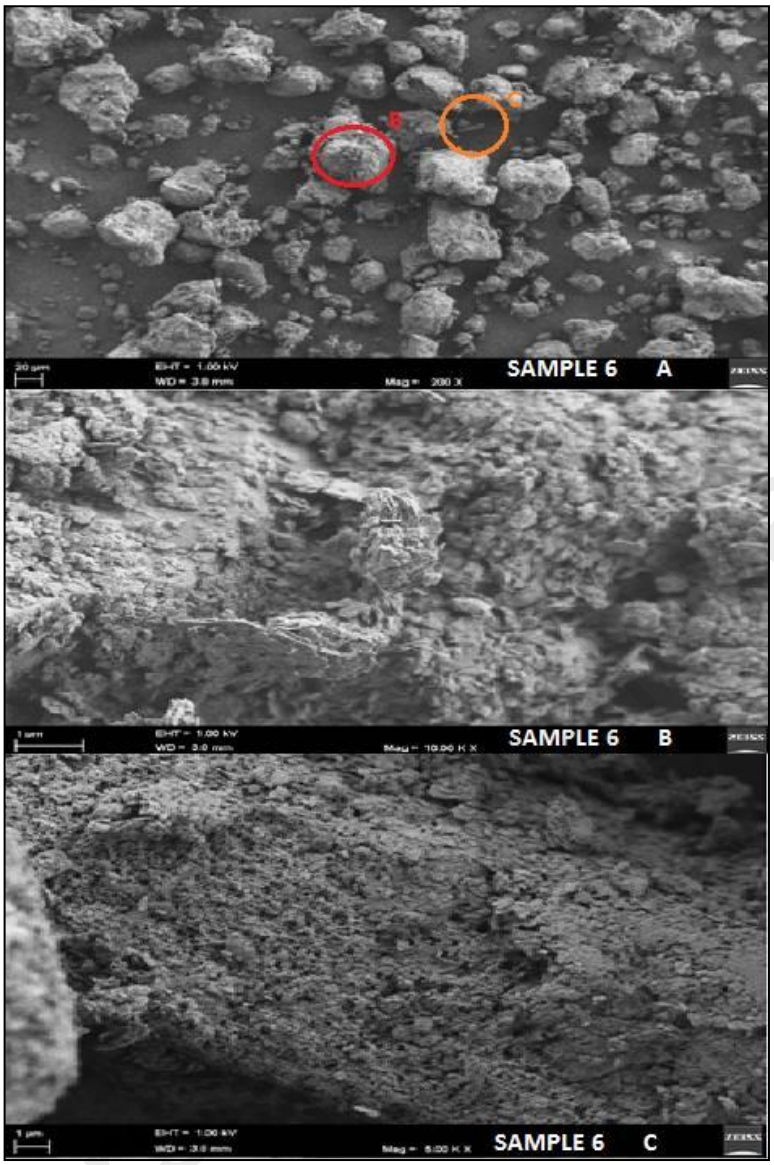

Figure 4.10 : Sample 6 A. 2.00 x, B. 10.00Kx, C. 6.00 Kx magnified SEM image of the clay dry-pressed at room temperature, in C. the silt texture is found and B. is clay.

All the magnified SEM image on sample 4 (Figure 4.8)showed the clay with capillary surface in sample 4 as the result of LDPS proved the concentration of clay is high in sample 4 after sieved.

The pores of particles in sample 5 (Figure 4.9)were more and smaller than sample 4 therefore it can be seen the particles performed in larger size with smoother surface rather than the sample 4 but the close shot of images proved the high concentration of sample is

clay but different type of clay (Markgraf et al., 2006) as the arrangement of clay cell is different in this sample.

Sample 6 (Figure 4.10) was the sample with highest concentration of silt based on the result of laser diffraction particle size distribution, therefore observing of cancellous surface (high pores) and cubical shape is regular. Moreover the outlook of sample 6 (Figure 4.10) was with roughness but the higher porosity images illustrated that the plates were steacked on top of this rhough surface.

4.4 Rheometry of Fine Sediments

The six series of sieved samples were examined to determine the rheological properties that lead to discover the effect of soil type and particle diameter on flow and sedimentation. Therefore the characteristics of particle tracer for using in particle image velocimetry were explored. The rheometry of fine sediments had done in two types of test, flow curve test and in condition of constant shear rate, then oscillatory test with controlled shear deformation. The significance of rheometry is because of the effect of rheological behavior on fine particles movement in fluid (Muhanned, 2013).

4.4.1 Flow Curve Test

Below figures demonstrates the results related to the flow curve test with the constant shear rate. The viscosity along the time decreases in a concentration of 70% Figures 4.11 in all the samples with the Parallel Plates (PP) 25mm and 50mm.

University of Malaya

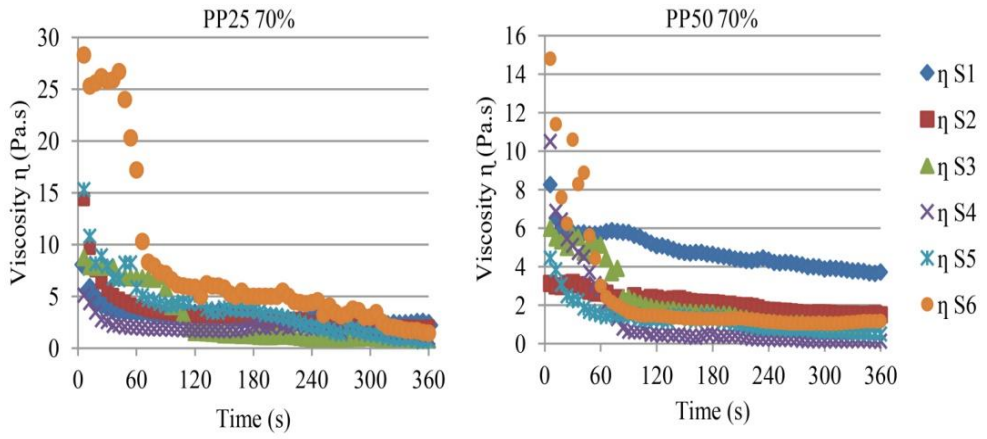

Figure 4.11 : Graphs of the variation of viscosity in time with constant shear rate (100Pa-Herschel-Bulkley) sieved soil samples using Parallel Plates 25 and 50 in concentration of 70%.

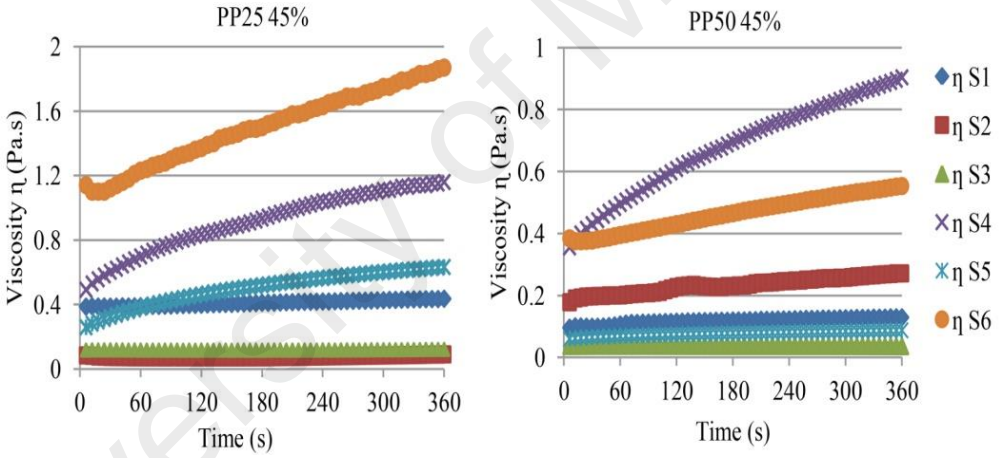

Figure 4.12 : Graphs of the variation of viscosity in time with constant shear rate (100Pa-Herschel-Bulkley) sieved soil samples using Parallel Plates 25 and 50 in concentration of 45%.

In 45% (Figure 4.12), the sieved soil samples show non-Newtonian, shear thinning to shear thickening behavior that illustrates a curve in time. Practically all the materials that are shear thinning are thixotropic. Moreover, because the microstructural elements that result are shear thinning, proper time is required for the rearrangement. Although with higher water content the samples tend to Newtonian behavior as the viscosity values

University of Malaya

variation is small, therefore with considering this issue they were assumed as non-Newtonian materials.

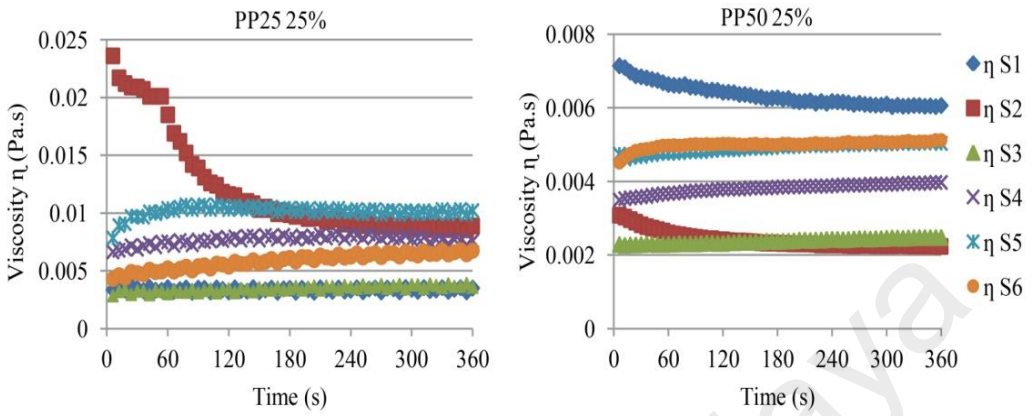

Figure 4.13 : Graphs of the variation of viscosity in time with constant shear rate (100Pa-Herschel-Bulkley) sieved soil samples using Parallel Plates 25 and 50 in concentration of 25%.

Figure 4.13 demonstrates the soil samples in concentration of 25 % with PP 50, PP 25, where the viscosity of fine particles in time behaves as shear thinning models in very low power; therefore, it would be acceptable to call this behavior as near-Newtonian, although sample 2 and even sample 1 exhibit a tendency to decrease the viscosity over time (shear thinning). This supports the notion highlighting shear thinning in higher concentrations.

The viscosity of soils decreases corresponding to the increase of the water content of the samples; this means η 70% > η 45% > η 25%. The plots show that sample 3 has a constant behavior with different conditions while the other samples have variations during time. Besides, the vicissitudes of viscosity in time indicates that all the samples have a thixotropic behavior, although in concentrations of 45% and 25% samples 4 and 5 appear different, and these samples show a shear thickening behavior as samples 4 and 5 contain higher volume of clay and this phenomenon is normal.

University of Malaya

Sample 6 with 70 percent volumetric fine sediment concentrate (Figures 4.14 - 15) shows as the pseudoplastic behavior at the first since it is included silt behaves like a real fluid instead of solid matter when it is forced to move (Greiser & Wurpts, 2008). The viscosity is shear rate and time dependent in this experiment. Higher volume of the water content could be the other reason for the visco-plastic behavior of the samples. Even in the concentration of 25% with lower viscosity in comparison with other concentrations, the Newtonian behavior can be observes as shown by the presented graphs.

Figure 4.14 illustrates the flow test of the fine particles in the concentration of 70% with Parallel Plate 25 mm. Seemingly, the soils exhibit a similar behavior that they act with PP50. All samples generally performed in similar characteristic using PP50 and PP25, just the rate of shear stress τ (Pa) values using PP25 is varied in higher rate than PP50, that the reason can be the area or diameter of plates, the amount of force is changed as the area got smaller. The rheological behavior of samples is shear thinning and more visco-plastic behavior can deduce of the plots.

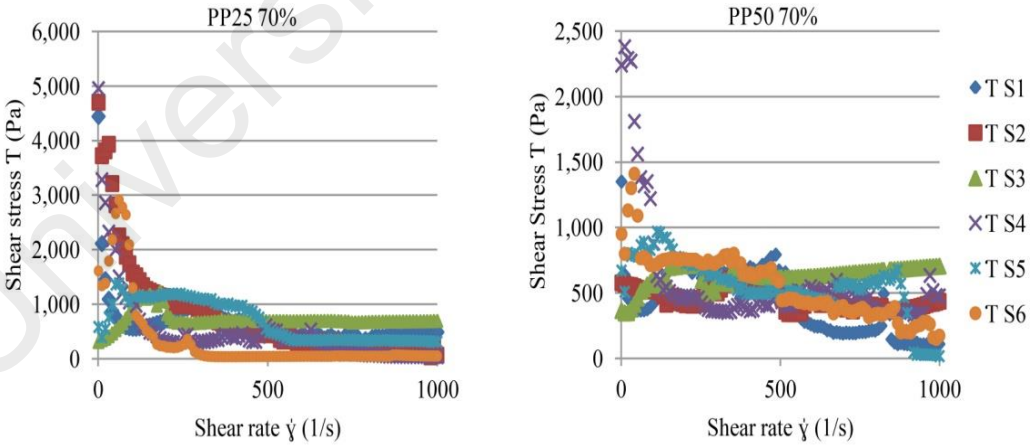

Figure 4.14 : Graphs of the flow curve with constant shear rate (Herschel-Bulkley) of the sieved soil samples using Parallel Plates 25mm and 50mm in the concentrations of 70%

University of Malaya

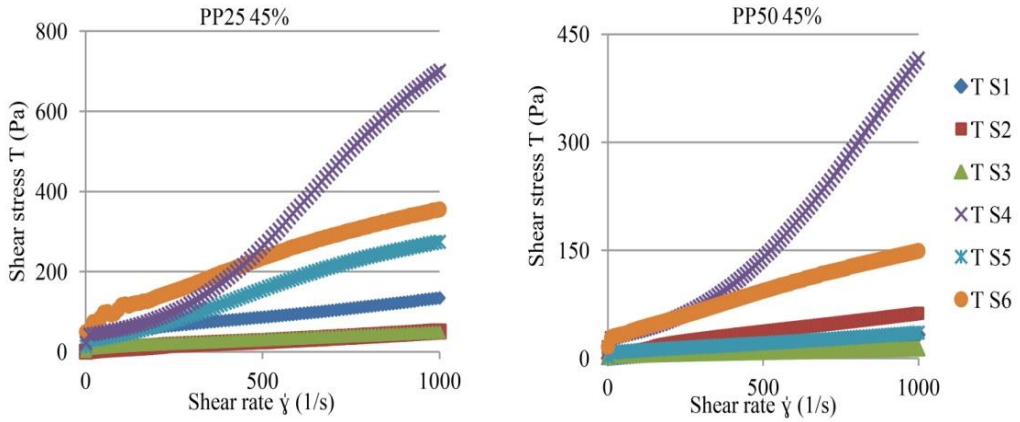

Figure 4.15 : Graphs of the flow curve with constant shear rate (Herschel-Bulkley) of the sieved soil samples using Parallel Plates 25mm and 50mm in the concentrations of 45%

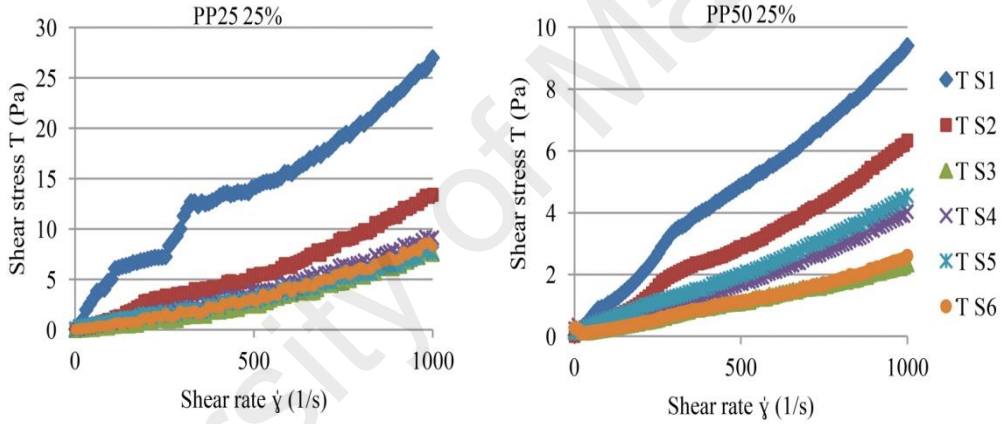

Figure 4.16 : Graphs of the flow curve with constant shear rate (Herschel-Bulkley) of the sieved soil samples using Parallel Plates 25mm and 50mm in the concentrations of 25%

Figures 4.15 and 4.16 display the 45% and 25% fine particle samples that prove the idea that viscosity η reduces with higher water contents. With a concentration of 25%, the behavior of the soils was near to Newtonian. Furthermore, the viscosity (η) variation with PP 25 was higher than PP50 during the time; henceforth, this would insinuate the relation between the force and area implying that the diameter of the parallel plate 25mm was smaller than 50 mm; thus, the energy of the force was spread other than 50mm.

University of Malaya

4.4.2 Oscillation Test

The graphs related to the storage and loss modulus (G′ and G″) were generated automatically during a test and stored electronically. These graphs illustrate three stages. The first stage or phase was a duration when the material exhibited an elastic behavior. A linear viscoelastic (LVE) range (Figure 4.17) and the included deformation limit γ_L are the parameters which are needed to quantify the 'stored elasticity' of a viscoelastic material, such as the soil (Markgraf et al., 2012). Next, the material begins a transition between the elastic and Newtonian behaviors; in the second stage it is shown that G′=G″. The collapsed stage was the last stage in which a viscous character prevailed; substances were creeping or running, represented by the Newtonian behavior in the ideal case.

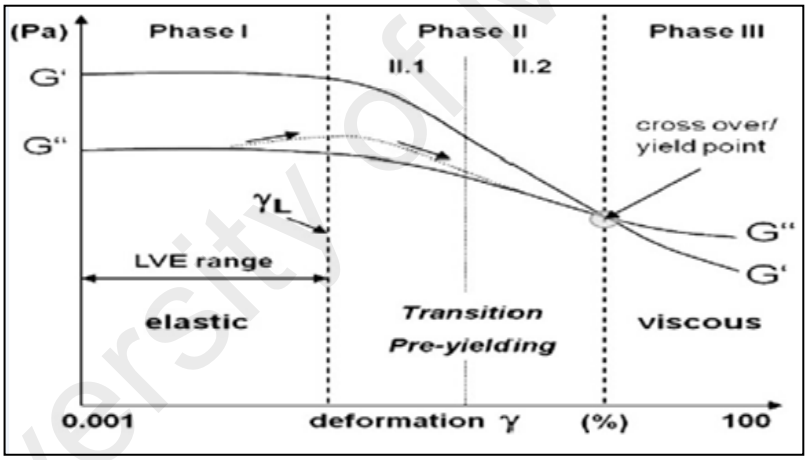

Figure 4.17 : Idealized plot of storage modulus G′ (Pa) and loss modulus G″ (Pa) vs. deformation γ (%).In general, three stages of elasticity loss can be defined, showing a gradual transition of an elastic (G′>G″) to a viscous (G′<G″) character(Markgraf et al., 2012)

Figures 4.18 and 4.19 describe the amplitude sweep test with PP50 and PP25 in two concentrations of 70% and 45%. The soils with the concentration of 25% almost indicate the Newtonian behavior; accordingly, the amplitude sweep test was not really applicable

University of Malaya

for the aforementioned concentration since this test is used for viscoelastic materials (Markgrafa, 2010).

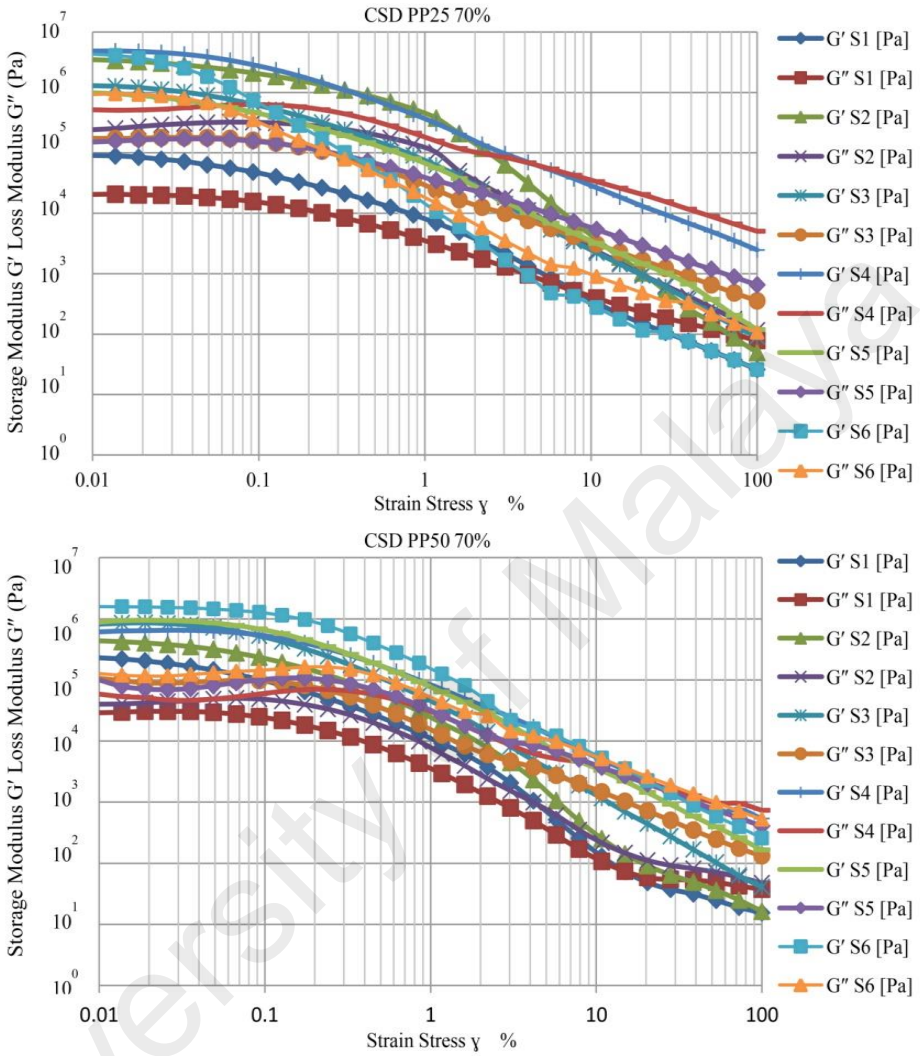

Figure 4.18 : Resulting graphs with storage modulus G′ and loss modulus G″ as functions of γ of the conducted amplitude sweep tests (AST) at the concentration of 70% (70% soil+30% distilled water) with parallel plates 25 mm and 50 mm diameter; the power of G′ and G″ decreased in graph of PP50.

University of Malaya

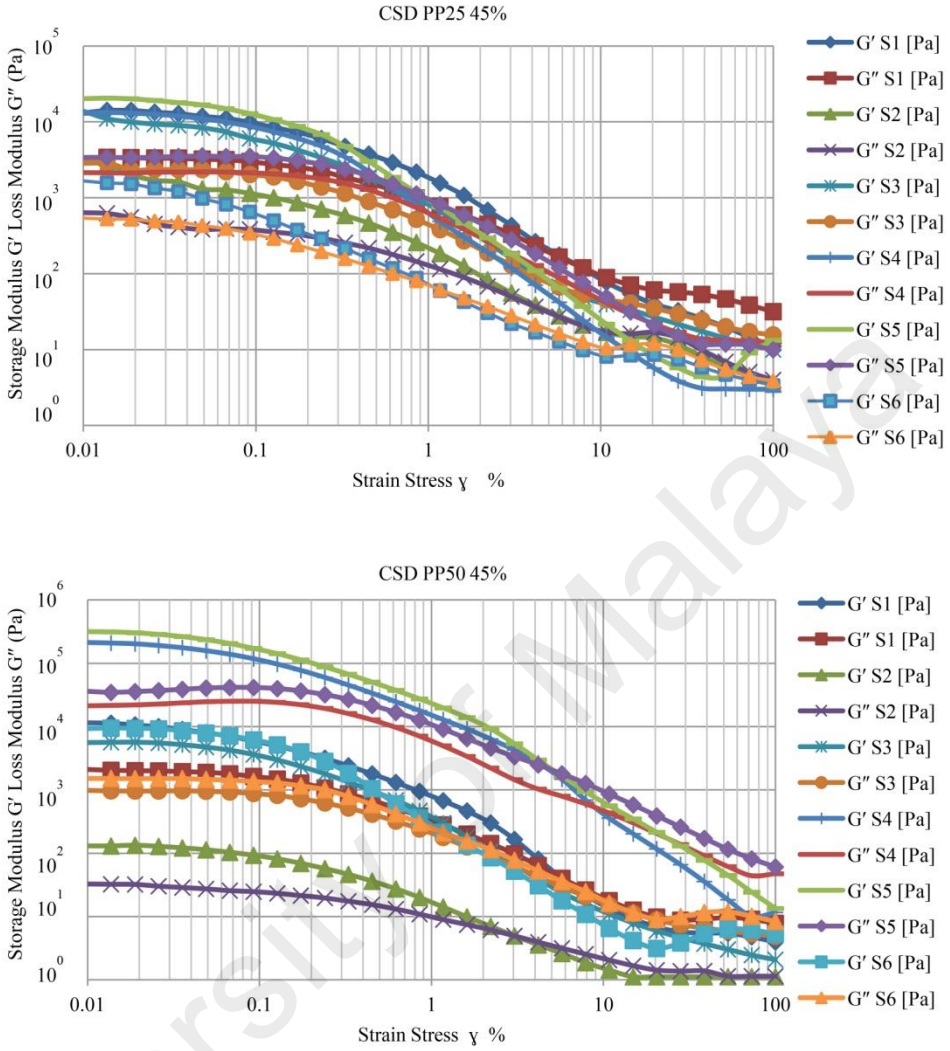

Figure 4.19 : Resulting graphs with storage modulus G′ and loss modulus G″ as function of γ of the conducted amplitude sweep tests (AST) at the concentration of 45% (45% soil+55% distilled water) with parallel plates 25 mm and 50 mm diameter; the cross over point using PP50 happened prior to using PP25mm. The power of G′ and G″ decreased in graph of PP50; the comparison between sample 2 powers can show this phenomenon clearly.

The difference between values of cross over point or strain stress amount of sieved samples is discussed in conclusion chapter. The plots illustrate the amounts of storage

University of Malaya

and loss modulus (G' and G") is begun in higher rate (10^7 Pa) within 70% concentration (70% soil+30% water) which the reason of this phenomenon needs to discuss. In all samples the storage modulus is bigger than the loss modulus and decreased after the cross over point. Moreover the sample 1 graph described the low value of storage and loss modulus in oscillation test which proved the influence of fine sand in this sample in compare of other samples.

4.5 Relation of Particle Size, Shape and Texture with Rheological Properties

Total results between the flow curve test (Constant Shear rate) and the amplitude sweep test applied using rheometer MCR 302, Anton Paar, USA with a profiled parallel-plate measuring systems 50 mm and 25 mm in diameter indicated that there was no difference between the results in variation and both plates corroborated their results with the overlap curves in the plots. Nonetheless, the viscosity rate, storage modulus, and loss modulus proved the idea that PP25 was an appropriate instrument for testing the soil; ever since the studied parameters values (amounts) of the samples which were determined by PP25 were less than PP50 and the pressure ratio of the surface area in different levels of the water content was obvious. Besides, the flow curve (Figures 4.14-16) demonstrated that the smaller area spread the force in all angles with less tension in viscosity as the shear stress and viscosity reduction during the test by Parallel Plate 25mm (PP25) differed from the variations of Parallel Plate 50mm (PP50) (Markgraf et al., 2012). The next reason for insisting on the above averment is the amount of the samples consumed. By PP50 mm, a greater volume of the substance was used. The shear stress at low shear rates is much higher for the upward than for the downward curve in sample 1 and 2 with 70% concentration in Figures 4.14-16 and show a minimum at higher shear rates. It is defined as a structural collapse that is irreversible at short time scales (Van Kessel & Blom, 1998).

University of Malaya

According to BS5930:1999 and BS1377:1990, fine particles of the soil exhibit physical characteristics and the appearance was influenced by cohesion and plastic properties (plasticity) associated with the mineral composition and the water content. Therefore, the fine sediments that incorporated fine sand, silt, and clay could make the viscoelasticity and plasticity behaviors. In this study, after being mixed with the distilled water, all the samples found a cohesive structure which depended on the rate of each type of soil. This structure behaved differentially. By means of higher fraction of fine sand in fine sediment accumulation is attributed the flow inhibition and the clay particles is not moved in water column as expected (Kirby, 2011). Figure 3.2 illustrates the color of each sample; the pink color verifies the clay and brown shows the sandy material while dark gray is because of silt-rich sample 6. It is investigated that the concentration (C) of the fine grain soils had an influence on the flow (Figures 4.18-19) and sedimentation where the water content was higher offering little resistance to deformation (Rensbergen et al., 2003).

In addition to the soils concentration and fine sediment influencing rheological behavior, a clay known as the non-Newtonian behavior effect in the rheological analysis was distinguished as it was apparent in samples 4 and 5. It can be concluded that observing the non-Newtonian behaviors in samples 4 and 5 with higher concentrations of the clay was logical although based on the clay type this property changed (Markgraf et al., 2006) and with a higher volume of water the shear thinning behavior changed to shear thickening (Figures 4.14-16). The flow curves obtain in linear at 45% and 25% fine sediments concentration and behave near Newtonian (Figures 4.15-16).

Classification of the soils flows based on the particle size distribution was investigated by Costa (1987). It has been asserted that the processes which control the flow behavior depend on the deformation rate of the fine grained size particles which is rate independent frictional and viscous forces dominate. Moreover, they (Costa & Wieczorek, 1987)

University of Malaya

categorized three flow phases based on the particle size distribution and the water content that started with normal stream flow to visco-plastic or hyper concentrated, continuing with sudden increase in yield strength overlapping with the liquefaction behavior (slurry flow) at last leading to granular flow when the loss of the ability to liquefy is transacted. Additionally, regarding the texture influencing the rheological behavior, Markgraf (2006), quoted Kutilek (1994) that the shear strength and the soil water ratio of the soils were small after any mechanical disturbance (deformation) and increased with time. It was also noted that the soil water ratio and the volumetric soil water content was time dependent not only in swelling but also the thixotropic behavior and strongly reduced in the subsoil due to the overburden pressure in the topsoil (Lowe, 1976). This occurrence was detectable in the flow curve depending on the water ratio.

Moreover, the pore scale influence as well as studying the rheological properties of the soil hydrology should be emphasized; for instance, sample 6 with a different texture (Figure 4.10) demonstrated the abovementioned notion. Therefore, based on the pore size and the saturation with water the soil rheological properties can be varied. By means of the stress and force are applied the size of pore spaces decreased and the particle arrangement changes homogenous. The water concentration in stress can influence on soil fabric with different pore size as it will be composed of particles with several clay layers and aggregates with a large number of particles. Therefore the fine particles would be closer to each other so the flow in fine sediments with lower water content rate can be near Newtonian (Al-Mukhtar et al., 1996). Thus, the pore quantity and size of samples can be observed in images of SEM in Figure 4.6 sample2C, Figures 4.7-8 sample3C and sample4C, and Figures 4.9-10 sample5C and sample 6C, in addition the influence water content ratio with pores and soil fabric in flow curve plots. Furthermore, it is observed the shear strength has a constant relation with the density (Fontein & Van der Wal , 2006).

University of Malaya

The variation of viscosity in the Constant Shear Rate (CSR) test by PP25 and PP50 verifies initial viscosity at the low shear phase for 12 seconds followed by the high shear phase (time-and rate dependent) for about 36 seconds; it then happens at the last recovery phase (Zhang, 2004). The flow curve of sample 1 in a concentration of 45% with PP50 exhibited the Newtonian behavior while it displayed the shear thinning behavior with PP25; moreover, in both plots the viscosity decreased during the time corresponding to the rise in the speed and torque, implying that in such a concentration sample 1 acts as an ideal elastic (HOOK Law) and viscoelastic material. The oscillatory force on Sample 1 with a concentration of 45% described a weak strain overshoot face; therefore, in the Linear Viscoelastic (LVE) point, the material would exhibit an elastic behavior; subsequently, the second phase started the transition or pre yielding (the plastic region of the material); then the cross over point is considered as the yield point but beyond that any region is assumed to be viscous (Hyun et al., 2011). Although Sample 1 with a concentration of 25% revealed a weak behavior of thixotropic in the lower value as it could be assumed as Newtonian, the higher water concentration in this stage resulted in the Newtonian mode. The plot related to the concentration of 25% illustrated the elastic and pre-yielding phases, excluding the viscous phase. Moreover, the moisture effect showed that a higher water concentration contributed to previewing on the quicker fluid phase. Values associated with Sample 2 in each three concentrations described the thixotropic fluid. Sample 2 in concentrations of 70%, 45%, and 25% showed the shear thinning behavior (thixotropic) with a yield stress response. The only effect of the water content in sample 2 made a lower viscosity value with a higher water ratio. As it was mentioned earlier, samples 3, 4, and 5 revealed an almost identical flow curve in definition as these samples showed the shear thinning (pseudoplastic fluids) behavior in a concentration of 70%. This led to shear thickening while the viscoplastic fluids with a higher water ratio as regards sample 3 $_{25\%}$ showed the Newtonian (viscous) behavior

University of Malaya

(Fontein & Van der Wal, 2006). However, the range of the variation in samples 4 and 5 were more apparent than sample 3 (Figures 4.14-16).This truth might have happened because of a different texture and soil particle distribution as the bases of samples 4 and 5 were from the clay while sample 3 contained the fine sand and silt in the identical volume. Sample 6 had a shear thinning behavior in concentrations 70% and 45%; subsequently, with an increase in the water content in the concentration of 25%, it transformed the Newtonian fluid with low viscosity and remained constant.

In the amplitude sweep test, higher values for G′ and G″ (Figures 4.18-19) showed that the product had a higher η value. A higher η value means a high Molecular weight (Mw) or longer structures. The slope of the curve provides us with the information on the Molecular weight distribution (MWD) or if the structure breaks at once or partially. The steeper slope illustrated the narrower MWD. For a structured product all the bonds broke with the same force. Moreover, the frequency rate was significant because it could lead the Non-linear behavior (LVE). A cross-over point at a lower frequency means a higher Mw and that the product is less elastic at a higher impact. A higher modulus at the cross-over point indicates a narrower MWD.

The amplitude sweep tests as applied in the surveys in the current research included more data on the possible textural effects, influenced by fine sediments and the water content, apart from the flow curve behavior in both the viscoelastic and plastic materials. A different shear behavior due to the textural effects became obvious when the primary levels of G′ of the loss material are compared with six types of fine soils. In the amplitude sweep test, the sample with higher water content had a lower deformation (comparison of samples in concentrations 70% and 45% as shown in Figures 4.18-19). The higher volumetric fine sediment concentration with their rheological properties could lead the thixotropic behavior as develop shear strength after deposition and will grow the critical

University of Malaya

limits during the time (Fontein & Van der Wal , 2006).The influence of the texture on the curve was apparent in case sample 1 $_{70\%}$ with fine sand rich as the primary level of G′ was at 10^5 of G″ at 10^4 even with two plates (50mm and 25mm), for samples 4 $_{70\%}$and $5_{70\%}$ with higher clay and silt textures the primary level of G′ was between 10^6 and 10^7 of G″ at 10^5. A higher input of deformation could be observed here.

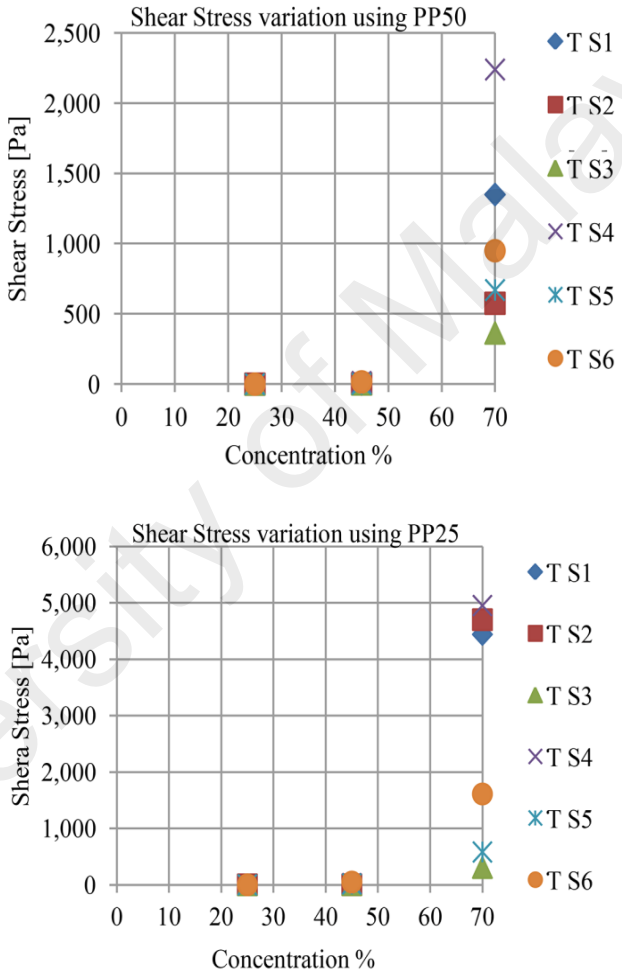

Figure 4.20 : The graphs demonstrate the effect of water content and Parallel Pate diameters

Based on the plots, it is obvious that the soil sample in the concentration of 70% exhibited a thixotropic behavior as the viscosity decreased during the time. These changes in the fluid's viscosity over time indicate the time-dependent behavior (Costa & Wieczorek,

University of Malaya

1987). In the amplitude sweep test, storage modulus G′ (Pa) was bigger than loss modulus G″ (Pa) and the distance of these two lines proved that the fine particle samples performed as viscoelastic materials in samples 1 to 6, except samples 4 and 5 that had more visco-plastic bases with yield points. In addition, the decrease of the two parameters after the cross over point illustrated the strain thinning behavior (Markgraf et al., 2006) although the material reached the fluid phase with PP25 earlier than PP50. Based on the presented graphs (Figures 4.18-19), the distances between G′andG″ in samples 4 and 5 were more than the other samples, indicating more visco-plasticity. As the difference between storage modulus and loss modulus of sample 1 was far than sample 2, the difference of the molecular weight distribution could be observed in these two samples (fine sand). Sample 2 substantiates the influence of the particle size distribution on the rheological behavior as it had a lower power of G′ and G″ in comparison with the other samples. In particular, a comparison between G′ and G″ powers of samples 2, 3, and 4 could clarify the deviations (Markgraf et al., 2006). As demonstrated through the graph (Figures 4.18-19), Sample 4 with the clay content was placed higher than samples 2 and 3 as such a behavior was shown in sample 3 with higher silt and less fine sand contents to sample 2 with basically the highest volume of fine sand. Moreover, graphs in Figure 4.18 and Figure 4.19 demonstrate earlier deformation of samples in two variables; first, the samples reached the yield point in the concentration of 45% earlier than 70%, proving that the higher water content contributed to the reduction of viscosity (Figure 4.20). Furthermore, the faster deformation of samples in concentration of 45% using PP50 (Figure 4.19) demonstrated less levelling and less sagging of the samples in such a concentration. In addition, the samples reached the yield point and the viscous phase faster by using parallel plate 25mm.

University of Malaya

4.6 Particle Image Velocimetry

The particle image velocimetry method was developed to investigate the two-dimensional hydrodynamic behavior of the fine sediment model in this study based on several key features: inlet and outlet elevation, outlet locations, depths of water, different points in the sediment basin, and two water flow rates. The study of 3D fluid flow onto 2D technique creates a visualization of vector velocity in two directions, and it omits the effects of velocity in the third or the z-direction (Giordano et al., 2006; Hoque et al., 2015; Lad et al., 2011). The Correction of misalignment is done using the calibration and various types of analysis (FFT, cross correlation, etc) (Adrian, 2005), and algorithms transformation which improves the neglected of z direction in images (Lad et al., 2011; Tokgoz et al., 2012).

The series of images captured, which represent fine particle movement in the water flow in the designed basin was input into the Dantec program. All 100 images were analyzed and a vector statistics map of particle movement in the studied frame was finalized to visualize the displacement of particles in flow. The flow was from the left to the right side. In the following process, it was understood that fine particles have positive and negative vector values. Since the particles moved from left to right, they produced positive values while in the opposite direction the values were negative. Therefore, this result signifies the reason for siltation. In particle settling, different parameters have effect, such as particle size, viscosity, and fluid density.

PIV was the best technique to directly visualize the fine sediment hydrodynamic behavior in water, although there was a limitation with the amount of real soil concentration as the machine failed in turbid water (Van Doorne & Westerweel, 2007; Weitbrecht et al., 2002; Yang et al., 2012; Yu & Liu, 2007). However, using seeding particles with similar

University of Malaya

characteristics to real fine particles supported the capturing of images close to the natural behaviour of fine particles.

The experiment investigates the movement of fine particles under different pressures and stress after 15 minutes of seeding the fluid, using 2 different size samples in one frame in middle of tank. The Reynolds number was evaluated 12000 in higher flow rate. The frame size under study was 30×15 cm^2. Then to demonstrate the flow direction of fine particles in different region of tanks, 5 different area of tank were studied by using the FPP sample (20-50μm).

4.6.1 The Displacement Path of Fine Particles

The results represent an overview of the fine sediment movement mechanism under different stresses in the entire sediment basin. The experiment repeated for each zone to prohibit and reduce the mistakes in velocity of tracked vectors. In particle settling, different parameters have effect, such as particle size, viscosity, and fluid density. Hence, each studied location are named as zone a the surface area; zone b Near the inlet, upper level of the sediment basin (b-NIU); Zone c, Near the inlet, bottom of the sediment basin (c-NIB); zone d, Near the outlet, bottom of the sediment basin (d-NOU) ; zone e, Near the outlet, upper sediment basin (e-NOB).

4.6.1.1 Water surface (a)

At the water surface, fine particles with higher flow rate (11 L/m) dispersed very fast (Figure 4.22). The water flow direction was from left to right, and particles in top layers moved downward or changed direction to the right. The vector map implies that fine particles settled, but in lower layers the layer viscosity pushed the particles upward. Figure 4.22 demonstrates the mobility of fine particles at lower flow rate (5.5 L/m) at the water surface level. The particles collided with the eddy zone, therefore the direction of

University of Malaya

fine particle transport was inclined toward the right and transferred to lower layers. The influence of water flow and walls of tank collision, and gravity force could be the two possibilities of this fact; other reasons are discussed in following. However, part of the particles settled, but the real action of fine particles at this water level was dispersion and obstruction in the layers. The velocity of fine particle displacement was high at the surface and by moving downward their velocity decreased; especially in the lower velocity section (blue in the map), the eddy zone with greater diffusion of fine particles were observed. Generally, the U/Umax increased with distance, which explains the siltation behavior and increasing velocity with particle settling (Figure 4.21).

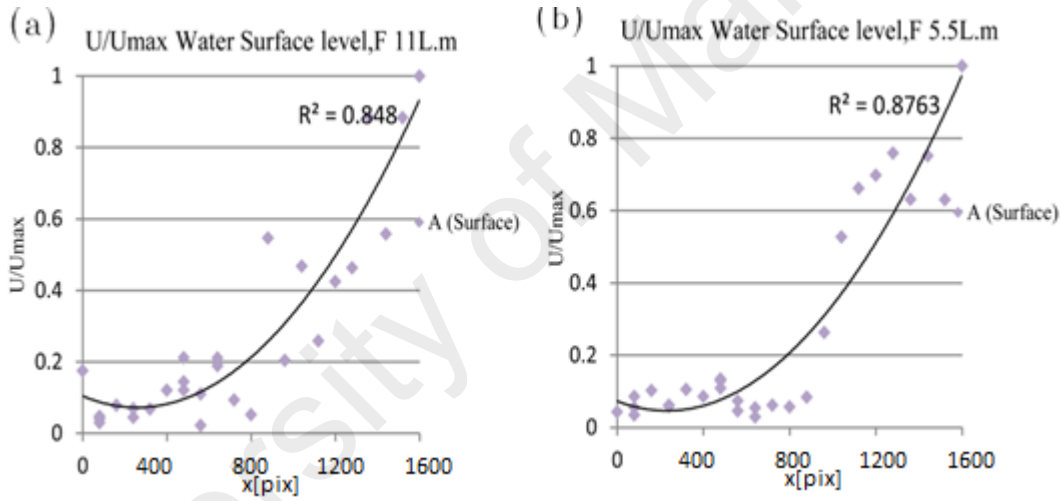

Figure 4.21 : U/Umax graph at two flow rates of 11 L/m (a) and 5.5 L/m (b) at water surafce (Zone a)

The hydrodynamic behavior of fine particles at the water surface, near the sediment basin center and lower flow rate (5.5 L/m) was different than at a higher flow rate (11 L/m). Although this difference is evident from the vector map, the findings from the graph prove that the U/Umax variation in values tended to be on the same line as the higher flow rate. In the first image angle (Figure 4.22), a circulation zone was observed that distributed the eddy zone toward the front. In addition, the fine particles re-suspended upon reaching a new flow stream at the bottom of the frame.

University of Malaya

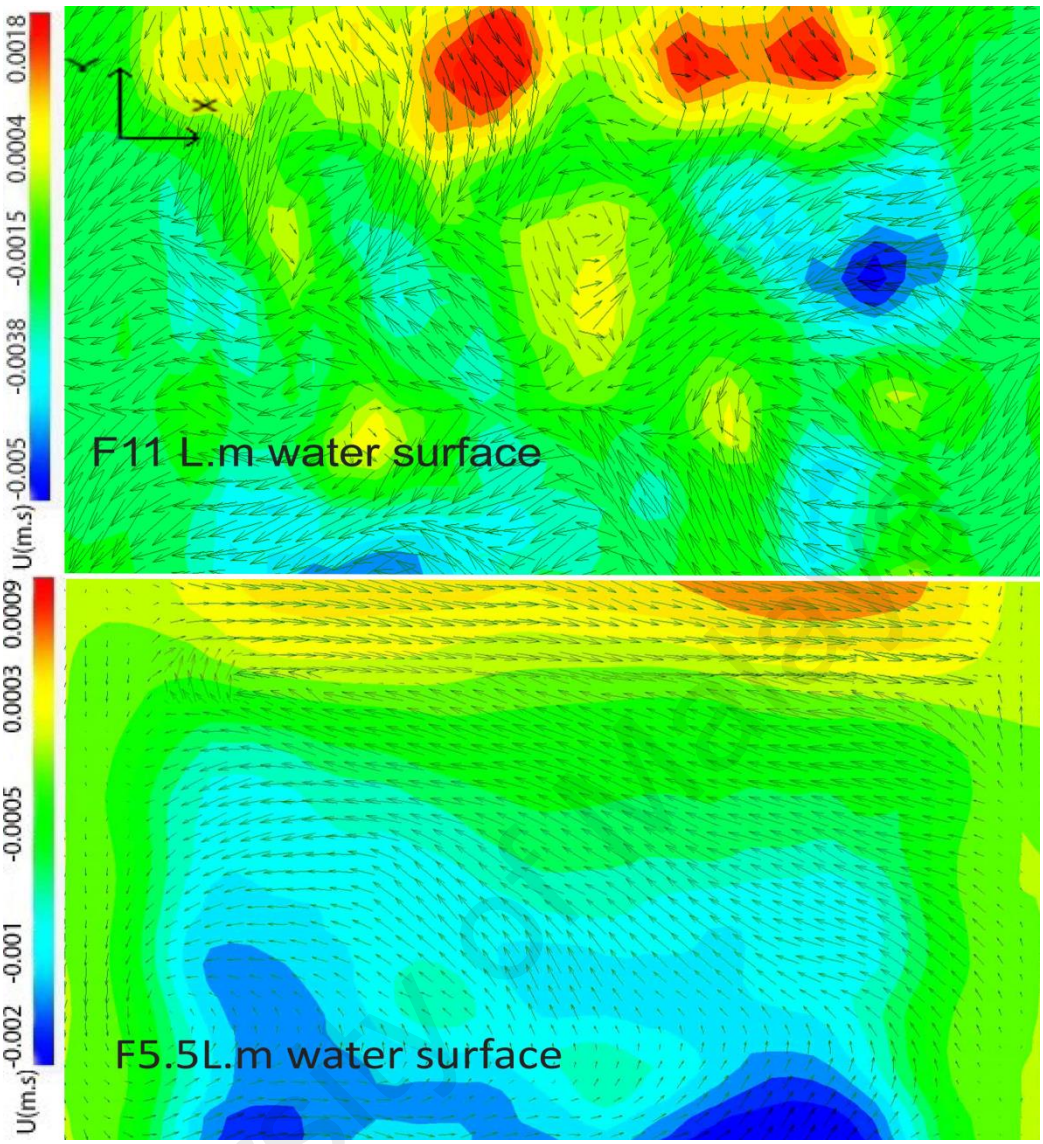

Figure 4.22 : Overlay of scalar and vector maps of fine particle movement at flow rates of11 L/m (a) and 5.5 L/m (b) at the water surface level (zone a)

4.6.1.2 Near the inlet, upper level of the sediment basin (b-NIU)

This zone is called by b-NIU means the near inlet upper side of tank and showed by “b”. Figures 4.23-24 show the transport map of fine particles at two different flow rates in the middle of the sediment basin near the inlet. It is observed that fine particles had higher velocity at higher flow rate (Q of 11 L/m), and because the dischage rate was higher this phenomon was normal. The fine particles ambulated in near-laminar motion over most of the studied section, but some re-suspended in the upper layers at the right wall due to

the wall boundray. Moreover, the studied section was near the inlet and basin wall, so when the flow approached the basin wall the particles returned to an upper direction. The other interesting result is evident at the bottom of the figure that shows that with travel toward the bottom of the tank, the upward movement increased. Then the particles became suspended at the top, where flow from the layers below had influence.

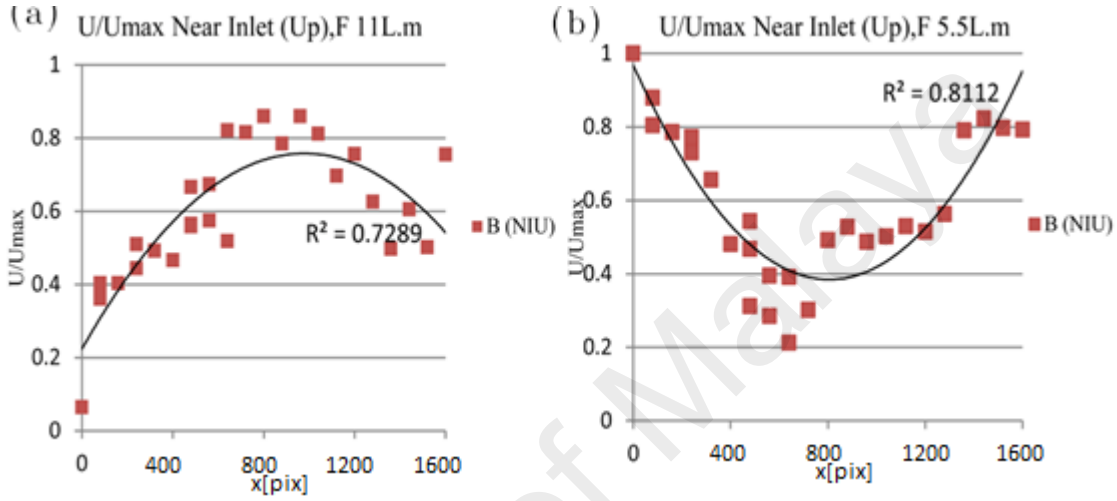

Figure 4.23 : U/Umax graph at two flow rates, 11 L/m (a) and 5.5 L/m (b), near the inlet, upper basin (zone b)

At lower flow rate, the motion of fine particles was distinct. The U/Umax graph shows the difference in fine particle movement at Q 5.5 L/m. The decreased flow rate indicates that the fine particles near the inlet settled quickly at the first vertical water column, after which flow hauled them upwards. The influence of particle drag force was observed at the beginning of transport, then the eddy of the layer below pulled the fine particles. The variation in presurre made a circulation zone at the left side of the frame that carried the fine particles on the Z-axis, which is outside the study zone. It is concluded that the particles near the inlet were transported with flow, but with decreasing flow rate the settling tendency of fine particles enhanced. However, the basin wall boundary resuspended the fine particles.

University of Malaya

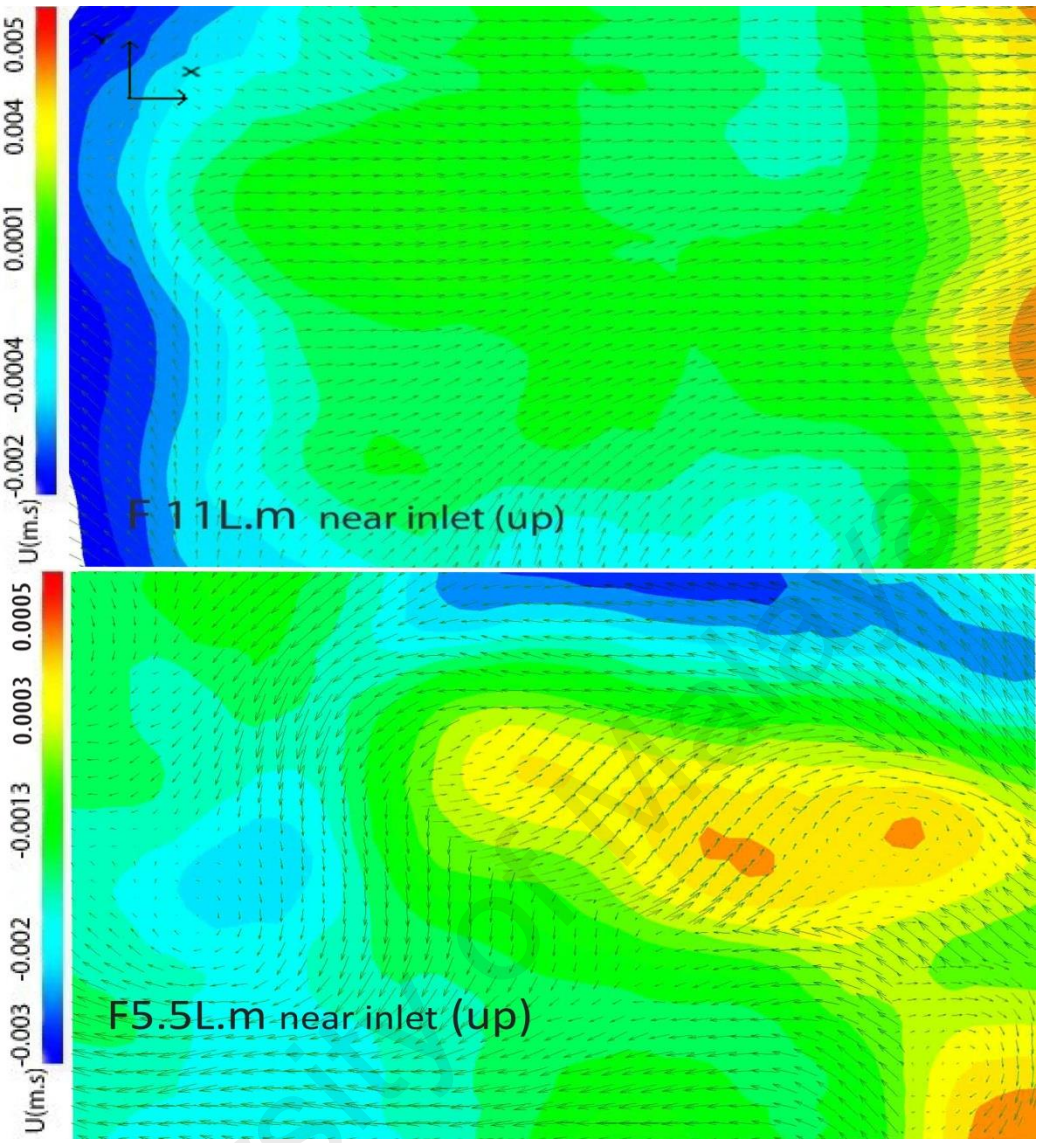

Figure 4.24 : Overlay of scalar and vector maps of fine particle movement at flow rates of 11 L/m (a) and 5.5 L/m (b) near the inlet, upper level of the basin (zone b)

4.6.1.3 Near the inlet, bottom of the sediment basin (c-NIB)

The study frame was shifted to the bottom of the sediment basin to investigate the movement of fine particles near the inlet at the bottom of the retention structure. The exprimental results were similar for both flow rates, and the same tendency of U/Umax was observed in the measured area. The rise in U/Umax demonstrated in the graph (Figure 4.25) signifies the re-suspension of fine particles due to bed shear stress. Meanwhile, the particle displacement velocity was slow at lower flow rate (5.5 L/m) than at 11 L/m.

Figure 4.26 illustrates that the majority of fine particles were carried up with flow. However, at greater depth there was a stream elimination line that indicates the particles' settling trend. In the left corner of the vector map, the impact of bed shear stress and wall boundaries made the particles spurt. If the frame could be adjusted closer to the inlet wall, this phenomon would be more apparent.

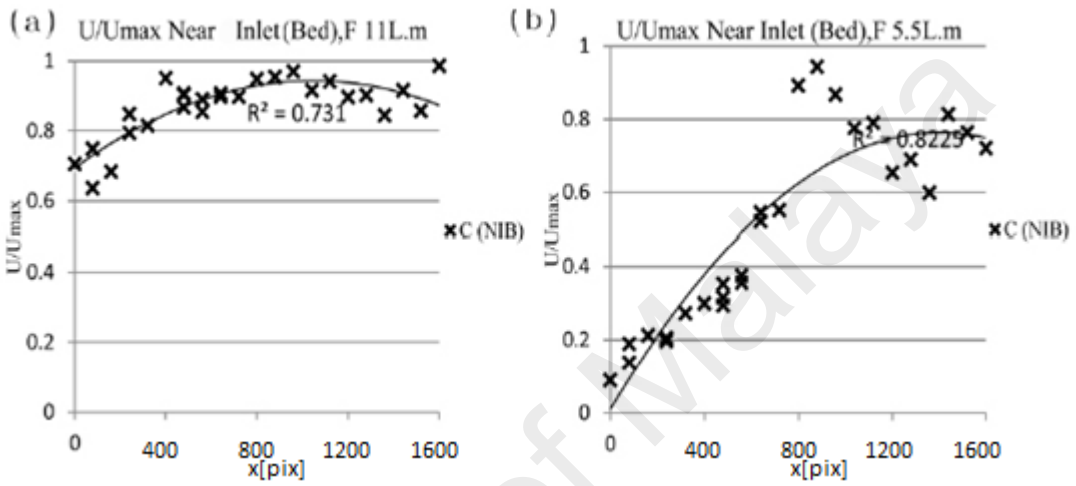

Figure 4.25 : U/Umax graph at two flow rates of 11 L/m (a) and 5.5 L/m (b), near the inlet, bottom of the basin (zone c)

At lower flow rate similar dispersion was estimated, though the image (Figure 4.26) shows more suspension of fine particles. The large blue spot and fine particle direction asserts the flow of fine particle displacement in the upper studied frame. Moreover, the conjunction of particle directions proves the lower settling tendency to the bottom at this flow rate, therefore more suspended particles were predicted. It is inferred that drag force enhanced at the bottom of the retention structure and with decreasing flow rate, the suspension level rose.

University of Malaya

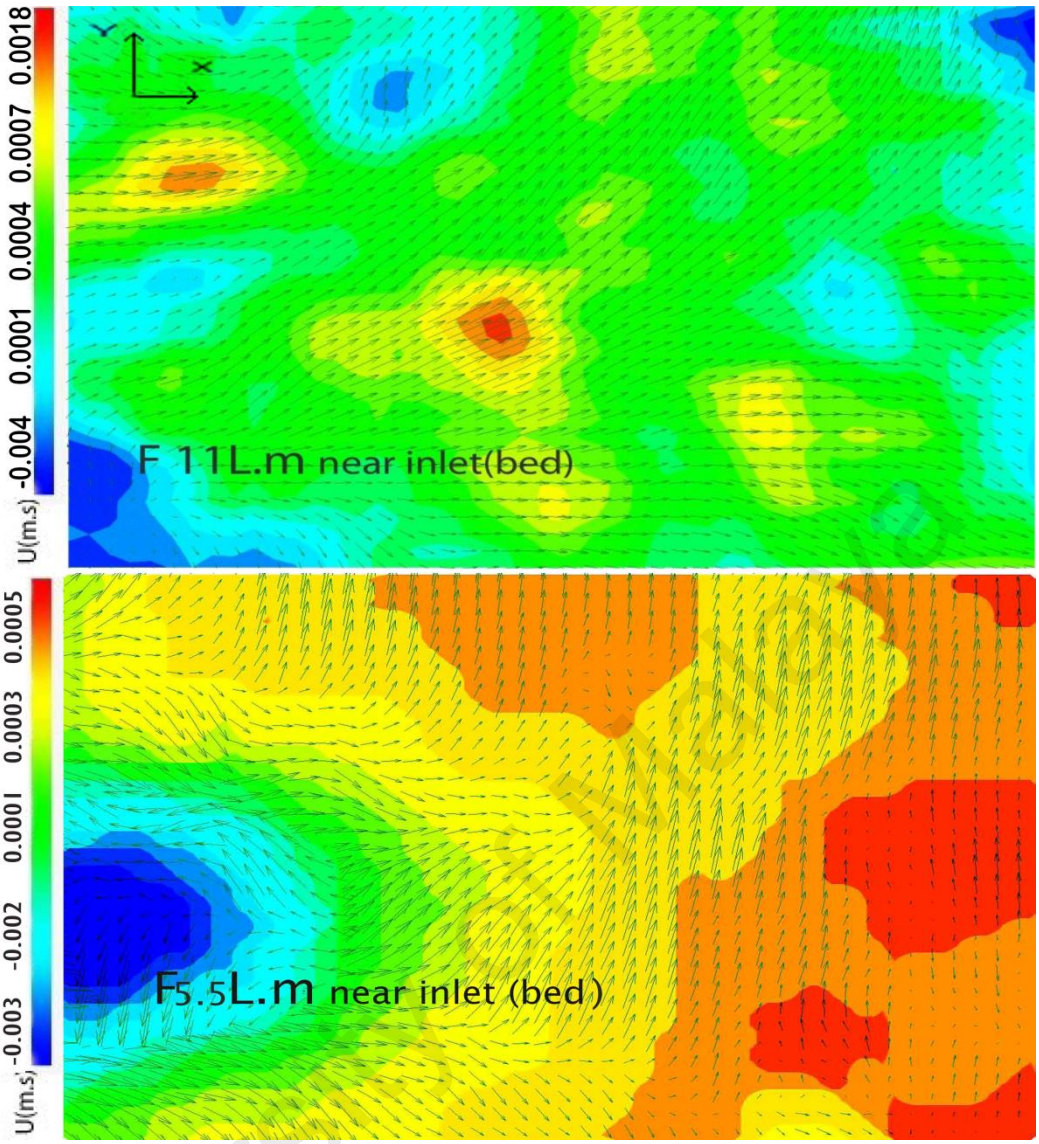

Figure 4.26 : Overlay of scalar and vector maps of fine particle movement at flow rates of 11 L/m (a) and 5.5 L/m (b), near the inlet, bottom of the basin (Zone c)

4.6.1.4 Near the outlet, bottom of the sediment basin (d-NOU)

For the last experimental evaluation stage, the studied frame was adjusted to the bottom, close to the outlet to investigate the mechanism of fine particle displacement in a different corner of the sediment basin. The graph (Figure 4.27) displays that fine particles tended to re-suspend and settle at higher flow rate and flow to the outlet at lower flow rate. However, the fine particles were slower at lower flow rate, and a suspension zone was

detected at the left of the image (Figure 4.28). This motion occurred at the back of the tank and is necessary to define the Z-axis.

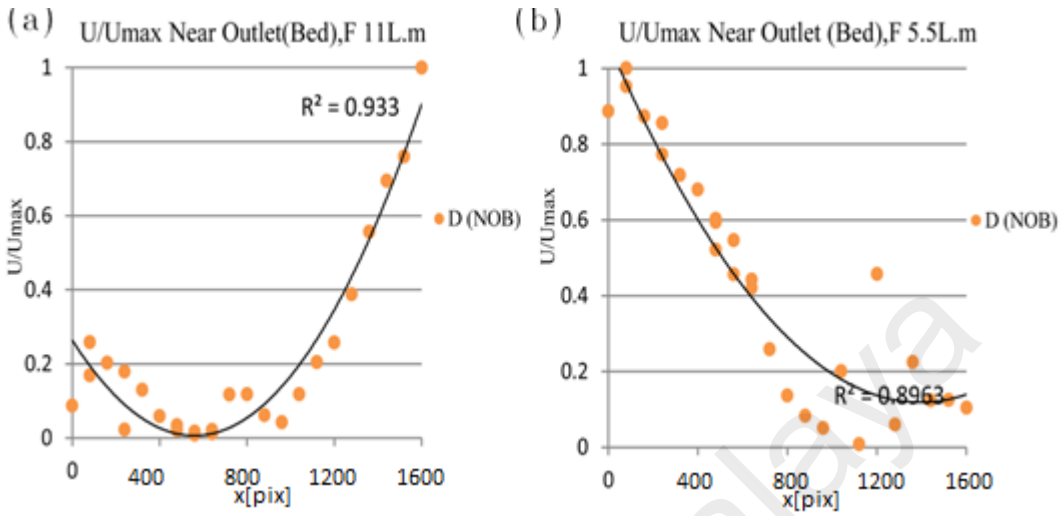

Figure 4.27 : U/Umax graph at two flow rates of 11 (a) and 5.5 L/m (b) near the outlet, bottom of the basin (zone d)

Apparently, the outlet influence was greater at lower flow rate, as the fine particles moved toward that point. But by increasing the flow rate to 11 L/m the velocity line increased in the graph (Figure 4.27) and fine particles tended to re-suspend in the water column more. Moreover, the shear bed stress and the basin's bottom wall boundary moved the fine particles upward and produced an eddy zone in the middle of the tank although the force of inlet flow was very small in this section (Figure 4.28). All vector map changes are clear in the U/Umax graph.

University of Malaya

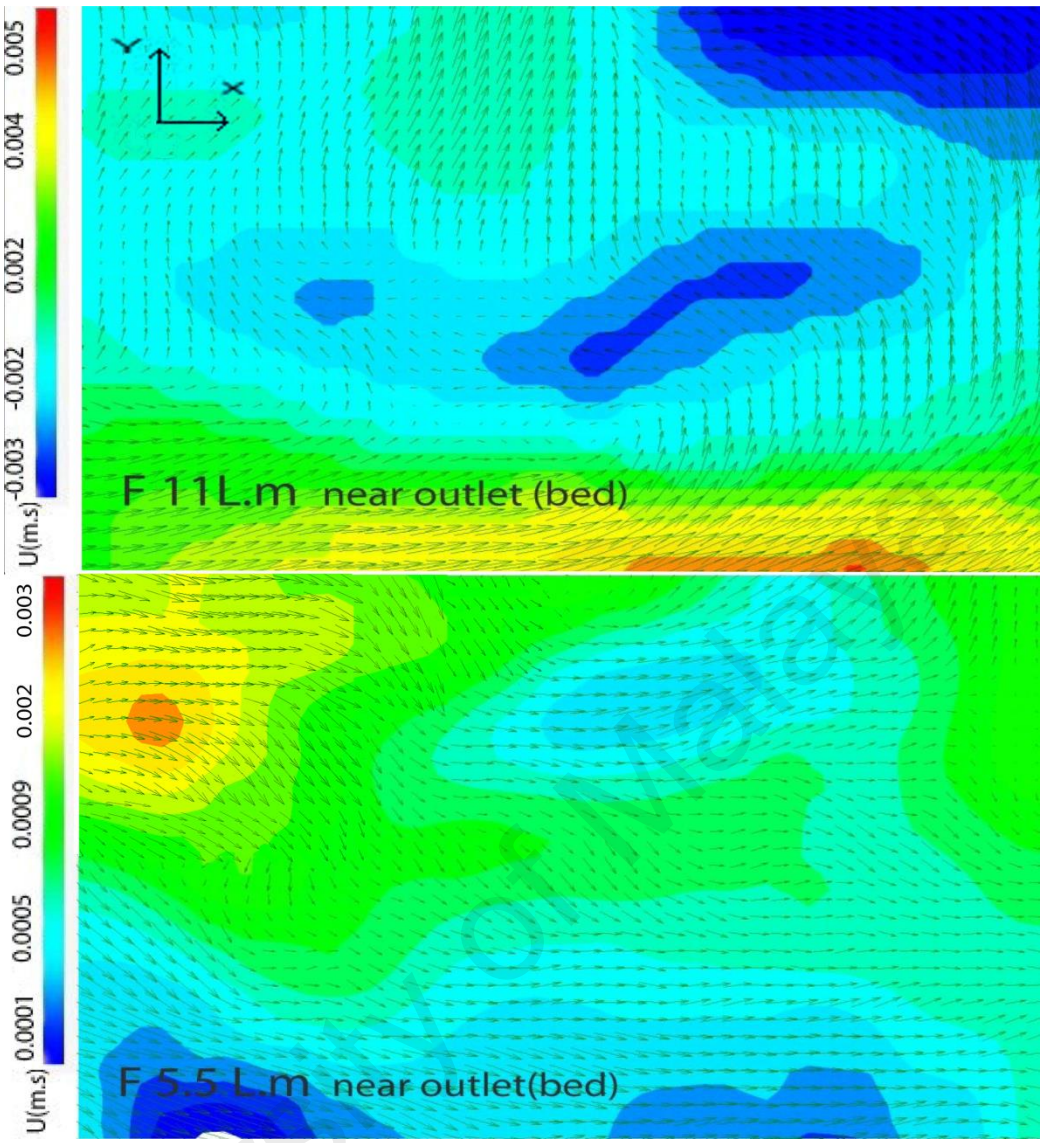

Figure 4.28 : Overlay of scalar and vector maps of fine particle movement at flow rates of 11 L/m (a) and 5.5 L/m (b), near the outlet, bottom of the basin (zone d)

4.6.1.5 Near the outlet, upper sediment basin (e-NOB)

The hydrodynamic behavior of fine sediment at the upper level of the sediment basin near the outlet was explored using PIV. Figure 4.30 displays the movement of fine particles at two flow rates, 11 L/m and 5.5 L/m. By tracking the fine particles on the vector map at a lower flow rate (5.5 L/m, Figure 4.29) it appears they settled in this section; however, the path deviated to the bottom right where the outlet was placed due to the elevation of the inlet and outlet. Nevertheless, at the left side of the studied frame there was more tendency

toward the left as well as settling. The U/Umax increased as the fine particle flow approached the outlet wall. On the other hand, this particle velocity variation was much smaller than at higher flow rate of 11 L/m.

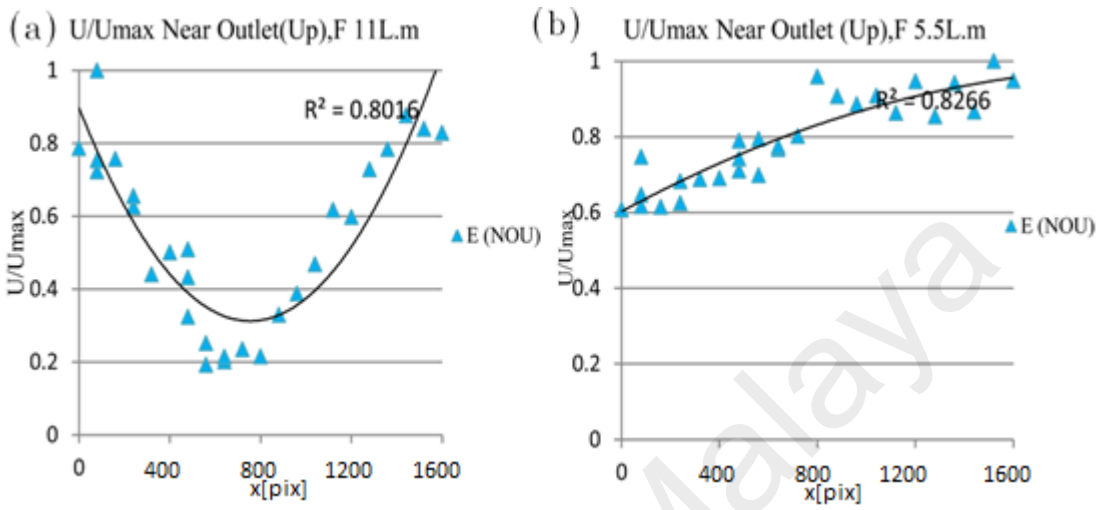

Figure 4.29 : U/Umax graph at two flow rates, 11 (a) and 5.5 L/m (b), near the outlet, upper basin (zone e)

The U/Umax graph demonstrates the variation in fine particle velocity at higher flow rate as decreasing at the left and increasing towards the right. The mechanism of fine particle movement at 11 L/m was different than at lower flow rate. The settling rate was higher at this experimental level, although the higher pressure dispersed the particles more and the circulation zones had lower velocity, which deflected the motion to the left. At the bottom left corner of the image, a re-suspension zone was detected that shows the eddy force of the water layers. Additionally, by increasing the velocity of particle displacement, the flow tended toward the outlet. Thus, it can be said that the higher flow rate created a greater circulation zone and pressure difference, which changed the fine particles' direction more than the lower flow rate. Generally, minor suspension was estimated at this sediment basin level.

University of Malaya

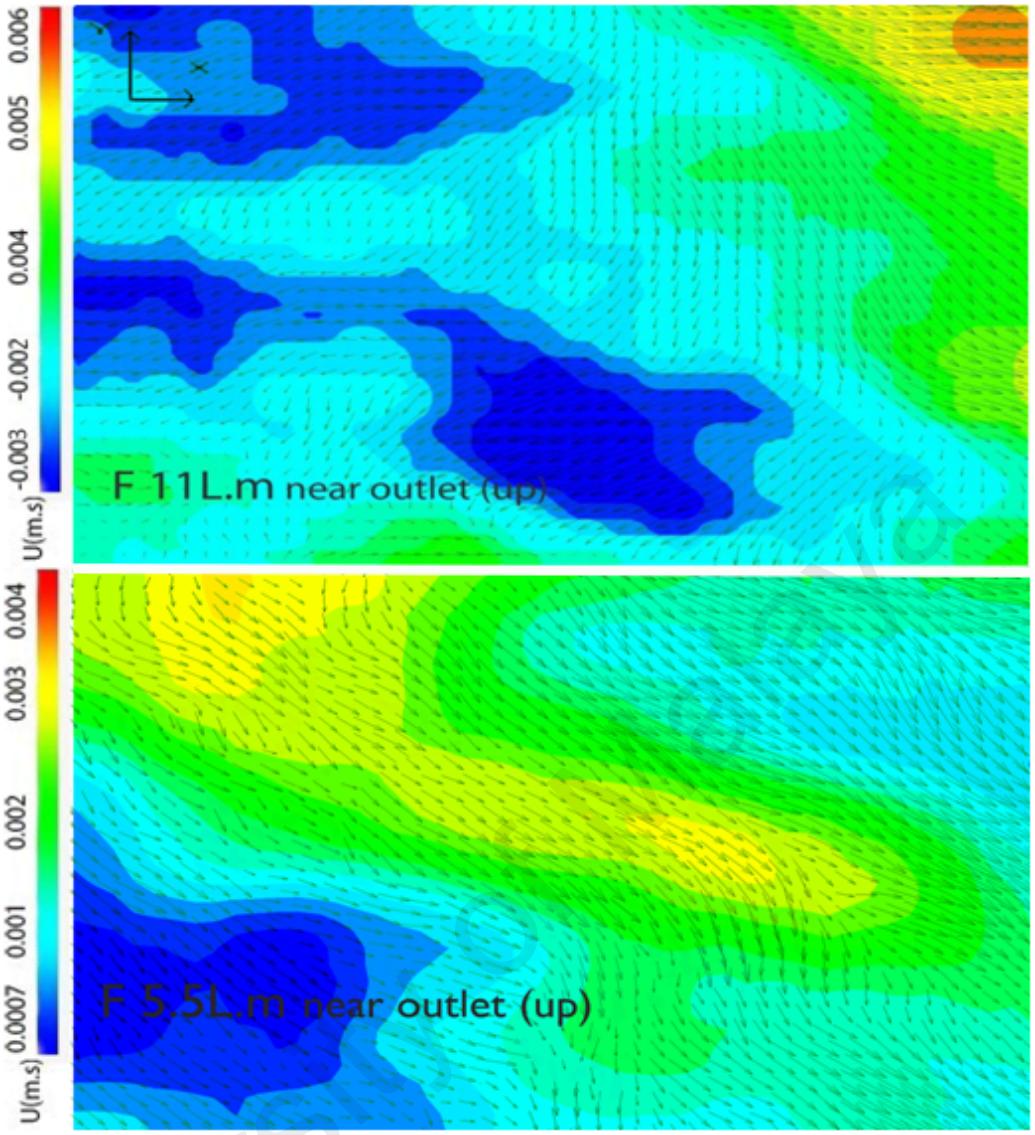

Figure 4.30 : Overlay of scalar and vector maps of fine particle movement at flow rates of 5.5 L/m (a) and 11 L/m (b) near the outlet, upper basin (zone e)

The overall view of these 5 zones showed the particles had higher velocity and faster hydrodynamic behaviour through the 11 L/m flow rates and the shape of tank caused the circulation of water after reaching to the wall therefore, many vortex zones has been created during the time and trapped the fine particles in different region.

4.6.2 Fine Sediment Dynamics within the Retention Structure

The key factor in using seed particles was the similarity in physical and transport properties between fine sediment and fine soil particles (15%) mixed with tracer particles

(Guasto et al., 2006; Maleoszewski et al., 2006; Spencer et al., 2011). The experimental method focused on non-cohesive particles, since soil particles at high concentration absorb water and floc size increases with time. The water flow was in transitional condition; therefore, during fine sediment transport in the sediment basin, different circulation was created in each area. It should be noted that the study assumption concerns fine spherical particles. Ebel (2009) identified the particle smaller than 10µm with velocity more than 0.001 m/s remains suspended.

The study observations proved that part of the fine sediment passed through the outlet pipe or settled in the pipe due to the pipe boundary (Kaminsky et al., 2008). Moreover, a minor part of the particles settled in the rest of the test and produced a homogenized fluid, though with a low particle concentration (Adrian, 2005). The variation in flow rate proved that the mechanism of particle mobility changed and the lower flow rate instigated particle flow with regular motion while the influence of gravitational force enhanced. Moreover, the studied particles' flow velocity in the studied point confirmed the decline in flow rate from the inlet to the other side of the tank on the X-axis (Jones & Wadzuk, 2013). The overall findings from the examination demonstrate that the detention structure with medium water level had a greater siltation problem at high flow rate and the fine sediment concentration decreased with distance (Li et al., 2007). Therefore, the combination of particle size (<63µm - 20-50 µm), water level (25 cm), water flow rate, and retention surface shape helped understand the settling mechanism of fine sediment with the studied method (Nichols et al., 2013).

The retention structure was made with two vertical layers. The upper layer showed that the fine particles displaced faster toward the first level of water above the bottom and tended to settle; thus, gravitational force was stronger at the upper level. Hence, the layer of fluid below demonstrated the suspension of fine particles in the water column, which

University of Malaya

is evidence of bed shear stress and Newton's third law that states that reaction force is of the same magnitude but in the opposite direction. Therefore, by approaching the bottom of the basin, the particles went upward with the flow (Mitchell & Burgess, 2004; Rex & Petticrew, 2011).

The surface motion dispersed the fine particles in different directions. The motion in this layer was somewhat greater, and by approaching the inlet, the flow rate and flow rate power reached this layer with less variation. The influence of wind on siltation was ignored (Kunkel et al., 2013). The fine particles went downward to the water depth level near the inlet, and then adjacent to the bottom the particles diffused by bed shear stress and the eddy boundary. Therefore, the resistance force enhanced in fine particles, which suspended in the water column. Although the higher flow rate increased the frictional force at the bottom of the basin, the erosion rate escalated.

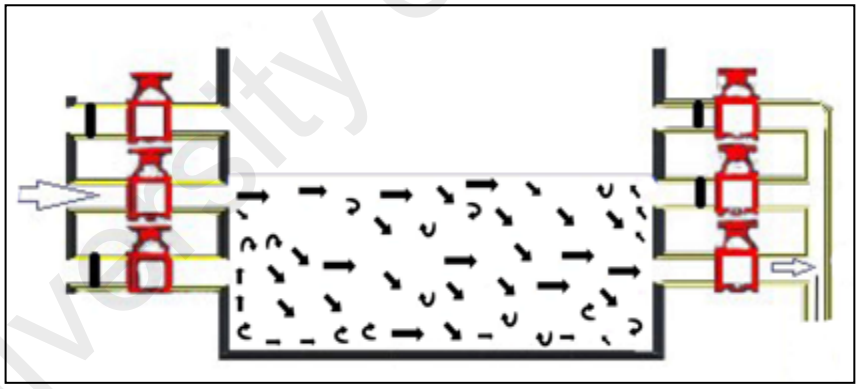

Figure 4.31 : A schematic of fine particles circulation

The displacement of fine particles in the bottom layer varied with distance: the nearer the flow was to the inlet, the more the particles dispersed and re-suspended at higher flow rate. By approaching the outlet, the fine particles moved with frictional force toward the outlet. Therefore, an undesirable outlet condition at higher flow rate was more likely. The lower flow rate caused a higher rate of fine particle settling; however, the resistance of the bed re-suspended the particles in the water body. Moreover, the outlet's dragging

University of Malaya

force was greater at low flow rate, thus the density increased at low flow rate (Lindken & Merzkirch, 2002; Spencer et al., 2011). The low flow rate maps (Figures 4.28 and 4.29) display more steady flow conditions. It can be concluded that during no-flow condition the fine particles settled easily. Thus, as high flow rate disperses the particles more, water quality declines during high seasonal flow (Wong et al., 2006).

The studied area dimensions affected fine sediment movement. As such, the sediment basin size changed the motion result, which is a phenomenon called volume pond efficiency (Khan et al., 2013; Senatore et al., 2013). The effect of fluid viscosity and density were more identifiable in fine particle transport. Since the fine particles had small diameters, the impact of density in the upper water layer, especially near the outlet, as well as viscosity resistance at mid-water depth (Figure 4.30) were apparent (Barnard et al., 2013; Bo et al., 2013). Overall, the hydrodynamic behavior of fine sediment was classified based on the position in the retention structure. In deeper water, the suspension level of fine sediments enhanced, although a lower flow rate helped diminish it. Additionally, the drag force and density value increased near the outlet (Paris et al., 2010; Tu et al., 2001).

4.6.3 Impact of Water Depth, Inlet and Outlet Configuration

The test was run for same condition as last experiment with changing the difference in height of water to 20 and 44 cm to study the effect of depth on hydrodynamic behaviour of fine sediment. In here, the place of outlet was varied between two locations. First the inlet and outlet placed in same height, then they set with elevation from each other, Figure 3.5 illustrates the conditions.

University of Malaya

4.6.3.1 Fine particle mechanism in different depths

The results of fine particle seeds settling down in sample one at 20 cm water depth showed that at higher flow rate (Q=11 L/m) they were transported faster than at lower flow rate (Q=5.5 L/m). Although there is greater change in velocity at lower flow rate (-0.002 to 0.004 m/s), the fine particles (D=20-50 μm) were re-suspended from the bottom of the tank where they had lower velocity as they returned to the flow direction, when they remained in regular lines and their velocity tended to decrease. The analyzed images of fine particle movement at different flow rates demonstrated that fine particles of clay in sample one (20-50 μm) settled down at the higher flow rate (Q of 11L/m). However, at Q of 5.5 L/m the fine particles displaced more slowly and the vector map illustrates that the particles moved on a steady curve (turbulent boundary layer) to the left and they tended to settle beyond this distance.

University of Malaya

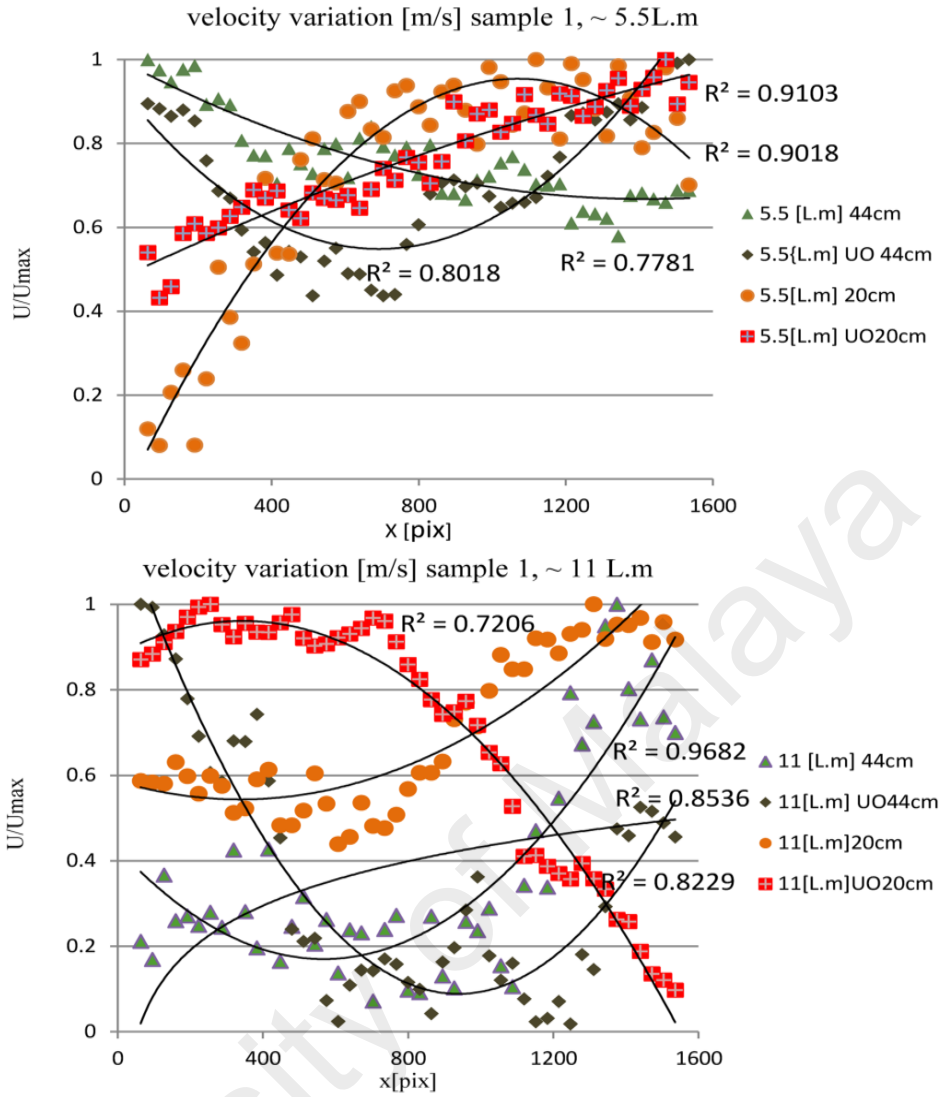

Figure 4.32 : U/Umax graph of sample one (D=20-50 µm) at different water flow rates (Q=11 and 5.5 L/m) in two water depths, 20 cm and 44 cm. Upper Outlet shown by UO

Evidently, at higher flow rate the fine particles dispersed more and at the left side of the image (Figure 4.34) a flux toward the outlet was detected. It can be concluded that the particles traveled downward towards the outlet. Therefore, the suction power of the outlet pulled the fine particles in the left direction, although the particles were pushing up at the end side of the frame at 5.5 L/m flow rate, which showed the weakness of gravity force on the eddy layer of water. The influence of inlet and outlet elevation was more evident at higher flow rate, as the fine particles displaced disorderedly in water. The velocity variation of fine particles at higher flow rate in the graph illustrates the amount of pressure

University of Malaya

on the movement of particles was higher and the viscosity of water decreased with rising flow rate. This means that higher stress made the fine particles flow through the water body.

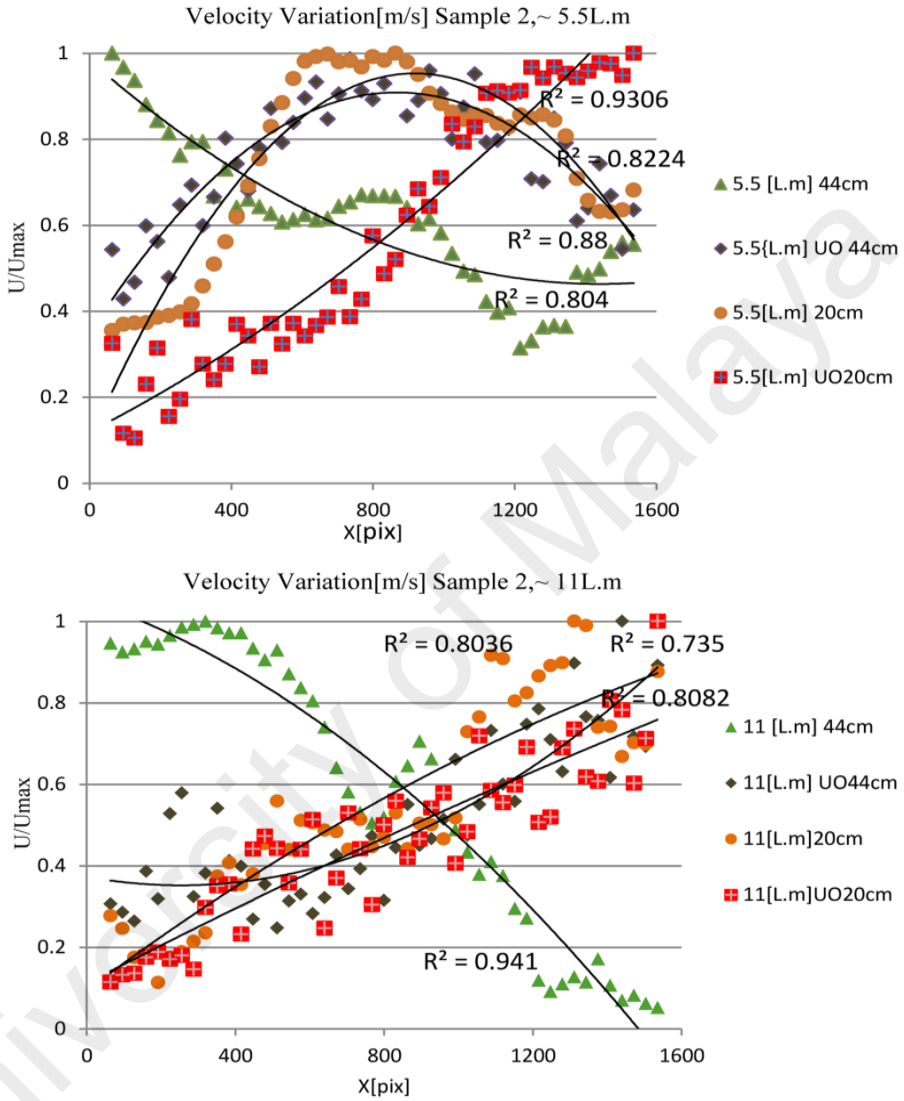

Figure 4.33 : U/Umax graph for sample two (D=1-20 µm) at different water flow rates (Q=11 and 5.5 L/m) and two water depths, 20 cm and 44 cm. Upper Outlet shown by UO

By changing the outlet height, the inlet pipe height was adjusted accordingly, and the behavior of fine particles transformed. Fine seeded particles in sample one at 11 L/m flow rate started settling down at regular flow. The graph in Figure 4.32 visualizes this conversion of particle flow when the velocity of fine particles decreased with time. Lower

University of Malaya

water flow rate (Q of 5.5 L/m) carried the fine particles (D 20-50µm) in steady lines to the bottom of the basin. The direction of the arrows on the vector map illustrates that a forward-driving force was acting on the particles at a flow rate of 5.5 L/m. This potentially happened due to the boundary layers, which hindered the settling velocity at this water level in the existing condition. Based on the result, the fine particles at both flowrates tended to settle down. Although, this behavior differed at higher flow rate, whereby the terminal velocity (vt) of fine seeded particles in sample one was higher and fine particles at 11 L/m flow rate increased the particles' density and decreased the fluid's viscosity (v_t= 0.0004-0.006 m/s). Therefore, fine particles (20-50 µm) in water depth of 20 cm (h) moved faster at higher flow rate and tended to settle down at the same inlet and outlet heights.

University of Malaya

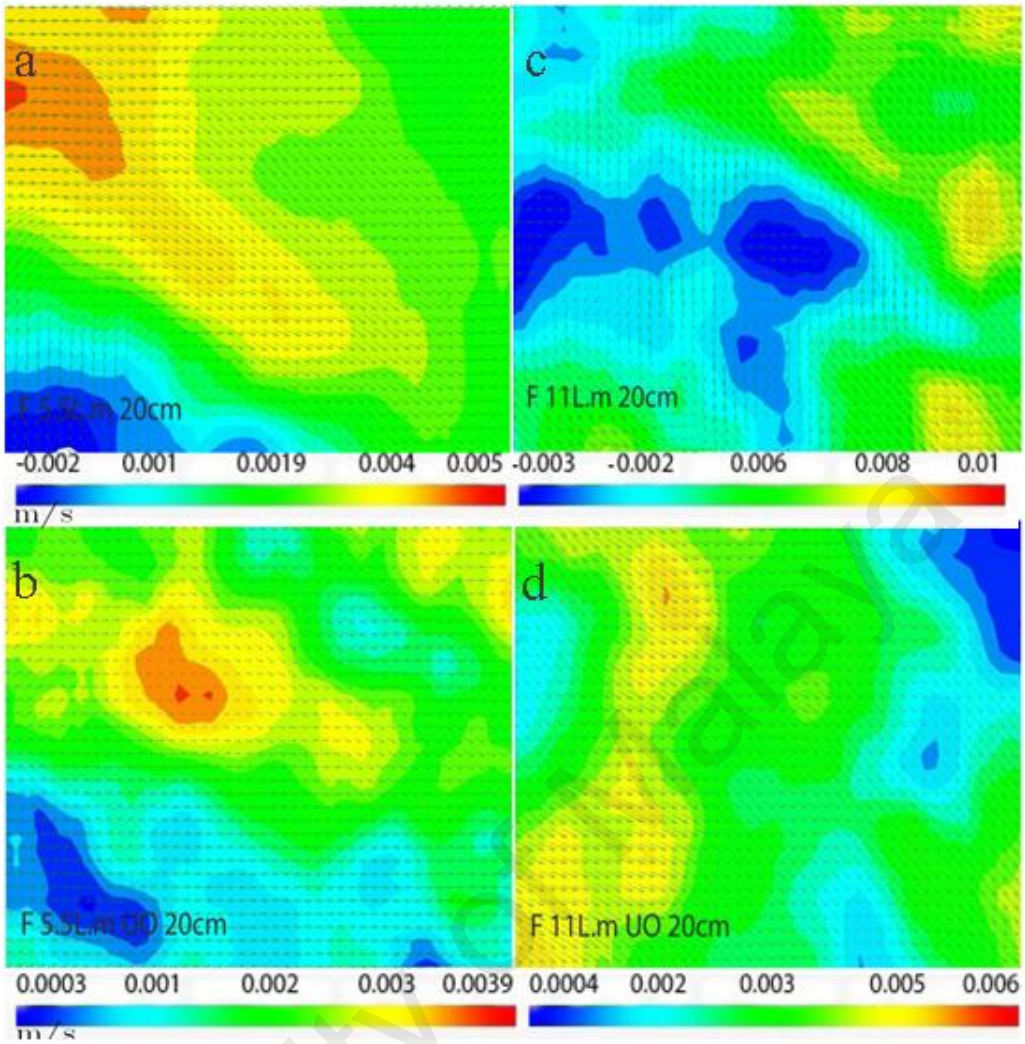

Figure 4.34 : Vector overlap and scalar map of sample one (20-50 µm) at 20 cm depth in variation of flow rate (Q=11 and 5.5 L/m) with different outlet placements (UO-images b and d)

The homogenized mix of fine soil and water seeded with fluorescent particles having smaller particle size diameters (1-20µm) at 20 cm depth was tested in the same condition as that used for the first type of fine particles. The resulting graph (Figure 4.33) demonstrates the investigation of sample two at lower flow rate of 5.5 L/m. Here, the velocity ratio (U/Umax) increased and the fine particles' velocity ratio exhibited a curve that indicates the influence of the outlet as all particles moved downward. However, it must be noted that only part of the particles settled down and the rest went out with the flow. At 11 L/m, when approaching the outlet zone, fine particles (D 1-20µm) were

transported to the right side and followed the flow steadily. The left side of the frame (Figure 4.35) shows that the fine particles were trapped in circulation zones and revolved towards the left, then settled down. The shear velocity of sample two at 11 L/m was higher (almost 0.009 m/s) than the lower flow rate. Generally, sample one with larger diameter (20-50 µm) had greater mean velocity than sample two in a similar condition.

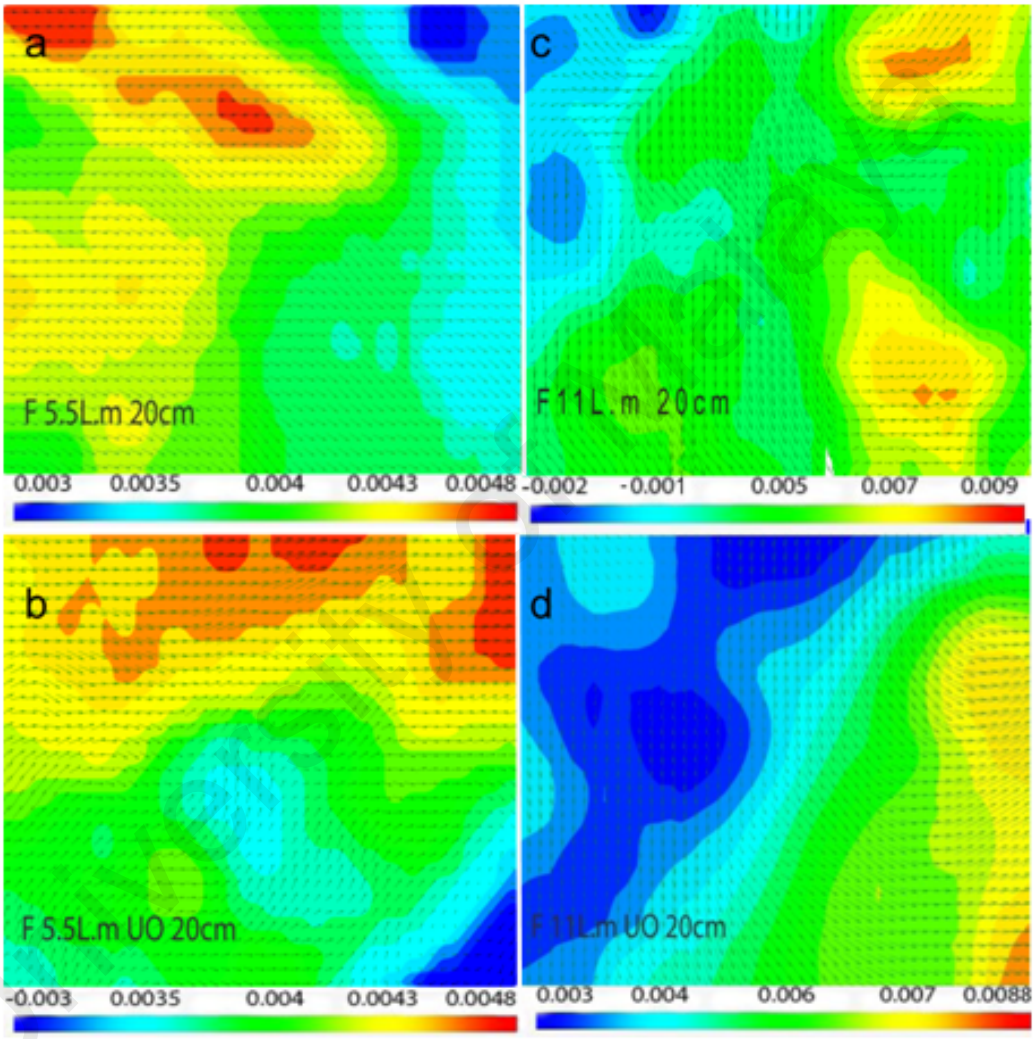

Figure 4.35 : Vector overlap and scalar map of sample two (1-20 µm) at 20 cm depth with flow rates of 5.5 L/m (a and b), 11 L/m (c and d) and different outlet placement (b and d)

The results revealed that the smaller particles in sample two were transported differently at 5.5 L/m after adjusting the upper outlet (UO). The outlet pressure decreased while the bed layer boundaries and hindered settling produced turbulence in the particle movement.

The captured frame was at mid-depth, between the inlet and outlet. Thus the re-suspension of particles from the bed layer was apparent. A circulation zone was spotted at the right side of the frame, which occurred due to the turbulence of fine particles. At higher Q, fine particles (1-20 µm) settled down near the inlet and were pushed up when approaching the outlet. In the examined water circulation, when the fine particles encountered higher pressure, their density reached a value higher than water. The particles then settled down, but on the X-axis, close to the outlet the re-suspended particles were interrupted by the bed wall, moved up and became suspended in water. The U/Umax values indicate a similar velocity attitude for both flow rate and outlets with the actual value difference based on flow rate. According to Stokes' law the gravitational force was stronger at the same inlet and outlet levels, therefore the tendency to settle was enhanced.

4.6.3.2 Fine particle hydrodynamic behavior in different depths

The next variable that was investigated in the study was the impact of water depth on fine particle movement, or settling. The studied tank was filled with water and fine soil (15% volumetric concentration) up to 44 cm (h) depth and was then seeded with fluorescent particles (20-50 µm and 1-20 µm). Then the same tank area was explored by capturing images of the light emitted by seed particles (PIV technique). The remaining condition for the method was the same as that examined for 20 cm water depth.

The U/Umax graph (Figure 4.32) displays the transport of fine particles in sample one (20-50 µm) at flow rates, 11 L/m and 5.5 L/m. The result signifies the same variation in velocity ratio over distance. This proves the decrease in mean velocity at this depth, which means the particles, reached a point of higher stability and tended to settle.

The combination of scalar and vector maps for sample one at higher flow rate and a depth of 44 cm demonstrates the re-suspension of particles at the left side and their tendency to

University of Malaya

settle at the right side of the frame. The detected suspension occurred due to bed wall or bed shear stress that moved the particles upward in the water. Then, with the release of bed layer pressure the particles were propelled to the outlet, so the outlet suction pressure was stronger. The apparent impact of depth variation on fine particle movement was the velocity ratio, where the particles were transferred more slowly with increasing water depth (maximum U/Umax 0.0009m/s (44cm), 0.01m/s (20cm)). Figure 4.38 demonstrates the hydrodynamic behavior of sample one at lower water flow rate (5.5 L/m) and low pressure position, which caused the steady linear movement of particles toward the outlet. This is because the outlet was near the basin's bed and the wall boundaries diminished the transport velocity of particles at lower flow rate (5.5 L/m). At 44 cm depth, the displacement (x) of fine particles over time at flow rate (Q) of 5.5 L/m was higher than at 11 L/m. This result is opposite the findings at 20 cm depth. Therefore, it can be concluded that with increasing depth, fine particles (20-50 µm) were transported quicker than at 11 L/m. It shows the higher flow rate dispersed particles in the layers above. Due to collisions with the boundary layers, the eddy zone was observed and particle movement accelerated. Another reason for this issue is that the water surrounding the area with particles reduced the gravitational force, therefore the water diffusion dispersed the particles.

University of Malaya

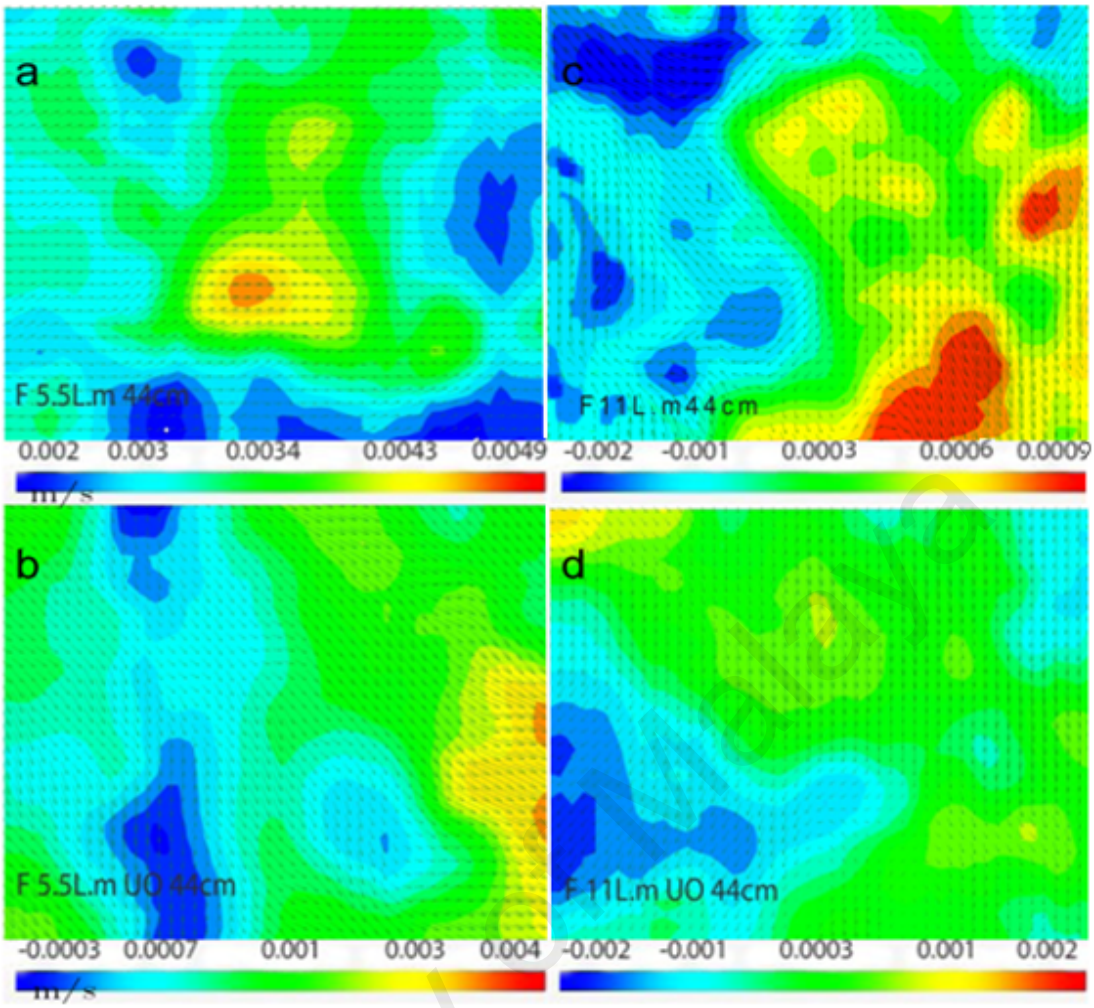

Figure 4.36 : Vector overlap and scalar map of sample one (20-50 µm) at 44 cm depth with flow rates of 5.5 L/m (a and b), 11L/m (c and d), and different outlet placements (b and d)

Next, the elevation between the inlet and outlet diminished and they were adjusted to be in a line, thus the impact of the upper outlet (UO) was studied. It was found (Figure 4.32) that the ratio of displacement velocity (U/Umax) developed along the same curve shape and the variation in U/Umax tended toward a convex function at both flow rates (Q). Moreover, the dispersion of particles decreased quickly, and at both flow rates fine particle settling was observed. Evidently, with higher outlet, the incoming pressure from the outlet on the fine particles diminished, so the particles settled steadily. However, the terminal velocity (Vt) increased in the UO condition compared with the elevated inlet. It

is inferred that by increasing the water depth and adjusting the inlet and outlet to the same height, fine particles (D=20-50µm) settled and their suspension rate reduced with the closed outlet. This behavior supports the theory that settling velocity increases when approaching bed water level.

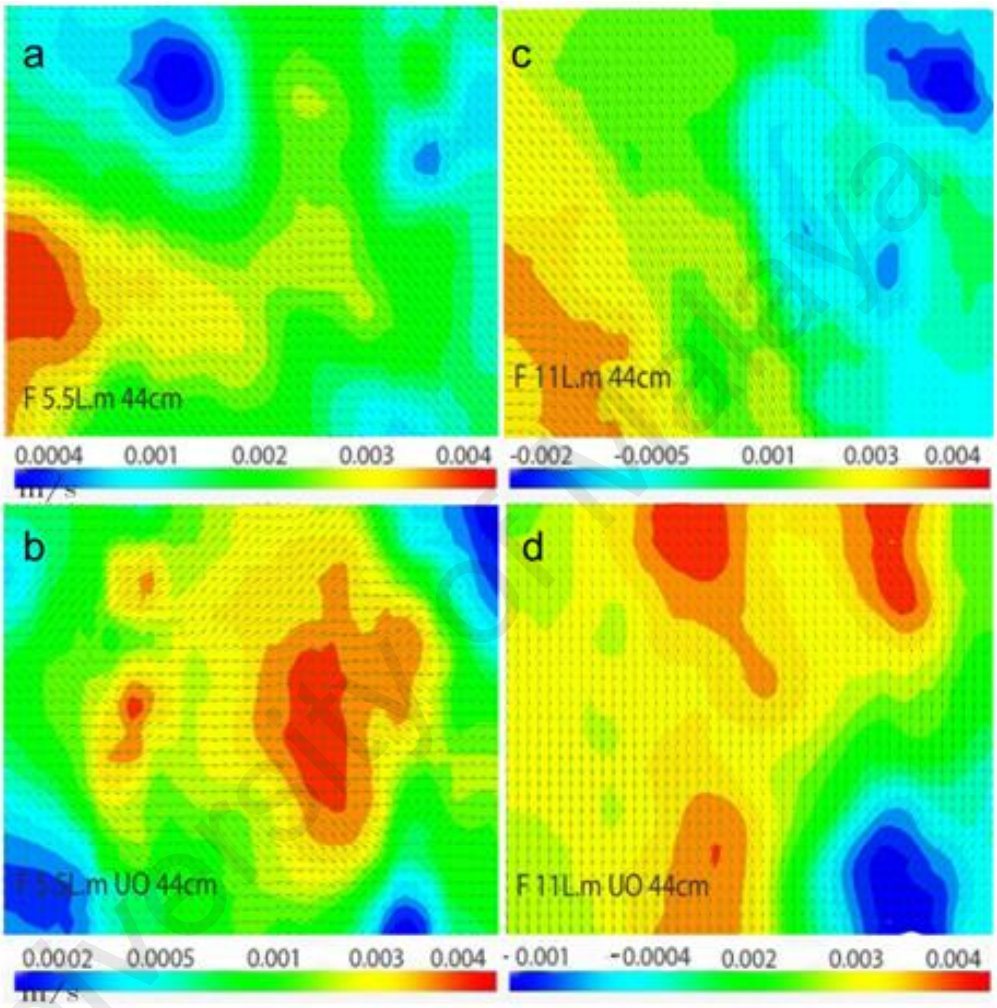

Figure 4.37 : Overlap of vector and scalar map of sample two (1-20 µm) at 44 cm depth in two flow rates of 11 L/m and 5.5 L/m, by different outlet placements (b and d)

Figure 4.37 demonstrates the different tendencies of fine particle (1-20 µm) movement in both flow rates (Q). The concave function of fine particles (1-20µm) at lower flow rate (5.5 L/m) and elevated inlet and outlet was observed. However, the hydrodynamic behavior of fine particles (1-20 µm) in the operating Q (5.5 L/m) was to settle, the fine particles followed the force of gravity and there was no viscosity resistance for the fine

particles. Similar behavior was detected for particles at higher flow rate (11 L/m) although the U/Umax graph shows the velocity ratio distribution was increasing linearly with a less convex curve. Fine particles were transported with higher values of velocity (Vt) at higher flow rates, which was different for particles with larger diameter. The phenomenon occurred because of the impact of particle diameter and flow rate on depth. The smaller the particle diameter, the more rapid the speed of particle displacement was. By altering the outlet to a higher position (UO), the U/Umax value decreased in the area. Thus, diverse tendencies of particles with larger diameters were discovered, though the fine particles (1-20 µm) settled at higher fluid flow rate (11 L/m). Additionally, at UO and 5.5 L/m flow rate the fine particles (1-20 µm) resisted the gravitational force and were transported to the upper layer. On the other hand, finer particles behaved differently from all studied conditions in this step and tended more toward the action of particles at 20 cm depth. In Figure 4.37 an eddy layer was observed in the middle of the scalar map that interspersed the flow above and pushed the particles down; a small circulation zone was also seen near the outlet wall. Bed shear stress and wall boundary influenced the smaller particles at lower flow rate. Consequently, fine particles were expected to suspend in the water body; however, by approaching the bed, the pressure decreased.

4.6.4 Impact of Depth and Outlet Location on Fine Particles Movement Mechanism

The fine sediments were assumed to be spherical. Based on the results, the drag resistance of fine particles rather than to gravitational force varied at different flow rates (Q). According to other studies, there is a correlation between the function of Reynolds number (Re) CD =24/R that is constant ~ 0.4 for 10^3 <Re < R crit ~ 3 for 10^5 based on the Stokes law (Jiménez & Madsen, 2003) and particle diameter size. It was observed (Figures 4.35 and 4.37) that fine particles exhibited more resistance at lower flow rate

University of Malaya

and were suspended in the water body when the inlet and outlet were elevated. The finer particles (1-20μm) were transported smoothly with flow and their direction was influenced by the different forces in this case, although with rising water depth at lower discharge (Q) re-suspension behavior was detected. In addition, the suspended bed load detected at this point of the study was higher than when using an upper outlet. Generally, the fine particles had viscoplastic behavior and the water reached a critical content state. Thereafter, the particles exhibited viscous behavior without further changes in water content (Mahajan &Budhu, 2008). By varying the water depth (h), the explained behavior appeared clearly in the settling velocity and movement of fine particles. The fine particles traveled to the bottom of the basin constantly by increasing the distance between the water surface and bottom of the basin. It was demonstrated that the influence of depth on velocity ratio decreased the rate of suspension in rising water level. However, the outlet point was a major factor in this behavior. By elevating the inlet and outlet, the particles moved in the outlet's direction and their path changed to the right. The placement of the inlet and outlet in a line in water caused a decline in the suspension of particles and enhanced siltation level.

The impact of stream power on the fine particle transport mechanism was investigated by varying the flow rate (Q) by means of a pump. The variation of discharge Q displayed that higher flow rate transported particles over the distance faster, and when the particles were smaller the rate of dispersion enhanced (Figures 4.33 and 4.35). Thus, the dispersion of fine particles in fluid with less raise was higher and more suspension was found (Ali et al., 2011; Huang, 2007; Hadad, 2013). Varied flow rates caused faster pond siltation, therefore the difference in fine particle transport mechanism was obvious (Harrison et al., 2007). However, the roles of particle diameter (D) were essential, and mean velocity increased with smaller diameters (Jones &Wadzuk, 2013). Higher flow rates generated tidal hydrodynamics in the water body, which controlled fine sediment transport and

University of Malaya

encouraged the resistance of fine particles in the middle of the tank (Shi et al., 2006; Yu et al., 2013). The mobility of fine particles at greater depth increased their settling and decreased suspension (Mitchell et al., 2006). The incoming fine particles altered their direction with outlet placement and depth of water; the elevation of the inlet and outlet (Figure 4.34) generated a surge in the lower fluid layer that carried the fine particles at different angles (Mitchell, 2010). The mobility and direction of fine particles at greater depth revealed the correlation between depth and particle settling. By traveling from the inlet and being carried out by the outlet force, the fine particles tended to form siltation more and at higher flow rate their settling rate augmented (Tang & Wang, 2009; Toriman et al., 2009; Tu et al., 2001).

Near the bed, velocity was higher when the inlet and outlet were elevated, therefore water flow transported sediments faster (Figures 4.36 and 4.37). The 20 cm water level somewhat showed the fine sediment transport mechanism near the water surface layer, the increasing settling mean velocity and the linear transport of fine particles with increasing water levels (Bayani Cardenas, 2008; Mitchell & Burgess, 2004). Darcy's law that defines all positive velocity U (m/s) proves that particles moved from a high pressure area to low pressure; therefore the result was positive. The near-bed velocity of particle displacement was lower at higher water levels; even the influence of outlet relocation was not great on fine particle displacement velocity in the area. At 20 cm depth, the impact of water flow rate on particle size was apparent, as larger particles displaced faster and showed less resistance to falling, thus gravitational force was more powerful.

4.6.5 The Impact of Inlet on Hydrodynamic Behavior of Fine Particle

The sediment basin was filled up to three levels of water: 16.5, 19, and 22 cm. The adjusted depth allowed for the investigation of fine particle displacement in the designed sediment basin with different incoming water conditions. The three water inflow stages

University of Malaya

were named according to the distance of the inlet pipe from the water surface, i.e. U (Upper), M (Middle) and L (Lower). The assumption was that the retention had one inlet and one outlet, thus the upper inlet pipe at 20 cm water level was open and two different outlets were explored. The maximum power for the pump to produce the water flow rate was around 11 L/m, so the water flow rate varied between 11 L/m and 5.5 L/m. Based on the Reynolds number, the water flow could be described as transitional flow (near laminar flow) and the fine particles were moving in water close to natural behavior.

4.6.5.1 Inlet higher than the water surface level

The first instance studied was a water level of 16.5 cm, which was below the inlet pipe. Thus the values for this condition are given as U (The upper than the water level). In this part of the test, the outlet was the lowest pipe at the opposite side of the tank. The sediment basin was controlled according to the water flow to find the best place for using PIV to eliminate bubble errors in analysis. Since the distance or height of the inlet compared to the water level caused higher incoming water pressure based on the gravity force in falling water, oxygen was released in water, creating bubbles in the first tank area.

University of Malaya

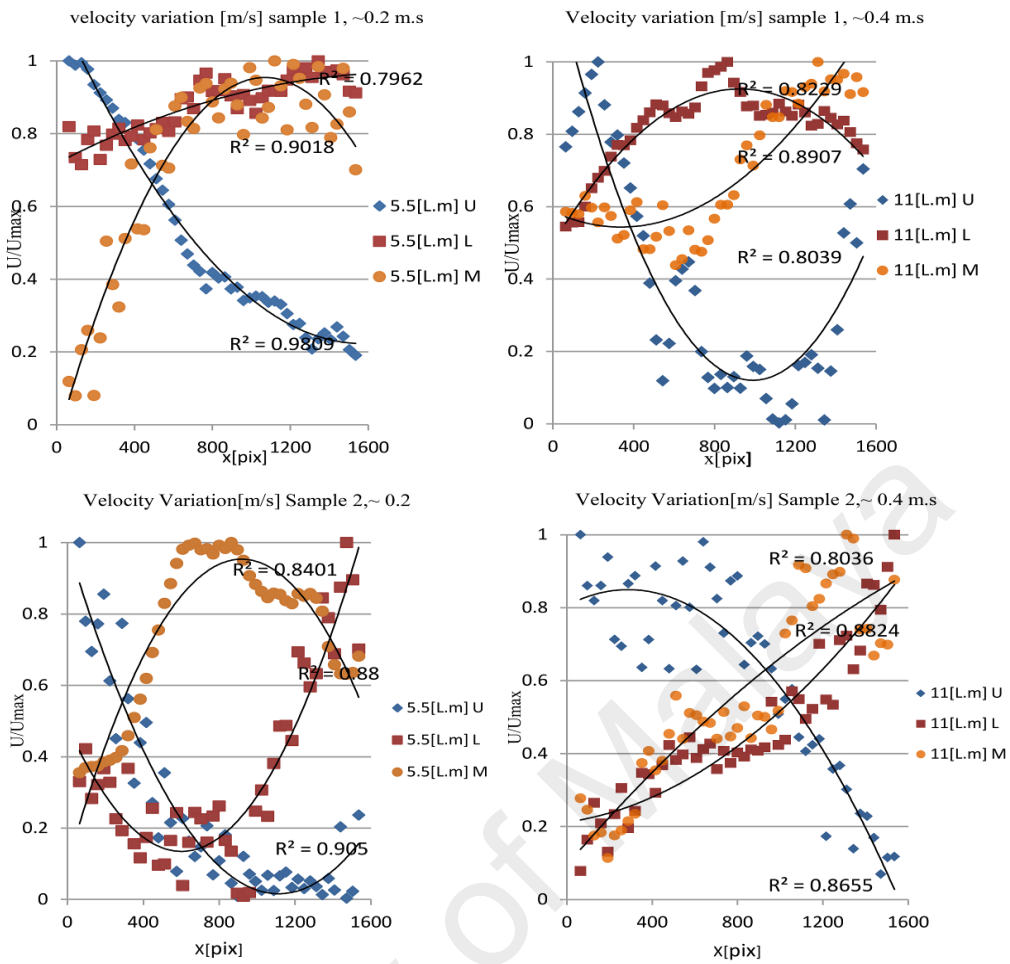

Figure 4.38 : Graphs of sample one and sample two with a lower outlet

Therefore, the study focused on the first, horizontal part of the tank without bubbles. The nearest place from the inlet was selected to begin the test on fine particle movement. In addition, all images in different test conditions were taken from the same area. The result of sample one (20-50 µm) in U condition (Figure 4.38) indicates the high dispersion of fine particles in the middle of the water body. At a flow rate of 11 L/m, the mixing of fine particles in water flow created turbulence that trapped some fine particles; thus particles began to disperse at this water level due to the water flow impact. It showed there is a linear increase in transport capacity with increasing mean flow(Zhang et al., 2011). The recirculation zone upstream of the frame showed that the particles re-suspended in the water body with the flow force. Such effect of deflection angle in the presence of

University of Malaya

recirculation zones is probably due to the role of the screen deviation angle, which in turn influences the longitudinal pressure distribution (Figures 4.39).

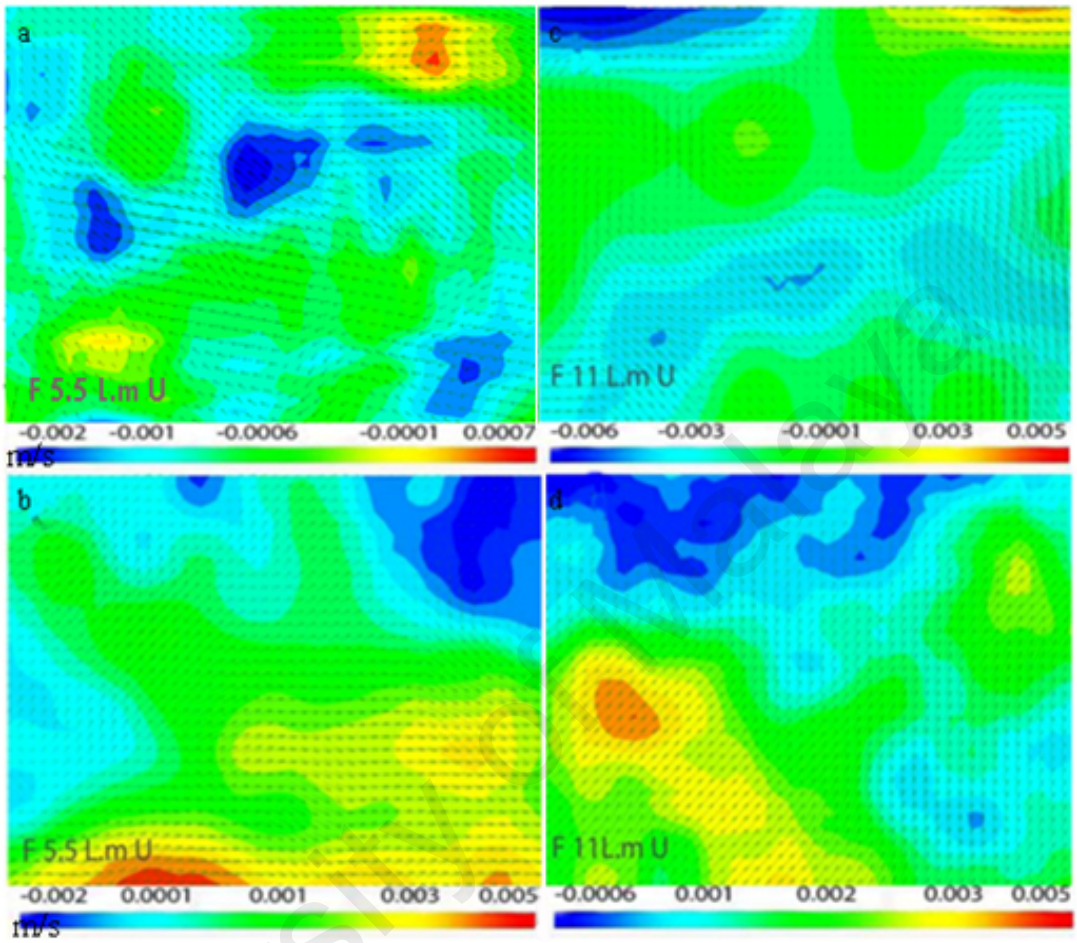

Figure 4.39 : Scalar and vector static maps of sample 1(a and b), and sample 2(c and d) at upper inlet pipe placement, a and c flow rate of 5.5 L/m and, b and d flow rate of 11L/m.

The mean shear velocity decreased with time as fine particles moved on the abscissa; moreover, the change in particle velocity from negative, -0.6 (mm/s), to positive velocity of 0.5 (mm/s) proved that the inlet flow swerved the fine particles (Figure 4.39). Therefore, the particles re-suspended from the bottom of the tank to the upper water layers and settled down in the next horizontal layers in front.

As described in the flow rate graph, at around 5.5 L/m the fine particles veered their direction from bottom to top, and some small recirculation zones were detected. Although

the particles' movement was much slower than at higher flow rate (11L/m), still the lower water level condition from the inlet caused the dispersion of particles. The incoming water penetrated the water layers and broke down the van der Waals force of water molecules. The high pressure reached near the bed, dispersed the fine particles and changed their direction or re-suspended them. The results of mean velocity signify that fine particles settled better in a lower flow rate range. Moreover, the second type of fluorescent particle size (1-20μm) result shows that in the L condition (Figure 4.38) fine particles moved up again, but the difference in particle size between samples two and one was the amount of deviation from the path.

At a flow rate of 5.5 (L/m), the particles moved forward in laminar flow. In addition, the arrows show that the particles followed the streamline in a parallel direction. It can be observed that particles suspended in the middle of the tank moved slowly. Fine particles in sample two with a flow rate of 11 (L/m) in the U condition were transported to upper layers with a curve, but the intensity of particle movement differed from sample one since no recirculation zone was observed (Figure 4.39).

4.6.5.2 Middle inlet pipe flow

The second condition was tested in this study by adjusting the water level to the middle of the pipe. Here, we tried to investigate the influence of water level height from the inlet. In this stage, the water level was nearly 19 cm and water was gushing from the middle of the inlet pipe (middle of inlet, M). The valve of the lowest outlet pipe was open. Sample one with a flow rate of 11 (L/m) followed the flow steadily (Figure 4.40), although at a certain angle of the image frame re-suspended particles returning to the settling flow were detected. The scalar map of the lower flow rate (5.5 L/m) shows that the fine particles glided in the water body and tended to settle down, which is the opposite of the U

University of Malaya

condition (Figure 4.41). At higher flow rate (11 L/m) the fine particles in sample one settled down, moved on the horizontal axis, and displayed conical circulation.

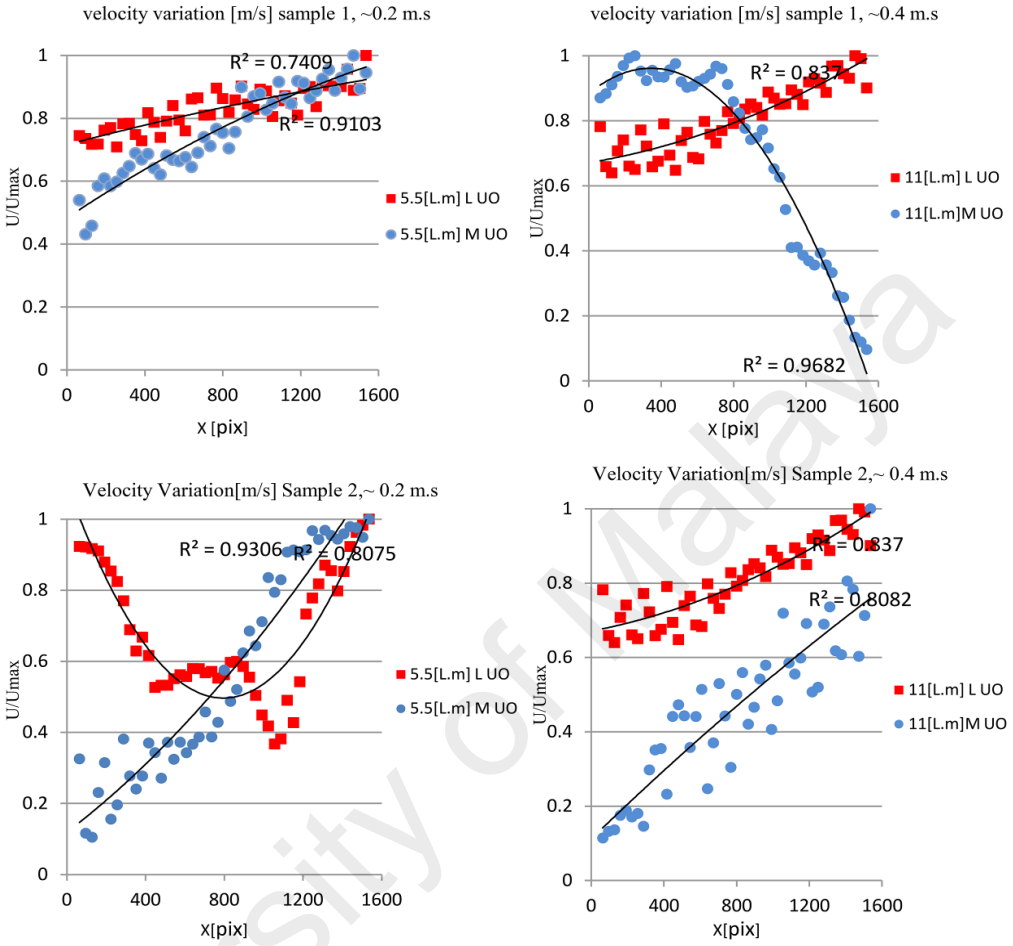

Figure 4.40 : Graphs of sample one and sample two with an upper outlet

The decrease in flow rate caused higher settling velocity at 5.5 L/m, which represents the greater effect of gravity force. Water is a low viscosity material, and the fluid of soil and water at low concentration as used in the study exhibited near Newtonian behavior (Markgraf et al., 2012).

Therefore, the fine particles of various sizes (20-50 µm) traveled to the bottom of the tank, where the gravity force is higher than the drag force. The velocity ratio showed a decrease in setup operation velocity at 11 (L/m) and an increase in this condition at 5.5(L/m). The figure shows that the fine particles in sample one moved anti-clockwise at

University of Malaya

high flow rate. This happened because of two recirculation zones that propelled the particles downwards, unlike the majority of fine particles. However, the velocity variation was small (around 0.0001 m/s). Particles tended to steadily settle down at 5.5 (L/m) more so than at 11 (L/m). The graph of particle movement proved this movement tendency toward the outlets. In the designed sediment basin the first condition attempted did not allow to convert the place of outlet pipe to other model as the water level was lower than the selected outlet for all different outlet locations. Nevertheless, by increasing the water level (depth), the water surface rose and reached the upper outlet pipe. Therefore, in the M condition, the lower pipe was closed and new water circulation was developed to study the effect of outlet location on fine particles settling. In order to achieve this, the pipe that was placed on the opposite side of the inlet pipe at the same level (upper outlet, UO) was opened and the tests were run with the same variables (Figure 4.40).

University of Malaya

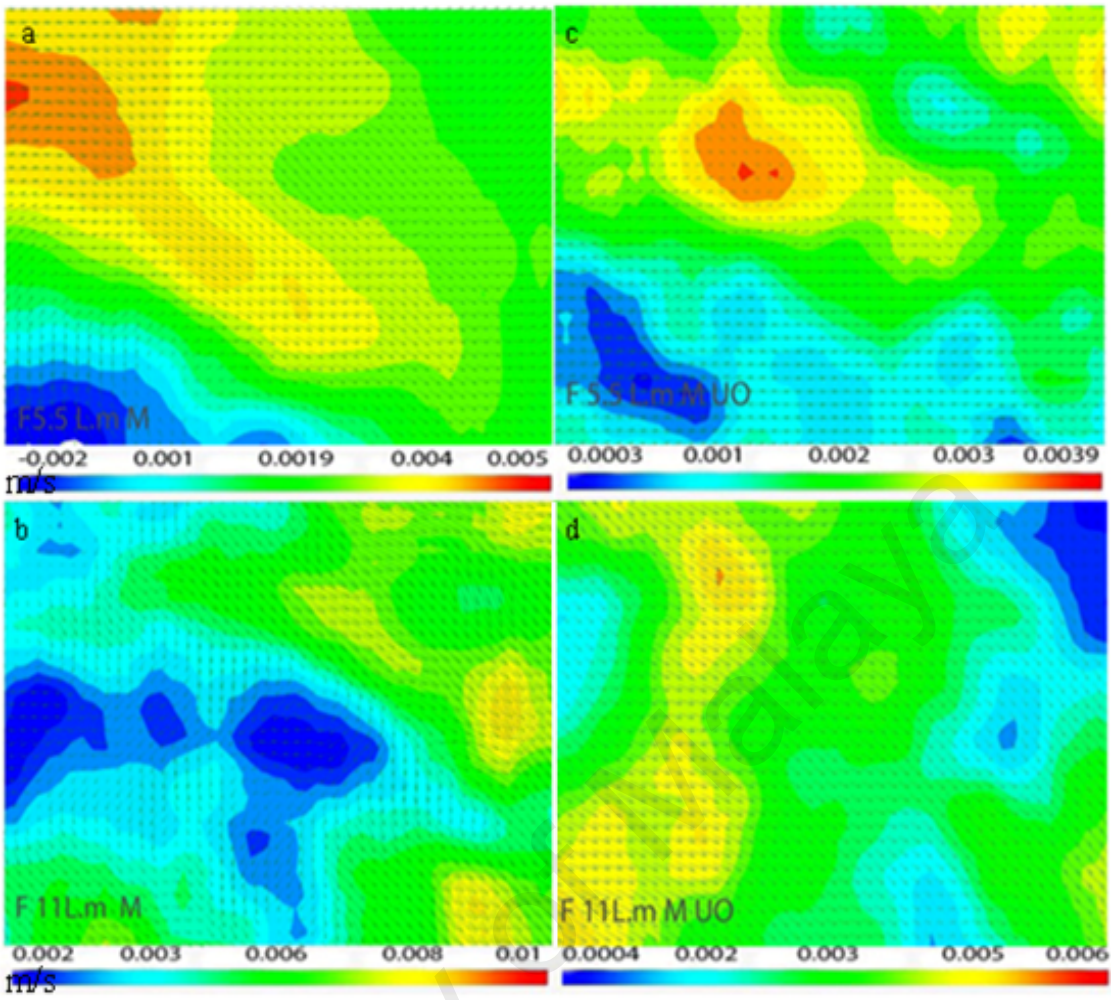

Figure 4.41 : Scalar and vector static maps of sample 1, middle inlet pipe flow, a. flow rate of 5.5 L/m and, b. flow rate of 11L/m using lower outlet, c. flow rate of 5.5 L/m and, d. flow rate of 11L/m using upper outlet.

Sample one during higher water flow (11L/m) with UO settled to the bottom of the tank with decreasing velocity and exhibited laminar flow in some parts of the frame (Figure 4.41 and Figure 4.45). According to the results, the particles in sample one altered their path to settle down under the influence of flow to the right side. They were transported more steadily and along the line without a circulation zone.

Thus, the flow with adjusted inlet and outlet on the same line made the particles in sample one move with greater order, and it seemed the fine particles tended to settle down as the outlet location changed. The result of sample one with lower water inflow (5.5 L/m) and

OU confirmed the outlet location in this flow did not alter the particles' behavior of settling at lower flow rates; however, the mean velocity difference was smaller when using the upper outlet (Figure 4.41). Therefore, it can be concluded that water flow with an upper outlet guided the particles in a calmer streamline in the tank than a lower outlet pipe. This happened because of the pressure difference rate, and when the water flow distanced itself from the inlet it lost its original force. But as the water flow approached the outlet, the pressure rose in the bottom water layer, so more dispersion or disorder was exhibited (Vu & Tan, 2010).

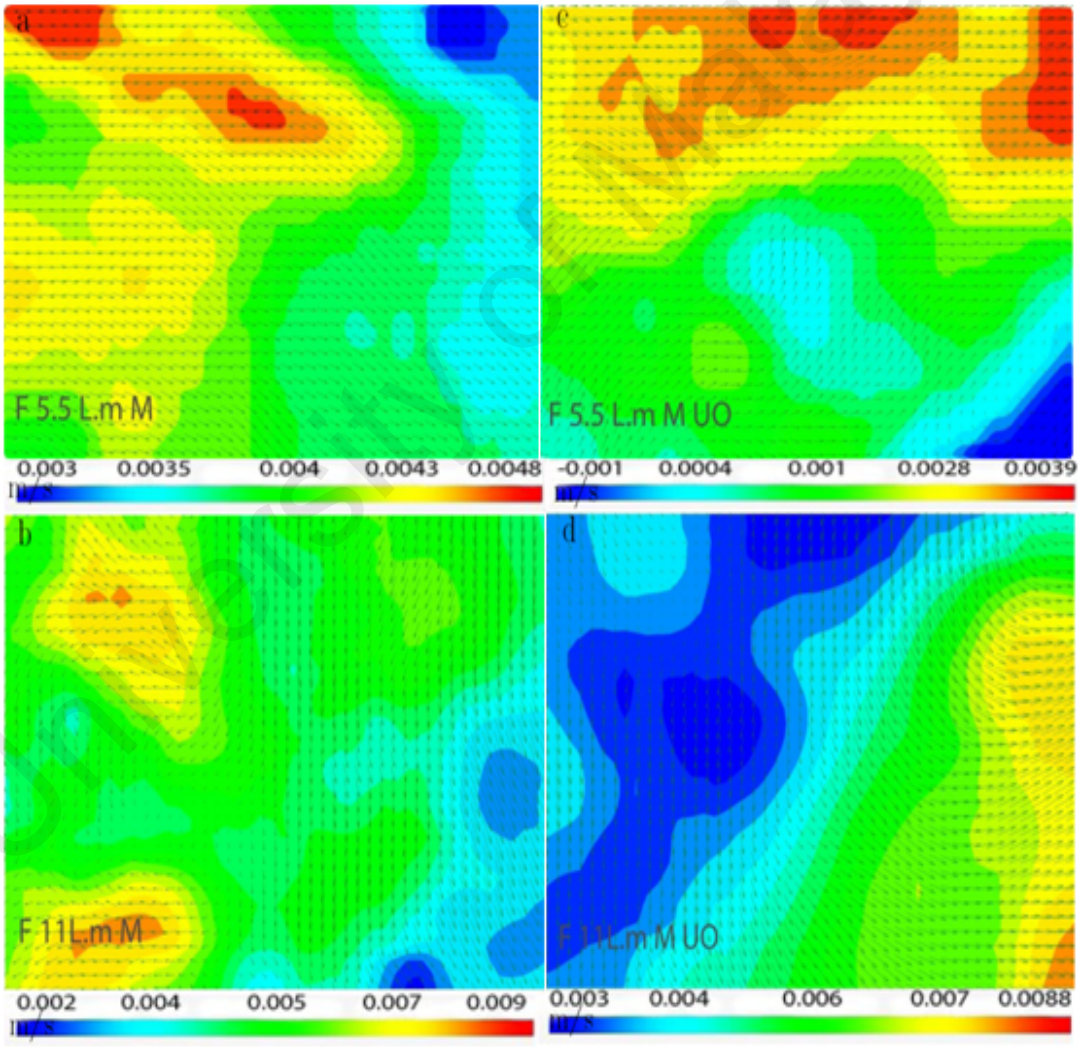

Figure 4.42 : Scalar and vector static maps of sample 2, middle inlet pipe flow, a. flow rate of 5.5 L/m and, b. flow rate of 11L/m using lower outlet, c. flow rate of 5.5 L/m and, d. flow rate of 11L/m using upper outlet.

The vector map of sample two (Figure 4.42) illustrates that finer particles had higher average velocity in particle displacement. Figure 4.42 shows that sample two in M condition formed two different behaviors. At one side near the inlet, the particles re-suspended in the upper layers then followed the gravity force to settle down. Curve irregularity was noted in some parts, and after a while, with increasing distance from the inlet pipe the graph tended to settle down. As the water flow pressure varied with distance from the inlet, the particles got out of inlet flow order (Figure 4.38) and followed the gravity force. At the lower water flow rate (5.5L/m), fine particles (sample two) dragged to the bottom and more settling action was observed (Figure 4.42).

Moreover, an evaluation of the vector map for flow rate of 5.5 (L/m) in both samples demonstrated similar particle settling at different velocities (Jones & Wadzuk, 2013). Owing to the smaller particle size of sample two than sample one, higher settling velocity was recorded. The tendency of particles to settle was higher in sample one at lower flow rate. It was found that samples sized 1-20 µm experienced re-suspension at a lower flow rate (5.5 L/m) and for upper outlet UO (Figure 4.40), while by approaching the outlet wall, the flow tended to change direction and settle the particles back at the bottom. Fine particles were investigated at a higher flow rate in the same water surface level condition and inlet pipe. The upper outlet resisted more and transported particles towards the bottom layers directly rather than following the water flow in the outlet direction (Wong et al., 2006). This minimal circulation is evident in the right corner of the image, where particles in sample two with smaller diameter settled back down. Although at higher water inflow (11 L/m) fine particles behaved similar to the previous outlet location, they gyrated to the bottom left of the tank directly and strained toward the upper layer when approaching outlet pressure. The impact of gravity force appeared better with sample two.

University of Malaya

4.6.5.3 Water level higher than the inlet pipe

The final examination setup had two similar variations as described above. First the water level was raised higher than the inlet pipe, to 22 cm. Then the lowest outlet pipe was opened.

Sample one at both flow rates tended to settle steadily to the bottom of the tank (Figure 4.43). The biggest difference in particle movement between these two different water levels was about the ratio of particles' mean velocity (Figure 4.38). The particles of 20-50 µm moved faster at higher inflow rate than 5.5 (L/m). The achieved result for sample two (1-20 µm) showed similar tendencies of particles descending to the bottom (Figure 4.42). However, the fine particles had a more wavy motion at the 11 (L/m) inflow rate (Figure 4.44). The movement of sample two at 11 (L/m) flow rate is described in the graph as raising the velocity values during the first period of image recording, after which both conditions exhibited a similar decrease in velocity (Figure 4.38).

University of Malaya

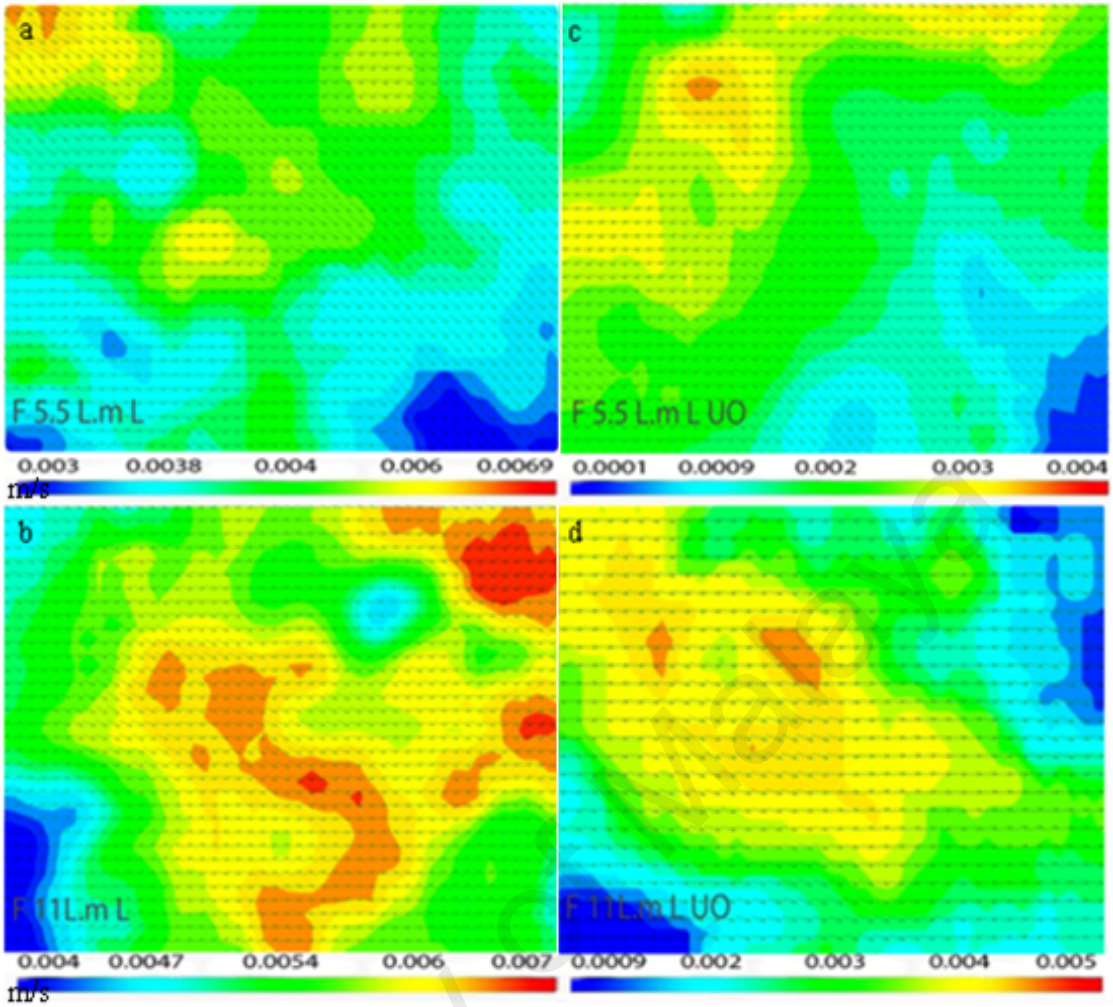

Figure 4.43 : Scalar and vector static maps of sample 1, water level higher than the inlet pipe, a. flow rate of 5.5 L/m and, b. flow rate of 11L/m using lower outlet, c. flow rate of 5.5 L/m and, d. flow rate of 11L/m using upper outlet, with displacement velocity

The fine particles in sample one replicated their behavior with the transfer of the outlet towards the top, so the vector maps show the same motion (Figure 4.43). However, in reality the particles' dragging velocity increased in upper outlet condition. As such, this result verified that the same line of inlet and outlet and upper water surface level improved the extent of siltation in the middle of the tank.

The effect of this stage of water income on the settling of sample two displayed that a higher flow rate (11 L/m) guided the particles to settle. However, some water wave circulation was spotted in the middle of the frame but at the end the particles descended

to the bottom. The same condition with flow rate of 5.5 (L/m) revealed the same motion as sample one. Therefore, it could be established that this level of water income (above the pipe) was an effective model of incoming water. Sample two performed differently with upper outlet adjustment, whereby at higher flow rate (11 L/m) the particles passed in order without any wave motion, but acted with fluctuating values at flow rate of 5.5 (L/m) (Figure 4.40). It seemed the upper outlet caused greater pressure for lighter particles at lower flow rate, therefore it divided into two groups (Figure 4.44): in the first group the particles were settling down, and in the second group they tended to rise in the water level. Somehow, those particles remained suspended in the middle of the tank.

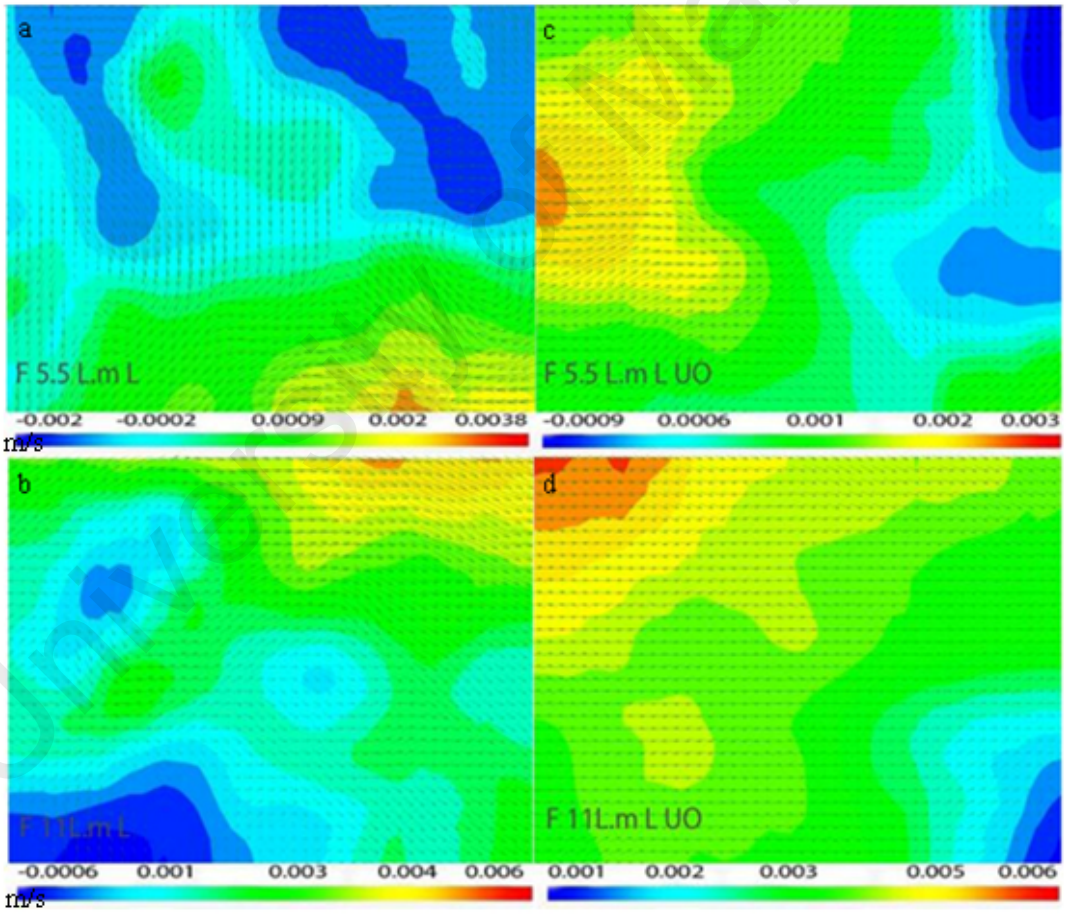

Figure 4.44 : Scalar and vector static maps of sample 2, water level higher than the inlet pipe, a. flow rate of 5.5 L/m and, b. flow rate of 11L/m using lower outlet, c. flow rate

of 5.5 L/m and, d. flow rate of 11L/m using upper outlet, with displacement velocity in m/s

4.6.6 Effect of Inlet on Dispersion of Fine Particles

The results signify that the space between the water inlet and water surface level had an impact on fine particle displacement. As the inlet was higher than the water surface level, the water layer changed, driving the water flow with more force to forward layers. Therefore, the fine particles lost their drag force and loaded to the bottom of the tank then went forward again. Moreover, the fine particles collided with each other so a circulation zone was observed in the U condition. However, as the inlet approached the water surface level, the effect of density and viscosity were clearer as the undercurrent flow was more calm (Paris et al., 2010). According to the results, the fine particles resisted force and frictional force in the middle of the basin under the M and L conditions at 11 L/m flow rate. The density phenomenon can influence the results of the fine particles in the basin because the low Reynolds number characterized the flow (Barnard et al., 2013; Maleoszewski et al., 2006).

It was proved that water pressure reduced in the middle of the tank under this condition and gravity force carried the particles towards bottom layers. The pond volume efficiency was considered, whereby it could affect the behavior of fine particles and the laboratory facility could limit the data (Maleoszewski et al., 2006; Persson et al., 1999).

Nonetheless, it should be noted that varying results were obtained because the performance of the studied forces was tested at different ranges of morphologic conditions. With variation in flow rate at the stream, the fine particles' settling direction changed and their average velocity varied. This is because the higher flow rate of 11 L/m caused more dispersion of the fine particles in sample one (Figures 4.41-43). Although,

University of Malaya

the smaller particles of sample two showed greater variation with flow, and the suspension behavior of the particles (<63µm) (Jones & Wadzuk, 2013) during siltation was coherent.

It is worth mentioning that the frame under study was in the middle of the tank, therefore it was far from the peak flow and the flow rate was approximate in the studied location. The result of sample two with smaller particle diameter size emphasized that the decay coefficient was highly dependent on particle size (Nichols et al., 2013; Hadad, 2013; Yu et al., 2013).

In the study the impact of wind in siltation neglected since the laboratory technique limited the nature condition, therefore lift force of air was not considered (Kunkel et al., 2013). In addition, the fine particles settling determined under influence of switched outlets to explore the influence of outlet in fine particles settling (Nichols et al., 2013). Fine particles movement in the sediment basin was transformed depend on the water circulation as it realized the upper outlet or the construction of inlet and outlet in same height was effective in keeping the fine particles movement in steady lines (Figure 4.41,and 4.42) and avoid the eddy and dispersion zones (Talling et al., 2012). The place of outlets shown the impact of gravitational acceleration improved more with using upper outlet and fine particles incline to settling down. Also it happened when the lower valve was opened then pressure of water flow in outlet drafted the particles to the bottom but the influence of bed shear stress enhanced the re-suspension and created eddy of particles or circulation zone, thus particles remained suspend in water body, hence the place of outlet role a barrier to siltation (Sharip & Zakaria, 2007).

It was explored different hydraulic variables such as stream power, shear stress, and effective stream power had influence on the fine particles transport in tank (Ali et al., 2011). Although it should note widely, varying results were obtained because the

University of Malaya

performances of studied forces were tested in different ranges of morphologic conditions. With variation of flow rate at the stream the fine particles settling direction was changed and the average velocity of fine particles had varied; as the higher flow rate of 11L/m caused more dispersion in fine particles of sample one (Figure 4.43, 4.45). Although smaller particle of sample two shown more variation with flow and the suspension behavior of fine particles (<63μm) (Jones & Wadzuk, 2013) during siltation was coherent. It should note the frame of study was in the middle of tank therefore it was far from the peak flow and the flow rate was approximate in the studied location. The result of sample two with smaller particle diameter size emphasized that the decay coefficient being highly dependent on particle size (Nichols et al., 2013; Hadad, 2013; Yu et al., 2013). The wide varied of fine particles direction passed through the water proved smaller particles with lower flow rate could suspend in water level that in the width of pond settled down in time (Li et al., 2007) therefore, longer path affected in decreasing the fine particles suspension.

4.7 Sedimentation Efficiency

In this section, an attempt is made to develop the PIV method results and examine the rate of collecting efficiency in the designed settlement basin. Therefore, Stoke's law is used to make a comparison between different flow rates and the depth influence on the sedimentation rate or collecting efficiency of the tank. It should be clarified that the experiment result analysis was done for elevated inlets and outlets, although it was realized that having the outlet at the bottom of tank decreased the efficiency of the sediment basin and is thus not suitable for wastewater treatment. The collecting efficiency demonstrated the effect of particle size on the settling velocity of particles, which was calculated with Stoke's law and the ratio between the settling velocities resulting from PIV. The calculated velocity was introduced as the collecting efficiency. Muhanned

University of Malaya

(2013) showed that the settling velocity of particles significantly varies according to particle path during settling. The study showed that the spherical particles pursue a vertical path during settling, and the irregular-shaped particles follow different paths and orientations, like springing, circular, oscillating and unstable paths. These orientations decrease the settling velocity of irregular-shaped particles (Muhanned, 2013).

4.7.1 Collecting Efficiency in Different Locations

The collection efficiency rate is determined based on the PIV results in sections 4.6.1 and 4.6.3 for the displacement path of fine particles in 4 zones of the rectangular tank and impact of depth, respectively. The collecting efficiency is dependent on tank size and flow rate. In this study, the tank was divided into different areas and the different tank frames were investigated in the same water flow and fluid depth conditions. Subsequently, the effect of different depths, inlets and outlets on collection efficiency was evaluated.

Higher flow rates caused lower collecting efficiency, which means that higher turbulence occurred with higher flow rates. It should be noted that the resulting graph regarding the collection efficiency is related to the rectangular reservoir designed.

4.7.1.1 The effect of flow on siltation

According to section 4.6.1, four regions, A, B, C and D were named in the tank and the influence of particle size, flow rate and study location was explored. It was found that flow rate can affect the settling velocity of particles. Two flow rates of 11 L/min and 5.5 L/min were applied to survey the behavior of fine particles in four different locations of the sedimentation tank. In two dimensions PIV study, the velocity of vectors in U and V components illustrated. Hereby, the V component represents the settling velocity in this

University of Malaya

study. Thus, the settling velocity rate over the calculated settling velocity of different particle size shows the collection efficiency in each location.

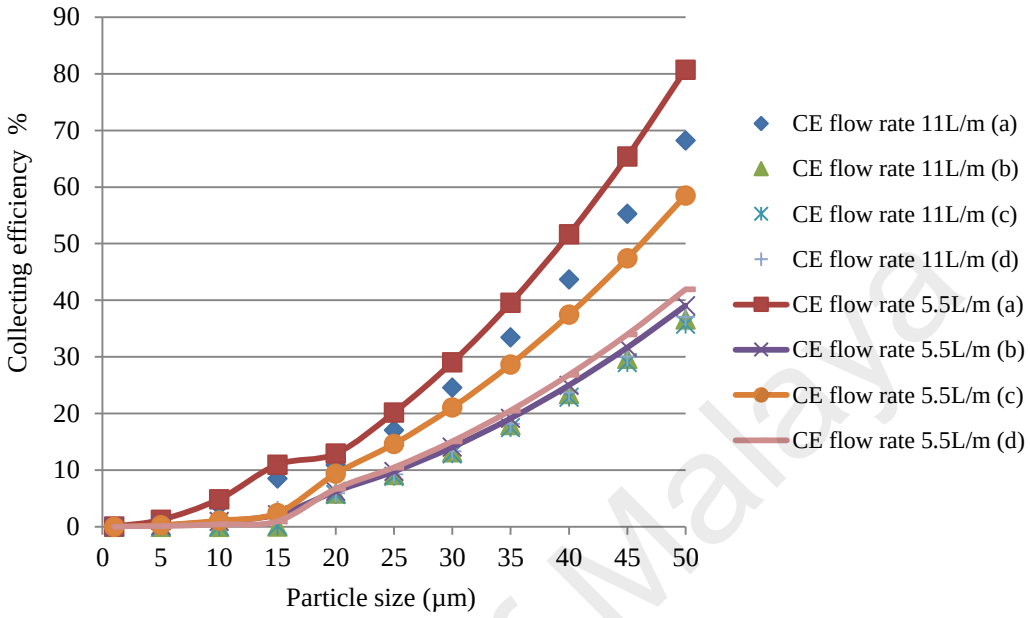

Figure 4.45 : Collecting efficiency at the 4 zones of tank (a – b - c and d) in two different flow rates

The 5.5 L/min flow rate exhibited higher efficiency compared to 11 L/min in all directions, which proved the effect of Q on sedimentation.

Based on the graph (Figure 4.43), the highest sedimentation happened in the surface (A) column of water, then the inlet close to the bottom (C), followed by the outlet near the bottom (D), and then the pipe near the inlet (B). This result can be studied based on the vector direction and movement using particle image velocimetry (PIV). According to Figure 4.21, the particles exhibited the lowest velocity in the U direction at the surface and it can be assumed that the flow pressure reached the lowest power there, therefore the particles started to move downward. The particles tended toward the bottom of the tank in locations C and D and the highest dispersion was found in location B, which is the

University of Malaya

nearest to the inlet flow (Figures 4.23, 4.25, 4.27), where it is obvious the flow pushed the particles to the front or other directions except downward.

The settling efficiency in different areas of the tank except the surface area proved that the settling velocity changes over higher flow rates are almost the same in most areas of the rectangular tank. The analysis demonstrated that the collection efficiency (Figure 4.43) has lower rates in locations B and D, which could be a direct effect of inlet and outlet flow on these two locations, therefore the flow can lead particles to go out with the outlet flow in location D.

4.7.1.2 Collecting efficiency in differential of depth

From the other outcomes of the PIV study in the tank, two other variations, namely of depth and outlet location besides various flow rates are analyzed to evaluate the collection efficiency. In this method, one location in the middle of tank was selected and studied with PIV testing. Once again, the same method was applied to survey the influence of the mentioned variations on collection efficiency or sedimentation rate. Two different depths of 20 and 44 cm were studied in a single constant frame in the middle of the tank (section 4.6.3). The results showed that greater depth had more influence on sedimentation rate, since at 44 cm, fine particles settled more. This proves the idea of longer settling time, whereby greater depth can increase the sedimentation rate and wastewater treatment. Subsequently, the outlet location's effect on settling rate was investigated. The outlet in the tank was changed in two conditions: once the inlet and outlet were at the same height and in front of each other, and then the elevation of the inlet and outlet was studied. For better clarification, the inlet and outlet were designed at the same tank level but the other outlet near the bottom was also studied to determine the impact of outlet location on sediment removal. From graph 4.44 it is apparent that the difference in inlet and outlet elevation reduced the sedimentation rate at both depths; therefore, it can be concluded

University of Malaya

that in the sediment tank design, the best option is to have the same inlet and outlet height. The graph indicates that the influence of the outlet location is greater than that of water depth, therefore the outlet placement had the most important role in the sedimentation tank. This is because the dispersion of particles was higher while there is elevation between inlet and outlet in the rectangular tank.

At lower flow rate, the difference between outlets was much higher than at 11 L/m flow rate (Figure 4.44). This proves that a lower flow rate at the deepest water level and with an upper outlet having the optimum settling velocity may indicate a dead zone.

The hydrodynamic behavior of fine particles can change under the influence of depth and flow rate, and the other most significant parameter is the outlet location.

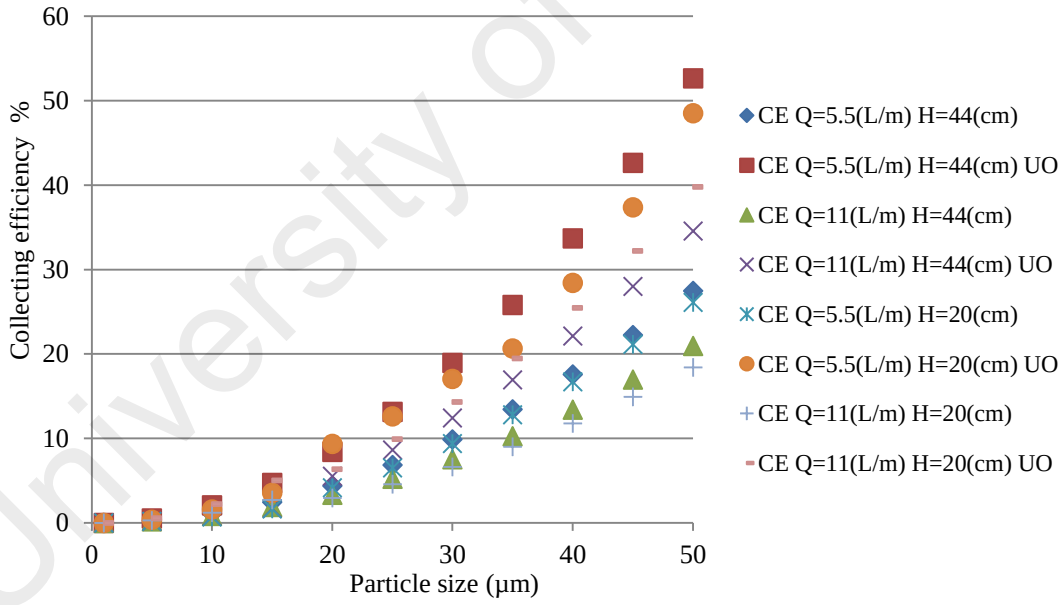

Figure 4.46 : Collecting efficiency at different depths (20 cm and 44cm) and outlet locations in two flow rates of 11 L/m and 5.5 L/m

University of Malaya

4.7.2 Impact of Hydraulic parameters on Collecting Efficiency

The terminal velocity and settling velocity of sediment particles are known as key variables in understanding the effect of sediment transport on the suspension, mixing, deposition and exchange processes. On the other hand, it is difficult to predict the transport velocity, even for a single particle (Zhiyao et al., 2008). Therefore, many equations have been developed to predict the settling velocity of particles (Ahrens, 2000; Cheng, 1997; Guo, 2002; She et al., 2005; Zhu & Cheng, 1993). Still, all equations are weak in predicting the settling velocity of fine particles. Nonetheless, using a method to obtain the real and direct velocity of fine particles in water would increase the chances of observing the real behavior of fine particles with reduced error of equations.

According to different studies (Althaus et al., 2011; Boyle et al., 2005; Camnasio et al., 2011; Dufresne et al., 2010a, 2010b; Hidayah & Karnaningroem, 2012; Jamshidnia & Firoozabadi, 2010; She et al., 2005) that were investigated the numerical and simulation of the refine sediment from water body, instead of the direct investigation in laboratory. It is understood that many factors can affect the sedimentation efficiency of a tank, such as inlet and outlet location, discharge rate, particle size and depth. Variations in these conditions could change the hydrodynamic behavior of fine particles besides the efficiency of settling in a tank. The various influential parameters are discussed below.

4.7.2.1 The impact of inlet and outlet on collecting efficiency

In the design of a sediment basin it is proven that various elements, such as the position of inflow and outflow; outlet location and size; and inflow direction and distribution, are important to create high energy to enhance the level of sedimentation and affect runoff in a tank (Cholette & Cloutier, 1959; Rosenthal, 1982; Westers, 1995). Various studies have indicated that fine particles are not removed by pre-treatment and generally act as pollutants in a pond. Therefore, studying fine particles' hydrodynamic behavior is

University of Malaya

significant and can assist with gaining better understanding of how to decrease and remove them from water surfaces (Cripps & Bergheim, 2000).

Many researchers have designed sedimentation tanks without attention to the flow patterns within, which leads to tank failure (Matko et al., 1996). Flow pattern is significant, particularly since the flow pattern in rectangular tanks is more unpredictable as it depends on tank geometry and water inlet characteristics (Levenspiel, 2002). Moreover, the quantification of the velocities' characterization, eddies and recirculation zones, is essential for engineering applications (Camnasio et al., 2011). It is well-known that rectangular basins with a lack of mixing uniformity produce dead and by-passing volumes, a phenomenon that is more pronounced in settlement basins with an inlet (López et al., 2008). Rostami et al. (2011) studied the effect of the inlet on fluid distribution and aimed to reduce the circulation zone to enhance particle flow. The resulting dispersion zones at the inlet area produced similar results to the PIV study, due to the impact of the inlet on the region near the inlet in figure 4.45 during fine particle movement. Studies by Dufresne et al. (2010b) proved there is a deposition zone near the inlet at the bottom of a rectangular tank, therefore the resulting settling velocity in this zone (C) illustrates the greater efficiency with a lower flow rate.

The settling velocity of sediment particles decreases from the inlet to the outlet. Moreover, the decrease in velocity between the inlet and outlet with increasing depth reduces as well (Boyle et al., 2005; Hidayah & Karnaningroem, 2012). The velocity distribution in the sedimentation tank greatly influences the hydrodynamic behavior of particles, hence the outlet location improves the particle settling rate (W. Zhang et al., 2010). The location of the inlet and outlet at one height but in opposite directions has the highest effect on deposition (Camnasio et al., 2013). The other finding by Dufresne et al. (2010b) demonstrated that the higher settling rate to the bottom layers from the surface

University of Malaya

(zone A) occurs in the tank length where the flow velocity decreases from the inlet to the outlet (Mohammadpour et al., 2013).

Bajcar et al. (2011) described that during the continuous settling process, the material re-suspends in water, and a vortex area where a recirculation zone with locally lower velocities occurs is observed in some regions near the bottom of the settlement basin. This occurs depending on the flow rate pressure in the tank. Thus, the population of settled particle moves slowly in the direction of the flow nears the bottom of the settling tank (Figure 4.45 bottom, near the inlet or outlet). At the inlet regions (B and C) of the tank, the mean velocity shows a higher settlement rate that can alter with different particle sizes and flow rates (Camnasio et al., 2013; Jamshidnia & Firoozabadi, 2010).

4.7.2.2 Impact of particle size on settlement

The particle size and scale effect on sedimentation efficiency in the settling tank is studied (Bajcar et al., 2010). Gravitational force has an important role in particle settling, but sometimes the influence of particle diameter can overcome the gravity effect and change the rules. With decreasing particle diameter in fluid flow, fine particles suspend in the water layers, hence the flow effects are more intense than gravity on smaller particles (Hidayah & Karnaningroem, 2012). Particles smaller than 10 µm showed almost the same variation in collecting efficiency, as discussed by (Cripps & Bergheim, 2000), and this has been proven even with the flotation method or foam fractionation where for particles smaller than 10 µm the removal efficiency is similar (Chen et al., 1993). Thus, the removal of particles smaller than 10 µm is different from the physical assumption. The falling velocities of natural particles are affected by particle geometry (She et al., 2005). Therefore, sandy silt particles settle faster than clay particles (Ginsberg & Aliotta, 2011). Besides particle size, particle shape could affect their movement, as discussed in the rheology section (Southard, 2006).

University of Malaya

The mean particle size distributions for the fine particles collected from the LD and SEM tests displayed that the coarsest and finest particle curves in rheometry performed differently based on fluid concentration. This could lead to differences in settling velocity and even the horizontal (sediment transport) movement of particles from the inlet and outlet (Karlsson et al., 2010). It has been experimentally observed that some fine particles settled inside the inlet and outlet pipes. It should be noted that the finer particles and those of 15 µm exhibited almost the same values and behavior, and the smaller particles got suspended in the water body and reached the outlet location (Marsalek et al., 1997).

4.7.2.3 Influence of flow rates on fine particles movement

Many factors are at play in the hydrodynamic behavior of fine particles in rivers and ponds (Zakaria et al., 2010). Minor changes in the speed of inflow can have severe impact on the operation of a settling tank when essential suspension parameters are not changed (Bajcar et al., 2010). Kinetic energy has the highest role in sediment travel in a basin, therefore the impact of flow rates on particle movement can be realized (Hidayah & Karnaningroem, 2012). The highest sedimentation efficiency in a rectangular tank generally occurs where the settlement area is the greatest and velocities are usually low, similar to the results obtained from the PIV method analysis, where particle settling was enhanced (Bajcar et al., 2011).

The turbulence intensity decreases as the particles tend to settle more (Ginsberg & Aliotta, 2011). Therefore, at a lower flow rate, less dispersion or loop patterns are found in the resulting map (Kemker, 2014). Thus, during higher flow rates such as in flooding, the rate of suspended sediments increases. The stress rate near the outlet is also higher (Ginsberg & Aliotta, 2011). Research on flow patterns has revealed that in case of higher flow rates, the water circulation at the outer wall and the bottom of the model settling tank causes more particle dispersion (Bajcar et al., 2011). This re-suspension flow spreads a part of

University of Malaya

the particle current at the bottom of the tank towards the upper parts (Bajcar et al., 2011), thus enabling an extended residence time for the settling particles (Figure 4.45). Higher flow rates create bigger dead zones in a rectangular tank (López et al., 2008).

Several parameters have been found to influence the waste load (Cripps & Bergheim, 2000). The tank dimensions, flow rates and size of settling particles have an important role in the flow pattern in a sediment basin. The influence of the ratio between suspension compositions, such as size of particles and suspension flow rate on the flow field should be considered in order to enhance the design and optimize settling tanks (Bajcar et al., 2011). Studies have shown that temperature can increase the rate of solid suspension, and changes in flow rate could adjust the rate of sedimentation in water (Cripps & Bergheim, 2000). The difference between flow rates may not change the pattern of flow but it has an influence on the velocity of particles under flow pressure (López et al., 2008). Thus, a lower flow rate would decrease the rate of mixing and is more suitable for sedimentation.

It is obvious that without any asymmetric boundary in a tank, there is a symmetric flow in process. The variation between conditions alters the symmetric and asymmetric flow in a tank (Dufresne et al., 2011). In particle settling, the shear stress τ_0 in the boundary layer of a basin bed lightens the discharge flow rate that washes the bed, or it can move the particles from the bed (bedload or suspended load). Thus, shear stress can be introduced as another boundary in sedimentation rate (Kemker, 2014). In the absence of a wall slope in the study, the role of bed shear stress decreased (Southard, 2006). Increasing the flow rate increases the stress on the bed, more likely leading the water flow to initiate sediment resuspension; nonetheless, particle size *d* has influence as well. Moreover, higher velocity enhances the erosion rate as flow overcomes the shear stress of sediment (Kemker, 2014).

University of Malaya

4.7.2.4 Impact of depth on fine particles settling

All symmetric and asymmetric flow patterns are a result of the ratio between the depth and width of the tank (Camnasio et al., 2011). The basin designed in this study had an appropriate size to prevent extending the experimentation and to not be influenced by the scale and wall effects. The geometrical parameters, meaning the length and width of the tank and hydraulic parameters influenced the flow-field typology (Camnasio et al., 2011; Dufresne et al., 2010a). The depth and retention time are related and influence the hydrodynamic behavior of sediment (Ghani & Mohammadpour, 2015). Increasing the length and depth of a tank can be effective on increasing siltation (Dufresne et al., 2011; Wang et al., 2010). Therefore, the deposition pattern could be changed by varying these parameters. It should be noted that concentration has a significant role, since the viscosity (Figures 4.15-19) can be varied with concentration; however, the study was carried out with constant concentration. The numerical solution and simulation proved that the rate of flow and ratio of width to length also have an important role in sediment deposition (Guo, 2002).

There is a connection between retention time and depth, since a deeper tank allows more time for particles to flow. Kiat et al. (2008) found that the amount of sediment delivery will decrease with time, proving that higher retention time at greater depth helps particles settle, as higher collecting efficiency was found at 44 cm depth and in the bottom area (Figure 4.46). Greater tank length and depth facilitated more particles settling over time. This concept proved the impact of particle size and water depth on treatment leading for the wash-off of finer particles (Ellis & Revitt, 1982; Karlsson et al., 2010).

Consequently, it can be realized that the settling of particles in a tank is affected by many factors that are interlinked like a chain. Camnasio et al. (2013) described non-uniform and time-dependent roughness, such as large eddy simulations leading to higher

University of Malaya

deposition. Ab Ghani et al. (2011) discovered an increase in the conjunction of flow discharge with flow depth. In their study, the coarser particle settlement in the open channel studied showed that the highest accumulation rate was near the inlet and at lower depth, which indicates that coarser particles were trapped near the inlet.

The settling velocity of particles adjusts in each water body layer; for instance, a higher amount of particles settled in the first surface layer (Shahidan et al., 2012). Thus, the collecting efficiency represents almost the same results as other research findings. Based on (Bajcar et al., 2011) flow re-circulates at the water surface, after which the path seen is corrected.

From Hidayah and Karnaningroem (2012) it can be concluded that there are more changes in the hydrodynamic behavior in rectangular sediment basins at the surface, which dissipates along with the length and depth of the sedimentation basin. Bed-load transport may be observed based on particle diameter size at the bottom of the tank due to shear stresses. The movement of particles near the bed (bottom of the tank) illustrates the differing velocity of particles under the influence of flow rate (Brethour & Burnham, 2010). Controlling the hydrodynamics of a rectangular tank using equipment to circulate flow could improve the level of sediment release by the mixing process (Althaus et al., 2011).

4.8 Assessment of Settling Velocity

The resulting graph (Figure 4.47) indicates that the equation calculated almost the same values for very fine particles. It is concluded that less changes are observed for particles of less than 15 μm, but with increasing the particle size to 50 μm, the equation's sensitivity reduced. Therefore, the settling velocity result of the equation is in conflict with the PIV results.

University of Malaya

Table 4.1 : Comparison between the predicted settling velocity (m/s) and collected settling velocity (m/s) by PIV(under various coditions) for particle size of 1, 20 and 50 µm

Particle Size (µm)	Zhu and Cheng (1993)	Cheng (1997)	Ahrens (2000)	Guo (2002)	She (2005)	H=20cm Q=5.5L/m	H=20cm Q=11L/m	H=44cm Q=5.5L/m	H=44cm Q=11L/m
1	5.66E-08	5.7047E-08	5.69E-08	5.70E-08	4.826E-08	1.1E-05	4.058E-06	1.0318E-05	0.000966
20	2.26E-05	2.2817E-05	2.27E-05	2.27E-05	3.051E-05	0.00389	0.0002196	0.0020723	0.004867
50	0.000140	1.42E-04	0.000141	0.000140	0.0002039	0.00428	0.0020324	0.0047514	0.007595

The reason for this difference may be the lack of flow rate role in these equations, and the other rationale is the weakness of the created equations for finer particle sizes. The proposed formulas demonstrate that the predicted results can be used only for large sediment, such as sand and gravel (Cheng, 2008).

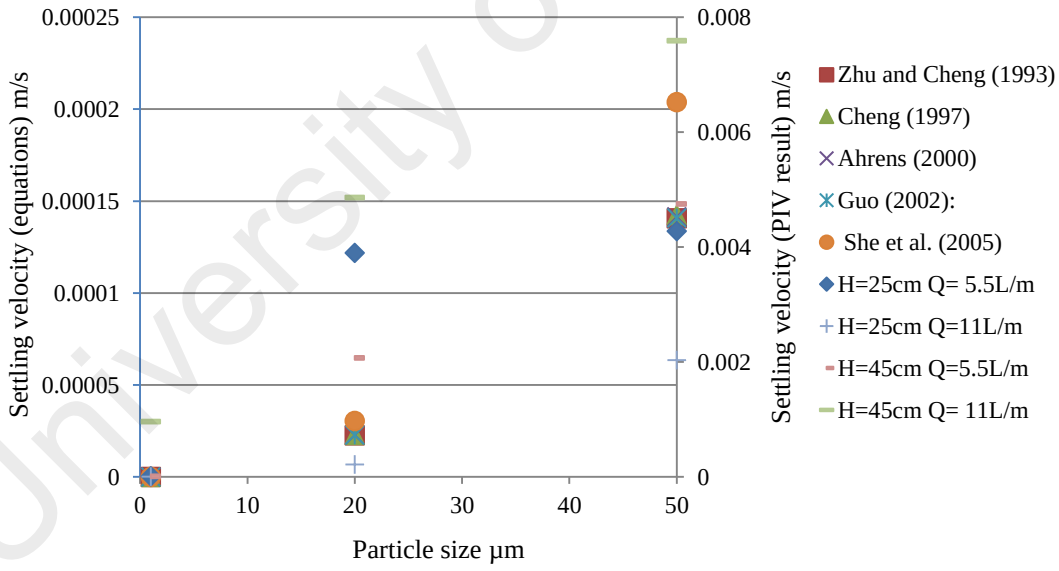

Figure 4.47 : The graph of settling velocity estimation through the equations and PIV, the H shows the depth and Q is flow rate.

Therefore, the practice of a technique with a direct look at fluid flow is essential. Furthermore, the PIV method employed assists to develop better understanding of flow

University of Malaya

inside a rectangular tank. Particles smaller than 10 µm were not uniformly distributed (Curtis et al., 1979).

4.9 Shear Velocity as a Correlation between the Rheological Behavior, Fine Particle's Texture and Displacement

The way to linked all data together and find out the relationship between the rheological behavior defines the parameters by shear velocity, therefore, the result of shear stress at 25% volumetric concentration of 6 sieved soil samples are used to measure the shear velocity in these six samples. At the end the collected velocity of fine particles in two flow rates with upper outlet was used to demonstrate the influence of texture and the particle size smaller than 62 µm on shear velocity over velocity rate.

Different researches attempted to find the correlation between shear stress and the flow velocity of particles, beside they tried to look at the particle size as well. The aim of more studies was about the coarser particles and their behavior near the bed but when we reach to discuss about fine particles the result would be different and constant law can't be describe.

It is concluded the sample one with higher rate of particle diameter size such as loam and fine sand texture shown different aspect rather than the other, although the type of clay has influence in the rate of shear velocity over velocity in other samples as well. Each the particle size increased the shear velocity would increase as well, thus settling velocity increases. However, it is proved there are no direct significant correlation between mean size of particles and the shear velocity but there is relationship between particle with fine size diameter and velocity.

University of Malaya

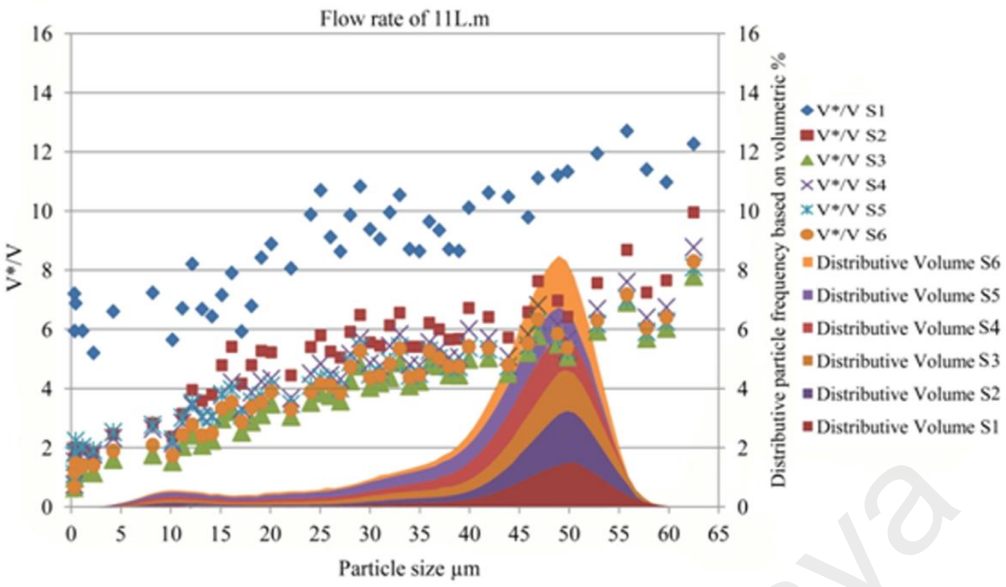

Figure 4.48 : Correlation between the particle texture, rheological behavior, and settling velocity at flow rate of 11 L/m

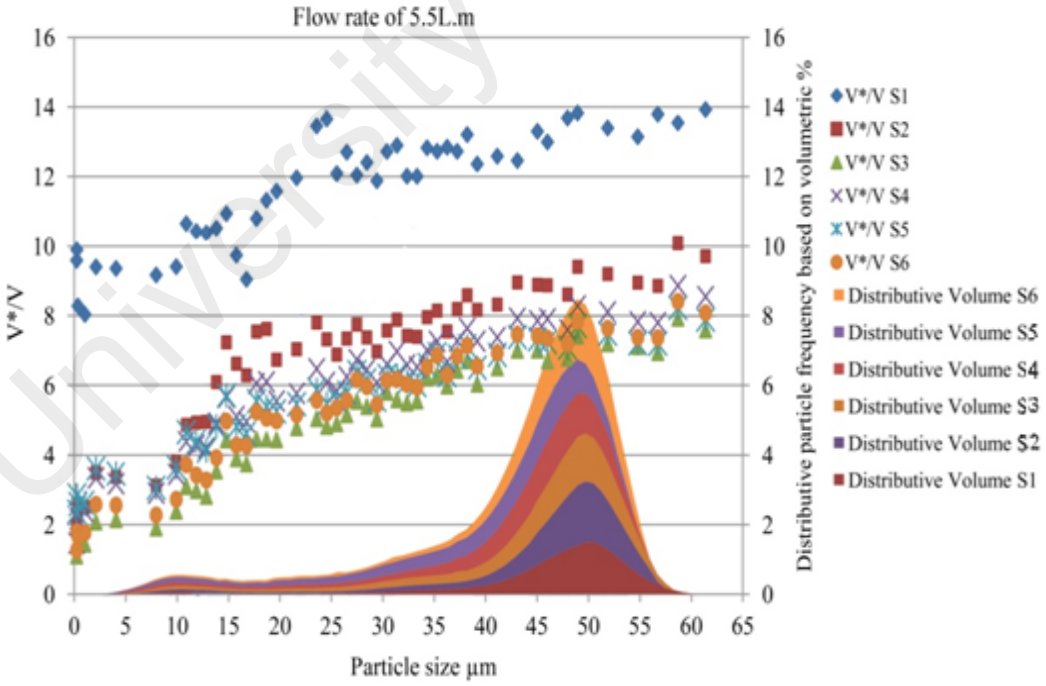

Figure 4.49 : Correlation between the particle texture, rheological behavior, and settling velocity at flow rate of 5.5 L/m

University of Malaya

CHAPTER 5: CONCLUSION AND RECOMMENDATIONS

5.1 Conclusion

A variety of methods were applied in this study to achieve the current research objectives. A clear vision of fine sediment hydrodynamic behavior was established to explore the effects of hydraulic and physical properties on retention structures. It was identified that fine particles with higher porosity function more with near-Newtonian behavior under stress. With increasing water content, the stability of fine particles decreased and a greater effect of flow velocity and hydraulic parameters was obvious. The fundamental physical and dynamic behavior governing fine sediment dispersions and accumulation was established by PIV technique. The PIV results were analyzed in terms of collecting efficiency and shear velocity to comprehend the effectiveness of physical and hydraulic parameters on fine sediment movement in retention structures. The research led to a number of conclusions with respect to the research objectives through employing laboratory methods and analyzing the results with a qualitative approach.

1. Investigating the physical parameters of fine sediment using SEM and LDSA:

It was discovered that clay and loam have the largest diversity in terms of volume and distribution among sieved soil particles. Under rheometry testing, the difference in rheological reactions of soil particles evidently showed that scanning electron microscopy was necessary to illustrate the shape and size of particles with direct access. Thus, based on the results, the researcher's notion about the effect of different clay shapes on fine particle movement in water was verified. It was concluded that higher porosity significantly affects fine particle dynamic behavior, and the diverse types of clay and loam could also affect water management systems.

The test findings are classified in two groups: first, the effect of water ratio on fine sediments, and second, the effect of particle size and shape. There is a direct correlation

University of Malaya

between water concentration and particle shape. The result of 25% concentration fine particle slurry substantiated the behavior of this water suspension level, which proved the correlation between rheology and PIV.

2. Exploring the rheological behavior and hydrodynamic behavior of fine sediment: The results obtained for the samples with 25% volumetric concentration represent real-world conditions in ponds and coasts well. The results suggest that the near-Newtonian behavior of fine sediments in these regions is the main contributor to suspension and the consequent slow sedimentation of these particles. It is deduced that the near-Newtonian behavior of fine sediments encouraged them towards the outlet, suggesting the most productive point for fine sediment collection. It can be concluded that a different type of clay could be attributed to different rheological properties and the water mix percentage created a specific behavior in fine particles. Moreover, the findings elaborate that the plate diameters affect the soil particle percentage. In addition, the results signify that mixing fine particles with water produced a paste with characteristics that could enhance the sheer volume with smaller plate diameters, although fine particles (<63μm) acted like ash in some ways.

It was found that higher water content affected the viscosity of the fine particle sample. In a mixture with higher water content, the fine sediment became suspended in a water column, and the rheological behavior was dependent on the fine sediment particles' ability to form bonds.

It was particularly observed that the soils' texture and microstructure, and water ratio caused variations in the rheological curve and material characteristics such as shear behavior and viscosity. In general, high clay content led to sliding shear behavior in contrast to silty soil, which represented more turbulent shear behavior. It is concluded that the force over a smaller area may facilitate a viscous state of fine particles earlier on

University of Malaya

than particles with larger diameters. Nonetheless, it can be concluded that fine particle movement in smaller areas with the same force value instigates greater transport than in larger areas. Thus, a rheometer with a parallel plate-measuring device is applicable for the detection of small-scale interactions.

The study suggests there is a significant correlation between flow velocity, fine sediment and fine particle settling; besides, there is a relation between fine sediment characteristics, water depth and fine particle settling. Thus, the concluding results from the effects of hydraulic parameter variations on fine particle hydrodynamic behavior were described based on the effects of flow rate, and inlet and outlet configuration. The greatest factor in enhancing the level of settling in basin was outlet. In all different experiments, it was determined that by increasing the flow rate to 11 L/m the fine particle velocity increased up to 0.01 m/s and the particle settling efficiency decreased down to 20%; therefore, the ideal condition occurred during a lower flow rate.

It was confirmed that the distance of the inlet from the water surface affected how fine particles settled, and when the inlet was below the water surface the fine particles collided more. The particles' diameter size had an impact on the direction in which particles settled and the smaller the particles, the lower the resistance of particles against the water flows was. It is concluded that when the inlet and outlet were at the same level in the basin's cubic dimensions, the siltation level between 50 to 80% enhanced. The overall study findings verify that controlling the hydraulic parameters affects fine particle transport, more so in terms of siltation.

3. Evaluating the effect of hydraulic parameters on collecting efficiency and settling velocity:

The results prove that part of the fine particles settled in the outlet pipe. An overview of the results demonstrates that fine particles were transported in different directions at the

University of Malaya

surface with a high dispersion rate of 70-80%. In terms of varying flow rates, the fine particles moved faster with higher flow rates, while lower flow rates helped the particles remain suspended longer and improved their settling efficiency by around 40% more than the others. It is concluded that nearly 50% of fine sediment settled with increasing gravitational force and with increasing distance from the inlet and decreasing flow rate. The outlet force (suction power) effectively contributed to the settlement of fine particles by carrying these to the bottom layer and in the outlet's direction. In the bed layer, erosion and frictional forces were evident, which re-suspended the fine particles in the water body with time. The changing mechanism of fine particles in this layer at different flow rates was evaluated, and it was noted that the particles re-suspended more at higher flow rates (zone b, c, and d). Hence, the particles followed the flow in the outlet's direction at lower flow rates. The findings demonstrate that at different inlet and outlet elevations, the hydraulic forces affected and changed the fine particles' movement near the outlet.

Higher flow rates dispersed the fine particles greatly. In this study, the impact of wall slope was neglected, and the obtained result was corrected for the rectangular-shaped sediment basin. There was a correlation between flow rate and particle size. Moreover, the water depth influenced the mechanism of fine particle transport, whereby as the depth increased to 44 cm the particles were directed towards the bottom. Nonetheless, the outlet placement influenced the direction of particles carried by flow and declined the collecting efficiency by 30 to 40%. Though the particles followed the gravitational force and settled at lower depths with an elevated inlet and outlet, the force of the outlet pulled the fine particles towards the right. As an impressive factor, moving the outlet to the upper pipe augmented the re-suspension rate and upward mobility of particles. Greater water depths calmed the water body, thus the particles moved to the bottom of the basin and the bed shear stress diminished. The motion of fine particles with collecting efficiency of 50%

University of Malaya

and above was the same when the inlet and outlet were at the same altitude and for both examined depths.

4. Correlation between flow rate, texture of particles and shear velocity:

Though the effects of Froude number, Brownian motion, interaction between particles and many other laws have been detected in the hydrodynamic behavior of fine particles, the direct examination method yields valuable data pertaining to fine particles in a retention structure. The low concentration of fine particles affirmed the hindered water level; therefore the influence of the mentioned laws is lesser than higher particle concentrations. On this note, clay had a remarkable role in the settlement and hydrodynamic behavior of particles, since higher particle porosity helped retain them in a suspended state. Moreover, the larger particles with less porosity as well as loam significantly altered the sediment stability. The ratio of shear velocity to settling velocity besides the rheometry results corroborate this phenomenon in sample with fine sand, thus the rapid settling of this type of fine particles was predictable. The morphology and tank dimensions substantially affected the hydrodynamic behavior of fine sediment. A wider and deeper tank enhanced the settlement by 5 to 20%. Moreover, the outlet and inlet being located at the same height increased fine particle settling by over 30%. It is inferred that the reduced flow rate clearing the water body of fine, settling particles with high porosity such as clay, advances the retention structure's competence. Although, the settling velocity for particles smaller than 15 μm was nearly the same. The consequential conclusion regarding the hydrodynamic behavior of fine sediment is the direct relations between displacement velocity and particle size, as well as depth, reserve ratio and flow rate. Furthermore, the outlet's location is a more decisive factor in particle settlement compared to depth. Therefore, the turbidity and siltation problems could be extremely mitigated in retention structures like ponds by considering the inherent attributes of fine particles. Consequently, the specifications of other notable hydraulics parameters for

University of Malaya

lessening turbidity are classified as water flow rate, inlet and outlet configuration and depth.

5.2 Recommendations

For further future studies, a number of recommendations are introduced below. These suggestions could expand new knowledge towards superior achievements in water management. The recommendations will enhance a valid vision of the dynamics of fine particles and will assist with determining natural and environmentally friendly solutions for the diminution of siltation.

- Research could be expanded in 3D or stereo vision using PIV. 3D visualization is accomplished with two cameras adjusted to 90° degrees between them. Therefore, three displacements for each vector in the dx, dy and dz from a pair of two-dimensional displacements from each camera can be investigated.
- Different retention structure shapes and widths could be applied to understand the effect of length on the hydrodynamic behavior of fine particles. Studies via indirect techniques have proven that the length of the basin may be effective on the collecting efficiency and settling velocity of particles, particularly fine particles. Thus, using a direct technique to determine the displacement of particles in a tank with the mentioned specifications could bring new knowledge to light.
- The number of soil samples could be increased to investigate the rheological behavior of different soils and identify the characteristics of soils in Malaysia. This fact would improve the level of knowledge about different types of clay and other parts of soil, specifically in Malaysia, which could assist with developing better solutions for stormwater management.

University of Malaya

- Modeling with the COMSOL Multiphysics program can facilitate new awareness regarding the effect of various hydraulic parameters under the influence of physics. The COMSOL Multiphysics interfaces employ the finite element method to solve constituent partial differential equations (PDEs).
- Field study investigations using PIV should be developed. By enhancing the quality of cameras and light source types, studying ponds and lakes directly in the environment would be more feasible. The collected results would be greatly effective in controlling siltation.

University of Malaya

REFERENCES

Ab Ghani, A., Azamathulla, H. M., Lau, T. L., Ravikanth, C., Zakaria, N. A., Leow, C. S., & Yusof, M. A. M. (2011). Flow pattern and hydraulic performance of the REDAC Gross Pollutant Trap. *Flow Measurement and Instrumentation, 22*(3), 215-224.

Ab Ghani, A., Mohd Sidek, L.T., Yusof, M. F., Chang, C. K. (2004). *Application of Bio-Ecological Drainage System (BIOECODS) in Malaysia*. Retrevied October.07.2012, from: redac.eng.usm.my/html/USWM/SUDS.htm

Adrian, R. (1999). Dynamic ranges of velocity and spatial resolution of particle image velocimetry. *Measurement Science and Technology, 8*(12), 1393.

Adrian, R. J. (1984). Scattering particle characteristics and their effect on pulsed laser measurements of fluid flow- Speckle velocimetry vs particle image velocimetry. *Applied optics, 23*(11), 1690.

Adrian, R. J. (1991). Particle-imaging techniques for experimental fluid mechanics. *Annual review of fluid mechanics, 23*(1), 261-304.

Adrian, R. J. (2005). Twenty years of particle image velocimetry. *Experiments in fluids, 39*(2), 159-169.

Adrian, R. J., & Westerweel, J. (2011). *Particle image velocimetry*: Cambridge University Press.

Afonso, A., Oliveira, P., Pinho, F., & Alves, M. (2011). Dynamics of high-Deborah-number entry flows: a numerical study. *Journal of Fluid Mechanics, 677*, 272-304. http://dx.doi.org/10.1017/jfm.2011.84

Ahmad, M., Dong, P., Mamat, M., Wan Nik, W., & Mohd, M. (2011). The critical shear stresses for sand and mud mixture. *Applied Mathematical Sciences, 5*(2), 53-71.

Ahrens, J. P. (2000). A fall-velocity equation. *Journal of waterway, port, coastal, and ocean engineering, 126*(2), 99-102.

Al-Mukhtar, N., Belanteur, N., Tessier, D., & Vanapalli, S. (1996). The fabric of a clay soil under controlled mechanical and hydraulic stress states. *Applied Clay Science, 11*(2), 99-115.

Al-Mutairi, N., Hamoda, M., & Al-Ghusain, I. (2004). Coagulant selection and sludge conditioning in a slaughterhouse wastewater treatment plant. *Bioresource technology, 95*(2), 115-119.

Alagarsamy, R. (2006). Distribution and seasonal variation of trace metals in surface sediments of the Mandovi estuary, west coast of India. *Estuarine, Coastal and Shelf Science, 67*(1), 333-339.

University of Malaya

Alison R, K., Cristiane Q, S., & Danielle C, U. (2012). Coliform bacteria: The effect of sediments on decay rates and on required detention times in stormwater BMPs. *Journal of Environmental Protection, 3*(8A), 11. doi:10.4236/jep.2012.328094

Althaus, J., Isabella, J. M., De Cesare, G., & Schleiss, A. (2011). *Fine sediment release from a reservoir by controlled hydrodynamic mixing.* Paper presented at the Proceedings of the 34th IAHR World Congress.

Andrews, S., Nover, D., & Schladow, S. G. (2010). Using laser diffraction data to obtain accurate particle size distributions: the role of particle composition. *Limnology and Oceanography: Methods, 8*(10), 507-526.

Angamuthu, M., & Ramalingam, A. (2011). Balanced key tree management for multi-privileged groups using (N, T) policy. *Security and Communication Networks, 5*(5), 545-555. 10.1002/sec.351

Auer, B., Elzer, U., & Arndt, H. (2004). Comparison of pelagic food webs in lakes along a trophic gradient and with seasonal aspects: influence of resource and predation. *Journal of plankton research, 26*(6), 697-709.

Axtell, N. R., Sternberg, S. P. K., & Claussen, K. (2003). Lead and nickel removal using Microspora and Lemna minor. *Bioresource technology, 89*(1), 41-48.

Ayon, A., Bayt, R., & Breuer, K. (2001). Deep reactive ion etching: a promising technology for micro-and nanosatellites. *Smart materials and structures, 10*(6), 1135.

Ayub, K. R., Sidek, L. M., Ainan, A., Zakaria, N. A., Ghani, A. A., & Abdullah, R. (2005). Storm water treatment using Bio-Ecological Drainage System. *International Journal of River Basin Management, 3*(3), 215-221.

Bajcar, T., Gosar, L., Širok, B., Steinman, F., & Rak, G. (2010). Influence of flow field on sedimentation efficiency in a circular settling tank with peripheral inflow and central effluent. *Chemical Engineering and Processing: Process Intensification, 49*(5), 514-522.

Bajcar, T., Steinman, F., Širok, B., & Prešeren, T. (2011). Sedimentation efficiency of two continuously operating circular settling tanks with different inlet-and outlet arrangements. *Chemical Engineering Journal, 178*, 217-224.

Barnard, P. L., Schoellhamer, D. H., Jaffe, B. E., & McKee, L. J. (2013). Sediment transport in the San Francisco Bay Coastal System: An overview. *Marine Geology, 345*, 3-17. doi:10.1016/j.margeo.2013.04.005

Bastiaans, R. J. M. (2000). *Cross-correlation piv; theory, implementation and accuracy*: Eindhoven University of Technology, Faculty of Mechanical Engineering. Netherlands.

Basualto, S., Tapia, J., Cruces, F., Peña-Cortés, F., Hauenstein, E., Bertrán, C., & Schlatter, R. (2006). The effect of physical and chemical parameters on the structure and composition of the phytoplankton community of Lake Budi (IX Region, Chile). *Journal of the Chilean Chemical Society, 51*(3), 993-999.

University of Malaya

Bayt, R. L., Breuer, K. S., & by Institutions, F. (2001). *Design and performance of hot and cold supersonic microjets.* Paper presented at the 39th Aerospace Sciences Meeting and Exhibit.

Bhat, M. M., Yazdani, T., Narain, K., Yunus, M., & Shukla, R. N. (2009). Water Quality Status of Some Urban Ponds of Lucknow, Uttar Pradesh. *Journal of Wetlands Ecology, 2*(1), 67-73.

Biswas, P., Godiwalla, K., Sanyal, D., & Dev, S. (2002). A simple technique for measurement of apparent viscosity of slurries: sand–water system. *Materials & design, 23*(5), 511-519.

Bo, T.-L., Zheng, X.-J., Duan, S.-Z., & Liang, Y.-R. (2013). The influence of sand diameter and wind velocity on sand particle lift-off and incident angles in the windblown sand flux. *Sedimentary Geology, 290*, 149-156. doi:10.1016/j.sedgeo.2013.03.013

Bogner, A., Jouneau, P.-H., Thollet, G., Basset, D., & Gauthier, C. (2007). A history of scanning electron microscopy developments: towards "wet-STEM" imaging. *Micron, 38*(4), 390-401.

Bonard, J.-M., Dean, K. A., Coll, B. F., & Klinke, C. (2002). Field emission of individual carbon nanotubes in the scanning electron microscope. *Physical review letters, 89*(19), 197602.

Born, M., & Wolf, E. (1999). *Principles of optics: electromagnetic theory of propagation, interference and diffraction of light*: Cambridge university press.

Boyle, J. F., Manas-Zloczower, I., & Feke, D. L. (2005). Hydrodynamic analysis of the mechanisms of agglomerate dispersion. *Powder Technology, 153*(2), 127-133.

Brethour, J., & Burnham, J. (2010). Modeling sediment erosion and deposition with the FLOW-3D sedimentation & scour model. *Flow Science Technical Note, FSI-10-TN85*, 1-22.

Britannica, E. (1964). *Encyclopaedia Britannica*: Encyclopaedia britannica. Retrieved June. 02. 2013.

Brown, R. L. (1931). OE MILWAUKEE: Google Patents. Retrieved October.09. 2012.

Brown, R. M., McClelland, N. I., Deininger, R. A., & Tozer, R. G. (1970). A water quality index: do we dare? . *Water Sewage Works, 117*, 339-343.

Brücker, C. (1993). Study of vortex breakdown by particle tracking velocimetry (PTV). *Experiments in fluids, 14*(1-2), 133-139.

Brücker, C., & Althaus, W. (1992). Study of vortex breakdown by particle tracking velocimetry (PTV). *Experiments in fluids, 13*(5), 339-349.

University of Malaya

Bryanston-Cross, P., Judge, T., Quan, C., Pugh, G., & Corby, N. (1995). The application of digital particle image velocimetry (DPIV) to transonic flows. *Progress in Aerospace Sciences, 31*(3), 273-290.

Bukhari, A. A. (2008). Investigation of the electro-coagulation treatment process for the removal of total suspended solids and turbidity from municipal wastewater. *Bioresource technology, 99*(5), 914-921.

Cammem, L. (1982). Effect of particle size on organic content and microbial abundance within four marine sediments. *Marine ecology progress series. Oldendorf, 9*(3), 273-280.

Camnasio, E., Erpicum, S., Orsi, E., Pirotton, M., Schleiss, A. J., & Dewals, B. (2013). Coupling between flow and sediment deposition in rectangular shallow reservoirs. *Journal of Hydraulic Research, 51*(5), 535-547.

Camnasio, E., Orsi, E., & Schleiss, A. J. (2011). Experimental study of velocity fields in rectangular shallow reservoirs. *Journal of Hydraulic Research, 49*(3), 352-358. doi:10.1080/00221686.2011.574387

Casey, R., Shaw, A., Massal, L., & Snodgrass, J. (2005). Multimedia evaluation of trace metal distribution within stormwater retention ponds in suburban Maryland, USA. *Bulletin of environmental contamination and toxicology, 74*(2), 273-280.

Chang, T. P., Wilcox, N. A., & Tatterson, G. B. (1984). Application of image processing to the analysis of three-dimensional flow fields. *Optical Engineering, 23*(3), 283-280.

Chen, S., Timmons, M. B., Bisogni Jr, J. J., & Aneshansley, D. J. (1993). Suspended-solids removal by foam fractionation. *The Progressive Fish-Culturist, 55*(2), 69-75.

Cheng, N.-S. (1997). Simplified settling velocity formula for sediment particle. *Journal of Hydraulic Engineering, 123*(2), 149-152.

Cheng, N.-S. (2008). Comparison of settling-velocity-based formulas for threshold of sediment motion. *Journal of Hydraulic Engineering, 134*(8), 1136-1141.

Cheng, Y. (2008). Sediment Discharge from a Storm-Water Retention Pond 1. *Journal of Irrigation and Drainage Engineering, 134*(5), 606-612.

Cholette, A., & Cloutier, L. (1959). Mixing efficiency determinations for continuous flow systems. *The Canadian Journal of Chemical Engineering, 37*(3), 105-112.

CIRIA. (2000). Sustainable Urban Drainage System - Design for England and Wales. Retrieved March.15.2013, from: http://www.ciria.org/service/Web_Site/AM/ContentManagerNet/ContentDisplay.aspx?Section=Web_Site&ContentID=8945

Clarke, I. C. (1974). Articular cartilage: a review and scanning electron microscope study II. The territorial fibrillar architecture. *J. Anat., 118*(2), 261-280.

University of Malaya

Cooke, B. C., Jones, A. R., Goodwin, I. D., & Bishop, M. J. (2012). Nourishment practices on Australian sandy beaches: A review. *Journal of environmental management, 113*, 319-327.

Costa, J. E., & Wieczorek, G. F. (1987). *Debris flows/avalanches: process, recognition, and mitigation* (Vol. 7): Geological Society of America.

Cottingham, K. L., & Carpenter, S. R. (1998). Population, community, and ecosystem variates as ecological indicators: phytoplankton responses to whole-lake enrichment. *Ecological Applications, 8*(2), 508-530.

Craig, D., Fallowfield, H., & Cromar, N. (2002). *Decay rates of faecal indicator organisms and pathogens: use of microcosm and in situ studies for the estimation of exposure risk in recreational waters.* Paper presented at the the American Water Works Association, United States.

Cranfield, U. (2014). Soil-Net.com. Retrieved May.10.2013, from: http://www.soilnet.com/dev/page.cfm?pageid=casestudies_diatoms&loginas=anon_casestudies

Cripps, S. J., & Bergheim, A. (2000). Solids management and removal for intensive land-based aquaculture production systems. *Aquacultural engineering, 22*(1), 33-56.

Curtis, W. F., Meade, R. H., Nordin, C. F., Price, B. N., & Sholkovitz, E. R. (1979). Non-uniform vertical distribution of fine sediment in the Amazon River. *Nature, 280*, 381-383. doi:0028083679310381

Cybulski, A., & Mucha, Z. (1997). Laser keyholes in liquids. *Welding international, 11*(3), 212-220.

Danielle, N. (2010). The Importance of Rewriting Storm Water Regulations [New research project to tackle water pollution from agriculture]. Retrieved from Retervived April. 01.2013, from: https://sites.google.com/a/brvgs.k12.va.us/water-pollution/home/research-paper

Davies, J.-M., Roxborough, M., & Mazumder, A. (2004). Origins and implications of drinking water odours in lakes and reservoirs of British Columbia, Canada. *Water research, 38*(7), 1900-1910.

Debs, C. (2013). A Review Of Fresh Cement And Concrete Rheology. *The Masterbuilder ,Indian Premier Construction Magazine,* 138-144.

Denn, M., & Porteous, K. (1971). Elastic effects in flow of viscoelastic liquids. *The Chemical Engineering Journal, 2*(4), 280-286.

Di Felice, F., & Pereira, F. (2008). Developments and applications of PIV in naval hydrodynamics *Particle Image Velocimetry* (pp. 475-503): Springer.

Di Stefano, C., Ferro, V., & Mirabile, S. (2010). Comparison between grain-size analyses using laser diffraction and sedimentation methods. *biosystems engineering, 106*(2), 205-215.

University of Malaya

Dinkelacker, F., Schäfer, M., Ketterle, W., Wolfrum, J., Stolz, W., & Köhler, J. (1992). Determination of the third velocity component with PTA using an intensity graded light sheet. *Experiments in fluids, 13*(5), 357-359.

Divakaran, R., & Sivasankara Pillai, V. (2002). Flocculation of river silt using chitosan. *Water Research, 36*(9), 2414-2418.

Dowd, P. (2010). University Engineering Education in Australia. *Accessed June, 12*, 2010.

Dudderar, T., Meynart, R., & Simpkins, P. (1988). Full-field laser metrology for fluid velocity measurement. *Optics and Lasers in Engineering, 9*(3), 163-199.

Dufresne, M., Dewals, B. J., Erpicum, S., Archambeau, P., & Pirotton, M. (2010a). Classification of flow patterns in rectangular shallow reservoirs. *Journal of Hydraulic Research, 48*(2), 197-204.

Dufresne, M., Dewals, B. J., Erpicum, S., Archambeau, P., & Pirotton, M. (2010b). Experimental investigation of flow pattern and sediment deposition in rectangular shallow reservoirs. *International Journal of Sediment Research, 25*(3), 258-270.

Dufresne, M., Dewals, B. J., Erpicum, S., Archambeau, P., & Pirotton, M. (2011). Numerical investigation of flow patterns in rectangular shallow reservoirs. *Engineering Applications of Computational Fluid Mechanics, 5*(2), 247-258.

Ebel, E. J. (2009). Principle and process of sediment transport. Retrieved November.11.2015.

Einsten, A. (1903). Investigations On The Theory Of The Brownian Movement. *Ann. d. Phys., 11*, 170-188.

Ekhwan, T. M., Mokhtar, M., Gasim, M. B., Abdullah, S. M. S., Jaafar, O., & Aziz, N. A. A. (2009). Water resources study and modeling at North Kedah: a case of Kubang Pasu and Padang Terap water supply schemes. *Research journal of earth sciences, 1*(2), 35-42.

Ellis, J. B., & Revitt, D. M. (1982). Incidence of heavy metals in street surface sediments: solubility and grain size studies. *Water, Air, and Soil Pollution, 17*(1), 87-100.

EPA. (2001). Retrieved April. 10. 2013, from: http://water.epa.gov/scitech/swguidance/standards/criteria/aqlife/methylmercury/index.cfm

Eshel, G., Levy, G., Mingelgrin, U., & Singer, M. (2004). Critical evaluation of the use of laser diffraction for particle-size distribution analysis. *Soil Science Society of America Journal, 68*(3), 736-743.

Estproc. (2003). *The transport of fine sediment in the Humber estuary*. Retervied April. 10. 2013, from: http://www.estproc.net/documents/report04.pdf

Fang, H., Zhao, H., Shang, Q., & Chen, M. (2012). Effect of biofilm on the rheological properties of cohesive sediment. *Hydrobiologia, 694*(1), 171-181.

University of Malaya

FAO. (2012). Retrieved May.18. 2013, from http://www.fao.org/index_en.htm.

Federal Highway Administration. (2006). Geotechnical Aspects of Pavements Reference Manual. *Geotechnical Aspects of Pavements Reference Manual*. FHWA, U.S. Department of Transportation. Retrieved March. 07. 2013, from: http://www.fhwa.dot.gov/engineering/geotech/pubs/05037/05a.cfm

Ferreira, R. M. (2011). Turbulent flow hydrodynamics and sediment transport: Laboratory research with LDA and PIV *Experimental Methods in Hydraulic Research* (pp. 67-111): Springer.

Fink, J. C. (2005). *The Effects Of Urbanization On Baird Creek, Green Bay, Wisconsin.* (Master Of Science in Environmental Science And Policy), University of Wisconsin-Green Bay, Wisconsin-Green Bay. Retrieved March.20.2013, from: http://www.uwgb.edu/watershed/fink/Fink_Thesis.pdf

Fontein W., & Van der Wal J. (2006). *Assessing Nautical Depth Efficiently In Terms Of Rheological Characteristics.* Paper presented at the the International Hydrographic Conference'Evolutions in Hydrography', Antwerp, Belgium.

Ghani, A., & Mohammadpour, R. (2015). Temporal variation of clear-water scour at compound Abutments. *Ain Shams Engineering Journal*. doi:10.1016/j.asej.2015.07.005

Ginsberg, S., & Aliotta, S. (2011). *Sediment Transport, Chapter 14: Sediment Transport Circulation Pattern through Mesotidal Channels System.* 275-294. India: INTECH Open Access Publisher.

Giordano, R., Astarita, T., & Carlomagno, G. M. (2006). Correction of misalignment errors in stereoscopic PIV systems. Retrieved May.17.2014, from: http://www.aivela.org/Giordano_paper03.pdf

Goswami, P. K., & Mishra, J. K. (2013). Climatic and tectonic controls on the sedimentary processes of an alluvial fan of the western Ganga Plain, India. *Geological Magazine, 150*(02), 240-253.

Gotoh, S., & Nawa, T. (2012). On Rheological Approach to Estimate Fractal Dimension of Aggregate in Concentrated and Flocculated Suspension. *Nihon Reoroji Gakkaishi, 40*(4), 157-164.

Grant, I. (1997). Particle image velocimetry: a review. *Proceedings of the Institution of Mechanical Engineers, Part C: Journal of Mechanical Engineering Science, 211*(1), 55-76. doi:10.1243/0954406971521665

Grant, I., Zhao, Y., Tan, Y., & Stewart, J. (1991). *Three component flow mapping-Experiences in stereoscopic PIV and holographic velocimetry.* Paper presented at the Laser Anemometry-Advances and Applications.

Greiser, N., & Wurpts, R. (2008). *Microbiological Impact On Formation And Rheological Properties Of Fluid Mud.* Paper presented at the Chinese-German Joint Symposium on Hydraulic and Ocean Engineering, Darmstadt.

University of Malaya

Guasto, J. S., Huang, P., & Breuer, K. S. (2006). Statistical particle tracking velocimetry using molecular and quantum dot tracer particles. *Experiments in fluids, 41*(6), 869-880.

Guo, J. (2002). Logarithmic matching and its applications in computational hydraulics and sediment transport. *Journal of Hydraulic Research, 40*(5), 555-565.

Hackley, V. A., & Ferraris, C. F. (2001). *Guide to rheological nomenclature: Measurements in ceramic particulate systems*: National Institute of Standards and Technology Gaithersburg, MD, USA.

Hadad, T., & Gurka, R. (2013). Effects of particle size, concentration and surface coating on turbulent flow properties obtained using PIV/PTV. *Experimental Thermal and Fluid Science, 45*, 203–212

Harrison, E. T. (2007). *The impact of fine sediment accumulation on benthic macroinvertebrates: implications for river management.* Paper presented at the Proceedings of the 5th Australian Stream Management Conference. Australian rivers: making a difference, Charles Sturt University, Thurgoona, New South Wales.

Harrison, E. T., Norris, R. H., & Wilkinson, S. N. (2008). Can an indicator of river health be related to assessments from a catchment-scale sediment model? *Hydrobiologia, 600*(1), 49-64.

Hashimoto, T., Turukawa, T., & Mori, N. (2005). Flow property and micellar structures in capillary flows of surfactant solutions. *Journal of the Society of Rheology ;Japan, 33*(1), 1-8.

Hassan, Y., Blanchat, T., & Seeley Jr, C. (1992). PIV flow visualisation using particle tracking techniques. *Measurement Science and Technology, 3*(7), 633.

Hawai'I, U. o. (2012). Retrieved July. 02. 2013, from: http://www.soest.hawaii.edu

Heath, J. R., Knobler, C. M., & Leff, D. V. (1997). Pressure/temperature phase diagrams and superlattices of organically functionalized metal nanocrystal monolayers: the influence of particle size, size distribution, and surface passivant. *The Journal of Physical Chemistry B, 101*(2), 189-197.

Hern, T. K., Hin, L. S., Ibrahim, S., Nik Sulaiman, N. M., Sharifi, M., & Abe, S. (2014). Impact of Fine Sediment on TSS and Turbidity in Retention Structure. *Journal of Geoscience and Environment Protection, 2*(4), 1-8. doi:10.4236/gep.2014.24001

Hidayah, E., & Karnaningroem, N. (2012). The implementation of hydrodynamic model in water treatment to estimate turbidity removal. *International Journal of Environmental Sciences and Research, 2*(1), 129-133.

HMK, T. (2014). Laser Diffraction Particle Size Analysis. In H. T. c. A China Land Reliable Industrial Supplier (Ed.). China. Retrieved June.05.2013.

University of Malaya

Hooke, R. (1931). A Description of Helioscopes 1676 London. Reprinted in RT Gunther. *Early science in Oxford, 8*, 140-141.

Hopkins, J. (2014). Department of Mechanical Engineering,Johns Hopkins University Johns Hopkins University

Hoque, M. M., Sathe, M. J., Mitra, S., Joshi, J. B., & Evans, G. M. (2015). Comparison of specific energy dissipation rate calculation methodologies utilising 2D PIV velocity measurement. *Chemical Engineering Science,137*, 752–767.

Horton, B., & DeCelles, P. (2001). Modern and ancient fluvial megafans in the foreland basin system of the central Andes, southern Bolivia: Implications for drainage network evolution in fold-thrust belts. *Basin research, 13*(1), 43-63.

Hsu, T.-J., Yu, X., Ozdemir, C. E., & Balachandar, S. (2012). A 3D numerical investigation of fine sediment transport in an oscillatory channel. *Coastal Engineering Proceedings, 1*(33), 9.

http://www.iq.usp.br/mralcant/About_Rheo.html. (2013). Retrieved May.12.2013.

Huang, S. L. (2007). Effects of using different sediment transport formulae and methods of computing Manning's roughness coefficient on numerical modeling of sediment transport. *Journal of Hydraulic Research, 45*(3), 347-356.

Hyun, K., Wilhelm, M., Klein, C. O., Cho, K. S., Nam, J. G., Ahn, K. H., McKinley, G. H. (2011). A review of nonlinear oscillatory shear tests: Analysis and application of large amplitude oscillatory shear (LAOS). *Progress in Polymer Science, 36*(12), 1697-1753.

Ismail T., M. A., Othman, A. B., Fadzil1, S. B., Harun, & Zainuddin., Z. M. (2010). *Deposition ff Sediments in Detention Pond*. Paper presented at the International journal of conservation science.

Iverson, R. M. (2003). The debris-flow rheology myth. *Debris-flow hazards mitigation: mechanics, prediction, and assessment, 1*, 303-314.

Jahanmiri, M. (2011). *Particle Image Velocimetry Fundamentals and Its Applications*. Retrieved from Göteborg, Sweden:

Jamshidnia, H., & Firoozabadi, B. (2010). Experimental Investigation of Ba e E ect on the Flow in a Rectangular Primary Sedimentation Tank.

Jeffreys, H. (1929). *On the transport of sediments by streams.* Paper presented at the Mathematical Proceedings of the Cambridge Philosophical Society.

Jewel M.A.S., M.M. Rahman, & M.A. Sarker. (2006). Effects of environmental parameters on the cyanobacterial bloom in a lake of Bangladesh,. *Bangladesh Journal of Progressive Science and Technology, 4*(2), 159-164.

Johnson, B., Leishman, J. G., & Sydney, A. (2009). *Investigation of sediment entrainment in brownout using high-speed particle image velocimetry.* Paper presented at the 65th Annual Forum of the American Helicopter Society, Grapevine, TX.

University of Malaya

Jones, G. D., & Wadzuk, B. M. (2013). Predicting Performance for Constructed Storm-Water Wetlands. *Journal of hydraulic engineering, 139*(11), 1158-1164.

Kaide, A. S., T. (2012). Rheology of Silica Gel Obtained From Alkaline Sol Transition. *Journal of Society of Rheology Japan, 40*(40), 165-170.

Kamarudin, M. K., Toriman, M. E., Mastura, S. S., Hj, M., Jamil, I. N., & Gazim, M. B. (2009). Temporal variability on lowland river sediment properties and yield. *American Journal of Environmental Sciences, 5*(5), 657.

Kaminsky, R., Kallweit, S., Rossi, M., Morbiducci, U., Scalise, L., Verdonck, P., & Tomasini, E. P. (2008). PIV measurements of flows in artificial heart valves *Particle Image Velocimetry* (pp. 55-72): Springer.

Karageorgis, A., Anagnostou, C., Sioulas, A., Chronis, G., & Papathanassiou, E. (1998). Sediment geochemistry and mineralogy in Milos bay, SW Kyklades, Aegean Sea, Greece. *Journal of Marine Systems, 16*(3), 269-281.

Karlsson, K., Viklander, M., Scholes, L., & Revitt, M. (2010). Heavy metal concentrations and toxicity in water and sediment from stormwater ponds and sedimentation tanks. *Journal of hazardous materials, 178*(1), 612-618.

Kemker, C. (2014). Sediment Transport and Deposition. Retrieved from: http://www.fondriest.com/environmentalmeasurements/parameters/hydrology/sediment-transport-deposition/

Khan, S., Melville, B. W., & Shamseldin, A. (2013). Design of Storm-Water Retention Ponds with Floating Treatment Wetlands. *Journal of Environmental Engineering, 139*(11), 1343-1349.

Kiat, C. C., Ab Ghani, A., Abdullah, R., & Zakaria, N. A. (2008). Sediment transport modeling for Kulim River–A case study. *Journal of Hydro-environment Research, 2*(1), 47-59.

Kilic, S., Nam, K., & Aral, M. (2005). *Preliminary Analysis of Self-Cleaning Capacity of Lake Pontchartrain using Fugacity Analysis*. *98*, 100-117. MESL Research Group. Retrieved March.18.2013, from: http://www.mvn.usace.army.mil/pao/BRO/wat_res98/WaterRes98_9of16.pdf

King Kuok Kuok, & Po Chan Chiu. (2013). Particle Image Velocimetry for Measuring Water Flow Velocity. *International Journal of Environmental, Earth Science and Engineering, 7*(12), 45-51.

Kinnaman, A. R., Surbeck, C. Q., & Usner, D. C. (2012). Coliform Bacteria: The Effect of Sediments on Decay Rates and on Required Detention Times in Stormwater BMPs. *Journal of Environmental Protection, 3*(28), 787-797.

Kippax P. (2005). Measuring particle size using modern laser diffraction techniques *Paint & Coating Industry, 21*(8), 42-47.

University of Malaya

Kirby, R. (2013). Managing industrialised coastal fine sediment systems. *Ocean & Coastal Management, 79*, 2-9.

Kirby R. (2011). Minimising harbour siltation—findings of PIANC Working Group 43. *Ocean Dynamics, 61*, 233–244. doi:10.1007/s10236-010-0336-9

Komar, P. D. (1998). Beach processes and sedimentation. Retrieved August.10.2013, from: http://www.citeulike.org/group/11419/author/Komar:PD

Krishnappan, B.G. (1997). *A New Model of Fine Sediment Transport For the Fraser River* (DOE FRAP 1996-17). Retrieved June. 04. 2013, from: http://research.rem.sfu.ca/frap/9617.pdf

Krishnappan, B. G. (2000). Modelling cohesive sediment transport in rivers. *IAHS Publication(International Association of Hydrological Sciences)*(263), 269-276.

Krzaklewski, W., Barszcz, J., Małek, S., Kozioł, K., & Pietrzykowski, M. (2004). Contamination of forest soils in the vicinity of the sedimentation pond after zinc and lead ore flotation (in the region of Olkusz, southern Poland). *Water, Air, & Soil Pollution, 159*(1), 151-164.

Kumar, P., Wanganeo, R., Wanganeo, A., & Sonaullah, F. (2011). Preliminary study on Ichthyofaunal diversity of Shershah Suri pond, Sasaram, Bihar. *International Journal of Engineering Science and Technology, 3*(2), 1582-1588.

Kumar. P , & Wanganeo., A. (2012). Preliminary study on Ichthyofaunal diversity of a Eutrophic pond, Sasaram, Bihar. *Journal of Chemical, Biological and Physical Sciences, 2*(2),1107-1114.

Kunkel, E. A., Privette, C. V., Sawyer, C. B., & Hayes, J. C. (2013). Attachment of Escherichia coli to fine sediment particles within construction sediment basins. *Advances in Bioscience and Biotechnology, 4*(3A), 407-415.

Kuok, K. K., & Chiu, P. C. (2013). Particle Image Velocimetry for Measuring Water Flow Velocity. *International Scholarly and Scientific Research & Innovation, 7*(12), 664-670.

Kutílek, M., & Nielsen, D. R. (1994). *Soil hydrology: texbook for students of soil science, agriculture, forestry, geoecology, hydrology, geomorphology and other related disciplines*: Catena Verlag.

Lad, N., Aroussi, A., Adebayo, D., & Al-Atabi, M. (2011). Characterisation Of Multiphase Fluid-Structure Interaction Using Non-Intrusive Optical Techniques. *Journal of Engineering Science and Technology, 6*(2), 131-145.

Le Hir, P., Ficht, A., Silva Jacinto, R., Lesueur, P., Dupont, J.-P., Lafite , R., Cugier, P. (2001). Fine sediment transport and accumulations at the mouth of the Seine estuary (France). *Journal of Estuaries And Coasts, 24*(6), 950-963. doi:10.2307/1353009

Lenntech. (2011). Water pollution FAQ. Retrieved October.11.2013, from: http://www.lenntech.com/water-pollution-faq.htm#ixzz23J7OmVdP

University of Malaya

Lev, E., Spiegelman, M., Wysocki, R. J., & Karson, J. A. (2012). Investigating lava flow rheology using video analysis and numerical flow models. *Journal of Volcanology and Geothermal Research, 247-248*, 62-73.

Levenspiel, O. (2002). Modeling in chemical engineering. *Chemical Engineering Science, 57*(22), 4691-4696.

Li, Y., Deletic, A., & Fletcher, T. (2007). Modelling wet weather sediment removal by stormwater constructed wetlands: Insights from a laboratory study. *Journal of hydrology, 338*(3), 285-296.

Lim, W. L., Chew, Y. T., Chew, T. C., & Low, H. T. (1997). Steady flow velocity field and turbulent stress mappings downstream of a porcine bioprosthetic aortic valveIn Vitro. *Annals of biomedical engineering, 25*(1), 86-95.

Lindken, R., & Merzkirch, W. (2002). A novel PIV technique for measurements in multiphase flows and its application to two-phase bubbly flows. *Experiments in fluids, 33*(6), 814-825.

LLC, R. (2014). A Basic Introduction to Viscometers & Viscometry. USA. Retrieved October.15.2013.

Longe, E., & Balogun, M. (2010). Groundwater Quality Assessment Near a Municipal Landfill, Lagos, Nigeria. *Research journal of applied sciences, engineering and technology, 2*(1), 39-44.

López, P. R., Lavín, A. G., López, M. M. M., & de las Heras, J. L. B. (2008). Flow models for rectangular sedimentation tanks. *Chemical Engineering and Processing: Process Intensification, 47*(9), 1705-1716.

Lowe, D. R. (1976). Subaqueous liquefied and fluidized sediment flows and their deposits. *Sedimentology, 23*(3), 285-308.

Lucas, R., Courties, C., Herbland, A., Goulletquer, P., Marteau, A. L., & Lemonnier, H. (2010). Eutrophication in a tropical pond: Understanding the bacterioplankton and phytoplankton dynamics during a vibriosis outbreak using flow cytometric analyses. *Aquaculture, 310*(1), 112-121.

Mackay, D. (2001). *Multimedia environmental models: the fugacity approach*: CRC press. New York,US. Retrieved November.06.2013.

Mackay, D., & Paterson, S. (1991). Evaluating the multimedia fate of organic chemicals: a level III fugacity model. *Environmental Science & Technology, 25*(3), 427-436.

Maleoszewski, P., Wachniew, P., & Czuprynski, P. (2006). Hydraulic characteristics of a wastewater treatment pond evaluated through tracer test and multi-flow mathematical approach. *Polish Journal of Environmental Studies, 15*(1), 105-110.

Marett, J. (1967). *Techniques of modern photography*: Evans Bros. Retrieved October.19.2013.

University of Malaya

Markgraf, W., Horn, R., & Peth, S. (2006). An approach to rheometry in soil mechanics—Structural changes in bentonite, clayey and silty soils. *Soil and Tillage Research, 91*(1), 1-14.

Markgraf, W., Watts, C. W., Whalley, W. R., Hrkac, T., & Horn, R. (2012). Influence of organic matter on rheological properties of soil. *Applied Clay Science, 64*, 25-33.

Markgrafa, W. (2010). *Quantifying microstructural stability of South-Brazilian soils by the application of rheological techniques and zeta potential measurements.* Paper presented at the Proceedings of the 19th World Congress of Soil Science: Soil solutions for a changing world, Brisbane, Australia, 1-6 August 2010., Brisbane, Australia.

Marsalek, J., Watt, W., Anderson, B., & Jaskot, C. (1997). Physical and chemical characteristics of sediments from a stormwater management pond. *Water Quality Research Journal of Canada, 32*(1), 89-100.

Matko, T., Fawcett, N., Sharp, A., & Stephenson, T. (1996). Recent progress in the numerical modelling of wastewater sedimentation tanks. *Process safety and environmental protection, 74*(4), 245-258.

Maxwell, J. C. (1867). On the dynamical theory of gases. *Philosophical transactions of the Royal Society of London*, 49-88.

Mazzeo, F. A. (2008). *Importance of Oscillatory Time Sweeps in Rheology*. Retrieved January.11.2014, from New Castle DE, USA.

Meade, R. H. (1972). Transport and deposition of sediments in estuaries. v. 133, p. 91-120. doi: 10.1130/MEM133-p91

Mehmet, N., & Turkemen., M. (2005). Phytoplankton biomass and species composition of Lake Golbasi (Hatay – Turkey). *Turkish Journal of Biology, 29*, 49-56.

Meijer, L. E., & Avnimelech, Y. (1999). On the use of micro-electrodes in fish pond sediments. *Aquacultural engineering, 21*(2), 71-83.

Melling, A. (1997). Tracer particles and seeding for particle image velocimetry. *Measurement Science and Technology, 8*(12), 1406.

Milliman, J. D., & Syvitski, J. P. (1992). Geomorphic/tectonic control of sediment discharge to the ocean: the importance of small mountainous rivers. *The Journal of Geology,100*(5), 525-544.

Mitchell, S., & Burgess, H. (2004). Effect On Estuarine Fine-Sediment Transport Of Intermittent Pump Discharge At Pagham Harbour, West Sussex. *Water and Environment Journal, 18*(1), 39-43.

Mitchell, S., Burgess, H., & Pope, D. (2006). Stratification and fine sediment transport mechanisms in a semi-enclosed tidal lagoon (Pagham Harbour, West Sussex). *Water and Environment Journal, 20*(4), 248-255.

University of Malaya

Mitchell, S., Burgess, H., Pope, D., & Theodoridou, A. (2008). Field studies of velocity, salinity and suspended solids concentration in a shallow tidal channel near tidal flap gates. *Estuarine, Coastal and Shelf Science, 78*(2), 385-395.

Mitchell, S., Lawler, D., West, J., & Couperthwaite, J. (2003). Use of continuous turbidity sensor in the prediction of fine sediment transport in the turbidity maximum of the Trent Estuary, UK. *Estuarine, Coastal and Shelf Science, 58*(3), 645-652.

Mohammadpour, R., Ghani, A. A., & Azamathulla, H. M. (2013). Numerical modeling of 3-D flow on porous broad crested weirs. *Applied Mathematical Modelling, 37*(22), 9324-9337.

Muhanned, A. (2013). Studying the Factors Affecting the Settling Velocity of Solid Particles in Non-Newtonian Fluids. *College of Engineering Journal (NUCEJ), 16*(1), 41-50.

Murray, A. S., & Olley, J. M. (2002). Precision and accuracy in the optically stimulated luminescence dating of sedimentary quartz: A status review. *Journal on Methods and Applications of Absolute Chronology, 21*, 1-16.

Myrhaug, D., & Holmedal, L. E. (2007). Mobile layer thickness in sheet flow beneath random waves. *Coastal engineering, 54*(8), 577-585.

National Hydraulic Research Institute of Malaysia (NAHRIM). (2012). Ministry of Natural Resources and Environment (NRE). Retrieved October.11.2013, from: www.nahrim.gov.my/index.php/en.

Nègre, M., Leone, P., Trichet, J., Défarge, C., Boero, V., & Gennari, M. (2004). Characterization of model soil colloids by cryo-scanning electron microscopy. *Geoderma, 121*(1), 1-16.

New Mexico Environment Department, N. (2014). *State of New Mexico Clean Water Act Section 303(d)/Section 305(b) Integrated Report*. New Mexico: Water Quality Control Comission. Retrieved from: http://www.nmenv.state.nm.us/swqb/303d-305b/2014-2016/2014.2016NMReport.pdf.

Nichols, M., Nearing, M., Polyakov, V., & Stone, J. (2013). A sediment budget for a small semiarid watershed in southeastern Arizona, USA. *Geomorphology, 180*, 137-145.

Nielsen, D. (2012). *The Importance of Rewriting Storm Water Regulations.* Retrieved October.22.2013, from: https://sites.google.com/a/brvgs.k12.va.us/water-pollution/home/research-paper

Novotny, V. (2003). *Water quality: Diffuse pollution and watershed management*: John Wiley & Sons.

Oakley, T. R., Loth, E., & Adrian, R. J. (1996). Cinematic particle image velocimetry of high-Reynolds-number turbulent free shear layer. *AIAA journal, 34*(2), 299-308.

University of Malaya

Olhero, S., & Ferreira, J. (2004). Influence of particle size distribution on rheology and particle packing of silica-based suspensions. *Powder Technology, 139*(1), 69-75.

Önal, S. (2010). *Investigation of flow characteristics around a single and staggered slotted-cylinders.* (PhD), Çukurova University, Adana. Retrieved September.08.2013, from: http://library.cu.edu.tr/tezler/8052.pdf

Ongley, E. D. (1996). *Control of water pollution from agriculture*: Food & Agriculture Org.

Oram, B., & PG. (2012). Monitoring the Quality of Surface water. Retrieved October.09.2012, from: http://www.water-research.net/index.php/water-treatment/water-monitoring/monitoring-the-quality-of-surfacewaters

Pan, J., & Center, L. T. (1995). *Procedures for Reducing the Size of Coverage-based Test Sets.* Paper presented at the Proceedings of International Conference on Testing Computer Software.

Paris, R., Fournier, J., Poizot, E., Etienne, S., Morin, J., Lavigne, F., & Wassmer, P. (2010). Boulder and fine sediment transport and deposition by the 2004 tsunami in Lhok Nga (western Banda Aceh, Sumatra, Indonesia): a coupled offshore–onshore model. *Marine Geology, 268*(1), 43-54.

Persson, J., Somes, N., & Wong, T. (1999). Hydraulics efficiency of constructed wetlands and ponds. *Water science and technology, 40*(3), 291-300.

Pidwirny, M. (2006). *Streamflow and Fluvial Processes* (2nd Edition ed.): Fundamentals of Physical Geography.

Prasad, A. K. (2000a). Particle image velocimetry. *Current Science-Bangalore, 79*(1), 51-60.

Prasad, A. K. (2000b). Stereoscopic particle image velocimetry. *Experiments in Fluids, 29*(2), 103-116

Prasad, A. K., & Jensen, K. (1995). Scheimpflug stereocamera for particle image velocimetry in liquid flows. *Applied Optics, 34*(30), 7092-7099.

Prestlglacomo, A. R., Effler , S. W., O'Donnell', D., Hassett, J. M., M. Mlchalenko, E., Lee' , Z., & Weldemann, A. (2007). Turbidity and suspended solids levels and loads in a sediment enriched stream: implications for impacted lotic and lentic ecosystems. *Lake and Re,eroir Management, 23*, 231-244.

Raffel, M., Kompenhans, J., Stasicki, B., Bretthauer, B., & Meier, G. (1995). Velocity measurement of compressible air flows utilizing a high-speed video camera. *Experiments in fluids, 18*(3), 204-206.

Raffel, M., Seelhorst, U., & Willert, C. (1998). Vortical flow structures at a helicopter rotor model measured by LDV and PIV. *Aeronautical Journal, 102*(1014), 221-227.

University of Malaya

Raffel, M., Willert, C. E., Wereley, S. T., & Kompenhans, J. (2007). *Particle Image Velocimetry ; A Practical Guide*. Berlin Heidelberg New York: Springer

Raffel, M., Willert, C. E., Wereley, S. T., & Kompenhans, J. (2007). *Post-processing of PIV data,; Particle Image Velocimetry* (pp. 177-208): Springer.

Reading, H. G. (2009). *Sedimentary environments: processes, facies and stratigraphy*. USA: Blackwell publishing.

Rensbergen, P., Hillis, R. R., Maltman, A. J., & Morley, C. K. (2003). *Subsurface sediment mobilization* (Vol. 216): Geological Society of London.

Rex, J. F., & Petticrew, E. L. (2011). *Fine Sediment Deposition at Forest Road Crossings: An Overview and Effective Monitoring Protocol*. Canada, University of Northern British Columbia: INTECH Open Access Publisher.

Rosenthal, H. (1982). *Water management in circular tanks of a commercial intensive culture unit and its effects on water quality and fish condition*: ICES Statutory meeting, C.M.

Rostami, F., Shahrokhi, M., Said, M. A. M., & Abdullah, R. (2011). Numerical modeling on inlet aperture effects on flow pattern in primary settling tanks. *Applied Mathematical Modelling, 35*(6), 3012-3020.

Rott, N. (1990). Note On The History Of The Reynolds Number. *Annu. Rev. Fluid Mech., 22*(I), 1-12. Retrieved November.03.2012, from: http://gram.eng.uci.edu/rangel/mae130a/osborne-reynolds.pdf

Rublee, P. A., & Bettez, N. (1995). Change of microplankton community structure in response to fertilization of an arctic lake. *Hydrobiologia, 312*(3), 183-190.

Saleh, W., Bowden, R., Hassan, I., & Kadem, L. (2010). Two-phase flow structure in dual discharges–Stereo PIV measurements. *Experimental Thermal and Fluid Science, 34*(8), 1016-1028.

Santiago, J. G., Wereley, S. T., Meinhart, C. D., Beebe, D., & Adrian, R. J. (1998). A particle image velocimetry system for microfluidics. *Experiments in fluids, 25*(4), 316-319.

Sargaonkar, A., & Deshpande, V. (2003). Development of an overall index of pollution for surface water based on a general classification scheme in Indian context. *Environmental monitoring and assessment, 89*(1), 43-67.

Sarnelle, O., Morrison, J., Kaul, R., Horst, G., Wandell, H., & Bednarz, R. (2010). Citizen monitoring: Testing hypotheses about the interactive influences of eutrophication and mussel invasion on a cyanobacterial toxin in lakes. *Water research, 44*(1), 141-150.

Schindler, D., & Hecky, R. (2009). Eutrophication: more nitrogen data needed. *Science, 324*(5928), 721-722.

University of Malaya

Schindler, D. W. (2006). Recent advances in the understanding and management of eutrophication. *Limnology and Oceanography*, 356-363.

Schowalter, W. R. (1978). *Mechanics of non-Newtonian fluids*: Pergamon press Oxford.

Schriver, P., J. Bøgestrand, E. Jeppesen, & Søndergaard., M. (1995). Impact of Submerged Macrophytes on Fish-Zooplankton-Phytoplankton Interactions - Large- Scale Enclosure Experiments in a Shallow Eutrophic Lake. *Freshwater Biology, 33* 255-270.

Schubel, J. R. (1977). Sediment and the quality of the estuarine environment: Some observations. *Fate of pollutants in the air and water environments. Part 1. Mechanism of interaction between environments and the mathematical modeling and the physical fate of pollutants*, 399-424. Retrevied May.06.2013, from: http://www.nerrs.noaa.gov/doc/siteprofile/acebasin/html/modules/watqual/wmturs ed.htm

Schütte, A., & Lüdeke, H. (2013). Numerical investigations on the VFE-2 65-degree rounded leading edge delta wing using the unstructured DLR TAU-Code. *Aerospace Science and Technology*, *24*(1), 56-65.

Segal, E., Shouse, P. J., Bradford, S. A., Skaggs, T. H., & Corwin, D. L. (2009). Measuring particle size distribution using laser diffraction: implications for predicting soil hydraulic properties. *Soil science, 174*(12), 639-645.

Senatore, C., Wulfmeier, M., Vlahinić, I., Andrade, J., & Iagnemma, K. (2013). Design and implementation of a particle image velocimetry method for analysis of running gear–soil interaction. *Journal of Terramechanics, 50*(5), 311-326.

Shahidan, N. F., Hasan, Z. A., Abdullah, M. Z., & Ghani, A. A. (2012). Mathematical Modelling of Flow and Sediment Pattern at Ijok Intake, Ijok River, Perak, Malaysia. *International Journal of Modelling and Simulation, 32*(3), 165.

Shamsad, S., Didar-Ul-Alam, M., Shamsuddoha, A., & Alam, M. N. (2010). Water Quality of Major Ponds of Comilla Town. *Bangladesh Journal of Scientific and Industrial Research, 45*(1), 57-62.

Shamsudin, S., Abd, R., Mohamad, I. N., & Rahman, A. A. (2012). Detention Pond Sediment Accumulation Prediction using Monte Carlo Simulation. *American Journal of Environmental Sciences, 8*, 25-34.

Sharip, Z., & Zakaria, S. (2007). *Lakes and reservoir in Malaysia: Management and research challenges.* Paper presented at the Proceedings of Taal 2007: The 12th World Lake Conference, Malaysia.

She, K., Trim, L., & Pope, D. (2005). Fall velocities of natural sediment particles: a simple mathematical presentation of the fall velocity law. *Journal of Hydraulic Research, 43*(2), 189-195.

Shields, J., Paul, E., St. Arnaud, R., & Head, W. (1968). Spectrophotometry measurement of soil color and its relationship to moisture and organic matter. *Canadian Journal of Soil Science, 48*(3), 271-280.

University of Malaya

Sipaúba-Tavares, L., Donadon, A., & Milan, R. (2011). Water quality and plankton populations in an earthen polyculture pond. *Brazilian Journal of Biology, 71*(4), 845-855.

Southard, J. (2006). The sediment transport rateSpecial topics: An introduction to fluid motions, sediment transport, and current-generated sedimentary structures. USA: Massachusetts Institute of Technology.

Spencer, K., Droppo, I., He, C., Grapentine, L., & Exall, K. (2011). A novel tracer technique for the assessment of fine sediment dynamics in urban water management systems. *Water Research, 45*(8), 2595-2606.

Stanković, A., Stojanović, Z., Veselinović, L., Škapin, S. D., Bračko, I., Marković, S., & Uskoković, D. (2012). ZnO micro and nanocrystals with enhanced visible light absorption. *Materials Science and Engineering: B, 177*(13), 1038-1045.

Stasicki, B., & Meier, G. (1995). *Computer-controlled ultra-high-speed video camera system.* Paper presented at the High-Speed Photography and Photonics: 21st International Congress.

Stephansen, D. A., Nielsen, A. H., Hvitved-Jacobsen, T., & Vollertsen, J. (2012). Bioaccumulation of heavy metals in fauna from wet detention ponds for stormwater runoff. *Urban Environment*, 329-338.

Stojanović, Z., & Marković, S. (2012). Determination of particle size distributions by laser diffraction. *Technics_New Materials 21, 67*, 11-20. Retrieved July.09.2013, from: http://www.itn.sanu.ac.rs/images/Stojanovic_Technics_67_11-20.pdf

Swann, C. (2001). The influence of septic systems at the watershed level. *Watershed Protection Techniques, 3*(4), 821-834.

Takahashi, Y., Kurosawa, K., Sato, Y., Nakamura, M., Makise, H., & Matsumoto, J. U. N. I. (1999). The Effect of Effluents from Fish Ponds on Eutrophication of the Midstream of the Abukuma River. *Journal of Water and Waste, 41*(12), 1097-1103.

Ted Pella, I. (2014). *Specimen Mounts, Holders and Consumables for the Phenom Desktop SEM*. In I. M. P. f. S. a. I. Ted Pella (Ed.). USA.

Tepe, Y., & Boyd, C. E. (2002). Sediment quality in Arkansas bait minnow ponds. *Journal of the World Aquaculture Society, 33*(3), 221-232.

Terrell, C. R., & Perfetti, P. (1996). *Water quality indicators guide: surface waters* (Vol. 161). Washington, DC, USDA Soil Conservation Service: Diane Publishing.

Thompson, B. J. (1989). *Holographic methods for particle size and velocity measurement-recent advances.* Paper presented at the 1989 Intl Congress on Optical Science and Engineering.

University of Malaya

Thomson, W. (1865). On the elasticity and viscosity of metals. *Proceedings of the Royal Society of London, 14*, 289-297.

Tokgoz, S., Elsinga, G. E., Delfos, R., & Westerweel, J. (2012). Spatial resolution and dissipation rate estimation in Taylor--Couette flow for tomographic PIV. *Experiments in fluids, 53*(3), 561-583.

Torgersen, T., Branco, B., & Bean, J. (2004). Chemical retention processes in ponds. *Environmental engineering science, 21*(2), 149-156.

Tu, J., Ishak, A., & Hassan, H. (2001). Prediction of suspended fine-sediment concentration and siltation at Kapar coastal region in Malaysia. *Coastal Engineering V: Computer Modelling of Seas and Coastal Regions, 5*, 43.

USEPA. (1999). *Importance of Turbidity,* USA: U.S. Environmental Protection Agency (Ed.). Retrieved October.11.2013.

Utami, T., & Ueno, T. (1984). Visualization and picture processing of turbulent flow. *Experiments in fluids, 2*(1), 25-32.

Valentine, E., Benson, I., Nalluri, C., & Bathurst, J. (2001). Regime theory and the stability of straight channels with bankfull and overbank flow. *Journal of Hydraulic Research, 39*(3), 259-268.

Van Doorne, C., & Westerweel, J. (2007). Measurement of laminar, transitional and turbulent pipe flow using stereoscopic-PIV. *Experiments in fluids, 42*(2), 259-279.

Van Kessel, T., & Blom, C. (1998). Rheology of cohesive sediments: comparison between a natural and an artificial mud. *Journal of Hydraulic Research, 36(*4), 591-612.

Van Rijn, L. C. (2007). *Manual sediment transport measurements in rivers, estuaries and coastal seas*. Amsterdam: Aqua publications.

Venditti, J., Dietrich, W., Nelson, P., Wydzga, M., Fadde, J., & Sklar, L. (2010). Effect of sediment pulse grain size on sediment transport rates and bed mobility in gravel bed rivers. *Journal of Geophysical Research, 115*(F3), F03039.

Vermeulen, T. (2004). *Sensitivity Analysis of Fine Sediment Transport in the Humber Estuary.* (Master), TU Delft, Delft University of Technology.

Victoria, U. O. (2000). *Introduction to Particle Size Analysis*. Department of Geography. Univesity of Victoria . Retrieved June.06.2014, from: http://www.geog.uvic.ca/dept2/faculty/smithd/477/manuals/techniques/10%20Geog%20477.pdf

Vincent, S. J. (2001). The Sis palaeovalley: a record of proximal fluvial sedimentation and drainage basin development in response to Pyrenean mountain building. *Sedimentology, 48*(6), 1235-1276.

Vu, T. T., & Tan, S. K. (2010). Laboratory investigation of hydraulic performance of silt screens. *Journal of Hydrodynamics, Ser. B, 22*(5), 312-317.

University of Malaya

Walker Jr., W.W. (1987). Phosphorus removal by urban runoff detention basins. *Lake Reservoir Management 3*(1), 314-328.

Wang, X. L., Li, T., Lang, J., Zhou, S. S., Zhang, L. L., & Chen, M. X. (2010). Numerical Analysis of Solid− Liquid Two-Phase Flow on Sandstone Wastewater of Hydropower Stations in a Rectangular Sedimentation Tank. *Industrial & Engineering Chemistry Research*, *49*(22), 11714-11723.

Weiss, J. D., Hondzo, M., & Semmens, M. (2006). Storm water detention ponds: Modeling heavy metal removal by plant species and sediments. *Journal of Environmental Engineering*, *132*(9), 1034-1042.

Weitbrecht, V., Kühn, G., & Jirka, G. (2002). Large scale PIV-measurements at the surface of shallow water flows. *Flow Measurement and Instrumentation*, *13*(5), 237-245.

Weitbrecht, V., Uijttewaal, W., & Jirka, G. H. (2004). 2-D particle tracking to determine transport characteristics in rivers with dead zones. *Shallow flows*,*12*(10), 477-484.

Weitz, D., Wyss, H., & Larsen, R. (2007). Oscillatory rheology: Measuring the viscoelastic behaviour of soft materials. *GIT laboratory journal Europe, 11*(3-4), 68-70.

Westers, H. (1995). *Feed and feeding strategies to reduce aquaculture waste.* Paper presented at the Aquaculture Bioengineering Corporation, Aquaculture Engineering and WasteManagement: In Proceeding from the Aquaculture Expo VIII and Aquaculture in theMid-Atlantic Conference.

Westerweel, J. (1993). *Digital particle image velocimetry: theory and application*. Netherlands: TU Delft, Delft University of Technology.

Westerweel, J., & Nieuwstadt, F. (1991). *Performance tests on 3-dimensional velocity measurements with a two-camera digital particle-image velocimeter.* Paper presented at the Laser Anemometry-Advances and Applications.

Whalley, W. B., & Krinsley, D. H. (1974). A scanning electron microscope study of surface textures of quartz grains from glacial environments. *Sedimentology, 21*(1), 87-105.

Whipple W., & J.V. Hunter. (1981). Settleability of Urban Runoff Pollution. *Journal of the Water Pollution Control Federation*, *53*, 451-464.

Wikipedia. (2012). *Sediment* (Vol. 2012, pp. 1): the Wikimedia Foundation, Inc. Retrieved October.11.2013.

Willert, C. E., & Gharib, M. (1991). Digital particle image velocimetry. *Experiments in fluids, 10*(4), 181-193.

Williamson, S. J., & Cummins, H. Z. (1983). *Light and color in nature and art* (Vol. 1): Wiley-VCH. Retrieved October.20.2013

University of Malaya

Wilson, P. C. (2010). Water Quality Notes: Water Clarity (Turbidity, Suspended Solids, and Color). Retrieved December.09.2013.

Wong, T. H., Fletcher, T. D., Duncan, H. P., & Jenkins, G. A. (2006). Modelling urban stormwater treatment—a unified approach. *Ecological Engineering, 27*(1), 58-70.

Woo, H. S., Julien, P. Y., & Richardson, E. V. (1986). Washload and fine sediment load. *Journal of Hydraulic Engineering, 112*(6), 541-545.

World Bank. (2012). Rural Water Supply, Volum 1, Design Manual. In T. W. B. O. Manila (Ed.), (pp. 212). Manila- Philippines Water Partnership Program.

Xie, P., Iwakuma, T., & Fujii, K. (1998). Changes in the structure of a zooplankton community during a Ceratium (dinoflagellate) bloom in a eutrophic fishless pond. *Journal of plankton research, 20*(9), 1663-1678.

Xu R. (2000). Particle Characterization: Light Scattering Methods . from Kluwer Academic Publishers

Yamamoto, T., & Sawa, K. (2011). Numerical Analysis of Shear Banding Flow of Wormlike Micelle Solutions between Parallel Channels using a Network Scission Model. *Journal of the Society of Rheology ;Japan, 39*(3), 105-111.

Yang, B., Wang, Y., & He, W. B. (2012). *Application of Micro-PIV on the Microscale Flow and a Modified System Based on Ordinary 2-D PIV.* Paper presented at the Advanced Materials Research.

Yang, B., Wang, Y., & Liu, J. (2011). PIV measurements of two phase velocity fields in aeolian sediment transport using fluorescent tracer particles. *Measurement, 44*(4), 708-716.

YemenWater. (2013). *Water Pollution*. Yemen: water and Environment center. Retrieved February.01.2014.

Yu, X.-J., & Liu, B.-J. (2007). Stereoscopic PIV measurement of unsteady flows in an axial compressor stage. *Experimental Thermal and Fluid Science, 31*(8), 1049-1060.

Yu, X., Hsu, T.-J., & Balachandar, S. (2013). A spectral-like turbulence-resolving scheme for fine sediment transport in the bottom boundary layer. *Computers & Geosciences, 61*, 11-22. doi:10.1016/j.cageo.2013.07.021

Yunus, K., Ahmad, S. W., Ong, M. C., & Bidai, J. (2010). Spatial distribution of lead and copper in the bottom sediments of Pahang river estuary, Pahang, Malaysia. *Sains Malaysiana, 39*(4), 543-547.

Zakaria, N. A., Azamathulla, H. M., Chang, C. K., & Ghani, A. A. (2010). Gene expression programming for total bed material load estimation—a case study. *Science of the total environment, 408*(21), 5078-5085.

Zhang, J., Qi, S., Xing, X., Tan, L., Gong, X., Zhang, Y., & Zhang, J. (2011). Organochlorine pesticides (OCPs) in soils and sediments, southeast China: a case study in Xinghua Bay. *Marine pollution bulletin, 62*(6), 1270-1275.

University of Malaya

Zhang, K. (2004). *Rheological characterization of dental waxes.* (Doctrol), Universitätsklinik.

Zhang, W., Zou, Z., & Sui, J. (2010). Numerical simulation of a horizontal sedimentation tank considering sludge recirculation. *Journal of Environmental Sciences, 22*(10), 1534-1538.

Zhiyao, S., Tingting, W., Fumin, X., & Ruijie, L. (2008). A simple formula for predicting settling velocity of sediment particles. *Water Science and Engineering, 1*(1), 37-43.

Zhu, L., & Cheng, N. (1993). Settlement of settling particles. *River and Harbour Engineering Department, Nanjing Hydraulic Research Institute, Nanjing (in Chinese)*.

University of Malaya

LIST OF PUBLICATIONS AND PAPERS PRESENTED

PUBLICATIONS

Masoumeh Moayeri Kashani, Lai S Hin, Shaliza B Ibrahim, Nik Meriam B Nik Sulaiman, Teo F Yenn, 2015, An Investigation into the Effects of Particle Texture, Water Content and Parallel Plates' Diameters on Rheological Behaviour of Fine Sediment, International Journal of Sediment Research.(ISI cited)

Masoumeh Moayeri Kashani, Lai S Hin, Shaliza B Ibrahim, Nik Meriam B Nik Sulaiman. 2015, A Study on Hydrodynamic Behavior of Fine Sediment in Retention Structure Using PIV, Water Environment Research. (ISI cited)

Masoumeh Moayeri Kashani, Lai S Hin, Shaliza B Ibrahim, Nik Meriam B Nik Sulaiman. 2016, Tracking the Hydrodynamic Behavior of Fine Sediment Using Particle Image Velocimetry, Environmental Earth Sciences. (ISI cited)

PAPERS PRESENTED

Masoumeh Moayeri Kashani, Lai S Hin, Shaliza B Ibrahim, Nik Meriam B Nik Sulaiman. 2015, Influence of Particles Texture, and Structure on Rheological Behaviour of Fine Sediment Slurry International conference of CleanWAS 2015 Kuala Lumpur Malaysia. (ISI conference)

University of Malaya